POLSKIE TOWARZYSTWO MIKROBIOLOGÓW
POLISH SOCIETY OF MICROBIOLOGISTS

Polish Journal of Microbiology

2015

Polish Journal of Microbiology
formerly Acta Microbiologica Polonica
2015, Vol. 64, No 3

CONTENTS

INSTRUCTIONS FOR AUTHORS
Submission of manuscripts: http://www.pjm.indexcopernicus.com/
Instructions for authors: http://www.pjmonline.org

Polish Journal of Microbiology
2015, Vol. 64, No 3

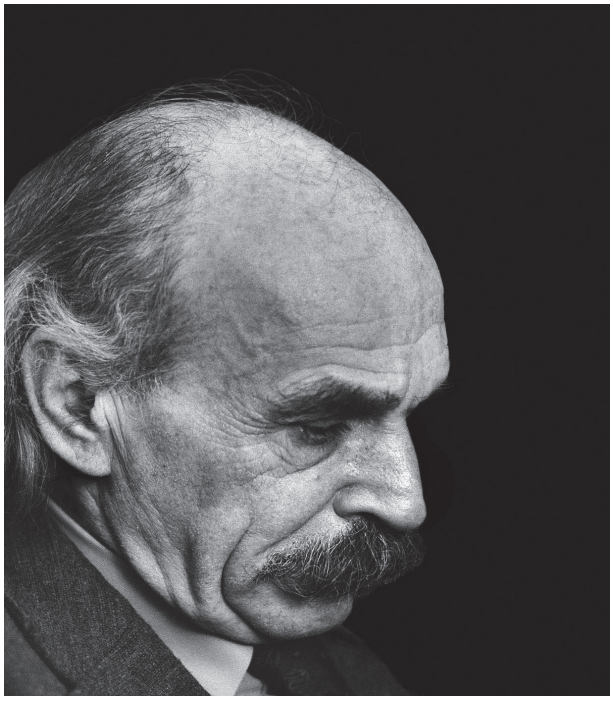

The 16th conference in the series

"*Molecular biology in the diagnostics of infectious diseases and biotechnology* – DIAGMOL 2015"

will be held on the 28th of November 2015,
in the Crystal Hall of the WULS-SGGW in Warsaw

This year's conference will be devoted to the memory of professor Władysław Kunicki-Goldfinger, on the 20th anniversary of his death.
The program of the first conference session will embrace memories about the Professor's life and accomplishments, presented by his colleagues, collaborators and students.

The faculty of the Department of Bacterial Genetics,
Institute of Microbiology, University of Warsaw

Polish Journal of Microbiology
2015, Vol. 64, No 3, 193–202

MINIREVIEW

CRISPR-Cas Systems in Prokaryotes

MICHAŁ BURMISTRZ[1] and KRZYSZTOF PYRĆ[1, 2]*

[1] Microbiology Department, Faculty of Biochemistry Biophysics and Biotechnology, Jagiellonian University, Krakow, Poland
[2] Malopolska Centre of Biotechnology, Jagiellonian University, Krakow, Poland

Submitted 29 April 2015, accepted 6 May 2015

Abstract

Prokaryotic organisms possess numerous strategies that enable survival in hostile conditions. Among others, these conditions include the invasion of foreign nucleic acids such as bacteriophages and plasmids. The clustered regularly interspaced palindromic repeats-CRISPR-associated proteins (CRISPR-Cas) system provides the majority of bacteria and archaea with adaptive and hereditary immunity against this threat. This mechanism of immunity is based on short fragments of foreign DNA incorporated within the hosts genome. After transcription, these fragments guide protein complexes that target foreign nucleic acids and promote their degradation. The aim of this review is to summarize the current status of CRISPR-Cas research, including the mechanisms of action, the classification of different types and subtypes of these systems, and the development of new CRISPR-Cas-based molecular biology tools.

Key words: CRISPR-Cas, prokaryotes

Introduction

Prokaryotes inhabit many hostile environments that are often inaccessible to other organisms. Regardless of their environment, prokaryotes are able to adapt and adjust to the changing world by developing new tactics to promote survival. One of the systems constituting a natural defense mechanism is the ability to distinguish self from non-self nucleic acids. Nucleic acids may be inserted into prokaryotic cells by infection, transduction, conjugation, or transformation, and may have harmful effects. The defense mechanisms include the restriction-modification, abortive infection, and surface exclusion systems, all of which act in an innate, non-specific manner (Samson *et al.*, 2013). However, a unique defense system involving clustered regularly interspaced palindromic repeats-CRISPR-associated proteins (CRISPR-Cas) was reported recently. This system is present in most archaeal species and approximately half of all bacterial species. A unique feature of the CRISPR-Cas system is that it provides adaptive and hereditary immunity against foreign nucleic acids, mimicking in some ways the immune systems of eukaryotes.

The first reports of the CRISPR-Cas system originate from as early as 1987, but these repeat regions were not associated with a specific function (Ishino *et al.*, 1987). In 2002, they were discovered in other bacteria and named CRISPR (Jansen *et al.*, 2002). Since then, numerous roles of CRISPR-Cas systems have been postulated, including chromosomal rearrangements, modulation of gene expression, replicon partitioning, and DNA repair (Babu *et al.*, 2011; Jansen *et al.*, 2002; Makarova *et al.*, 2002; Mojica *et al.*, 1995). Discovery of the similarity between some CRISPR spacer sequences and sequences from viruses and plasmids led to the suggestion that CRISPRs play roles in adaptive immunity against foreign nucleic acids (Makarova *et al.*, 2006). Later, spacers homologous to chromosomal genes of the host were discovered (Bolotin *et al.*, 2005; Mojica *et al.*, 2005), suggesting that, in addition to phage immunity, CRISPR-Cas systems may play a role in autoimmunity or as a regulatory mechanisms (Sorek *et al.*, 2008; Stern *et al.*, 2010).

Components of the CRISPR-Cas system

The CRISPR-Cas system comprises genomic (CRISPR) and proteomic (Cas) components. The genomic component is a DNA loci containing short fragments of targeted nucleic acid sequences (spacers) interspaced by short repeated sequences (repeats). These

* Corresponding author: K. Pyrć, Microbiology Department, Faculty of Biochemistry Biophysics and Biotechnology, Jagiellonian University, Krakow, Poland; **e-mail: k.a.pyrc@uj.edu.pl.**

spacer sequences can be of either foreign or self-origin (Stern *et al.*, 2010; Vercoe *et al.*, 2013). The proteomic component is responsible for the incorporation of new template sequences, processing them into a form that enables base pairing with target nucleic acids, as well as for scanning and cleavage of target DNA or RNA. Of note, not all CRISPR-Cas systems discovered to date are active (Haft *et al.*, 2005; van der Ploeg, 2009).

Structure of the CRISPR-Cas system

The genomic component of the CRISPR-Cas system is formed by a series of variable spacers, which in some cases share sequence similarity with viruses, plasmids, or bacteria. These regions are interspaced with repeat sequences that are identical or almost identical within a single CRISPR cassette. The length of the repeat sequences varies between 25 and 40 nt, whereas the length of the spacer sequences varies between 21 and 72 nt. As mentioned above, some spacers show high homology with foreign nucleic acids, but the origin of a significant percentage of spacers remains unknown. The sequence homology between the spacer and the target is the major determinant of nucleic acid degradation of the target. Some bacterial species contain more than one CRISPR locus within their genome (Louwen *et al.*, 2014). Depending on the specific bacterial species or strain, a CRISPR locus may contain from a few to several hundred repeat spacer units; however, most commonly, a single CRISPR locus contains approximately 50 units. The CRISPR repeat sequences play an important role during both the acquisition of new spacers and the transcription and maturation of CRISPR RNA (crRNA). Based on the sequence similarity, the CRISPR repeats are assigned into groups (Kunin *et al.*, 2007). These groups were taken into account in the current classification of CRISPR-Cas systems (Makarova *et al.*, 2011). Although most CRISPR arrays are located on chromosomal DNA, there are examples of CRISPRs located on plasmids (Godde and Bickerton, 2006). In general, CRISPR loci are flanked by A/T rich leader sequences containing promoter elements and binding sites for regulatory proteins (Jansen *et al.*, 2002; Yosef *et al.*, 2012).

CRISPR arrays are usually located in close proximity to a set of genes encoding Cas proteins. Members of this large group of proteins are required for CRISPR activity and have multiple functions as nucleases, polymerases, helicases, and nucleic acid binders. The exact number and types of Cas proteins depend on the specific CRISPR-Cas class.

Similar to other immune systems, the CRISPR-Cas system requires differentiation between self and non-self species to avoid autoimmunity. The CRISPR array is the most susceptible to autoimmune events as it contains spacers used for target recognition. In most cases, the CRISPR-Cas system deals with this problem by utilizing protospacer adjacent motifs (PAMs) (Sashital *et al.*, 2012),which are present in the target DNA but not the CRISPR array. DNA cleavage occurs only if the correct PAM sequence is present (Jinek *et al.*, 2012; Semenova *et al.*, 2011; Westra *et al.*, 2013). However, in type III CRISPR-Cas systems the safety mechanism

Table I
Subtypes of CRISPR-Cas system.

Type	Type hallmarks	Sub-type	Subtype hallmarks	crRNA processing*	Effector complex	Targeted nucleic acid	Exemplary organism
I	Cas3	I-A	Cas8a	Cas6 homologues, Cascade	Cascade	DNA	*Sulfolobus islandicus* (Held *et al.*, 2013)
		I-B	Cas8b				*Clostridium difficile* (Soutourina *et al.*, 2013)
		I-C	Cas8c, repeat group 3	Cas5d			*Xanthomonas oryzae* (Semenova *et al.*, 2009)
		I-D	Cas10	Cas6 homologues			*Thermofilum pendens* (Hrle *et al.*, 2014)
		I-E	Cse1, repeat group 2				*Escherichia coli* (Westra *et al.*, 2010)
		I-F	Csy1, repeat group 4				*Pseudomonas aeruginosa* (Bondy-Denomy *et al.*, 2013)
II	Cas9, repeat group 10	II-A	Csn2	RNase III, unknown nuclease	Cas9		*Streptococcus thermophilus* (Barrangou *et al.*, 2007)
		II-B	Cas4				*Francisella novicida* (Sampson *et al.*, 2013)
		II-C	lack of Csn2 and Cas4				*Neisseria meningitides* (Zhang *et al.*, 2013)
III	Cas10	III-A	Csm2	Cas6 homologues, Csm	Csm		*Staphylococcus epidermidis* (Marraffini and Sontheimer, 2008)
		III-B	Cmr5	Cas6 homologues, Cmr	Cmr	RNA	*Thermus thermophilus* (Staals *et al.*, 2013), *Sulfolubus solfataricus* (Zhang *et al.*, 2012b)

*An alternative crRNA biogenesis was described for *Neisseria* spp. of type II (details within main text).

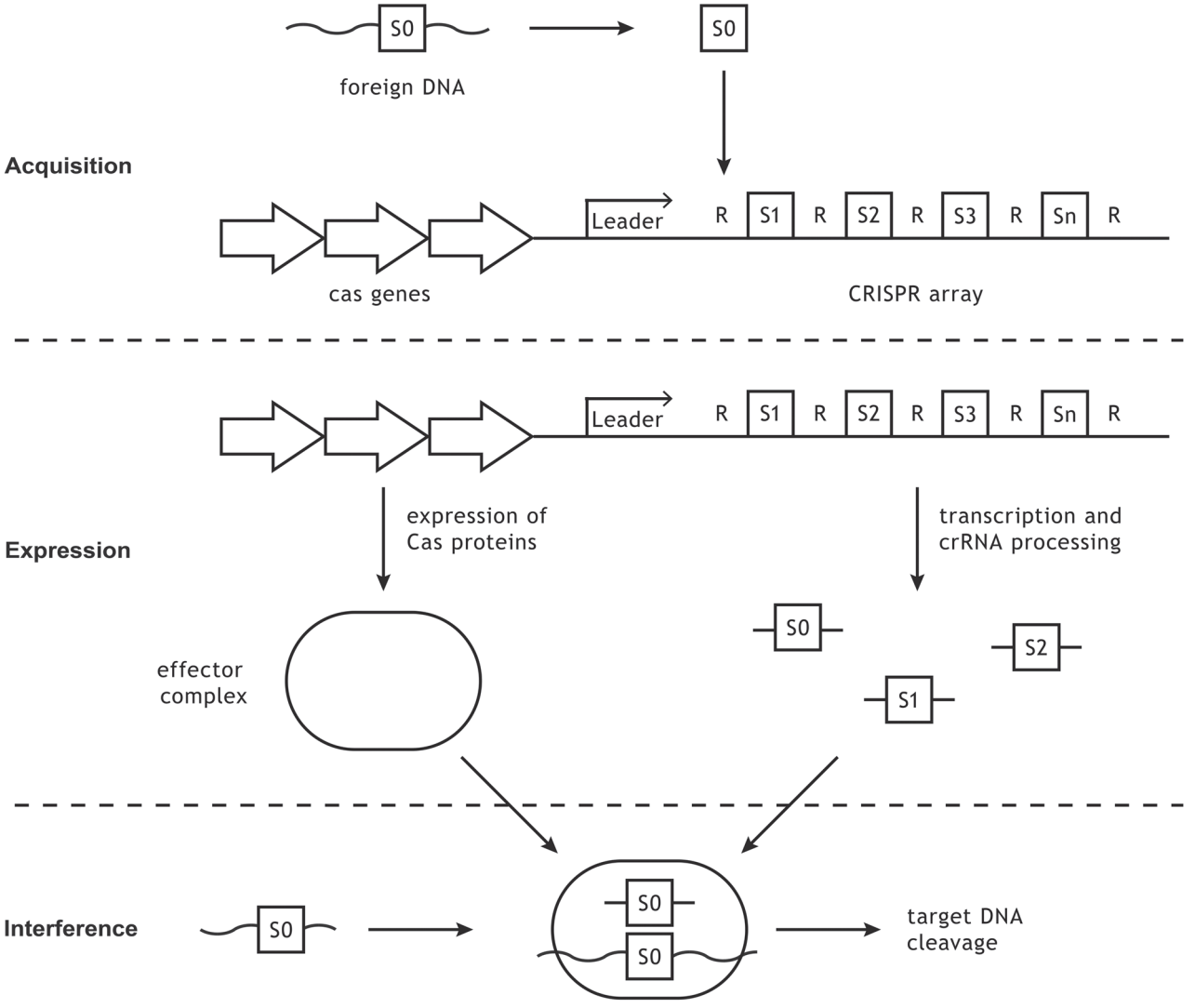

Fig. 1. Scheme of CRISPR-Cas system. S0, S1, S2, … , Sn stands for spacer sequences. R stands for repeat sequence.

is PAM-independent and is based on the proximity of a repeat sequence to a spacer sequence in the CRISPR locus, which hinders its cleavage (Marraffini and Sontheimer, 2010).

The current classification of CRISPR-Cas systems is based on the sequences of the *cas* genes, the sequences of the repeats within the CRISPR arrays, and the organization of the *cas* operons (Makarova *et al.*, 2011). The classification distinguishes three main types of CRISPR-Cas systems (types I–III). Each type is also divided into subtypes, including I-A to I-F, II-A to II-C, III-A and III-B. The *cas1* and *cas2* genes are common to all three CRISPR-Cas types. The major criterion for classification includes the presence or absence of certain Cas proteins. For example, the Cas3, Cas9, and Cas10 proteins are hallmarks of CRISPR/Cas types I, II and III, respectively. Systems that do not have the specific hallmarks of types I–III are grouped as unclassified (type U). A description of the CRISPR-Cas subtypes is provided in Table I.

Mode of action

Profound studies of the mode of action of the CRISPR-Cas system revealed that the process can be divided into three distinct phases: (1) the acquisition of spacers following exposure to foreign nucleic acids, (2) the transcription of spacers and transcript processing to produce a crRNA that guides target recognition, and (3) target recognition and cleavage. Figure 1 shows a schematic overview of the CRISPR-Cas mode of action, and each phase is discussed in detail below.

Spacer acquisition

The most important feature of the CRISPR/Cas system is its capacity to respond dynamically to external stimuli. This adaptation relies on the ability to insert fragments of foreign nucleic acids into the CRISPR array, such that they serve as a template for the generation of crRNA, which mediates the subsequent

degradation of targeted nucleic acids. In this manner, bacteria are able to learn the patterns present in nucleic acids during invasion of foreign genetic elements. The mechanism responsible for the recognition, processing, and integration of new spacers has not been characterized fully; nevertheless, a number of factors involved in the process were identified.

New spacers are incorporated into the leader end of the CRISPR array in an orderly manner (Barrangou *et al.*, 2007; Pourcel *et al.*, 2005). Such unilateral insertion of new spacers converts the CRISPR array into a timeline containing a chronological database of foreign nucleic acid encounters. Prior to the incorporation of a new spacer sequence into the CRISPR array, foreign nucleic acids must be recognized and fragmented. A study performed in *Streptococcus thermophiles* indicated that the restriction-modification system can supply the CRISPR-Cas system with potential substrates for integration (Dupuis *et al.*, 2013). However, several factors are important for the incorporation of novel nucleic acids into the cell's genome. For example, the presence of a PAM (Deveau *et al.*, 2008) sequence flanking the protospacer sequence, is necessary for the selection of spacers (Mojica *et al.*, 2009). A positively selected protospacer sequence is then processed into a precursor (Swarts *et al.*, 2012). To enable integration of this precursor into the CRISPR array, the repeat adjacent to the leader end sequence is nicked at the 3' ends of both of its strands, and the precursor is subsequently integrated between two single-stranded repeat sequences (Díez-Villaseñor *et al.*, 2013). It has been hypothesized that an interaction between the leader sequence and Cas proteins ensures proper orientation of newly integrated spacers within the CRISPR array (Yosef *et al.*, 2012). The last step of spacer integration is reconstruction of the second strands of the repeat; as a result, the repeat sequence is duplicated during the integration process (Yosef *et al.*, 2012). In addition to PAM, other sequence motifs that affect the rate of spacer incorporation were also discovered in proto spacers. An example of such a sequence motif is the acquisition affecting motif, which comprises a dinucleotide AA and is located at the 3' end of a protospacer (Yosef *et al.*, 2013).

In addition to genetic factors, the process of spacer acquisition also involves protein components. Among the many factors involved in spacer acquisition, the Cas1 and Cas2 proteins seem to be the most important. Both of these proteins are important for spacer integration (Yosef *et al.*, 2012) and are conserved in all CRISPR-Cas systems (Haft *et al.*, 2005; Makarova *et al.*, 2011). A study in *Escherichia coli* showed that Cas1 and Cas2 form a protein complex that interacts with the CRISPR locus (Datsenko *et al.*, 2012; Yosef *et al.*, 2012). Despite the identification of a number of activities and structural motifs of these proteins (Babu *et al.*, 2011; Beloglazova *et al.*, 2008; Nam *et al.*, 2012a; Reeks *et al.*, 2013; Wiedenheft *et al.*, 2012; Wiedenheft *et al.*, 2009), their exact function in spacer acquisition remains unknown. A side from Cas1 and Cas2, several other factors may also be involved in the CRISPR-Cas adaptation stage. In *E. coli*, the Cas1 protein interacts with housekeeping proteins involved in DNA maintenance, including the RecBCD and RuvB proteins (Babu *et al.*, 2011). Several recent findings also indicate the involvement of additional Cas proteins, namely, Cas3, Cas4, Csa1, and Csn2 (Arslan *et al.*, 2013; Jackson *et al.*, 2014; Makarova *et al.*, 2006; Makarova *et al.*, 2011; van der Oost *et al.*, 2009; Zhang *et al.*, 2012a). Csn2 is thought to be responsible for the recruitment of additional factors and stabilization of DNA breaks in the CRISPR array during spacer acquisition (Arslan *et al.*, 2013).

An interesting phenomenon linked with spacer acquisition has been described. Although one spacer is sufficient for target DNA degradation, a single CRISPR locus can contain multiple spacers originating from a single genetic entity. This finding led to the so-called hypothesis of "primed spacer acquisition", in which the presence of one spacer can trigger the acquisition of additional spacers from the same DNA target (Swarts *et al.*, 2012). This primed acquisition can also occur in the presence of mismatches between the spacer and protospacer sequences that prevent the interference (Datsenko *et al.*, 2012; Heler *et al.*, 2014). It is thought that the role of primed spacer acquisition is to counter possible evasion. The hypothesis that the effector complex slides across the target DNA was proposed to explain the mechanism of primed acquisition (Datsenko *et al.*, 2012; Fineran *et al.*, 2014; Li *et al.*, 2014). This hypothesis states that, after a failed interference attempt, the effector complex recruits Cas1 and Cas2, and then slides along the target strand to find suitable PAMs that enable the acquisition of new spacers. However, this proposed mechanism has not yet been confirmed.

Transcript processing

Spacers within the CRISPR array cannot interfere directly with foreign nucleic acids and need to be transcribed. In most cases, transcription is initiated by the leader sequence located upstream of the CRISPR array. As a result, a long precursor transcript called a pre-crRNA is created. Further processing of this transcript differs depending on the CRISPR-Cas system type; however, a notable exception has been described. In *Neisseria* spp., no pre-crRNA transcript is generated; instead, the crRNAs are transcribed separately from promoters embedded within repeat sequences, and their 5' ends are formed by transcription rather than maturation (Zhang *et al.*, 2013). Notably, these crRNAs can undergo type II processing (see below), although it is not required for their functionality (Zhang *et al.*, 2013).

In type I and III CRISPR-Cas systems, initial processing of the pre-crRNA is performed by Cas6 nuclease homologs carrying two repeat-associated mysterious protein domains (Reeks *et al.*, 2013). Cleavage of the pre-crRNA generates a product comprising a full spacer sequence flanked by repeat-derived handles on both ends. In most cases, the 5' handles are 8 nt (nucleotides) long (11nt in type I-C systems (Nam *et al.*, 2012b) and 13 nt in I-D systems (Scholz *et al.*, 2013), whereas the 3' handles have variable lengths depending on the specific CRISPR-Cas type. In some types, the 3' handles form hairpin structures (Carte *et al.*, 2010; Carte *et al.*, 2008; Niewoehner *et al.*, 2014; Wang *et al.*, 2011). In type I-C systems, initial processing is performed by Cas5 rather than Cas6 (Garside *et al.*, 2012; Nam *et al.*, 2012b), whereas in other CRISPR-Cas types, Cas5 is catalytically inactive and is thought to interact with the 5' handle of the crRNA (Wiedenheft *et al.*, 2011). In most type I and type III systems, after initial processing, the crRNA is transferred to CRISPR ribonucleoprotein (crRNP) complexes for secondary processing (Hatoum-Aslan *et al.*, 2011). In types I-A, I-B, I-C, and I-D, this processing results in shortening of the 3' handles. In both subtypes of type III, secondary processing generates two populations of products that differ in length by 6 nt (Hale *et al.*, 2012; Zhang *et al.*, 2012b). In contrast to the systems mentioned above, types I-E and I-F do not utilize secondary processing. After initial cleavage by Cas6 or its homolog, the Cas6 protein remains associated with the hairpin at the 3' handle of the crRNA. Subsequently, this sub-complex is incorporated into Cascade, the effector complex utilized by type I systems.

The mechanism of pre-crRNA processing in type II systems differs from those of type I and type III systems. First, an additional fragment encoding a trans activating crRNA (tracrRNA) is transcribed from the CRISPR locus. The tracrRNA contains a 25 nt sequence complementary to the repeat sequences within the pre-crRNA. Initial processing involves hybridization of the tracrRNA and pre-crRNA, and the hybrids are subsequently digested by RNase III associated with Cas9 (Deltcheva *et al.*, 2011; Jinek *et al.*, 2012). After cleavage, the hybrids attached to Cas9 undergo further trimming by an unidentified nuclease to yield functional, mature crRNA (Deltcheva *et al.*, 2011).

Target recognition and degradation

Mature crRNAs are incorporated into crRNP complexes. Depending on the type of CRISPR-Cas system, these effector complexes vary in their composition and mode of action; however, the general mechanism is common among types I–III. Initially, the crRNP complex scans nucleic acids for protospacer sequences. Base pairing between the crRNA spacer and the proto spacer begins in a 7–8 nt seed region (Semenova *et al.*, 2011). Further hybridization to the protospacer region results in formation of an R-loop structure, in which the crRNA is paired with one of the DNA strands and the displaced DNA strand remains single-stranded (Sashital *et al.*, 2012; Sorek *et al.*, 2013). This structure triggers a conformational change in the crRNP complex, thereby initiating type-dependent nuclease activity (Jore *et al.*, 2011; Spilman *et al.*, 2013; Wiedenheft *et al.*, 2011). During the degradation phase, to prevent the effector complex from digesting its own CRISPR array, it is essential to distinguish between foreign and self DNA. In type I and type II CRISPR-Cas systems, this safety mechanism is based on the presence of PAMs (Gasiunas *et al.*, 2012; Jinek *et al.*, 2012; Semenova *et al.*, 2011; Westra *et al.*, 2013). Within the targeted nucleic acids, the PAM sequence is localized in close proximity to the protospacer sequence, whereas the spacer sequence in the CRISPR array lacks this element; consequently, the CRISPR region is not cleaved. In type III CRISPR-Cas systems, discrimination between self and foreign DNAs is PAM-independent. In these systems, the 5' handle of a crRNA interacts with a repeat sequence in the CRISPR locus. This interaction probably prevents nuclease recruitment, thereby preventing cleavage of self DNA (Marraffini and Sontheimer, 2010).

The effector complexes of type I and type III systems share a significant level of structural similarity. The small subunits of these complexes include Csa5 and Cse2 in type I systems, and Csm2 and Cmr5 in type III systems. The large subunits include Cas8 homologs and Cas10 homologs in types I and III, respectively. The effect or complexes of all subtypes of type I CRISPR-Cas systems share significant similarities and are collectively referred to as Cascade complexes (Reeks *et al.*, 2013). A typical Cascade complex consist of Cse1 (one subunit), Cse2 (two subunits), Cas5 (one subunit), Cas7 (six subunits), and Cas6 (one subunit) (Jore *et al.*, 2011; van Duijn *et al.*, 2012). The type I-E Cascade complex from *E. coli* is the most well-characterized of all CRISPR-Cas systems. The backbone of the complex consists of six Cas7 units, along which the crRNA is positioned. The 5' and 3' handles of the crRNA are anchored at opposite sides of the complex to Cas5 and Cas6, respectively. The Cse1 protein located at the 5' crRNA end of the complex is responsible for the non-specific interaction with DNA during initial target scanning (Jore *et al.*, 2011). This protein is also responsible for interaction with the PAM motif located at the 3' end of the proto spacer (Sternberg *et al.*, 2012), and this interaction is thought to trigger hybridization of the crRNA and target DNA by destabilization of the DNA duplex (Sashital *et al.*, 2012). In type I-E systems, the seed region, which requires perfect hybridization for target degradation, is located at the 5' end of the spacer (positions 1–5,

7, and 8) (Künne *et al.*, 2014; Semenova *et al.*, 2011). A conformational change in the Cascade complex, linked with formation of the R-loop, triggers recruitment of the Cas3 protein (Westra *et al.*, 2012). Cas3 possesses metal-dependent nuclease and ATP-dependent helicase activities (Beloglazova *et al.*, 2011; Jackson *et al.*, 2014; Mulepati and Bailey, 2011), and initial DNA cleavage occurs on the strand displaced during formation of the R-loop (Sinkunas *et al.*, 2013). The subsequent degradation of the target proceeds in an exonucleolytic manner from the 3' to the 5' end (Beloglazova *et al.*, 2011; Westra *et al.*, 2012). The second strand of the DNA is digested in both endonucleolytic and exonucleolytic manners (Beloglazova *et al.*, 2011; Mulepati and Bailey, 2011; Westra *et al.*, 2012).

The mechanism of interference used by type II CRISPR-Cas systems differs from that of type I systems. In type II systems, interference depends on the Cas9-RNP complex, the structure of which is relatively less intricate than those of other CRISPR types and includes Cas9 and a single guide RNA (sgRNA) (Jinek *et al.*, 2014; Nishimasu *et al.*, 2014). The sgRNA is a duplex of crRNA and tracrRNA (Jinek *et al.*, 2012). Cas9 has two domains, an α-helical recognition domain and a nuclease domain; the first of these domains is responsible for coordinating the guide RNA, and the second takes part in PAM recognition and target DNA cleavage. The nuclease domain actually comprises two individual nucleases, namely, RuvC and HNH (Nishimasu *et al.*, 2014). The interference process begins with the incorporation of a sgRNA into Cas9, which results in a conformational change of Cas9 that enables the complex to bind DNA (Jinek *et al.*, 2014). Subsequently, DNA scanning proceeds in a similar manner to that in type I systems. The PAM motif of type II systems is located at the 5' end of the proto spacer (Deveau *et al.*, 2008; Mojica *et al.*, 2009). Recognition of this motif is considered to lead to displacement of the DNA strand and formation of the R-loop. Base pairing between the spacer and proto spacer starts from a 12 nt seed region (Jiang *et al.*, 2013; Sternberg *et al.*, 2014). Each strand of the target DNA is digested by a different nuclease domain of Cas9 protein; specifically, the HNH domain cleaves the strand hybridized with crRNA, and the RuvC domain cleaves the displaced strand (Jinek *et al.*, 2012; Jinek *et al.*, 2014).

Type III CRISPR-Cas effector complexes resemble those of the type I Cascade complex. The backbone of the type III crRNP complex is composed of multiple Csm3 (type III-A) or Cmr4 (type III-B) proteins (Rouillon *et al.*, 2013; Spilman *et al.*, 2013; Staals *et al.*, 2013). Like type I CRISPR-Cas effector complexes, the crRNA is positioned along the backbone in type III complexes (Rouillon *et al.*, 2013). Parallel to the backbone, the small subunits (Csm2 or Cmr5) form a secondary string connecting the two ends of the complex. The Csm4 (type III-A) or Cmr3 (type III-B) protein is located at the 5' end of the crRNA and is bound to the large subunit (Csm1 or Cmr2, respectively). Together with the Cmr6 protein, Csm5 or Cmr1 is located at the 3' end of the crRNA and bound to a small subunit (Csm2 or Cmr5). Functioning of type III systems is not as well-characterized as that of other types, but some important differences have been described. As mentioned earlier, in type III-A systems, discrimination between self and non-self DNA proceeds in a PAM-independent manner (Rouillon *et al.*, 2013), and the large subunit (Csm1) is thought to take part in the discrimination process (Hatoum-Aslan *et al.*, 2014). The presence of a seed sequence within the spacer sequence was proposed (Hatoum-Aslan *et al.*, 2014) but not confirmed fully. Type III-B systems are unique among other CRISPR types because they target RNA rather than DNA (Hale *et al.*, 2009); however, there are examples of type III-B systems targeting plasmid DNA *in vivo* (Deng *et al.*, 2013). Most type III-B effector complexes comprise six proteins (Cmr1-6) (Gasiunas *et al.*, 2014); however, in *Sulfolobus solfataricus*, these effector complexes contain an additional protein (Cmr7) (Zhang *et al.*, 2012b). Recognized target RNA is cleaved at regular intervals in the 3' to 5' direction (Staals *et al.*, 2013). This digestion pattern indicates the presence of multiple active sites within the backbone of the Cmr complex (Staals *et al.*, 2013), which is composed of multiple subunits of Cmr4 and Cmr5.

Other functions of the CRISPR-Cas system

Recognition and degradation of invading nucleic acids is a major function of the CRISPR-Cas system; however, several studies showed that it may have additional roles. One of the intriguing features of the CRISPR-Cas system is the presence of spacers that are complementary to bacterial genes (Bolotin *et al.*, 2005; Horvath *et al.*, 2009; Mojica *et al.*, 2005; Shah *et al.*, 2009). This feature suggests the possibility of recognition and cleavage of self nucleic acids and, consequently, may be considered a form of autoimmunity (Stern *et al.*, 2010; van der Ploeg, 2009). However, it is worth noting that CRISPR-Cas systems containing self-targeting elements often lack some *cas* genes or are non-functional (Haft *et al.*, 2005; Stern *et al.*, 2010; van der Ploeg, 2009). None the less, the presence of autoimmunity within CRISPR-Cas systems does not exclude their regulatory roles, and alteration of *cas* gene expression in response to stress is a commonly observed phenomenon (Perez-Rodriguez *et al.*, 2011; Viswanathan *et al.*, 2007). There are also several examples of Cas proteins involved in the regulation of bacterial virulence. *Francisella novicida* utilizes a CRISPR-Cas system to evade recognition by host pattern recognition receptors (Sampson

et al., 2013); this is achieved by down-regulation of the mRNA coding for bacterial lipoprotein, a surface protein that is recognized by the host's Toll-like receptor-2. Down-regulation of the mRNA encoding bacterial lipoprotein weakens the Toll-like receptor-2 induced pro-inflammatory cytokine response. *Neisseria meningitides* and *Campylobacter jejuni* employ Cas9 for the modulation of virulence (Louwen *et al.*, 2013; Sampson *et al.*, 2013); however, in these species, the exact mechanism of action has not been deciphered fully. Furthermore, in *Legionella pneumophila*, Cas2 plays an important role in intracellular survival and replication in amoebae *via* an unidentified mechanism (Gunderson and Cianciotto, 2013).

CRISPR-Cas-based technology

The first practical application of CRISPR-Cas systems was typing of bacterial diversity (Groenen *et al.*, 1993; Kamerbeek *et al.*, 1997). Several typing methods were developed based on CRISPR locus size, spacer content of a given locus, or point mutations within specific spacer and/or repeat sequences (Shariat and Dudley, 2014). Increasing knowledge of the mechanisms of action of CRISPR-Cas opened new avenues for applications of these systems. It became clear that easily reprogrammable, precisely controllable, sequence-specific nucleic acid cleavage is useful for molecular biology-based studies. To date, the most well-developed methods are based on the type II CRISPR-Cas effector complex, mainly because of its simplicity, in that it consists of Cas9 and sgRNA only (Jinek *et al.*, 2012). In addition, DNA cleavage by Cas9 is very efficient (Gasiunas *et al.*, 2012), and target recognition can be programmed by exchanging the sgRNA guiding sequence (Jinek *et al.*, 2012). The limitation of the application of this effector complex for molecular biology studies is the requirement for a PAM sequence within the desired target.

Eukaryotic DNA repair mechanisms can be used in combination with the CRISPR-Cas9 system can be used as a genome editing tool. Introduction of a crRNA-tracrRNA-Cas9 unit into eukaryotic cells results in sequence-specific DNA cleavage, and the cleaved strands undergo repair by an endogenous mechanism in the cell. Homologous recombination or non-homologous end joining of previously cleaved DNA enables genome editing (Cong *et al.*, 2013; Jinek *et al.*, 2013; Mali *et al.*, 2013b). In addition to dsDNA cleavage, Cas9-based systems can also be used for other purposes, such as nicking or binding DNA, which can be achieved by introducing mutations within the active sites of the Cas9 nuclease domains (HNH and RuvC) (Mali *et al.*, 2013a). The advantage of nicking DNA over blunt cutting is the possibility to create defined overhangs, thereby enabling direction of the specific recombination event (Mali *et al.*, 2013a). Mutation of both the HNH and RuvC domains converts Cas9 into a RNA-guided dsDNA binding protein (dCas9), and programming dCas9 to bind to a specific promoter region can efficiently prevent transcription of a gene of interest (Bikard *et al.*, 2013).

The use of Cas9 fused with other proteins also enables its employment for other applications. When fused with an activator domain, dCas9 enhances transcription (Bikard *et al.*, 2013); for example, dCas9 fused with the ω subunit of bacterial RNA polymerase recruits other subunits of the polymerase (Opalka *et al.*, 2010). Furthermore, fusion of Cas9 with green fluorescent protein enables its use in live cell imaging (Chen *et al.*, 2013). It could be speculated that other CRISPR-Cas modules will be used in molecular biology applications in the future, such as targeting of RNA by type III-B systems.

Concluding remarks

Since its discovery, the CRISPR-Cas system has been an intriguing object of study. Before the identification of the functionality of this system, adaptive immunity was considered to be associated exclusively with eukaryotic organisms (Goren *et al.*, 2012). Adaptations of the CRISPR-Cas system in response to environmental conditions are hereditary; therefore, this system is a fine example of Lamarckian inheritance (Koonin and Wolf, 2009). Enhanced understanding of the mechanism of action of the CRISPR-Cas system enabled the development of new tools for genome engineering that are efficient alternatives to transcription activator-like effector nucleases (Boch *et al.*, 2009) and zinc-finger nucleases (Bibikova *et al.*, 2003). The CRISPR-Cas system was also used to build phage resistance in an industrial strain of *Streptococcus thermophiles* (Barrangou *et al.*, 2013). This application is of significant value to microorganism-based industries, such as the dairy and biopharmaceutical markets. Certainly, new CRISPR-Cas-based methods will be developed in the future. Despite intensive research during recent years, many questions concerning the mode of action and possible applications of the CRISPR-Cas system remain unanswered.

Acknowledgements

This work was supported by the grant from the National Science Centre, Poland (2011/01/D/NZ6/00269) to KP.

The Faculty of Biochemistry, Biophysics and Biotechnology of the Jagiellonian University is a beneficiary of the structural funds from the European Union (grant No: POIG.02.01.00-12-064/08 – "Molecular biotechnology for health").

Faculty of Biochemistry, Biophysics and Biotechnology is a partner of the Leading National Research Center (KNOW) supported by the Ministry of Science and Higher Education.

The funders had no role in study design, data collection and analysis, decision to publish, or preparation of the manuscript.

The authors declare that they have no competing interests.

Literature

Arslan Z., R.Wurm, O. Brener, P. Ellinger, L. Nagel-Steger, F. Oesterhelt, l. Schmitt, D. Willbold, R. Wagner, H. Gohlke H. and others. 2013. Double-strand DNA end-binding and sliding of the toroidal CRISPR-associated protein Csn2. *Nucleic Acids Res.* 41: 6347–6359.

Babu M., N. Beloglazova, R. Flick, C. Graham, T. Skarina, B. Nocek, A. Gagarinova, O. Pogoutse, G. Brown, A. Binkowski and others. 2011. A dual function of the CRISPR-Cas system in bacterial antivirus immunity and DNA repair. *Mol. Microbiol.* 79: 484–502.

Barrangou R., C. Fremaux, H. Deveau, M. Richards, P. Boyaval, S. Moineau, D.A. Romero and P. Horvath. 2007. CRISPR provides acquired resistance against viruses in prokaryotes. *Science* 315: 1709–1712.

Barrangou R., A.C. Coûté-Monvoisin, B. Stahl, I. Chavichvily, F. Damange, D.A. Romero, P. Boyaval, C. Fremaux and P. Horvath. 2013. Genomic impact of CRISPR immunization against bacteriophages. *Biochem. Soc. Trans.* 41: 1383–1391.

Beloglazova N., G. Brown, M.D. Zimmerman, M. Proudfoot, K.S. Makarova, M. Kudritska, S. Kochinyan, S. Wang, M. Chruszcz, W. Minor and others. 2008. A novel family of sequence-specific endoribonucleases associated with the clustered regularly interspaced short palindromic repeats. *J. Biol. Chem.* 283: 20361–20371.

Beloglazova N., P. Petit, R. Flick, G. Brown, A. Savchenko and A.F. Yakunin. 2011. Structure and activity of the Cas3 HD nuclease MJ0384, an effector enzyme of the CRISPR interference. *EMBO J.* 30: 4616–4627.

Bibikova M., K. Beumer, J.K. Trautman and D. Carroll. 2003. Enhancing gene targeting with designed zinc finger nucleases. *Science* 300: 764.

Bikard D., W. Jiang, P. Samai, A. Hochschild, F. Zhang and L.A. Marraffini. 2013. Programmable repression and activation of bacterial gene expression using an engineered CRISPR-Cas system. *Nucleic Acids Res.* 41: 7429–7437.

Boch J., H. Scholze, S. Schornack, A. Landgraf, S. Hahn, S. Kay, T. Lahaye, A. Nickstadt and U. Bonas. 2009. Breaking the code of DNA binding specificity of TAL-type III effectors. *Science* 326: 1509–1512.

Bolotin A., B. Quinquis, A. Sorokin and S.D. Ehrlich. 2005. Clustered regularly interspaced short palindrome repeats (CRISPRs) have spacers of extrachromosomal origin. *Microbiology* 151: 2551–2561.

Bondy-Denomy J., A. Pawluk, K.L. Maxwell and A.R. Davidson. 2013. Bacteriophage genes that inactivate the CRISPR/Cas bacterial immune system. *Nature* 493: 429–432.

Carte J., R. Wang, H.Li, R.M. Terns and M.P. Terns M.P. 2008. Cas6 is an endoribonuclease that generates guide RNAs for invader defense in prokaryotes. *Genes Dev.* 22: 3489–3496.

Carte J., N.T. Pfister, M.M. Compton, R.M. Terns and M.P. Terns. 2010. Binding and cleavage of CRISPR RNA by Cas6. *RNA* 16: 2181–2188.

Chen B., L.A. Gilbert, B.A. Cimini, J. Schnitzbauer, W. Zhang, G.W. Li, J. Park, E.H. Blackburn, J.S. Weissman, L.S. Qi and others. 2013. Dynamic imaging of genomic loci in living human cells by an optimized CRISPR/Cas system. *Cell* 155: 1479–1491.

Cong L., F.A. Ran, D. Cox, S. Lin, R. Barretto, N. Habib, P.D. Hsu, X. Wu, W. Jiang, L.A. Marraffini and others. 2013. Multiplex genome engineering using CRISPR/Cas systems. *Science* 339: 819–823.

Datsenko K.A., K. Pougach, A. Tikhonov, B.L. Wanner, K. Severinov and E. Semenova. 2012. Molecular memory of prior infections activates the CRISPR/Cas adaptive bacterial immunity system. *Nat. Commun.* 3: 945.

Deltcheva E., K. Chylinski, C.M. Sharma, K. Gonzales, Y. Chao, Z.A. Pirzada , M.R. Eckert, J. Vogel and E. Charpentier. 2011. CRISPR RNA maturation by trans-encoded small RNA and host factor RNase III. *Nature* 471: 602–607.

Deng L., R.A. Garrett, S.A. Shah, X. Peng and Q. She. 2013. A novel interference mechanism by a type IIIB CRISPR-Cmr module in *Sulfolobus*. *Mol. Microbiol.* 87: 1088–1099.

Deveau H., R. Barrangou, J.E. Garneau, J. Labonté, C. Fremaux, P. Boyaval, D.A. Romero, P. Horvath and S. Moineau. 2008. Phage response to CRISPR-encoded resistance in *Streptococcus thermophilus*. *J. Bacteriol.* 190: 1390–1400.

Díez-Villaseñor C., N.M. Guzmán, C. Almendros, J. García-Martínez and F.J. Mojica F.J. 2013. CRISPR-spacer integration reporter plasmids reveal distinct genuine acquisition specificities among CRISPR-Cas I-E variants of *Escherichia coli*. *RNA Biol.* 10: 792–802.

Dupuis M., M. Villion, A.H. Magadán and S. Moineau. 2013. CRISPR-Cas and restriction-modification systems are compatible and increase phage resistance. *Nat. Commun.* 4: 2087.

Fineran P.C., M.J. Gerritzen, M. Suárez-Diez, T. Künne, J. Boekhorst, S.A. van Hijum, R.H. Staals and S.J. Brouns. 2014. Degenerate target sites mediate rapid primed CRISPR adaptation. *Proc. Natl. Acad. Sci. USA* 111: E1629–1638.

Garside E.L., M.J. Schellenberg, E.M. Gesner, J.B. Bonanno, J.M. Sauder, S.K. Burley, S.C. Almo, G. Mehta and A.M. MacMillan. 2012. Cas5d processes pre-crRNA and is a member of a larger family of CRISPR RNA endonucleases. *RNA* 18: 2020–2028.

Gasiunas G., R. Barrangou, P. Horvath and V. Siksnys. 2012. Cas9-crRNA ribonucleoprotein complex mediates specific DNA cleavage for adaptive immunity in bacteria. *Proc. Natl. Acad. Sci. USA* 109: E2579–2586.

Gasiunas G., T. Sinkunas and V. Siksnys. 2014. Molecular mechanisms of CRISPR-mediated microbial immunity. *Cell Mol. Life Sci.* 71: 449–465.

Godde J.S. and A. Bickerton. 2006. The repetitive DNA elements called CRISPRs and their associated genes: evidence of horizontal transfer among prokaryotes. *J. Mol. Evol.* 62: 718–729.

Goren M., I. Yosef, R. Edgar and U. Qimron. 2012. The bacterial CRISPR/Cas system as analog of the mammalian adaptive immune system. *RNA Biol.* 9: 549–554.

Groenen P.M., A.E. Bunschoten, D. van Soolingen and J.D. van Embden. 1993. Nature of DNA polymorphism in the direct repeat cluster of *Mycobacterium tuberculosis*; application for strain differentiation by a novel typing method. *Mol. Microbiol.* 10: 1057–1065.

Gunderson F.F. and N.P. Cianciotto. 2013. The CRISPR-associated gene cas2 of *Legionella pneumophila* is required for intracellular infection of amoebae. *MBio.* 4: e00074–00013.

Haft D.H., J. Selengut, E.F. Mongodin and K.E. Nelson. 2005. A guild of 45 CRISPR-associated (Cas) protein families and multiple CRISPR/Cas subtypes exist in prokaryotic genomes. *PLoS Comput Biol* 1: e60.

Hale C.R., P. Zhao, S. Olson, M.O. Duff, B.R. Graveley, L. Wells, R.M. Terns and M.P. Terns. 2009. RNA-guided RNA cleavage by a CRISPR RNA-Cas protein complex. *Cell* 139: 945–956.

Hale C.R., S. Majumdar, J. Elmore, N. Pfister, M. Compton, S. Olson, A.M. Resch, C.V. Glover, B.R. Graveley, R.M. Terns and others. 2012. Essential features and rational design of CRISPR RNAs that function with the Cas RAMP module complex to cleave RNAs. *Mol. Cell* 45: 292–302.

Hatoum-Aslan A., I. Maniv and L.A. Marraffini. 2011. Mature clustered, regularly interspaced, short palindromic repeats RNA (crRNA) length is measured by a ruler mechanism anchored at the precursor processing site. *Proc. Natl. Acad. Sci. USA* 108: 21218–21222.

Hatoum–Aslan A., I. Maniv, P. Samai and L.A. Marraffini. 2014. Genetic characterization of antiplasmid immunity through a type III–A CRISPR–Cas system. *J. Bacteriol.* 196: 310–317.

Held N.L., A. Herrera and R.J. Whitaker. 2013. Reassortment of CRISPR repeat-spacer loci in *Sulfolobus islandicus*. *Environ. Microbiol.* 15: 3065–3076.

Heler R., L.A. Marraffini and D. Bikard. 2014. Adapting to new threats: the generation of memory by CRISPR-Cas immune systems. *Mol. Microbiol.* 93: 1–9.

Horvath P., A.C. Coûté-Monvoisin, D.A. Romero, P. Boyaval, C. Fremaux and R. Barrangou. 2009. Comparative analysis of CRISPR loci in lactic acid bacteria genomes. *Int. J. Food Microbiol.* 131: 62–70.

Hrle A., L.K. Maier, K. Sharma, J. Ebert, C. Basquin, H. Urlaub, A. Marchfelder and E. Conti. 2014. Structural analyses of the CRISPR protein Csc2 reveal the RNA-binding interface of the type I-D Cas7 family. *RNA Biol.* 11(8): 1072–1082.

Ishino Y., H. Shinagawa, K. Makino, M. Amemura and A. Nakata. 1987. Nucleotide sequence of the *iap* gene, responsible for alkaline phosphatase isozyme conversion in *Escherichia coli*, and identification of the gene product. *J. Bacteriol.* 169: 5429–5433.

Jackson R.N., M. Lavin, J. Carter and B. Wiedenheft. 2014. Fitting CRISPR-associated Cas3 into the helicase family tree. *Curr. Opin. Struct. Biol.* 24: 106–114.

Jansen R., J.D. Embden, W. Gaastra and L.M. Schouls. 2002. Identification of genes that are associated with DNA repeats in prokaryotes. *Mol. Microbiol.* 43: 1565–1575.

Jiang W., D.Bikard, D. Cox, F. Zhang and L.A. Marraffini. 2013. RNA-guided editing of bacterial genomes using CRISPR-Cas systems. *Nat. Biotechnol.* 31: 233–239.

Jinek M., K. Chylinski, I. Fonfara, M. Hauer, J.A. Doudna and E. Charpentier. 2012. A programmable dual-RNA-guided DNA endonuclease in adaptive bacterial immunity. *Science* 337: 816–821.

Jinek M., A. East, A. Cheng, S. Lin, E. Ma and J. Doudna. 2013. RNA-programmed genome editing in human cells. *Elife* 2: e00471.

Jinek M., F. Jiang, D.W. Taylor, S.H. Sternberg, E. Kaya, E. Ma, C. Anders , M. Hauer, K. Zhou, S. Lin and others. 2014. Structures of Cas9 endonucleases reveal RNA-mediated conformational activation. *Science* 343: 1247997.

Jore M.M., M. Lundgren, E. van Duijn, J.B. Bultema, E.R. Westra, S.P. Waghmare, B. Wiedenheft, U. Pul, R. Wurm, R. Wagner and others. 2011. Structural basis for CRISPR RNA-guided DNA recognition by Cascade. *Nat. Struct. Mol. Biol.* 18: 529–536.

Kamerbeek J., L. Schouls, A. Kolk, M. van Agterveld, D. van Soolingen, S. Kuijper , A. Bunschoten, H. Molhuizen, R. Shaw, M. Goyal and others. 1997. Simultaneous detection and strain differentiation of *Mycobacterium tuberculosis* for diagnosis and epidemiology. *J. Clin. Microbiol.* 35: 907–914.

Koonin E.V. and Y.I. Wolf. 2009. Is evolution Darwinian or/and Lamarckian? *Biol. Direct.* 4: 42.

Kunin V., R.Sorek and P. Hugenholtz. 2007. Evolutionary conservation of sequence and secondary structures in CRISPR repeats. *Genome Biol.* 8: R61.

Künne T., D.C. Swarts and S.J. Brouns. 2014. Planting the seed: target recognition of short guide RNAs. *Trends Microbiol.* 22: 74–83.

Li M., R. Wang, D. Zhao and H. Xiang. 2014. Adaptation of the *Haloarcula hispanica* CRISPR-Cas system to a purified virus strictly requires a priming process. *Nucleic Acids Res.* 42: 2483–2492.

Louwen R., D. Horst-Kreft, A.G. de Boer, L. van der Graaf, G. de Knegt, M. Hamersma, A.P. Heikema, A.R. Timms, B.C. Jacobs, J.A. Wagenaar and others. 2013. A novel link between *Campylobacter jejuni* bacteriophage defence, virulence and Guillain-Barré syndrome. *Eur. J. Clin. Microbiol. Infect. Dis* 32: 207–226.

Louwen R., R.H. Staals, H.P. Endtz, P. van Baarlen and J. van der Oost. 2014. The role of CRISPR-Cas systems in virulence of pathogenic bacteria. *Microbiol. Mol. Biol. Rev.* 78: 74–88.

Makarova K.S., L. Aravind, N.V. Grishin, I.B. Rogozin and E.V. Koonin. 2002. A DNA repair system specific for thermophilic Archaea and bacteria predicted by genomic context analysis. *Nucleic. Acids. Res.* 30: 482–496.

Makarova K.S.,N.V. Grishin, S.A. Shabalina, Y.I. Wolf and E.V. Koonin. 2006. A putative RNA-interference-based immune system in prokaryotes: computational analysis of the predicted enzymatic machinery, functional analogies with eukaryotic RNAi, and hypothetical mechanisms of action. *Biol. Direct.* 1: 7.

Makarova K.S., D.H. Haft, R. Barrangou, S.J. Brouns, E. Charpentier, P. Horvath, S. Moineau, F.J. Mojica, Y.I. Wolf, A.F. Yakunin and others. 2011. Evolution and classification of the CRISPR-Cas systems. *Nat. Rev. Microbiol.* 9: 467–477.

Mali P., K.M. Esvelt and G.M. Church. 2013a. Cas9 as a versatile tool for engineering biology. *Nat. Methods* 10: 957–963.

Mali P., L. Yang, K.M. Esvelt, J.Aach, M. Guell, J.E. DiCarlo, J.E. Norville and G.M. Church. 2013b. RNA-guided human genome engineering via Cas9. *Science* 339: 823–826.

Marraffini L.A. and E.J. Sontheimer. 2008. CRISPR interference limits horizontal gene transfer in staphylococci by targeting DNA. *Science* 322: 1843–1845.

Marraffini L.A. and E.J. Sontheimer. 2010. Self versus non-self discrimination during CRISPR RNA-directed immunity. *Nature* 463: 568–571.

Mojica F.J., C. Ferrer, G. Juez and F. Rodríguez-Valera. 1995. Long stretches of short tandem repeats are present in the largest replicons of the Archaea *Haloferax mediterranei* and *Haloferax volcani*i and could be involved in replicon partitioning. *Mol. Microbiol.* 17: 85–93.

Mojica F.J., C. Díez-Villaseñor, J. García-Martínez and E. Soria E. 2005. Intervening sequences of regularly spaced prokaryotic repeats derive from foreign genetic elements. *J. Mol. Evol.* 60: 174–182.

Mojica F.J., C. Díez-Villaseñor, J. García-Martínez and C. Almendros. 2009. Short motif sequences determine the targets of the prokaryotic CRISPR defence system. *Microbiology* 155: 733–740.

Mulepati S. and S. Bailey. 2011. Structural and biochemical analysis of nuclease domain of clustered regularly interspaced short palindromic repeat (CRISPR)-associated protein 3 (Cas3). *J. Biol. Chem.* 286: 31896–31903.

Nam K.H., F. Ding, C. Haitjema, Q. Huang, M.P. DeLisa and A. Ke. 2012a. Double-stranded endonuclease activity in *Bacillus halodurans* clustered regularly interspaced short palindromic repeats (CRISPR)-associated Cas2 protein. *J. Biol. Chem.* 287: 35943–35952.

Nam K.H., C. Haitjema, X. Liu, F. Ding, H. Wang, M.P. DeLisa and A. Ke. 2012b. Cas5d protein processes pre-crRNA and assembles into a cascade-like interference complex in subtype I-C/Dvulg CRISPR-Cas system. *Structure* 20: 1574–1584.

Niewoehner O., M. Jinek and J.A. Doudna. 2014. Evolution of CRISPR RNA recognition and processing by Cas6 endonucleases. *Nucleic Acids Res.* 42: 1341–1353.

Nishimasu H., F.A. Ran, P.D. Hsu, S. Konermann, S.I. Shehata, N. Dohmae, R. Ishitani, F. Zhang and O. Nureki. 2014. Crystal structure of Cas9 in complex with guide RNA and target DNA. *Cell* 156: 935–949.

Opalka N., J. Brown, W.J. Lane, K.A. Twist, R. Landick, F.J. Asturias and S.A. Darst. 2010. Complete structural model of *Escherichia coli* RNA polymerase from a hybrid approach. *PLoS Biol* 8: e1000483

Perez-Rodriguez R., C. Haitjema, Q.Huang, K.H. Nam, S. Bernardis, A. Ke. and M.P. De Lisa. 2011. Envelope stress is a trigger of CRISPR RNA-mediated DNA silencing in *Escherichia coli*. *Mol. Microbiol.* 79: 584–599.

Pourcel C.,G. Salvignol and G. Vergnaud. 2005. CRISPR elements in *Yersinia pestis* acquire new repeats by preferential uptake of bacteriophage DNA, and provide additional tools for evolutionary studies. *Microbiology* 151: 653–663.

Reeks J., J. Naismith and M.F. White. 2013. CRISPR interference: a structural perspective. *Biochem. J.* 453: 155–166.

Rouillon C., M.Zhou, J. Zhang, A. Politis, V. Beilsten-Edmands, G. Cannone G., S. Graham, C.V. Robinson, L. Spagnolo and M.F. White. 2013. Structure of the CRISPR interference complex CSM reveals key similarities with cascade. *Mol. Cell* 52: 124–134.

Sampson T.R., S.D. Saroj, A.C. Llewellyn, Y.L. Tzeng and D.S. Weiss. 2013. A CRISPR/Cas system mediates bacterial innate immune evasion and virulence. *Nature* 497: 254–257.

Samson J.E., A.H. Magadán, M. Sabri and S. Moineau. 2013. Revenge of the phages: defeating bacterial defences. *Nat. Rev. Microbiol.* 11: 675–687.

Sashital D.G., B. Wiedenheft and J.A. Doudna. 2012. Mechanism of foreign DNA selection in a bacterial adaptive immune system. *Mol. Cell* 46: 606–615.

Scholz I., S.J. Lange, S. Hein, W.R. Hess and R. Backofen. 2013. CRISPR-Cas systems in the cyanobacterium *Synechocystis* sp. PCC6803 exhibit distinct processing pathways involving at least two Cas6 and a Cmr2 protein. *PLoS One* 8: e56470.

Semenova E., M. Nagornykh, M. Pyatnitskiy, I.I. Artamonova and K. Severinov. 2009. Analysis of CRISPR system function in plant pathogen *Xanthomonas oryzae*. *FEMS Microbiol Lett* 296: 110–116.

Semenova E., M.M. Jore, K.A. Datsenko, A. Semenova, E.R. Westra, B. Wanner, J. van der Oost, S.J. Brouns and K. Severinov. 2011. Interference by clustered regularly interspaced short palindromic repeat (CRISPR) RNA is governed by a seed sequence. *Proc. Natl. Acad. Sci. USA* 108: 10098–10103.

Shah S.A., N.R. Hansen and R.A. Garrett. 2009. Distribution of CRISPR spacer matches in viruses and plasmids of crenarchaeal acidothermophiles and implications for their inhibitory mechanism. *Biochem. Soc. Trans.* 37: 23–28.

Shariat N. and E.G. Dudley. 2014. CRISPRs: molecular signatures used for pathogen subtyping. *Appl. Environ. Microbiol.* 80: 430–439.

Sinkunas T., G. Gasiunas, S.P. Waghmare, M.J. Dickman, R. Barrangou, P. Horvath and V. Siksnys. 2013. In vitro reconstitution of Cascade-mediated CRISPR immunity in *Streptococcus thermophilus*. *EMBO J.* 32: 385–394.

Sorek R., V. Kunin and P. Hugenholtz. 2008. CRISPR--a widespread system that provides acquired resistance against phages in bacteria and archaea. *Nat. Rev. Microbiol.* 6: 181–186.

Sorek R., C.M. Lawrence and B. Wiedenheft. 2013. CRISPR-mediated adaptive immune systems in bacteria and archaea. *Ann. Rev. Biochem.* 82: 237–266.

Soutourina O.A., M. Monot, P. Boudry, L. Saujet, C. Pichon, O. Sismeiro, E. Semenova, K. Severinov, C. Le Bouguenec, J.Y. Coppée and others. 2013. Genome-wide identification of regulatory RNAs in the human pathogen *Clostridium difficile*. *PLoS Genet* 9: e1003493.

Spilman M., A. Cocozaki, C. Hale, Y. Shao, N. Ramia, R. Terns, M. Terns, H. Li and S. Stagg. 2013. Structure of an RNA silencing complex of the CRISPR-Cas immune system.

Staals R.H., Y. Agari, S. Maki-Yonekura, Y. Zhu, D.W. Taylor, E. van Duijn, A. Barendregt, M. Vlot, J.J. Koehorst, K. Sakamoto and others. 2013. Structure and activity of the RNA-targeting Type III-B CRISPR-Cas complex of *Thermus thermophilus*. *Mol. Cell* 52: 135–145.

Stern A., L. Keren, O. Wurtzel, G. Amitai and R. Sorek. 2010. Self-targeting by CRISPR: gene regulation or autoimmunity? *Trends Genet.* 26: 335–340.

Sternberg S.H., R.E. Haurwitz and J.A. Doudna. 2012. Mechanism of substrate selection by a highly specific CRISPR endoribonuclease. *RNA* 18: 661–672.

Sternberg S.H., S. Redding, M. Jinek, E.C. Greene and J.A. Doudna. 2014. DNA interrogation by the CRISPR RNA-guided endonuclease Cas9. *Nature* 507: 62–67.

Swarts D.C., C. Mosterd, M.W. van Passel and S.J. Brouns. 2012. CRISPR interference directs strand specific spacer acquisition. *PLoS One* 7: e35888.

van der Oost J., M.M. Jore, E.R. Westra, M. Lundgren and S.J. Brouns. 2009. CRISPR-based adaptive and heritable immunity in prokaryotes. *Trends Biochem. Sci.* 34: 401–407.

van der Ploeg J.R. 2009. Analysis of CRISPR in *Streptococcus mutans* suggests frequent occurrence of acquired immunity against infection by M102-like bacteriophages. *Microbiology* 155: 1966–1976.

van Duijn E., I.M. Barbu, A. Barendregt, M.M. Jore, B. Wiedenheft, M. Lundgren, E.R. Westra, S.J. Brouns, J.A. Doudna, J. van der Oost and others. 2012. Native tandem and ion mobility mass spectrometry highlight structural and modular similarities in clustered-regularly-interspaced shot-palindromic-repeats (CRISPR)-associated protein complexes from.

Vercoe R.B., J.T. Chang, R.L. Dy, C. Taylor, T. Gristwood, J.S. Clulow, C. Richter, R. Przybilski, A.R. Pitman and P.C. Fineran. 2013. Cytotoxic chromosomal targeting by CRISPR/Cas systems can reshape bacterial genomes and expel or remodel pathogenicity islands. *PLoS Genet* 9: e1003454.

Viswanathan P., K. Murphy, B. Julien, A.G. Garza and L. Kroos. 2007. Regulation of dev, an operon that includes genes essential for *Myxococcus xanthus* development and CRISPR-associated genes and repeats. *J. Bacteriol.* 189: 3738–3750.

Wang R., G. Preamplume, M.P. Terns, R.M. Terns and H. Li. 2011. Interaction of the Cas6 riboendonuclease with CRISPR RNAs: recognition and cleavage. *Structure* 19: 257–264.

Westra E.R., U. Pul, N. Heidrich, M.M. Jore, M. Lundgren, T. Stratmann, R. Wurm, A. Raine, M. Mescher, L. Van Heereveld and others. 2010. H-NS-mediated repression of CRISPR-based immunity in *Escherichia coli* K12 can be relieved by the transcription activator LeuO. *Mol. Microbiol.* 77: 1380–1393.

Westra E.R., P.B. van Erp, T. Künne, S.P. Wong, R.H. Staals, C.L. Seegers, S. Bollen, M.M. Jore, E. Semenova, K. Severinov and others. 2012. CRISPR immunity relies on the consecutive binding and degradation of negatively supercoiled invader DNA by Cascade and Cas3. *Mol. Cell* 46: 595–605.

Westra E.R., E. Semenova, K.A. Datsenko, R.N. Jackson, B. Wiedenheft, K. Severinov and S.J. Brouns. 2013. Type I-E CRISPR-cas systems discriminate target from non-target DNA through base pairing-independent PAM recognition. *PLoS Genet* 9: e1003742.

Wiedenheft B., G.C. Lander, K. Zhou, M.M. Jore, S.J. Brouns, J.van der Oost, J.A. Doudna and E. Nogales. 2011. Structures of the RNA-guided surveillance complex from a bacterial immune system. *Nature* 477: 486–489.

Wiedenheft B.,K. Zhou, M. Jinek, S.M. Coyle, W. Ma and J.A. Doudna. 2009. Structural basis for DNase activity of a conserved protein implicated in CRISPR-mediated genome defense. *Structure* 17: 904–912.

Wiedenheft B., S.H. Sternberg and J.A. Doudna. 2012. RNA-guided genetic silencing systems in bacteria and archaea. *Nature* 482: 331–338.

Yosef I., M.G. Goren and U. Qimron. 2012. Proteins and DNA elements essential for the CRISPR adaptation process in *Escherichia coli*. *Nucleic Acids Res* 40: 5569–5576.

Yosef I., D. Shitrit, M.G. Goren, D. Burstein, T. Pupko and U. Qimron. 2013. DNA motifs determining the efficiency of adaptation into the *Escherichia coli* CRISPR array. *Proc. Natl. Acad. Sci. USA* 110: 14396–14401.

Zhang J., T. Kasciukovic and M.F. White. 2012a. The CRISPR associated protein Cas4 Is a 5' to 3' DNA exonuclease with an iron-sulfur cluster. *PLoS One* 7: e47232.

Zhang J., C. Rouillon, M. Kerou, J. Reeks, K. Brugger, S. Graham, J. Reimann, G. Cannone, H. Liu, S.V. Albers and others. 2012b. Structure and mechanism of the CMR complex for CRISPR-mediated antiviral immunity. *Mol. Cell* 45: 303–313.

Zhang Y., N. Heidrich, B.J. Ampattu, C.W. Gunderson, H.S. Seifert, C. Schoen, J. Vogel and E.J. Sontheimer. 2013. Processing-independent CRISPR RNAs limit natural transformation in *Neisseria meningitidis*. *Mol. Cell* 50: 488–503.

Polish Journal of Microbiology
2015, Vol. 64, No 3, 203–210

ORIGINAL PAPER

Role of *SAP7-10* and Morphological Regulators (*EFG1*, *CPH1*) in *Candida albicans*' Hypha Formation and Adhesion to Colorectal Carcinoma Caco-2

MONIKA STANISZEWSKA[1]*, MAŁGORZATA BONDARYK[1], KAMIL ŻUKOWSKI[2] and MICHAŁ CHUDY[2]

[1] National Institute of Public Health-National Institute of Hygiene, Warsaw, Poland
[2] Faculty of Chemistry, Warsaw University of Technology, Warsaw, Poland

Submitted 16 August 2014, revised 25 January 2015, accepted 13 April 2015

Abstract

Secreted aspartic proteases (Saps) are considered as key virulence factors of *Candida albicans*. Hopefully our outlook will widen the knowledge of *SAP7*'s role in *C. albicans* pathogenesis. The goal of our study was to investigate *SAP7* expression during *C. albicans* adhesion to intestinal human cells. Another objective was to study the role of *SAP8-10* and transcriptional regulators: *EFG1* and *CPH1,* using the mutants: *Δsap*, *Δefg1*, *Δcph1* during growth on Caco-2 monolayer. *SAP7* expression was analyzed using real time RT-PCR; relative quantification was normalized against *ACT1* in cells after growth on Caco-2. Adherence assay of *C. albicans* to Caco-2 was performed in a 24-well-plate. The results proved that *SAP7* can play a role during the initial adaptation of *C. albicans* to intestinal tract and decreases over time. Up-regulation of *SAP7* occured in the absence of *SAP8* and *SAP10* (genetic alternations dependence). *SAP7* can be regulated by the morphogensis' regulators during *C. albicans* growth on epithelium. Adhesion of the mutants was indistinguishable from SC5314. The lack of neither *SAP8-10* nor *EFG1*/*CPH1* influences the adhesive behaviour of *C. albicans*. Deletion of *SAP8-10* resulted in no filamentation defects. The results help better understand the role of *SAP7* during adhesion and morphogenesis in *C. albicans*.

Key words: *Candida albicans*, adhesion, *SAP7* gene expression, secreted aspartyl proteinase Sap7-10, true hyphae

Introduction

The incidence and severity of candidiasis in immunocompromised or otherwise debilitated hosts, coupled with diagnostic difficulties and the high cost of treatment, have persuaded several investigators to focus on *Candida albicans* which is by far the most prevalent etiological agent of candidiasis. The most characteristic features of *C. albicans* are its extraordinary range of virulence factors, particularly adherence and spread on and/or through epithelial and endothelial tissues by inducing the filamentous growth and hyphal-associated aspartic proteases (Saps). Adherence to host tissues and morphological versatility are thought to be important in *C. albicans* virulence (Bertini *et al.*, 2013; Braga-Silva and Santos, 2011; Naglik *et al.*, 2011). *C. albicans* contains the hypha-associated genes: *EFG1* and *CPH1* that mediate adhesion of *C. albicans* to mucosal surfaces (Moazeni *et al.*, 2012; Lo *et al.*, 1997). Efg1 and Cph1 play a major role in promoting filamentous growth and regulate the expression of several genes with a crucial function in the invasion of host cells or in biofilm formation (Moazeni *et al.*, 2012; Staniszewska *et al.*, 2013). As adhesion and morphogenesis are crucial for the latter, it is fundamental to study the role of *EFG1* and *CPH1* associated with morphogenesis and adhesion during *C. albicans* epithelial cells colonization. The secreted aspartic protease (Sap) family encompasses at least ten members (Saps1-10) containing a signal peptide, which are secreted, except for Sap9 and Sap10 that remain bound to the cell wall. Individual *SAP* genes are expressed at various stages of the infection process (Correia *et al.*, 2010; Dalle *et al.*, 2010; Jackson *et al.*, 2007; Martin *et al.*, 2011; Pietrella *et al.*, 2013). Saps are characterized by a broad-spectrum proteolytic activity and virulence properties. Sap1-3 are active at acidic pH, whereas Sap4-6 are more active at neutral to slightly alkaline pH and are associated with hyphal growth (Aoki *et al.*, 2011; Cadicamo *et al.*, 2013; Naglik *et al.*, 2011). Saps directly attack and degrade host proteins that are involved in both innate as well as adaptive immunity (for example, complement, E-cadherin, histatins, antibodies),

* Corresponding author: M. Staniszewska, Independent Laboratory of Streptomyces and Fungi Imperfecti, National Institute of Public Health-National Institute of Hygiene, Warsaw, Poland; **e-mail: mstaniszewska@pzh.gov.pl**

and development of inflammations (Aoki *et al.*, 2011; Cassone and Cauda, 2012; Mayer *et al.*, 2013; Pietrella *et al.*, 2013). Although the combined role of Sap1-6 in virulence has now come into question, and the Sap9 and Sap10 isoenzymes' role in the cell surface integrity, cell separation, and adhesion, has been described (Albrecht *et al.*, 2006; Schild *et al.*, 2011), almost nothing is known of Sap7 and Sap8 competence (Taylor *et al.*, 2005). Therefore, we presented our outlook in the hope that it will lead to widening knowledge of the role of *SAP7-10* in *C. albicans* pathogenesis.

The goal of the present study was to investigate the aspartic protease *SAP7* gene expression during *C. albicans* adhesion to intestinal human cells. A further objective was to study the role of *SAP8-10* and of the transcriptional regulators: *EFG1* and *CPH1*, using the mutants: *Δsap*, *Δefg1*, *Δcph1* during growth on the Caco-2 monolayer. We tested the ability of the *Δsap8-10* mutants to form hyphae and to adhere to intestinal cells comparing them with the mutants: Δ*cph1* and *efg1* (attenuated in morphogenesis).

Experimental

Materials and Methods

Strains and Media. *C. albicans* strains used in the current study are listed in Table I (Lo *et al.*, 1997; Fonzi and Irwin, 1993; Gillum *et al.*, 1984; Liu *et al.*, 1994; Puri *et al.*, 2012; Schild *et al.*, 2011; Staniszewska, 2009). *C. albicans* (strain no 82) was isolated from blood samples from a patient treated for *Ependymoma anaplasticum* (Staniszewska, 2009; Staniszewska *et al.*, 2014a; 2014b). The clinical isolate had been previously identified according to colony colour on CHROMagar *Candida* medium and evaluated following API 20C AUX carbohydrate assimilation patterns (Staniszewska, 2009; Staniszewska *et al.*, 2012; Staniszewska *et al.*, 2014a; 2014b). Additionally, the identification procedure was confirmed with genetic methods using rDNA sequencing as previously described (Staniszewska, 2009; Staniszewska *et al.*, 2012; Staniszewska *et al.*, 2014b). All the strains used in the present study were stored on ceramic beads in Microbank tube (Prolab Diagnostics, Richmond Hill, ON, Canada) at –70°C. Prior to the respective examinations, routine culturing of strains for growth was conducted at 30°C for 18 h in YEPD (Ness *et al.*, 2010).

Cultivation and Infection of Caco-2 Cell Line (ATCC HTB27, LGC, Poland). Following the supplier's guidelines, monolayers of the colon adenocarcinoma derived cell line were cultured in the Eagle's Minimum Essential Medium (EMEM) containing 10% (v/v) FCS, 1mM pyruvic acid, without antibiotics or antifungal agents and maintained in a humidified incubator at 37°C in 5% (v/v) CO_2. For the experiment 1.2×10^5 of Caco-2 cells (/ml EMEM) were seeded into 24-well-plates (Corning, USA) and cultured up to 18 h. Next, after 18 h post seeding the Caco-2 monolayers

Table I
C. albicans strains used in this study

Strain	Parental strain	Relevant characteristics or genotype	Reference
Reference strains*			
SC5314	none	Prototrophic wild-type strain	(Gillum *et al.*, 1994)
CAI4	SC5314	*ura3Δ::imm434/ura3Δ::imm434*	(Fonzi and Irwin, 1993)
CAF2-1	SC5314	*ura3Δ::imm434/URA3*	(Fonzi and Irwin, 1993)
no 82	none	Prototrophic wild-type strain	(Staniszewska, 2009)
sap8Δ, sap9Δ, sap10 Δ and sap9/10 Δ mutants**			
Δsap8		*Δsap8::hisG/ Δsap8::hisG-URA3-hisG*	(Puri *et al.*, 2012)
Δsap9	CAI4	CAI4, *sap9Δ::hisG/sap9Δ::hisG* + pCIp10 (integration)	(Schild *et al.*, 2011)
Δsap10	CAI4	CAI4, *sap10Δ::hisG/sap10Δ::hisG* + pCIp10 (integration)	(Schild *et al.*, 2011)
Δsap9/10	CAI4	CAI4, *sap10Δ::hisG/sap10Δ::hisG sap9Δ::his/sap9Δ::hisG* + pCIp10 (integration)	(Schild *et al.*, 2011)
efg1Δ and *cph1Δ* mutants**			
Δcph1	CAI4	*ura3::1imm434/ura3::1imm434 cph1::hisG/cph1::hisG-URA3-hisG*	(Liu *et al.*, 1994)
Δcph1 (*CPH1*)	CAI4	*ura3::1imm434/ura3::1imm434 cph1::hisG/cph1::hisG(CPH1)*	(Lo *et al.*, 1997)
Δefg1	CAI4	*ura3::1imm434/ura3::1imm434 efg1::hisG/efg1::hisG-URA3-hisG*	(Lo *et al.*, 1997)
Δefg1 (*EFG1*)	CAI4	*ura3::1 imm434/ura3::1 imm434 efg1::hisG/efg1::hisG (EFG1)*	(Lo *et al.*, 1997)
Δcph1Δefg1 (*EFG1*)	CAI4	*ura3::1 imm434/ura3::1 imm434 cph1::hisG/cph1::hisG efg1::hisG/efg1::hisG (EFG1)*	(Lo *et al.*, 1997)

* apart from indicated features all strains are identical to their parental strain; ** full genotype

were inoculated with 10^5 log phase yeast cells (/ml EMEM) of *C. albicans* wild type and mutants. After 18 h of incubation the Caco-2 was lysed by adding sterile water resulting in recovery of *C. albicans* cells.

RNA Isolation, cDNA preparation and quantification. Total RNA from *C. albicans* cells was extracted as described by Amberg *et al.* (2005). Prior to further examinations *C. albicans* total RNA was stored at –20°C. RNA was reverse transcribed into first-strand cDNA using the Enhanced Avian HS RT-PCR kit (Sigma-Aldrich, USA) according to the manufacturer's instructions. Briefly, total reaction volume (10 µl) contained 1 µl of total RNA, and 1 µl of oligo $(dT)_{23}$ (3.5 µM), and 1 µl of dNTP mix (500 µM each dNTP), and 7 µl of water (nuclease-free) was prepared. Incubation step was carried out at 50°C for 10 min. Then subsequently, the remaining components: 1 µl of Enhanced avian AMV-RT (1 U/µl), 1 µl of 10 × buffer for AMV-RT, 8 µl of water (nuclease-free) were added to obtain 20 µl of final volume. The RT reaction was carried out at 50°C for 50 min. cDNA was quantified using the QuantiTect Taq-Man probe RT-PCR kit (Qiagen, Germany) according to the manufacturer's instructions. Appropriate Taq-Man primer and probe sets for *SAP7* (*SAP7-1* 5'-ATGGACACAGTGTGAAATATGAAGTG-3'; *SAP7-2* 5'-TCAGTGGAGGATGGACCATTAGA-3') and *ACT1* (ACT-1 5'-GACAATTTCTCTTTCAGCACTAGTAGTGA-3'; ACT-2 5'-GCTGGTAGAGACTTGACCAACCA-3') were designed as described previously by Naglik *et al.* (2008). For the real time RT-PCR analysis each reaction mixture contained 1 × RT-PCR buffer, 4 mM $MgCl_2$, 250 nM forward and reverse primer, 200 nM Taq-Man probe, HotStarTaq DNA polymerase, and template RNA (Naglik *et al.*, 2008). To validate our normalization we determined differences in the *SAP7* expression levels between *C. albicans* cells grown for 3 h and 18 h respectively on the Caco-2 cell line. Moreover, for reliable normalization of the *SAP7* gene expression data in *C. albicans* cells grown for 3 h and 18 h respectively we used the housekeeping gene *ACT1* as a reference gene. The real time RT-PCR reactions were performed as described previously by Naglik *et al.* (2008): at 95°C for 15 min, followed by 45 cycles of 15 s at 94°C and 1 min at 60°C with the LightCycler® 96 (Roche Diagnostics GmbH, Germany). The C_T values were provided from real time RT-PCR instrumentation and were imported into a spreadsheet Microsoft Excel 2010. The relative quantification was calculated using Eq. (Livak and Schmittgen, 2001), where

$$\Delta C_T = \text{Avg. } SAP7\ C_T - \text{Avg. } ACT1\ C_T;$$
$$\Delta\Delta C_T = \Delta C_T - \Delta C_{T\ \text{parental strain}} = 2^{-\Delta\Delta CT}.$$

Assay of adherence to human line Caco-2 epithelial cells. Adherence of *C. albicans* to the Caco-2 cell line (ATCC HTB-37™) was performed as described previously Hashash *et al.* (2011). Briefly, the Caco-2 cell line was cultivated in the EMEM containing 10% (v/v) FCS at 37°C at 5% (v/v) CO_2. After trypsinisation, with the use of 0.25% trypsin (Biomed-Lublin, Lublin, Poland) 1.2×10^5 Caco-2 cells (/ml EMEM) were incubated for at least 16 h on a 24-well-plate (Costar, Corning, NY, USA) to generate a confluent layer. Subsequently, the blastoconidia were grown overnight in the YEPD medium at 30°C. Then, 10^4 blastoconidial cells (/ml saline) were added to each well of the epithelial cells to be afterwards incubated for 90 min (adhesion phase). Next, the non-adherent cells were removed by standard rinsing, and the wells were overlaid with Sabouraud dextrose agar and allowed to solidify. After 18 h growth at 37°C, the number of adherent cells was determined by colony counting and compared with the controls on the Sabouraud dextrose agar plates. Adherence was expressed as a percentage of the total number of cells added (control cells).

Microscopy. The morphological transition from yeast-to-hyphal cells was performed by using LEXT 3D Measuring LASER Microscope OLS4000 (Olympus, USA) and Scanning Electron Tabletop Microscope TM 100 (Hitachi, Japan). Briefly, Caco-2 cells grown on 12 mm glass coverslips were inoculated for 21 days post seeding with 10^4 log phase yeast cells (/ml saline) of strains tested. After 90-min incubation at 37°C, the cells were washed three times with PBS to remove non-adherent yeast and then fixed in 2% glutaraldehyde for 10 min.

Statistical analysis. Each experiment was performed in triplicate on three separate occasions. The percentage of cell adhesion and the *SAP7* expression were formulated as a mean ± standard deviation. Statistical differences were evaluated through comparison with the Wilcoxon test, P values ≤ 0.05 were considered significant. Based on recently published data (Naglik *et al.*, 2008; Staniszewska *et al.*, 2014a), the latter method was used to calculate statistical differences between relative gene expression and cell adhesion.

Results

The *SAP7* gene expression during adhesion to the Caco-2 mMonolayer. The level of *SAP7* transcript normalized to the transcription of *ACT1* is presented in Table II. The expression of the *SAP7* gene in the cells of the parental strain CAF2-1 and Δ*sap8* decreased 1.7- and 1.3-fold respectively after 18-h growth on Caco-2. Conversely, in the cells of Δ*sap8*, *SAP7* mRNA increased 3.6- and 4.8-fold after 3-h and 18-h growth on the intestinal cells respectively compared to the parental strain CAF2-1. Moreover, the expression of *SAP7* decreased 2.3- and 1.1-fold in the cells of Δ*sap9*,

Table II
Analysis of the *SAP7* gene relative expression compared to the *ACT1* reference gene in *C. albicans* cells. The cells were grown on Caco-2 cell line at 37°C

C. albicans	$\Delta C_{(t)}$		$2^{-rrC(t)}$	
	3 h	18 h	3 h	18 h
SC5314	–0.07 ± 0.92	0.05 ± 1.15	[1]	[1]
CAF2-1	–0.53 ± 0.54	–1.23 ± 0.74	1.02 ± 0.63	0.60 ± 0.40
CAI4	–1.61 ± 0.40	–1.60 ± 1.20	1.10 ± 1.30	0.43 ± 0.35
Δ*cph1*	2.04 ± 0.60	0.90 ± 0.15	2.53 ± 1.40	1.10 ± 0.52
Δ*efg1*	–0.43 ± 1.02	–1.24 ± 0.11	0.73 ± 0.24	0.85 ± 0.23
Δ*sap8*	0.90 ± 1.75	0.50 ± 1.22	3.70 ± 3.00	2.90 ± 3.02
Δ*sap9*	–1.44 ± 2.44	–0.36 ± 1.34	1.48 ± 2.35	0.63 ± 0.48
Δ*sap10*	–3.03 ± 7.43	–0.29 ± 2.03	1.70 ± 1.60	1.68 ± 1.10
Δ*sap9/10*	–0.85 ± 2.40	–0.21 ± 1.45	1.45 ± 1.23	1.34 ± 1.50

$C_{(t)}$ – mean for three independent experiment ± SD; [1] strain SC5314 – calibrator in $2^{-\Delta\Delta C(t)}$

and Δ*sap9-10* respectively after 18-h growth on Caco-2. On the other hand, the *SAP7* mRNA slightly increased 1.1-fold in the null Δ*sap10* mutant. In the cells of the parental strain CAI4, *SAP7* decreased 2.5-fold after 18-h growth on Caco-2. After 3-h growth on Caco-2, *SAP7* was up-regulated in Δ*sap9*, Δ*sap10*, and Δ*sap9-10* (1.3-, 1.5- and 1.3-fold as compared respectively to the parental strain CAI4). After 18-h growth, *SAP7* was up-regulated in Δ*sap9*, Δ*sap10*, and Δ*sap9-10* (1.4-, 3.9-, and 3.1-fold as compared respectively to the parental strain CAI4). We showed that after 18-h growth, Δ*cph1* cells showed *SAP7* decreased 2.3-fold, while Δ*efg1* displayed a slight up-regulation of this gene (1.2-fold). The expression of *SAP7* on the line Caco-2 at 3 h post-inoculation was higher than in 18-h grown cells. The obtained results proved that *SAP7* can play a role during the initial adaptation of *C. albicans* to the intestinal tract and that it decreases over time.

Determination of *C. albicans* adhesion to Caco-2 monolayer. To study whether the genetic alternations found in *SAP* and *EFG1* and *CPH1* genes could have an impact on *in vitro* virulence, we investigated the adherence of the *C. albicans* null mutants in a model of epithelial cells, and compared them with that of the wild type strains: SC5314 and no 82 as well as the rescued strains. As depicted in Table III, the adherence ability varied within each species with the values from 0.533 ± 0.321 to 11.3 ± 10.324 for the wild type strains: SC5314 and no 82, and from 0.68 ± 0.593 to 11.8 ± 7.532 for the mutants. A significant trend toward an affected adhesion of morphogenesis mutants was noted by comparison with the wild type isolate no 82 ($P \leq 0.05$). Our results demonstrated that lack of Cph1 protein influence significant reduction in their adhesive ability ($P \leq 0.05$) compared to the wild type strain no 82. With *Δcph1* adhesion was significantly lower (16.6-fold) than with *Δefg1* (2.1-fold) compared to the wild type strain no 82. In opposition, the SC5314 and *Δcph1* strains showed almost similar adhesion, whereas *Δefg1* revealed 9.85-fold increase in adhesive mode compared to the parental strain (SC5314). In this particular case of *Δcph1*, reintroduction of the one copy of *CPH1* restored adhesion. Thus the presence or absence of *CPH1* affected the adhesiveness behaviour of *C. albicans* cells.

The adhesion properties depended on the morphogenesis mutants (compared to the wild type strain 82) while for the mutants *Δsap9* and *Δsap10* almost the same level of adhesion was observed ($P \geq 0.05$). Moreover, the mutant *Δsap8* adhered less efficiently to epithelial cells (6.2-fold reduction) compared to strain no 82. In the case of the *Δsap8* mutant, adhesion of the latter strain was reduced to statistically significant levels ($P \leq 0.05$). Moreover, when strain SC5314 was analyzed, there were no detectable differences in its percentage of adhesion in comparison to the mutants ($P \geq 0.05$,

Table III
Adherence of *C. albicans* morphologies in an *in vitro* model of intestinal candidiasis (monolayer of Caco-2 cell line ATCC). Data are expressed as the mean ± SD of three independent experiments

Strains 10^6 cells (ml saline)$^{-1}$	Percentage of cells adhesion
SC5314	0.533 ± 0.321
no 82	11.30 ± 10.32
Δsap8	**1.83 ± 1.55**
Δsap9	9.92 ± 8.10
Δsap10	11.80 ± 7.53
Δcph1	**0.68 ± 0.59**
Δcph1 (*CPH1*)	**2.60 ± 1.84**
Δefg1	**5.25 ± 6.72**
Δefg1 (*EFG1*)	**1.01 ± 1.11**
Δcph1Δefg1 (*EFG1*)	**1.45 ± 0.35**

Significant reduction of adhesive properties ($P \leq 0.05$) in bold (compared to the wild type strain no 82)

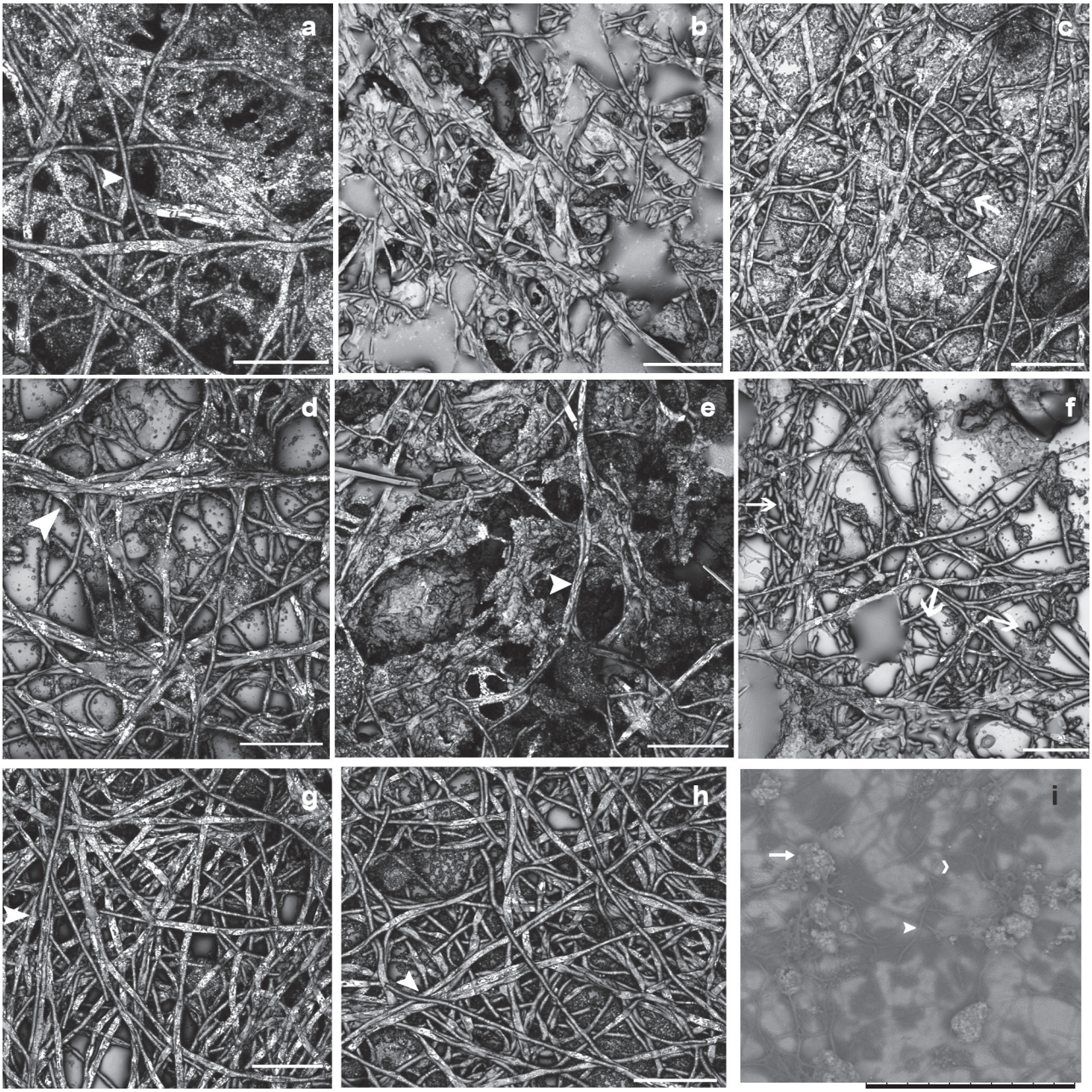

Fig. 1. Microscopic view of *C. albicans* strains hyphae production after 90-min incubation on Caco-2 monolayer at 35°C (5% CO_2).

(a) SC5314 presents true hyphal forms on the cell line surface (arrowhead). (b) The double Δ*cph1*/Δ*efg1* mutant containing an integrated copy of *EFG1* and (c) the Δ*efg1* mutant with one copy of *EFG1* display abundant true hyphae formation (arrowhead). In the case of the latter elongated blastoconidial cells can be seen (open arrow). (d) The Δ*cph1* mutant and (e) The Δ*cph1* strain reintroduced with one copy of *CPH1* show true hypha formation (arrowheads). (f) The Δ*efg1* mutant displays true hyphal forms and abnormally elongated blastoconidia (open arrows). (g) The strains: Δ*sap9* and (h) Δ*sap10* as well as (i) Δ*sap8*, display abundant hyphae formation (arrowheads) as well as conglomerate of morphologies (arrow) on enterocyte monolayer (open arrowhead). (a-h) Cells were imaged using LEXT 3D Measuring LASER Microscope OLS4000, bars 20 μm. (i) Cells were imaged using Scanning Electron Microscope TM100, bar 100 μm

Table III). In this regard, all the tested *C. albicans* strains were able to adhere to the epithelial cell line to a different degree.

***C. albicans* morphology on the intestinal Caco-2 monolayer.** Electron microscope studies revealed a, clearly reduced capacity of hyphal growth of the mutant *Δefg1* in comparison with the wild type strain SC5314 on enterocyte monolayer (Fig. 1). As shown microscope micrographs, following an 90-min attachment phase of yeast cells, we observed that all fungal strains had switched to hyphal growth form. The Δ*efg1* mutant latter strain showed morphologies tended to be slightly distorted compared to those of the wild type strain. Microscopically, no differences in the Δ*sap8-10* mutants' morphogenesis potential during adhesion to Caco-2 monolayer were observed after 90 min, indicating epithelial adherence and possibly cell proliferation.

Discussion

As far it is known (Cadicamo *et al.*, 2013; Correia *et al.*, 2010; Dalle *et al.*, 2010; Jackson *et al.*, 2007; Martin *et al.*, 2011; Naglik *et al.*, 2003; 2008; Taylor *et al.*, 2005), the increased expression of specific Saps at various stages of the infection plays a special role in tissue invasion. As the role of *SAP7* in *C. albicans* virulence had remained unknown, we showed in our study, that the level of the *SAP7* expression correlates with the importance of this gene for the early stage of the Caco-2 intestinal tissues invasion. It is worth noting, that differences in the *SAP7* expression between *C. albicans* cells colonizing Caco-2 depend on genetic alternations. These results showed clearly that the up-regulation of *SAP7* occurs in the absence of *SAP8* and *SAP10*. The compensation for the absence of Sap10 activity by Sap7 demonstrated their similar function. As showed Bocheńska *et al.* (2013) these two Saps out of 10 isoenzymes are unable to release bactericidal peptides from human Hb. As Sap10 participated in the processing of cell wall proteins (Schild *et al.*, 2011), the function of Sap7 was speculated and needed experimental verification. Our results perfectly agree with the previous study concerning Sap7 activity at neutral pH. We demonstrated (Staniszewska *et al.*, 2014a) that *SAP7* may help the fungus to cause systemic infections. We also showed that morphogenesis factors can be regulators of *SAP7* at early stage of epithelial infection. As desribed Pierce and Kumamoto (2012), Efg1 is a transcritional regulator of a large number of genes and many differences in the gene expression are suspected to occur in response to changes in the *EFG1* expression. Moreover, according to the latter authors, in the human gastrointestinal (GI) tract, wild type cells and cells with low Efg1 activity are expected to express factors that allow them to interact with host epithelial cells. We proposed that the *SAP7* activity provides a mechanism which allows the colonizing of human cells. As showed Nobile *et al.* (2012) *C. albicans* is one of the very few fungal species that can efficiently form biofilms in healthy mammalian cells. Following Nobile *et al.* (2012), we suggested that *SAP7* is involved in the biofilm network in *C. albicans* as a 'young' gene engaged in an early organisation of biofilm (adhesion to the intestinal monolayer). On the other hand, *C. albicans* hydrolytic enzymes might be regulated differently during various experiments and what is more, these genes' expression is strain-specific. Lermann and Morschhäuser (2008) showed that Saps are not required for the invasion of reconstituted human epithelia (RHE) by *C. albicans*. Therefore, environmental conditions have an important impact on the *SAP* expression pattern in *C. albicans*. Moreover, the proteinase encoded by the *SAP7* gene, if translated, may be associated with *C. albicans* early infection and is quite different from laboratory culture conditions (Cadicamo *et al.*, 2013; Taylor *et al.*, 2005).

C. albicans possesses a remarkable capacity to adhere to tissues (Dalle *et al.*, 2010; Yan *et al.*, 2013). Moreover, adhesion is influenced by enhanced expression and production of Saps (Albrecht *et al.*, 2006; Braga-Silva and Santos, 2011; Dalle *et al.*, 2010; Martin *et al.*, 2011; Seabra *et al.*, 2013). In our *in vitro* model of epithelial infection, Δ*sap8-10* and morphogenesis mutants displayed adherence to Caco-2 monolayer, where hyphae germinated. We characterized the morphology of the two morphogenesis mutants and four Δ*sap* compared to the wild type by CLSM, using the Caco-2 cell line. The strains proliferated, underwent morphogenesis and caused epithelial cells lysis. Although deletion of *CPH1* reduces hyphal growth on solid medium (Tsai *et al.*, 2013), we showed that it still forms hyphae during adhesion to a polarized monolayer of Caco-2 epithelial cells (Fig. 1). In stark contrast, *Δefg1* was slightly attenuated in developing filaments (Fig. 1). While, the extent of adhesion was strain-depended, a general trend was observed among all the strains tested, confirming a slightly reduced adhesion ability of the morphogenesis mutants, with *Δsap9* and *Δsap10* strongly adhering to the epithelial cells, followed by the wild type strain no 82 (Table III). Although, Cph1 appears to contribute to adhesion (*Δcph1* was reduced in this capacity, Table III), other factors, particularly agglutinin-like sequence (*ALS*) are the major contributor to epithelial cells adhesion (Tsai *et al.*, 2013). As discussed Brand (2012), deletion of one member of *SAP*s effected on the compensation of genes encoding surface proteins that are involved in adhesion i.e., *ALS3*, *HWP1*.

In our study, deletion of *SAP9* resulted in only slightly altered adhesion to Caco-2 compared to the wild type strains (Table III). To be more precise, *Δsap9* was more effective in adhesion than its parental strain SC5314. Strikingly, our data showed that adhesion activity of *Δsap10* was reduced in higher level compared to SC5314. We also found that strains were not adhesion activity correlated, pointing to a strain-dependent phenomenon rather than a significant association between Saps and adhesion. It was demonstrated that the ability of the mutants: Δ*sap,* Δ*efg1,* and Δ*cph1* to adhere to epithelial cells is not altered significantly compared with the wild types. Thus we suggested that a lack of morphogenesis factors as well as Δ*sap8-10* cannot be important for adhesion to the intestinal layer. Furthermore, deletion of the *SAP8-10* genes resulted in no filamentation defects; however these have not been reported to date. Overall, this analysis indicates that unlike SC5314, the significant differences in adhesion of Δ*sap*, Δ*efg1* and Δ*cph1* during the growth on Caco-2 relative to the clinical strain no 82 are not meaningful for this process if the strains genetic backgrounds are

too different. On the other hand, as reviewed by Naglik *et al.* (2011), Sap9 and Sap10 may indirectly contribute to adhesion by targeting covalently linked fungal cell wall proteins such as Cht2, Ywp1, Als2, Rhd3, Rbt5, Ecm33 and Pga4 and glucan cross-linking protein Pir1. Furthermore, the findings of Schild *et al.* (2011) on the *in vivo* expression profile of Saps1-6 supports a role of Sap1-3 in the adherence process to epithelial cells and Sap4 to Sap6 in assisting *C. albicans* cells to evade phagocytosis (Bertini *et al.*, 2013; Braga-Silva and Santos, 2011; Han *et al.*, 2011; Naglik *et al.*, 2011).

Conclusions. To our knowledge, ours is the first study of the role of *SAP7* in the early stage of the colorectal carcinoma Caco-2 invasion In order to benefit from these results in therapy (development of proper anti-fungal compounds or potentially effective combination vaccines including Sap7) additional *in vivo* experiments should be conducted.

Acknowledgements

The work was supported by the grant No DEC-2011/03/D/NZ7/06198 from National Science Center, Kraków, Poland. The authors would like to thank sincerely Prof. B. Hube for the strains CAF2-1, CAI4, *Δsap9*, *Δsap10*, *Δsap9-10*, *Δsap8*. We are extremely grateful to Professor Hsiu-Jung Lo from the National Health Research Institute in Zhunan (Taiwan) for providing us with the following strains: Can16, YLO323, HLC52, HLC74 and HLC84. We are very grateful to the Laboratory of Miniaturized Chemical System (Warsaw University of Technology) for access to confocal and electron microscopes.

Literature

Albrecht A., A. Felk, I. Pichova, J.R. Naglik, M. Schaller, P. de Groot, D. MacCallum, F.C. Odds, W. Schafer, F. Klis and others. 2006. Glycosylphosphatidylinositol-anchored proteases of *Candida albicans* target proteins necessary for both cellular processes and host-pathogen interactions. *J. Biol. Chem.* 281: 688–694.

Amberg D., D. Burke and J. Strathern. 2005. Yeast RNA isolations, Techniques and Protocols #6, pp. 127–131. In: Amberg D., D. Burke and J. Strathern (eds). *Methods in Yeast Genetics*. Cold Spring Harbor Laboratory Press, Cold Spring Harbor.

Aoki W., N. Kitahara, N. Miura, H. Morisaka, Y. Yamamoto, K. Kuroda and M. Ueda. 2011. Comprehensive characterization of secreted aspartic proteases encoded by a virulence gene family in *Candida albicans*. *J. Biochem.* 150: 431–438.

Bertini A., F. De Bernardis, L.A. Hensgens, S. Sandini, S. Senesi and A. Tavanti. 2013. Comparison of *Candida parapsilosis*, *Candida orthopsilosis*, and *Candida metapsilosis* adhesive properties and pathogenicity. *Int. J. Med. Microbiol.* 303: 98–103.

Bocheńska O., M. Rapala-Kozik, N. Wolak, G. Bras, A. Kozik, A. Dubin, W. Aoki, M. Ueda and P. Mak. 2013. Secreted aspartic peptidases of *Candida albicans* liberate bactericidal hemocidins from human hemoglobin. *Peptides* 48: 49–58.

Braga-Silva L.A. and A.L. Santos. 2011. Aspartic protease inhibitors as potential anti-*Candida albicans* drugs: impacts on fungal biology, virulence and pathogenesis. *Curr. Med. Chem.* 18: 2401–2419.

Brand A. 2012. Hyphal Growth in Human Fungal Pathogens and Its Role in Virulence. *Int. J. Microbiol.* 2012:517529.

Cadicamo C.D., J. Mortier, G. Wolber, M. Hell, I.E. Heinrich, D. Michel, L. Semlin, U. Berger, H.C. Korting, H.D. Holtje and others. 2013. Design, synthesis, inhibition studies, and molecular modeling of pepstatin analogues addressing different secreted aspartic proteinases of *Candida albicans*. *Biochem. Pharmacol.* 85: 881–887.

Cassone A. and R. Cauda. 2012. *Candida* and candidiasis in HIV-infected patients: where commensalism, opportunistic behavior and frank pathogenicity lose their borders. *Aids* 26: 1457–1472.

Correia A., U. Lermann, L. Teixeira, F. Cerca, S. Botelho, R.M. da Costa, P. Sampaio, F. Gartner, J. Morschhauser, M. Vilanova and others. 2010. Limited role of secreted aspartyl proteinases Sap1 to Sap6 in *Candida albicans* virulence and host immune response in murine hematogenously disseminated candidiasis. *Infect. Immun.* 78: 4839–4849.

Dalle F., B. Wachtler, C. L'Ollivier, G. Holland, N. Bannert, D. Wilson, C. Labruere, A. Bonnin and B. Hube. 2010. Cellular interactions of *Candida albicans* with human oral epithelial cells and enterocytes. *Cell Microbiol.* 12: 248–271.

Fonzi W.A. and M.Y. Irwin. 1993. Isogenic strain construction and gene mapping in *Candida albicans*. *Genetics* 134: 717–728.

Gillum A.M., E.Y. Tsay and D.R. Kirsch. 1984. Isolation of the *Candida albicans* gene for orotidine-5'-phosphate decarboxylase by complementation of *S. cerevisiae ura3* and *E. coli pyrF* mutations. *Mol. Gen. Genet.* 198: 179–182.

Han T.L., R.D. Cannon and S.G. Villas-Boas. 2011. The metabolic basis of *Candida albicans* morphogenesis and quorum sensing. *Fungal Genet. Biol.* 48: 747–763.

Hashash R., S. Younes, W. Bahnan, J. El Koussa, K. Maalouf, H.I. Dimassi and R.A. Khalaf. 2011. Characterisation of Pga1, a putative *Candida albicans* cell wall protein necessary for proper adhesion and biofilm formation. *Mycoses* 54: 491–500.

Jackson B.E., K.R. Wilhelmus and B. Hube. 2007. The role of secreted aspartyl proteinases in *Candida albicans* keratitis. *Invest. Ophthalmol. Vis. Sci.* 48: 3559–3565.

Lermann U. and J. Morschhäuser. 2008. Secreted aspartic proteases are not required for invasion of reconstituted human epithelia by *Candida albicans*. *Microbiology* 154: 3281–3295.

Liu H., J. Köhler and G.R. Fink. 1994. Suppression of hyphal formation in *Candida albicans* by mutation of a *STE12* homolog. *Science* 266: 1723–1726.

Livak K.J. and T.D. Schmittgen. 2001. Analysis of relative gene expression data using real time quantitative PCR and the 2(-Delta Delta C(T)) Method. *Methods* 25: 402–408.

Lo H.J., J.R. Kohler, B. DiDomenico, D. Loebenberg, A. Cacciapuoti and G.R. Fink. 1997. Non filamentous *C. albicans* mutants are avirulent. *Cell* 90: 939–949.

Martin R., B. Wachtler, M. Schaller, D. Wilson and B. Hube. 2011. Host-pathogen interactions and virulence-associated genes during *Candida albicans* oral infections. *Int. J. Med. Microbiol.* 301: 417–422.

Mayer F.L., D. Wilson and B. Hube. 2013. *Candida albicans* pathogenicity mechanisms. *Virulence* 4: 119–128.

Moazeni M., M.R. Khoramizadeh, P. Kordbacheh, Z. Sepehrizadeh, H. Zeraati, F. Noorbakhsh, L. Teimoori-Toolabi and S. Rezaie. 2012. RNA-mediated gene silencing in *Candida albicans*: inhibition of hyphae formation by use of RNAi technology. *Mycopathologia* 174: 177–185.

Naglik J.R., S.J. Challacombe and B. Hube. 2003. *Candida albicans* secreted aspartyl proteinases in virulence and pathogenesis. *Microbiol. Mol. Biol. Rev.* 67: 400–428.

Naglik J.R., D. Moyes, J. Makwana, P. Kanzaria, E. Tsichlaki, G. Weindl, A.R. Tappuni, C.A. Rodgers, A.J. Woodman, S.J. Challacombe and others. 2008. Quantitative expression of the *Candida albicans* secreted aspartyl proteinase gene family in human oral and vaginal candidiasis. *Microbiology* 154: 3266–3280.

Naglik J.R., D.L. Moyes, B. Wachtler and B. Hube. 2011. *Candida albicans* interactions with epithelial cells and mucosal immunity. *Microbes Infect.* 13: 963–976.

Ness F., V. Prouzet-Mauleon, A. Vieillemard, F. Lefebvre, T. Noel, M. Crouzet, F. Doignon and D. Thoraval. 2010. The *Candida albicans* Rgd1 is a RhoGAP protein involved in the control of filamentous growth. *Fungal Genet. Biol.* 47: 1001–1011.

Nobile C.J., E.P. Fox, J.E. Nett, T.R. Sorrells, Q.M. Mitrovich, A.D. Hernday, B.B. Tuch, D.R. Andes and A.D. Johnson. 2012. A recently evolved transcriptional network controls biofilm development in *Candida albicans*. *Cell* 148: 126–138.

Pierce J.V. and C.A. Kumamoto. 2012. Variation in *Candida albicans EFG1* expression enables host-dependent changes in colonizing fungal populations. *mBio* 3: e00117-00112.

Pietrella D., N. Pandey, E. Gabrielli, E. Pericolini, S. Perito, L. Kasper, F. Bistoni, A. Cassone, B. Hube and A. Vecchiarelli. 2013. Secreted aspartic proteases of *Candida albicans* activate the NLRP3 inflammasome. *Eur. J. Immunol.* 43: 679–692.

Puri S., R. Kumar, S. Chadha, S. Tati, H. Conti, B. Hube, P. Cullen and M. Edgerton. 2012. Secreted Aspartic Protease Cleavage of *Candida albicans* Msb2 Activates Cek1 MAPK Signaling Affecting Biofilm Formation and Oropharyngeal Candidiasis. *PLoS ONE* 7: e46020.

Schild L., A. Heyken, P.W. de Groot, E. Hiller, M. Mock, C. de Koster, U. Horn, S. Rupp and B. Hube. 2011. Proteolytic cleavage of covalently linked cell wall proteins by *Candida albicans* Sap9 and Sap10. *Eukaryot. Cell* 10: 98–109.

Seabra C.L., C.M. Botelho, M. Henriques and R. Oliveira. 2013. Differential adherence and expression of virulence traits by *Candida albicans* and *Candida parapsilosis* in mono- and dual-species cultures in arti icial saliva. *Mycopathologia* 176: 33–40.

Staniszewska M. 2009. Ph.D. Thesis, Search for *Candida albicans* virulence factors. Independent Laboratory of Streptomyces and Fungi Imperfecti. National Institute of Public Health-National Institute of Hygiene. Warsaw. Poland.

Staniszewska M., M. Bondaryk, K. Siennicka and W. Kurzatkowski. 2012. Ultrastructure of *Candida albicans* Pleomorphic Forms: Phase-Contrast Microscopy, Scanning and Transmission Electron Microscopy. *Pol. J. Microbiol.* 61: 129–135.

Staniszewska M., M. Bondaryk, E. Swoboda-Kopeć, K. Siennicka, G. Sygitowicz and W. Kurzątkowski. 2013. *Candida albicans* morphologies revealed by scanning electron microscopy analysis. *Braz. J. Microbiol.* 44: 813–821.

Staniszewska M., M. Bondaryk, T. Malewski and W. Kurzatkowski. 2014. Quantitative expression of *Candida albicans* aspartyl proteinase genes *SAP7*, *SAP8*, *SAP9*, *SAP10* in Human Serum *in vitro*. *Pol. J. Microbiol.* 63: 15–20.

Staniszewska M., Bondaryk M., Malewski T. and Schaller M. 2014. The expression of the *Candida albicans* gene *SAP4* during hyphal formation in human serum and in adhesion to monolayer cell culture of colorectal carcinoma Caco-2 (ATCC). *Centr. Eur. J. Biol.* 9: 796–810.

Taylor B.N., P. Staib, A. Binder, A. Biesemeier, M. Sehnal, M. Rollinghoff, J. Morschhauser and K. Schroppel. 2005. Profile of *Candida albicans*-secreted aspartic proteinase elicited during vaginal infection. *Infect. Immun.* 73: 1828–1835.

Tsai P.W., Y.T. Chen, P.C. Hsu and C.Y. Lan. 2013. Study of *Candida albicans* and its interactions with the host: A mini review. *BioMedicine* 3: 51–64.

Yan L., C. Yang and J. Tang. 2013. Disruption of the intestinal mucosal barrier in *Candida albicans* infections. *Microbiol. Res.* 168: 389–395.

Polish Journal of Microbiology
2015, Vol. 64, No 3, 211–216

ORIGINAL PAPER

The Participation of p53 and bcl-2 Proteins in Gastric Carcinomas Associated with *Helicobacter pylori* and/or Epstein-Barr Virus (EBV)

ANDRZEJ SZKARADKIEWICZ[1], TOMASZ M. KARPIŃSKI[1], JAN MAJEWSKI[2], KAMILA MALINOWSKA[1], OLGA GOŚLIŃSKA-KUŹNIAREK[1] and KRZYSZTOF LINKE[3]

[1] Department of Medical Microbiology, University of Medical Sciences in Poznań, Poznań, Poland
[2] Department of Clinical Pathomorphology, University of Medical Sciences in Poznań, Poznań, Poland
[3] Department of Gastroenterology, Human Nutrition and Internal Diseases, Poznań University of Medical Sciences, Poznań, Poland

Submitted 16 August 2014, revised 25 January 2015, accepted 13 April 2015

Abstract

In the presented studies p53 and bcl-2 proteins expression were evaluated in samples of gastric carcinomas in patients with *Helicobacter pylori* or EBV or without *H. pylori*/EBV infection. The studies were conducted on 64 adult patients with gastric adenocarcinomas: 16 patients with *H. pylori* (*cagA*+)-positivity (group 1), 14 with EBV-positive tumours (group 2), 12 with *H. pylori*/EBV-positive tumours (group 3) and 22 patients with *H. pylori*/EBV-negative tumours (group 4). *H. pylori* presence in gastric tumour specimens was detected using Giemsa staining and bacterial culture technique. Moreover, *cagA* gene was detected using PCR. EBV infection was detected based on EBER presence in the tissue by RNA *in situ* hybridization. Expressions of p53 and bcl-2 proteins were analysed using immunohistochemistry. Expression of p53 was noted in 14 (84%) patients from group 1, 8 (57%) patients from group 2, 7 (58%) patients from group 3, and 19 (86%) patients from group 4, whereas expression of bcl-2 was noted in 12 (75%) patients from group 1, in 10 (71%) patients from group 2, 9 (75%) patients from group 3, and 6 (27%) patients from group 4. The obtained results allow the conclusion, that *H. pylori* (*cagA*+)-associated development of the gastric adenocarcinoma is determined by abnormalities in the p53 *protein* function and overexpression of anti-apoptotic bcl-2 protein, whereas EBV-associated adenocarcinomas seem to be related with apoptosis resistance associated with bcl-2 overexpression.

Key words: *Helicobacter pylori*, bcl-2, Epstein-Barr virus, gastric adenocarcinoma, p53

Introduction

It has been well documented that pathogenesis of the gastric cancer is a complex and multi-stage process, with progression in lesions of the mucous membrane from chronic gastritis to chronic atrophic gastritis, intestinal metaplasia, dysplasia and finally gastric carcinoma (Konturek *et al*., 2003; Carcas, 2014). A significant role of infection with *Helicobacter pylori* (*H. pylori*) in the carcinogenesis process was also well established, defining this bacterium as a class I carcinogen for gastric cancer (IARC, 1994). Moreover, involvement of infection with the Epstein-Barr virus (EBV) in etiopathogenesis of gastric cancer was also documented (Czopek *et al*., 2003; Iizasa *et al*., 2012; Chen *et al*., 2012). It is estimated that gastric carcinomas are in approximately 80% cases associated with *H. pylori* infection, whereas in approximately 10% they are associated with EBV infection (Wu *et al*., 2000; HCCG, 2001; Czopek *et al*., 2003; Palli *et al*., 2007). In 40 to 100% of *H. pylori* strains isolated from patients with gastric carcinomas the *cagA* (cytotoxin-associated gene A) (Palli *et al*., 2007) was detected. Crucial role in the carcinogenesis process is played by p53 protein (tumour protein *p53*) and bcl-2 protein (B-cell leukemia/lymphoma-2) (Ozaki and Nakagawara, 2011; Moldoveanu *et al*., 2014; Czabotar *et al*., 2014). p53 has a suppressive effect on the cancerous transformation through induction of apoptosis in cells with defected genome (Vermeulen *et al*., 2003). As for bcl-2, it is the strongest apoptosis inhibitor among all known cell proteins (Mérino and Bouillet, 2009). Nevertheless, it remains unclear whether in gastric carcinoma *p53* abnormalities and bcl-2 expression are dependent on presence of *H. pylori* or EBV infection. Therefore, in this study we investigated p53 and bcl-2 expression in gastric carcinomas in patients with *H. pylori*/EBV or without *H. pylori*/EBV infection.

* Corresponding author: A. Szkaradkiewicz, Department of Medical Microbiology, University of Medical Sciences in Poznań, Poznań, Poland; **e-mail: szkaradkiewicza@poczta.onet.pl**

Experimental

Materials and Methods

Patients. The studies were conducted on 64 adult patients with histologically confirmed diagnosis of gastric adenocarcinoma. From patients who underwent routine upper endoscopy antral biopsies were taken. Cancer diagnosis (adenocarcinoma) was verified by analysis of hematoxylin and eosin stained preparations (Shibata *et al.,* 2001; Matsubara *et al*., 2004). Based on presence of infection with *H. pylori* or EBV, three study groups were distinguished. Group 1 included 16 *H. pylori*-positive patients (10 males and 6 females), 59 ± 12.4 years of age. The second group consisted of 14 EBV-positive patients (10 males and 4 females), 61 ± 6.7 years of age. The third group involved 12 *H. pylori*-positive and EBV-positive patients (9 males and 3 females), 62 ± 8.3 years of age. The fourth group included 22 *H. pylori*-negative and EBV-negative patients (17 males and 5 females), 65 ± 7.5 years of age.

H. pylori and *cagA* gene detection. Biopsies of gastric mucosa were plated on Columbia agar (bioMerieux) with 7% sheep blood with antibiotic supplement (*Helicobacter pylori* Selective Supplement (Dent), Oxoid). The incubation was conducted in microaerophilic conditions (Genbox microaer, bioMerieux) for 4 to 6 days at the temperature of 37°C. The isolated *H. pylori* strains were identified based on Gram staining as well as by production of urease, catalase, and oxidase (Szkaradkiewicz *et al*., 2010). For detection of *cagA* gene, the diagnostic kit of PCR-*H. pylori* (DNA Gdańsk) was used. PCR product was subjected to electrophoresis in the 2% agar gel and the result was read after staining with ethidium bromide. Presence of PCR reaction in form of a product of 445 base pairs in size was accepted as the positive test result. Moreover, presence of *H. pylori* was identified in the tissue sections using Giemsa staining (Lee and Kim, 2015).

Detection of EBER (EBER 1 and EBER 2) in tissue material. EBV DNA product in the form of untranslated RNA (EBER 1 and EBER 2) particles was detected in tissue material using *in situ* hybridization (ISH) (Niedobitek and Herbst, 2006; Izadi and Taheri, 2010). The tissue material was fixed in formalin and embedded in paraffin. Five μm thick sections were deparaffinised and digested with proteinase K for 30 min at 37°C, and washed in DEPC. This was followed by inactivation of proteinase K in 0.4% PFD solution for 20 min at 4°C. The hybridisation was performed using a fluorescein-labelled RNA probe of 15 nucleotides in length (PNA Probe/FITC; DakoCytomation) for 15 h at 37°C. After a thorough washing in SWS solution (DakoCytomation) the product was detected using FITC/AP-specific antibodies. BCIP/NBT (PNA ISH Detection kit; DakoCytomation) was used as a substrate.

Immunohistochemical analysis of TP53 protein (p53). Five μm thick sections from the same tumour blocks, used for EBER detection, were immunohistochemically analysed for the presence of p53 protein. Following removal of paraffin, rehydration and blocking of endogenous peroxidase activity with 3% H_2O_2 in distilled water, the tissue was incubated in 10 mM citrate buffer (pH 6.0) in a microwave oven (1000 W) for 15 min. Subsequently, the tissue was rinsed with phosphate-buffered saline (PBS) and treated with the primary antibody, DO-7 mouse anti-human p53 protein (DakoCytomation) in 1:50 dilution, employing 30 min incubation at room temperature. For visualisation of the reaction EnVision+ System-HRP (horseradish peroxidase) kit (DakoCytomation) was used. PBS was substituted for primary antibodies as the negative control. As a positive control, a section of colorectal cancer with high p53 expression was used. In all slides the cells stained per 1000 carcinoma cells were scored. The section was considered p53 positive when at least 10% cell nuclei were stained (Nasierowska-Guttmejer *et al*., 2000).

Immunohistochemical analysis of bcl-2 protein. Five μm thick sections from the same tumour blocks were immunohistochemically analysed for the presence of bcl-2 protein. Following removal of paraffin, rehydration and blocking of endogenous peroxidase activity with 3% H_2O_2 in distilled water, the tissue was incubated in 10 mM citrate buffer (pH 6.0) in a microwave oven (1000 W) for 15 min. Subsequently, the tissue was rinsed with phosphate-buffered saline (PBS) and treated with the primary antibody, FLEX monoclonal mouse anti-human bcl-2 oncoprotein (DakoCytomation) in 1:50 dilution, employing 30 min incubation at room temperature. For visualisation of the reaction EnVision+ System-HRP kit (DakoCytomation) was used. Finally, the site of immunoprecipitate formation was detected by applying diaminobenzidine (DAB; Sigma). PBS was substituted for primary antibodies as the negative control. As a positive control, a section of colorectal cancer with high bcl-2 expression was used. In all slides the cells stained per 1000 carcinoma cells were scored. The section was considered bcl-2 positive when at least 10% cell cytoplasms were stained (Nasierowska-Guttmejer, 2001).

Statistical analysis. Differences in frequencies of p53 and bcl-2 positive results were compared with Fisher's exact test. Relationships with *P*-values higher than 0.05 were considered insignificant.

Results

***H. pylori* and EBV infection.** Among studied patients with gastric carcinoma, were 16 (25%) patients with *H. pylori* infection constituted group 1 (Fig. 1), in which presence of *cagA* gene was detected in 14 iso-

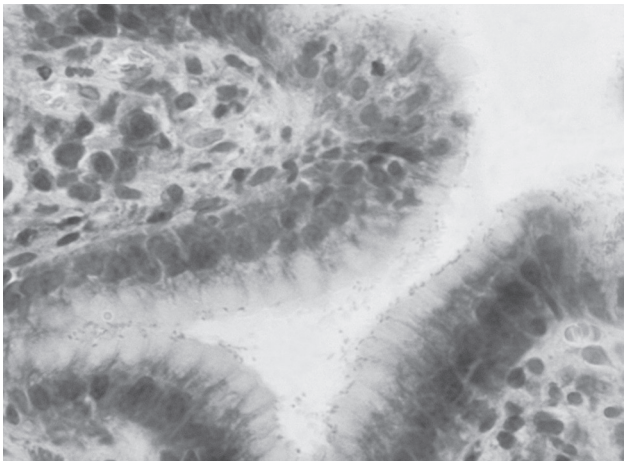

Fig. 1. *H. pylori*-positive gastric adenocarcinoma.

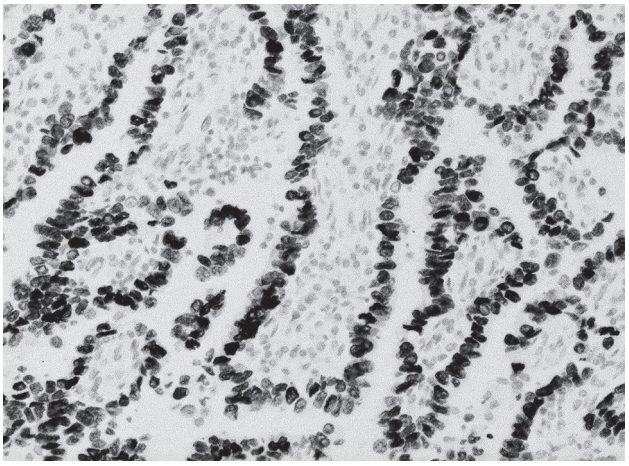

Fig. 3. Expression of p53 in *H. pylori* (*cagA*+)-positive gastric adenocarcinoma.

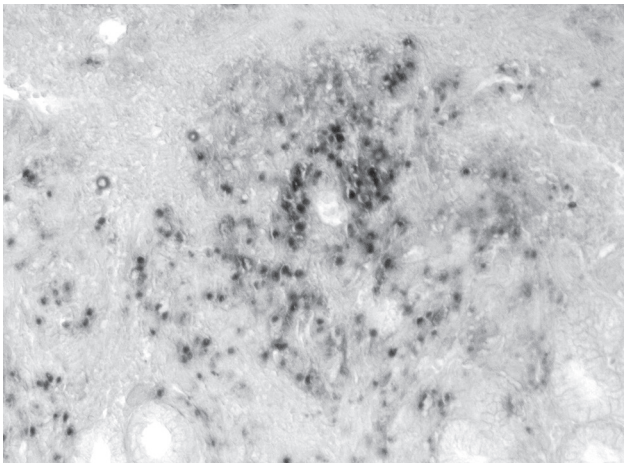

Fig. 2. EBER-positive gastric adenocarcinoma.

lated strains of the bacteria. Group 2 included 14 (22%) patients proved to be EBV-positive (Fig. 2). Group 3 included 12 (19%) patients found to be *H. pylori*-positive and EBV-positive. Group 4 included 22 (34%) patients in whom neither EBV infection nor *H. pylori* infection could be detected.

Expression of p53 protein. Results of detection of p53 protein are summarized in Table I. In group 1, among 16 patients with *H. pylori*-associated gastric carcinoma nuclear expression of p53 in most tumour cells was demonstrated in 14 (87%) cases (Fig. 3). In the remaining 2 (13%) cases no p53 could be detected. In group 2, among 14 patients with EBV-associated gastric carcinoma in 8 (57%) cases nuclear expression of p53 protein was noted in most tumour cells. In the remaining 6 (43%) cases no p53 could be detected. In group 3, among 12 patients with *H. pylori*-positive and EBV-positive gastric carcinoma in 7 (58%) cases nuclear expression of p53 protein was noted in most tumour cells. In the remaining 5 (42%) cases no p53 could be detected. In the group 4, among 22 patients with EBV-negative and *H. pylori*-negative gastric carcinoma, p53 protein nuclear expression was noted in most tumour cells in 19 (86%) cases. No p53 was detected in the remaining 3 (14%) cases. Expression of p53 in individual groups of patients, 1 to 3, with *H. pylori* and/or EBV infection, was not significantly more frequent than in patients without these infections ($P = 1.0000$, $P = 0.1111$ and $P = 0.0975$, respectively).

Expression of bcl-2 protein. Results of detection of bcl-2 protein are summarized in Table I. In group 1, among 16 patients with *H. pylori*-associated gastric carcinoma expression of bcl-2 was demonstrated in most tumour cells in 12 (75%) cases (Fig. 4). In the remaining 4 (25%) cases no bcl-2 could be detected. In

Table I
Expression of p53 and bcl-2 in gastric carcinoma in patients with or without documented infection with EBV or *H. pylori*.

Groups of patients with gastric carcinoma (n)	Number of patients with expression (%) of:			
	p53		bcl-2	
	(+)	(–)	(+)	(–)
Group 1 *H. pylori*-positive (cagA+) (n = 16)	14 (87%)	2 (13%)	12 (75%)*	4 (25%)
Group 2 EBV-positive (n = 14)	8 (57%)	6 (43%)	10 (71%)*	4 (29%)
Group 3 *H. pylori*-positive, EBV-positive (n = 12)	7 (58%)	5 (42%)	9 (75%)*	3 (25%)
Group 4 *H. pylori*-negative, EBV-negative (n = 22)	19 (86%)	3 (14%)	6 (27%)	16 (73%)

* significantly different as compared to group 4.

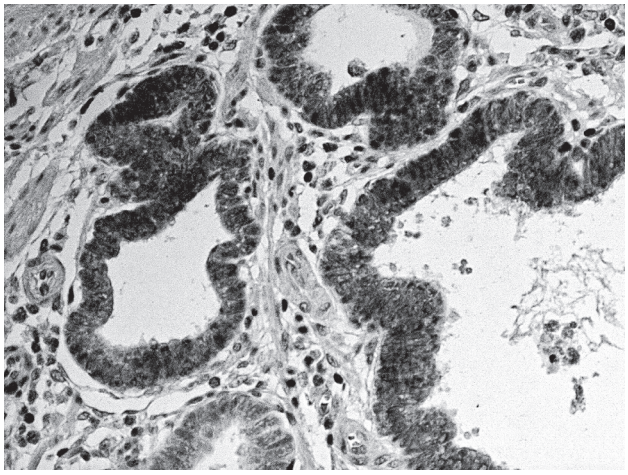

Fig. 4. Expression of bcl-2 in *H. pylori* (*cagA*+)-positive gastric adenocarcinoma.

group 2, among 14 patients with EBV-associated gastric carcinoma in 10 (71%) cases expression of bcl-2 protein was noted in most tumour cells. In the remaining 4 (29%) cases no bcl-2 could be detected. In the group 3, among 12 patients with *H. pylori*-positive and EBV-positive gastric carcinoma, bcl-2 protein expression was noted in most tumour cells in 9 (75%) cases. No bcl-2 was detected in the remaining 3 (25%) cases. In the group 4, among 22 patients with EBV-negative and *H. pylori*-negative gastric carcinoma, bcl-2 protein expression was noted in most tumour cells in 6 (27%) cases. No bcl-2 was detected in the remaining 16 (73%) cases. Expression of bcl-2 was found to be more frequent in the group of patients with *H. pylori* infection ($P = 0.0036$), the group of EBV-associated gastric carcinoma patients ($P = 0.0159$) and the group of *H. pylori*-positive and EBV- positive gastric carcinoma patients ($P = 0.0120$) but no difference in the frequency could be demonstrated in the groups of patients with EBV-negative and *H. pylori*-negative gastric carcinoma.

Discussion

In the present study, expressions of p53 and bcl-2 proteins have been examined in *H. pylori*- and/or EBV-associated and *H. pylori*/EBV-negative gastric carcinomas. Presence of *H. pylori* in the isolated samples of gastric tumour has been directly detected using Giemsa staining method of histological sections (Lee and Kim, 2015), and the bacterial culture from the obtained samples. In turn, infection with EBV has been detected on the basis of EBER presence in tumour cells. It has already been well documented that EBER is expressed in all forms of EBV latency and can always be detected by in situ hybridization (Murray and Young, 2002; Iizasa *et al*., 2012; Chen *et al*., 2012). Thus, the techniques employed in this study provided a reliable and a highly specific diagnosis of *H. pylori*/EBV infection.

The obtained results have shown that in most cases of both *H. pylori* (*cagA*+)-positive (group 1) and *H. pylori*-negative gastric carcinomas (group 4) a disturbed function of *p53* gene is observed. The data may suggest that *H. pylori* (*cagA*+) is not responsible for development of mutation in *p53* gene and the demonstrated overexpression of p53 in cancerous tissues. The suggestions are supported by results of earlier studies conducted by Berloco *et al.* (2003) and Targa *et al*. (2007). On the other hand, however, Suriani *et al.* (2008) demonstrated *H. pylori* CagA-specific antibodies in sera of 82.6% patients with *H. pylori*-negative gastric cancer. This indicates that patients with gastric carcinoma, even if *H. pylori*-negative at the time of this testing, might have been infected by *H. pylori* before onset of the disease and in the meantime the pathogen underwent eradication. Taking the above into account, it is possible that at least a proportion of group 4 patients have earlier been infected with *H. pylori* (*cagA*+). In addition, the percentage of patients manifesting expression of p53 in group 1 as well as in group 4 was high while results of p53 expression in all examined groups manifested no significant differences. In such a context it seems probable that *H. pylori* (*cagA*+) may induce *p53* mutations already at the early phase of carcinogenesis. The conclusion seems to be supported by studies of Kuniyasu *et al*. (2000) and of Kountouras *et al.* (2008) who detected *p53* mutations in at least 30% cases of intestinal metaplasia and in 58% patients with gastric dysplasia. Moreover, recent data indicate that infection with *H. pylori* may lead to an increased expression of *p53* apoptosis inhibitor (iASP), mediating the anti-apoptotic process (Meng *et al*., 2013). Thus, the pathogen may induce mutations of *p53* gene, and also its deregulation, which results in promotion of gastric cell proliferation and cancerous transformation.

However, proportions of patients with p53 expression were lower in the analysed groups 2 and 3. Thus, the obtained results may suggest that abnormalities in *p53* gene in gastric cancer are not EBV-dependent, consistent with results of our earlier study (Szkaradkiewicz *et al*., 2006). Such a suggestion is supported by other studies indicating that *p53* gene mutations are seldom identified or are absent from EBV-associated neoplasias (Petit *et al*., 2001; Wang *et al*., 2005). In addition, expression of p53 has been observed more frequently in group 4 than in groups 2 and 3. The observation corresponds to the earlier published studies of Ishii *et al.* (2004). The authors showed that frequency of p53 overexpression was lower in EBV-positive than in EBV-negative early stage gastric adenocarcinomas. Thus, the data might suggest that EBV interacts with *p53* gene, preventing or reducing expression of p53. In such a context, the suggestion that EBV infection promotes the development of gastric cancer by a *p53* pathway-dependent mechanism seems doubtful.

In turn, in analysis of our results devoted to bcl-2, we have documented expression of the anti-apoptotic protein in most cases of *H. pylori* (*cagA*+)-positive gastric carcinomas (group 1). In parallel, frequency of bcl-2 expression has been higher in patients of groups 1–3 than in patients of group 4. Therefore, it can be concluded that chronically developing infection with *H. pylori* (*cagA*+) determines an increase in bcl-2 expression, which in turn promotes development of gastric cancer. The conclusion finds support in earlier publications (Konturek *et al*., 2003; Lima *et al*., 2008). Moreover, Bartchewsky *et al*. (2010) demonstrated that in *H. pylori* infection, manifested by chronic gastritis, an increased Bax expression initiates cell apoptosis, but in patients with gastric cancer the pathogen induces the anti-apoptotic gene *bcl-2*. In addition, the presented *in vitro* investigations demonstrate that the *H. pylori*-secreted vacuolating cytotoxin – VacA exerts a pro-apoptotic effect on epithelial cells, acting in an opposite manner to anti-apoptotic activity of CagA (Oldani *et al*., 2009; Matsumoto *et al*., 2011). Therefore, the early period of infection with *H. pylori*, due to action of VacA, develops with overexpression of the pro-apoptotic protein while translocation of CagA to epithelial cells mobilizes overexpression of bcl-2 and, as a result, assures cellular survival. Recently presented data indicate also that CagA may activate human epidermal growth factor receptor 2 (HER2) in gastric cells (Shim *et al*., 2014). Activation of the oncogene plays an important role in cell proliferation and tumorigenesis (Gravalos and Jimeno, 2008; Bollig-Fischer *et al*., 2010).

In turn, results presented in this study, related to bcl-2 in patients carrying only EBV-positive (group 2) versus EBV-negative gastric carcinomas (group 4) have demonstrated significant differences in expression of the protein between the two groups. The results contradict studies of Ishii *et al*. (2001) and Lima *et al*. (2008) but are consistent with earlier results of Kume *et al*. (1999), who documented high bcl-2 expression in EBV-positive gastric carcinomas. The obtained by us data allow to conclude that EBV-infection induces bcl-2 expression in gastric epithelial cells. It is already well known that EBV latent membrane protein (LMP)-1 inhibits cell apoptosis, elevating levels of bcl-2 (Zimber-Strobl *et al*., 1996; Thompson and Kurzrock, 2004). Nevertheless, investigations on EBV gene expression in gastric carcinomas documented type I latency pattern, that used to be restricted to EBV nuclear antigen (EBNA)-1, the $EBER_s$, and secretion of BARF0 gene proteins (Thompson and Kurzrock, 2004; Sivachandran *et al*., 2012). At the same time, until now no reports have appeared which would document upregulation of bcl-2 – associated with EBNA-1 and BARF0 in epithelial cell lines (Fu *et al*., 2013). Nevertheless, EBERs may induce up-regulation of bcl-2 in immortalized nasopharyngeal epithelial cells, causing their tumorgenesis (Wong *et al*., 2005). Moreover, it is demonstrated that BARF0 may stimulate expression of HER2 in epithelial cells, which may point to involvement of still another molecular mechanism in pathogenesis of EBV-infected gastric carcinoma cells (Lin *et al*., 2007). Such data, in the context of results presented by us seem to indicate that also the development of EBV-associated gastric carcinomas is dependent on bcl-2 anti-apoptosis activity.

In conclusion, our current studies indicate that the development of *H. pylori* (*cagA*+)- positive gastric adenocarcinomas is linked to abnormalities in function of p53 protein and the overexpression of anti-apoptotic bcl-2. On the other hand, the development of EBV-positive gastric adenocarcinomas seems to be related with apoptosis resistance associated with bcl-2 overexpression.

Acknowledgements

The research was supported by a grant from Poznań University of Medical Sciences, Poland (502-01-02206316-02658).

Literature

Bartchewsky W.Jr., M.R. Martini, A.C. Squassoni, M.C. Alvarez, M.S. Ladeira, D.M. Salvatore, M.A. Trevisan, J.Jr. Pedrazzoli and M.L. Ribeiro. 2010. Effects of *Helicobacter pylori* infection on the expressions of Bax and Bcl-2 in patients with chronic gastritis and gastric cancer. *Dig. Dis. Sci.* 55(1): 111–116.

Berloco P., F. Russo, F. Cariola, M. Gentile, P. Giorgio, M.L. Caruso, A.M. Valentini, G. Di Matteo and A. Di Leo. 2003. Low presence of p53 abnormalities in *H. pylori*-infected gastric mucosa and in gastric adenocarcinoma. *J. Gastroenterol.* 38(1): 28–36.

Bollig-Fischer A., M. Dziubinski, A. Boyer, R. Haddad, C.N. Giroux and S.P. Ethier. 2010. HER-2 signaling, acquisition of growth factor independence, and regulation of biological networks associated with cell transformation. *Cancer Res.* 70(20): 7862–7873.

Carcas LP. 2014. Gastric cancer review. *J. Carcinog.* 13: 14.

Chen J.N., D. He, F. Tang and C.K. Shao. 2012. Epstein-Barr virus-associated gastric carcinoma: a newly defined entity. *J. Clin. Gastroenterol.* 46(4): 262–271.

Czabotar P.E., G. Lessene, A. Strasser and J.M. Adams. 2014. Control of apoptosis by the BCL-2 protein family: implications for physiology and therapy. *Nat. Rev. Mol. Cell Biol.* 15(1): 49–63.

Czopek, J. P., M., Stojak, A., Bińczak, T., Popiela, J., Kulig, Z., Rudzki, and J. Stachura. 2003. EBV-positive gastric carcinomas in Poland. *Pol. J. Pathol.* 54(2): 123–128.

Fu Q., C. He and Z.R. Mao. 2013. Epstein-Barr virus interactions with the Bcl-2 protein family and apoptosis in human tumor cells. *J. Zhejiang Univ. Sci. B* 14(1): 8–24.

Gravalos C. and A. Jimeno. 2008. HER2 in gastric cancer: a new prognostic factor and a novel therapeutic target. *Ann. Oncol.* 19(9): 1523–1529.

Helicobacter and Cancer Collaborative Group. 2001. Gastric cancer and *Helicobacter pylori*: a combined analysis of 12 case control studies nested within prospective cohorts. *Gut* 49(3): 347–353.

Iizasa H., A. Nanbo, J. Nishikawa, M. Jinushi and H. Yoshiyama. 2012. Epstein-Barr Virus (EBV)-associated gastric carcinoma. *Viruses* 4(12): 3420–3439.

International Agency for Research on Cancer. 1994. Schistosomes, liver flukes and *Helicobacter pylori*. Evaluation of carcinogenic

risks to humans. *IARC Monograph Evaluating Carcinogenic Risks to Humans* 61: 177–240.

Ishii H., G. Gobé, Y. Kawakubo, Y. Sato and Y. Ebihara. 2001. Interrelationship between Epstein-Barr virus infection in gastric carcinomas and the expression of apoptosis-associated proteins. *Histopathol.* 38(2): 111–119.

Ishii H.H., G.C. Gobe, J. Yoneyama, M. Mukaide and Y. Ebihara. 2004. Role of p53, apoptosis, and cell proliferation in early stage Epstein-Barr virus positive and negative gastric carcinomas. *J. Clin. Pathol.* 57(12): 1306–1311.

Izadi M. and S. Taheri. 2010. Significance of in situ hybridization results for EBV-encoded RNA in post-transplantation lymphoproliferative disorder setting: report from the PTLD. *Ann. Transplant.* 15(4): 102–109.

Konturek P.C., J. Kania, J.W. Konturek, A. Nikiforuk, S.J. Konturek and E.G. Hahn. 2003. *H. pylori* infection, atrophic gastritis, cytokines, gastrin, COX-2, PPAR gamma and impaired apoptosis in gastric carcinogenesis. *Med. Sci. Mon.* 9(7): SR53–66.

Kountouras J., C. Zavos, D. Chatzopoulos and P. Katsinelos. 2008. New aspects of *Helicobacter pylori* infection involvement in gastric oncogenesis. *J. Surg. Res.* 146(1): 149–158.

Kume T., K. Oshima, T. Shinohara, H. Takeo, Y. Yamashita, T. Shirakusa and M. Kikuchi. 1999. Low rate of apoptosis and overexpression of bcl-2 in Epstein-Barr virus-associated gastric carcinoma. *Histopathol.* 34(6): 502–509.

Kuniyasu H., W. Yasui, H. Yokozaki and E. Tahara. 2000. *Helicobacter pylori* infection and carcinogenesis of the stomach. *Langenbecks Arch. Surg.* 385(2): 69–74.

Lee J.Y. and N. Kim. 2015. Diagnosis of *Helicobacter pylori* by invasive test: histology. *Ann. Transl. Med.* 3(1): 10.

Lima V.P., M.A. de Lima, A.R. André, M.V. Ferreira, M.A. Barros and S.H. Rabenhorst. 2008. *H. pylori* (CagA) and Epstein-Barr virus infection in gastric carcinomas: correlation with p53 mutation and c-Myc, Bcl-2 and Bax expression. *World J. Gastroenterol.* 14(6): 884–891.

Lin J.H., C.H. Tsai, J.S. Chu, J.Y. Chen, K. Takada and J.Y. Shew. 2007. Dysregulation of HER2/HER3 signaling axis in Epstein-Barr virus-infected breast carcinoma cells. *J. Virol.* 81(11): 5705–5713.

Matsubara Y., H. Yanai, K. Ishiguro, S. Ryozawa, Y. Okazaki, N. Matsui and K. Okita. 2004. Clinical interpretation of the histological typing of gastric cancer using endoscopic forceps biopsy. *Hepatogastroenterol.* 51(55): 285–288.

Matsumoto A., H. Isomoto, M. Nakayama, J. Hisatsune, Y. Nishi, Y. Nakashima, K. Matsushima, H. Kurazono, K. Nakao, T. Hirayama and S. Kohno. 2011. *Helicobacter pylori* VacA reduces the cellular expression of STAT3 and pro-survival Bcl-2 family proteins, Bcl-2 and Bcl-XL, leading to apoptosis in gastric epithelial cells. *Dig. Dis. Sci.* 56(4): 999–1006.

Meng W.D., R.X. Chu, B.Z. Wang, L.P. Wang, L.L. Ma and L.X. Wang. 2013. *Helicobacter pylori* infection and expressions of apoptosis-related proteins p53, ASPP2 and iASPP in gastric cancer and precancerous lesions. *Pathologie Biologie (Paris)* 61(5): 199–202.

Mérino D. and P. Bouillet. 2009. The Bcl-2 family in autoimmune and degenerative disorders. *Apoptosis* 14(4): 570–583.

Moldoveanu T., A.V. Follis, R.W. Kriwacki and D.R. Green. 2014. Many players in BCL-2 family affairs. *Trends Biochem. Sci.* 39(3): 101–111.

Murray P.G. and L.S. Young. 2002. The role of the Epstein-Barr virus in human disease. *Front. Biosci.* 7: d519–540.

Nasierowska-Guttmejer A., L. Trzeciak, M.P. Nowacki and J. Ostrowski. 2000. p53 protein accumulation and p53 gene mutation in colorectal cancer. *Pathol. Oncol. Res.* 6(4): 275–279.

Niedobitek G. and H. Herbst. 2006. *In situ* detection of Epstein-Barr virus and phenotype determination of EBV-infected cells. *Methods Mol. Biol.* 326: 115–137.

Oldani A., M. Cormont, V. Hofman, V. Chiozzi, O. Oregioni, A. Canonici, A. Sciullo, P. Sommi, A. Fabbri, V. Ricci and P. Boquet. 2009. *Helicobacter pylori* counteracts the apoptotic action of its VacA toxin by injecting the CagA protein into gastric epithelial cells. *PLoS Pathogens* 5(10): e1000603.

Ozaki T. and A. Nakagawara. 2011. p53: the attractive tumor suppressor in the cancer research field. *J. Biomed. Biotechnol.* 2011: 603925.

Palli D., G. Masala, G. Del Giudice, M. Plebani, D. Basso, D. Berti, M.E. Numans, M. Ceroti, P.H. Peeters, H.B. Bueno de Mesquita et al. 2007. CagA+ *Helicobacter pylori* infection and gastric cancer risk in the EPIC-EURGAST study. *Int. J. Cancer* 120(4): 859–867.

Petit B., K. Leroy, P. Kanavaros, M.L. Boulland, M. Druet-Cabanac, C. Haioun, D. Bordessoule and P. Gaulard. 2001. Expression of p53 protein in T- and natural killer-cell lymphomas is associated with some clinicopathologic entities but rarely related to p53 mutations. *Human Pathol.* 32(2): 196–204.

Shibata A., T.A. Longacre, B. Puligandla, J. Parsonnet and L.A. Habel. 2001. Histological classification of gastric adenocarcinoma for epidemiological research: concordance between pathologists. *Cancer Epidemiol. Biomarkers Prev.* 10(1): 75–78.

Shim J.H., J.H. Yoon, S.S. Choi, H. Ashktorab, D.T. Smoot, K.Y. Song, S.W. Nam, J.Y. Lee, C.H. Park and W.S. Park. 2014. The effect of *Helicobacter pylori* CagA on the HER-2 copy number and expression in gastric cancer. *Gene* 546(2): 288–296.

Sivachandran N., C.W. Dawson, L.S. Young, F.F. Liu, J. Middeldorp and L. Frappier. 2012. Contributions of the Epstein-Barr virus EBNA1 protein to gastric carcinoma. *J. Virol.* 86(1): 60–68.

Suriani R., M. Colozza, E. Cardesi, D. Mazzucco, M. Marino, S. Grosso, S. Sanseverinati, I. Venturini, A. Borghi and M.L. Zeneroli. 2008. CagA and VacA *Helicobacter pylori* antibodies in gastric cancer. *Can. J. Gastroenterol.* 22(3): 255–258.

Szkaradkiewicz A., T.M. Karpiński, M. Drews, M. Borejsza-Wysocki, P. Majewski and E. Andrzejewska. 2010. Natural killer cell cytotoxicity and immunosuppressive cytokines (IL-10, TGF-beta1) in patients with gastric cancer. *J. Biomed. Biotechnol.* 2010: 901564.

Szkaradkiewicz A., W. Majewski, M. Wal, M. Czyzak, P. Majewski, J. Bierła and A. Kuch. 2006. Epstein-Barr virus (EBV) infection and p53 protein expression in gastric carcinoma. *Virus Res.* 118(1–2): 115–119.

Targa A.C., A.C. César, P.M. Cury and A.E. Silva. 2007. Apoptosis in different gastric lesions and gastric cancer: relationship with *Helicobacter pylori*, overexpression of p53 and aneuploidy. *Gen. Mol. Res.* 6(3): 554–565.

Thompson M.P. and R. Kurzrock. 2004. Epstein-Barr virus and cancer. *Clin. Cancer Res.* 10(3): 803–821.

Vermeulen K., Z.N. Berneman and D.R. Van Bockstaele. 2003. Cell cycle and apoptosis. *Cell Prolifer.* 36(3): 165–175.

Wang Y., B. Luo, L.P. Yan, B.H. Huang and P. Zhao. 2005. Relationship between Epstein-Barr virus-encoded proteins with cell proliferation, apoptosis, and apoptosis-related proteins in gastric carcinoma. *World J. Gastroenterol.* 11(21): 3234–3239.

Wong H.L., X. Wang, R.C. Chang, D.Y. Jin, H. Feng, Q. Wang, K.W. Lo, D. Huang, P.W. Yuen, K. Takada and others. 2005. Stable expression of EBERs in immortalized nasopharyngeal epithelial cells confers resistance to apoptotic stress. *Mol. Carcinogenesis* 44(2): 92–101.

Wu M.S., C.T. Shun, C.C. Wu, T.Y. Hsu, M.T. Lin, M.C. Chang, H.P. Wang and J.T. Lin. 2000. Epstein-Barr virus-associated gastric carcinomas: relation to *H. pylori* infection and genetic alterations. *Gastroenterol.* 118(6): 1031–1038.

Zimber-Strobl U., B. Kempkes, G. Marschall, R. Zeidler, C. Van Kooten, J. Banchereau, G.W. Bornkamm and W. Hammerschmidt. 1996. Epstein-Barr virus latent membrane protein (LMP1) is not sufficient to maintain proliferation of B cells but both it and activated CD40 can prolong their survival. *EMBO J.* 15(24): 7070–7078.

Polish Journal of Microbiology
2015, Vol. 64, No 3, 217–225

ORIGINAL PAPER

Bloodstream Infections due to *Enterobacteriaceae* Among Neonates in Poland – Molecular Analysis of the Isolates

AGNIESZKA CHMIELARCZYK, MONIKA POBIEGA*, JADWIGA WÓJKOWSKA-MACH, DOROTA ROMANISZYN, PIOTR B. HECZKO and MAŁGORZATA BULANDA

Chair of Microbiology, Kraków, Poland

Submitted 21 January 2014, revised 27 February 2015, accepted 17 March 2015

Abstract

Bloodstream infections (BSIs) are associated with a significantly increased risk of fatality. No report has been found about the molecular epidemiology of *Enterobacteriaceae* causing BSI in neonates in Poland. The aim of this work was to determine the antibiotic resistance profiles, virulence gene prevalence, the epidemiological and genetic relationships among the isolates from *Enterobacteriaceae* causing BSI in neonates with birth weight < 1501 g. Antimicrobial susceptibility testing was performed. PCR was performed to identify the presence of common beta-lactamase genes, virulence genes. PFGE and MLST were performed. The surveillance group contained 1,695 newborns. The incidence rate for BSIs was 5.9%, the fatality rate 15%. The most common species were *Escherichia coli* (n = 24) and *Klebsiella pneumoniae* (n = 16). CTX-M-15 was found in 6 *E. coli*, 8 *K. pneumoniae*, 1 *Enterobacter cloacae* strains. Among *E. coli fim*H (83.3%), *ibe*A (37.5%), *neu*C (20.8%) were the most frequent. PFGE demonstrated unique pulsotypes among *E. coli*. *E. coli* ST131 clone was found in 7 *E. coli* strains. PFGE of 16 *K. pneumoniae* strains showed 8 pulsotypes. Five isolates from one NICU belonged to one clone. MLST typing revealed 7 different ST with ST336 as the most prevalent. This study provides information about resistance, virulence and typing of *Enterobacteriaceae* strains causing BSI among neonates. *E. coli* and *Klebsiella* spp. isolated in this study have completely different epidemiology from each other.

Key words: *Enterobacteriaceae*, *Escherichia coli* ST131, *Klebsiella pneumoniae*, bloodstream infections, MLST, very-low birth weight neonates

Introduction

Bloodstream infections (BSIs) are the most common nosocomial infections among neonates, associated with a significantly increased risk of fatality (Stoll *et al.*, 2002). Newborns, especially those with very low birth weight (VLBW) are primarily at risk of developing late-onset BSIs (LO-BSIs), caused by organisms acquired perinatally or postnatally, usually as a consequence of nosocomial transmission. The main risk factors for LO-BSI include prematurity, prolonged stay in a neonatal intensive care unit (NICU) and administration of invasive procedures (Ozkan *et al.*, 2014). Consequently, the improved survival rates of small premature infants experiencing long stays in modern NICUs, which are better equipped for life-saving intensive care, has been a major factor in the increase in LO-BSI caused by Gram-negative bacteria (Cordero *et al.*, 2004; Wojkowska-Mach *et al.*, 2013). *Enterobacteriaceae* are second only to coagulase-negative staphylococci (CoNS) in causing LO-BSIs (Karlowicz *et al.*, 2000; Lutsar *et al.*, 2014). Prolonged use of broad-spectrum antibiotics in NICUs is associated with the occurrence of multi-drug resistant (MDR) bacteria. Selection of more broadly resistant Gram-negative enteric bacteria is linked with outbreaks of bacterial disease in NICUs (Cordero *et al.*, 2004).

Nosocomial isolates such as *Escherichia coli* and *Klebsiella* sp. often have extended spectrum β-lactamase (ESBL) phenotypes, and *E. coli* strains carrying these enzymes have disseminated into the community. One of the best examples of this trend is the global spread of the clonal *E. coli* sequence type (ST) 131 (ST131), which expresses CTX-M enzymes. (Birgy *et al.*, 2013) In contrast, among *Klebsiella* strains, relatively few of the serotypes (particularly K1 and K2) appear to be linked with invasive strains. Also, the hypermucoviscous phenotype, strongly associated with the presence of *rpm*A and *mag*A genes, is a virulence marker in clinical strains (Jung *et al.*, 2013). In *Klebsiella pneumoniae*, CTX-M-15 is mainly associated with quinolone-resistant strains, belonging to ST11 clone (Damjanova *et al.*, 2008; Oteo *et al.*, 2009).

Despite many reports of ESBL-producing isolates among Polish hospitals, no report has been found about the molecular epidemiology of *Enterobacteriaceae*

* Corresponding author: M. Pobiega, Chair of Microbiology, Krakow, Poland; **e-mail: monika.pobiega@gmail.com**

causing BSI in neonates. Here, we collected clinical isolates from *Enterobacteriaceae* family bacteria originating from BSIs of neonates hospitalized in six Polish NICUs to determine their antibiotic resistance profiles, virulence gene prevalence, and the epidemiological and genetic relationships among the isolates. Here we have focused on detailed molecular studies, data about epidemiology of bloodstream infections in newborns are included in other manuscripts (Wojkowska-Mach *et al.*, 2014).

Experimental

Materials and Methods

Study population. Prior to the study, a confirmatory ethics vote for the data collected in the Polish Neonatology Surveillance Network (PNSN) for the scientific purpose was approved by the Bioethics Committee of Jagiellonian University Medical College (No KBET/221/B/2011).

Continuous prospective target surveillance of infections was conducted from 1/1/2009 through 12/31/2011 at Polish NICUs (only teaching hospitals) which participated in PNSN. These tertiary NICUs provided care for 20% of all VLBW infants born in Poland annually. The surveillance included infants hospitalized in these NICUs whose birth weights were < 1500 grams (VLBW) at birth until they achieved a weight of 1800 grams or died. The study covered 1,695 newborns. The general fatality case rate was 16.3%. All VLBW infants of suspected or documented infected were subject to registration regardless of the time of occurrence according to criteria of Gastmeier *et al.* (2004) when they had clinical signs of a bloodstream infection (BSI) (Gastmeier *et al.*, 2004).

- at least 2 of the following: temperature > 38°C or < 36.5°C or temperature instability, tachycardia or bradycardia, apnea, prolonged capillary refill, metabolic acidosis, hypoglycemia and other signs of bloodstream infections such as lethargy;
- and patients who had 1 of the following criteria: C-reactive protein > 2.0 mg/dl, immature/total neutrophil ratio (I/T ratio) > 0.2, leukocytes < 5000/μl and platelets < 10000/μl.

LO-BSI was defined when diagnosed > 72 hours after delivery. Clinical sepsis represented an infant where signs of infection existed but on blood culture a causative organism was not identified.

Central venous catheter (CVC)-associated BSI (CVC-BSI) and peripheral intravenous catheter (PVC)-associated BSI (PVC-BSI) were defined as infections associated with the use of a central or peripheral venous catheter within the preceding 48 hours prior to the onset of the infection (Gastmeier *et al.*, 2004).

Bacterial strains. The present study examined 55 *Enterobacteriaceae* family isolates originating from BSIs: 4 from early onset infections (EOI), 51 from LOI. The majority originated from NICUs VI and II (25 and 12, respectively). The remainder were from V (8), I (5), III (3) and IV (2).

Culture and species identification. All blood specimens of at least 1 ml were injected into an aerobic blood culture bottle (Bactec Plus 26 Aerobic; Becton Dickinson, Poland), and cultured on MacConkey agar, Columbia agar (at 37°C, each for 24 h) and Sabouraud agar (at 37°C, 48 hours) (all from BIOCORP, Poland). Collection and identification of the bacterial strains was performed in the local microbiology laboratories of each hospital. Isolates were identified by the automated identification system (VITEK 2; bioMérieux, Warsaw, Poland). Bacterial strains were stored at −70°C and sent to Department of Microbiology, Krakow.

Antimicrobial susceptibility tests. Isolates were tested using disk diffusion antimicrobial susceptibility methods on Mueller-Hinton agar plates according to the current European Committee on Antimicrobial Susceptibility Testing (EUCAST) guidelines using clinical breakpoint tables v. 3.1 (http://www.eucast. org v.3.1, accessed: 11.02.2013). All discs were obtained from Oxoid, Basingstoke. ESBL activity was detected using a modified double-disk synergy test (Drieux *et al.*, 2008). ESBL-positive strains resistant to at least two other groups of antibiotics were considered to be MDR.

DNA isolation. DNA templates were extracted using a Genomic Mini kit (A&A Biotechnology, Poland) according to manufacturer's instructions.

Polymerase chain reaction (PCR) for extended-spectrum β-lactamase genes and virulence factor screening. PCR was performed to identify the presence of $bla_{\text{CTX-M}}$, bla_{SHV} and bla_{TEM} genes (Chmielarczyk *et al.*, 2013; Monstein *et al.*, 2007), products were sequenced by commercial company (Genomed, Warsaw, Poland).

E. coli was checked for the presence of selected virulence genes as described elsewhere (Chmielarczyk *et al.*, 2013; Johnson and Stell, 2000; Watt *et al.*, 2003).

The isolates were classified to 1 of the 4 main *E. coli* phylogenetic groups (A, B1, B2,and D) (Chmielarczyk *et al.*, 2013; Clermont *et al.*, 2000).

K. pneumoniae was tested for the presence of *rmp*A (regulator of mucoid phenotype A), *mag*A (mucoviscosity-associated gene A), *wab*G (involved in the biosynthesis of the outer core lipopolysaccharide), *uge* (encoding uridine diphosphate galacturonate 4-epimerase, which is responsible for capsule biosynthesis), *kfu* (iron uptake system), and *all*S (encoding the activator of the allantoin regulon) (Brisse *et al.*, 2009). PCR was performed with primer pairs specific for the *K. pneumoniae* capsule gene cluster (*cps*K1, *cps*K2)

(Fang *et al.*, 2007; Turton *et al.*, 2008). NCTC 5054 and NCTC 5055 were used as positive controls for *cps*K1 and *cps*K2, respectively.

Pulsed-field gel electrophoresis (PFGE). All isolates were analyzed using the standardized PFGE protocol developed at the Centers for Disease Control and Prevention by the PulseNet program. *Xba*I (Thermo Scientific) was used for DNA digestion. The digested products were separated on a CHEF III PFGE system (BioRad, Warsaw, Poland) in 0.5× Tris-borate-EDTA buffer at 14°C at 6 V for 20 h with a ramped pulse time of 2.2–54.2 s for *E. coli* and 14°C at 6 V for 22 h with a ramped pulse time of 2–35 s for *K. pneumoniae*, *Klebsiella oxytoca*, *Enterobacter cloacae* and *Serratia marcescens.* GelCompar (Applied Maths, Kortrijk, Belgium) was used for cluster analysis with the unweighted pair group method with an arithmetic mean and the Dice coefficient similarity require to be >90% for the pattern to be considered as belonging to the same type.

Multilocus sequence typing (MLST). MLST for *E. coli* was performed in accordance with (Wirth *et al.*, 2006) (http://mlst.ucc.ie/mlst/dbs/Ecoli), for *K. pneumoniae* was performed in accordance with (Diancourt *et al.*, 2005) (http://www.pasteur.fr/recherche/genopole/PF8/mlst/Kpneumoniae.html).

Results

The surveillance group contained 1,695 newborns with birth weight below 1500 g. Data on gestational age, mode of delivery, birth weight, multiple birth were previously published (Wojkowska-Mach *et al.*, 2014). In the study group, 100 cases of *Enterobacteriaceae* BSI were registered. Among all the etiological factors for BSI, bacteria belonging to Enterobacteriaceae family were responsible for 15.2% of such infections. The incidence rate for Enterobacteriaceae BSIs was 5.9%, while the fatality rate was 15%. The fatality rate for *E. coli* was 26.0% and for *Klebsiella* sp. 10.0% (p = 0.09). Of the 55 *Enterobacteriaceae* isolates included in our study, there were 24 *E. coli,* 16 *K. pneumoniae*, 4 *K. oxytoca*, 5 *E. cloacae*, 1 *Enterobacter sakazakii*, 4 *S. marcescens* and 1 *Morganella morganii* (Table I).

The CVC utilization rate was 0.45 and the PVC utilization rate was 0.16 (calculated by dividing the number of days of CVC/PVC by the total number of patient days). Among the infections caused by *E. coli*, 20.8% of LO-BSIs were associated with CVC use, while 8.3% were associated with PVC use. Among the LO infections caused by *K. pneumoniae*, 43.75% were associated with CVC and 18.75% with PVC.

Table I
Participation of particular isolates in species and NICU.

NICU	*Escherichia coli* (n = 24)			*Klebsiella pneumoniae* (n = 16)			*Enterobacter* sp. (n = 6)	*Klebsiella oxytoca* (n = 4)	*Serratia marcescens* (n = 4)	*Morganella morganii* (n = 1)
		ST	*Pulsotype*		*ST*	*Pulsotype*				
I (n = 5)	**1**	ST141	unique	**1**	ST153	unique	**2**			
	1	ST73	unique							
II (n = 12)	**4**	ST131	unique				**1**	**3**		
	2	ST69	identical (the same patient)							
	1	ST69	unique							
	1	ST75	unique							
III (n = 3)				**1**	ST336	unique			**1**	**1**
IV (n = 2)									**2**	
V (n = 8)	**2**	ST131	unique	**2**	ST17	identical (the same patient)		**1**		
	1	ST141	unique							
	1	ST69	unique							
	1	ST543	unique							
VI (n = 25)	**3**	ST998	unique	**5**	ST336	clone A	**3**		**1**	
	1	ST131	unique	**2**	ST11	clone B				
	1	ST141	unique	**2**	ST6	clone C				
	1	ST69	unique	**1**	ST6	unique				
	1	ST95	unique	**1**	ST153	unique				
	1	ST569	unique	**1**	ST870	unique				
	1	non typeable	unique							

Table II
Non-susceptible strains among different species of *Enterobacteriaceae* family.

	Escherichia coli n = 24 (%)	*Klebsiella pneumoniae* n = 16 (%)	*Enterobacter* sp. n = 6 (%)	*Klebsiella oxytoca* n = 4 (%)	*Serratia marcescens* n = 4 (%)	*Morganella morganii* n = 1 (%)
Penicillins						
Ampicillin	22 (91.7)	16 (100)	nd	4 (100)	nd	nd
Amoxicillin-clavulanate	13 (54.2)	9 (56.3)	nd	2 (50)	nd	nd
Piperacillin-tazobactam	0 (0)	2 (12.5)	1 (16.7)	0 (0)	0 (0)	0 (0)
Cephalosporins						
Cefepime	6 (25)	9 (56.3)	0 (0)	0 (0)	0 (0)	0 (0)
Cefotaxime	5 (20.8)	9 (56.3)	2 (33.3)	0 (0)	1 (25)	1 (100)
Ceftazidime	6 (25)	9 (56.3)	1 (16.7)	0 (0)	1 (25)	0 (0)
Cefuroxime	6 (25)	9 (56.3)	nd	0 (0)	nd	nd
Carbapenems						
Doripenem	1 (4.2)	3 (18.8)	0 (0)	0 (0)	0 (0)	0 (0)
Ertapenem	2 (8.3)	3 (18.8)	2 (33.3)	0 (0)	0 (0)	1 (100)
Imipenem	1 (4.2)	0 (0)	0 (0)	0 (0)	0 (0)	0 (0)
Meropenem	1 (4.2)	0 (0)	0 (0)	0 (0)	0 (0)	0 (0)
Monobactams						
Aztreonam	8 (33.3)	13 (81.3)	2 (33.3)	1 (25)	1 (25)	1 (100)
Fluoroquinolones						
Ciprofloxacin	5 (20.8)	7 (43.8)	0 (0)	0 (0)	0 (0)	0 (0)
Aminoglycosides						
Amikacin	2 (8.3)	2 (12.5)	0 (0)	0 (0)	0 (0)	0 (0)
Gentamicin	3 (12.5)	3 (18.8)	0 (0)	0 (0)	0 (0)	0 (0)
Tobramycin	6 (25)	8 (50)	0 (0)	0 (0)	0 (0)	1 (100)
Tetracyclines						
Tigecycline	0 (0)	0 (0)	0 (0)	0 (0)	0 (0)	0 (0)
Miscellaneous						
Chloramphenicol	1 (4.2)	3 (18.8)	0 (0)	0 (0)	0 (0)	0 (0)
Trimethoprim-sulfamethoxazole	10 (41.7)	6 (37.5)	0 (0)	0 (0)	0 (0)	0 (0)

The highest level of resistance among *E. coli* isolates was observed against AMP (91.7%), AMC (54.2%), SXT (41.7%) and ATM (33.3%). The highest level of resistance among *K. pneumoniae* isolates was observed against AMP (100%), ATM (81.3%), AMC (56.3%), all the cephalosporins investigated herein (56.3%), and CIP (43.8%) (Table II). The ESBL phenotype was found among 16 isolates (29%), with nine *K. pneumoniae*, six *E. coli* and one *E. cloacae*.

Molecular characterization showed that all ESBL-positive isolates carried the $bla_{\text{CTX-M}}$ gene: 15 of them had CTX-M-15 and one had CTX-M-3. Eleven isolates (68.8%) harbored the TEM-1 gene together with the CTX-M gene. Five isolates harbored the SHV-11 gene and one harbored SHV-1 together with CTX-M. Four isolates harbored CTX-M-15 gene together with TEM-1 gene and SHV-11 gene. One isolates harbored CTX-M-15 gene together with TEM-1 gene and SHV-1 gene. Ten of the ESBL-positive strains (5 *E. coli* and 5 *K. pneumoniae*) were regarded as MDR types.

The most frequently detected genes among the *E. coli* isolates were iron-related genes including *fhu*A (91.7%), *fec*A (75%), *iut*A (58.3%), *fyu*A (54.2%), *iro*N (50%) and *iuc*C (50%), *iha* (8.3%). The most frequently detected adhesion gene was *fim*H (found in 83.3% of the isolates). The *ibe*A gene was found in 37.5% of isolates, while the *neu*C gene was found in 20.8% of isolates.

Sixteen (66.6%) isolates clustered in the ECOR group B2, 6 (25.0%) in D, 1 (4.2%) in A, and 1 (4.2%) in group B1.

None of the *K. pneumoniae* strains tested here were the capsular K1 or K2 type. Additionally, the *mag*A gene was not identified in the isolates. In contrast, the gene *uge* was detected in all of the *K. pneumoniae* strains, while *wab*G was present in 11 of them (68.8%). Only one isolate harbored *all*S (no 75), while another harbored *kfu* and *rpm* genes (no 220).

PFGE typing demonstrated that almost all of the 24 *E. coli* isolates had unique pulsotypes. Two strains with identical pulsotypes were isolated from the same patient.

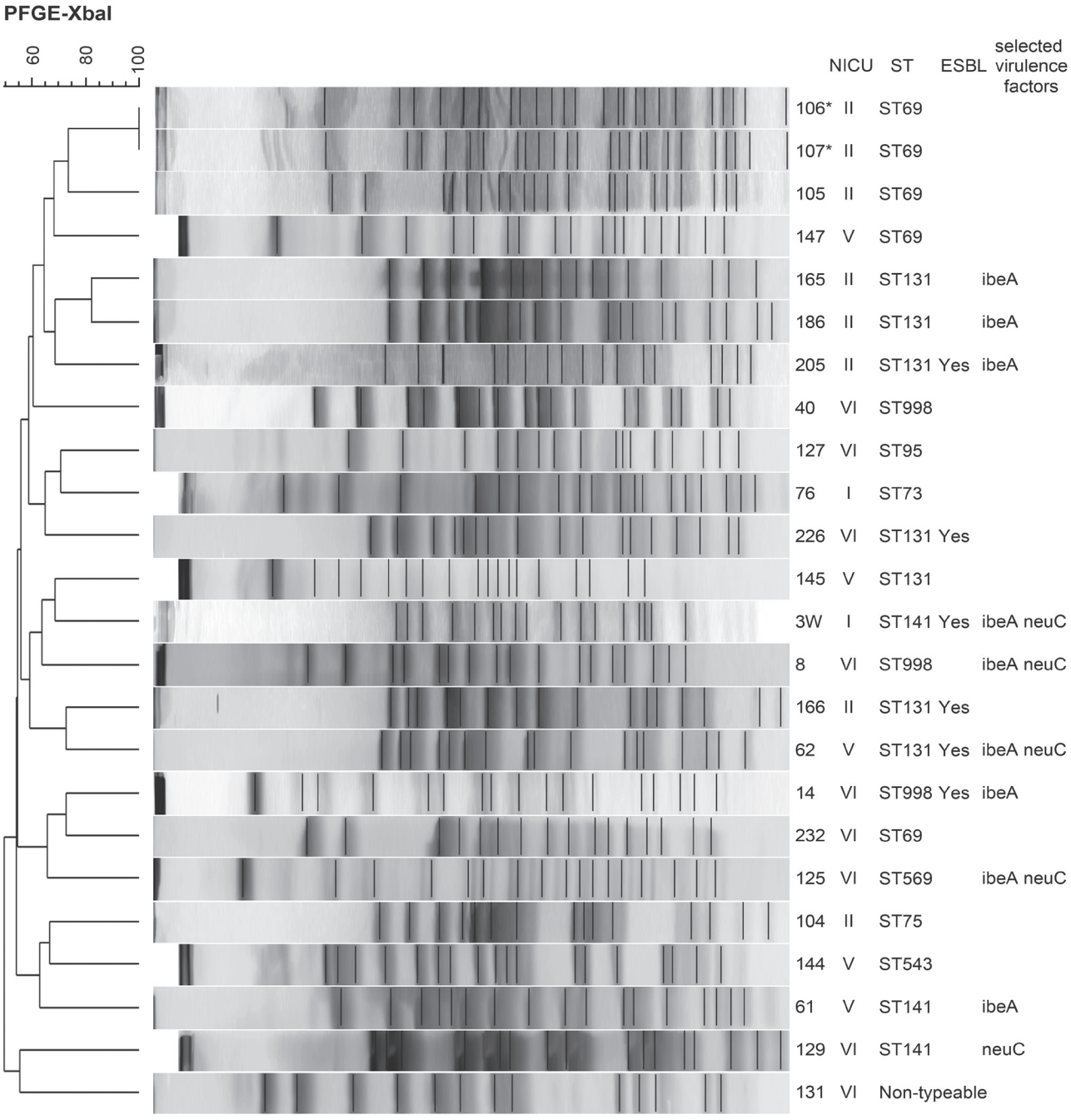

Fig. 1. Dendrogram of *E. coli* isolates. NICU was designated by Roman numerals. Asterisks indicate isolates derived from the same patient.

MLST typing revealed 10 different sequence types; these included ST131 (7 isolates), ST69 (5), ST141 (3), ST998 (3), ST73 (1), ST75 (1), ST95 (1), ST543 (1) and ST569 (1). One isolate could not be typed. Four among the ST131 isolates were from NICU II (Fig. 1). PFGE typing of 16 *K. pneumoniae* strains showed eight different pulsotypes. Five isolates from NICU VI belonged to one clone A. Those isolates were detected in 2009, 2010 and 2011. The mortality connected with those strains was 21.4%. Clone B consisted of two isolates similarly to clone C while the remaining five isolates had unique pulsotypes. MLST typing revealed seven different sequence types: ST 336 (6 isolates), ST6 (3), ST 11 (2) ST17 (2), ST153 (1), ST321 (1), and ST 870 (1). The main clone identified by PFGE was compatible with ST 336 (Fig. 2). PFGE typing of the *E. cloacae* strains revealed unique pulsotypes. Among *K. oxytoca*, two strains with identical pulsotypes were from the same patient, as was in the case for *S. marcescens* (data not shown).

Discussion

Enterobacteriaceae remain one of the most important, albeit not the most frequent, cause of BSIs. Septicaemia or BSI in neonates is an important cause of neonatal mortality and morbidity in developing

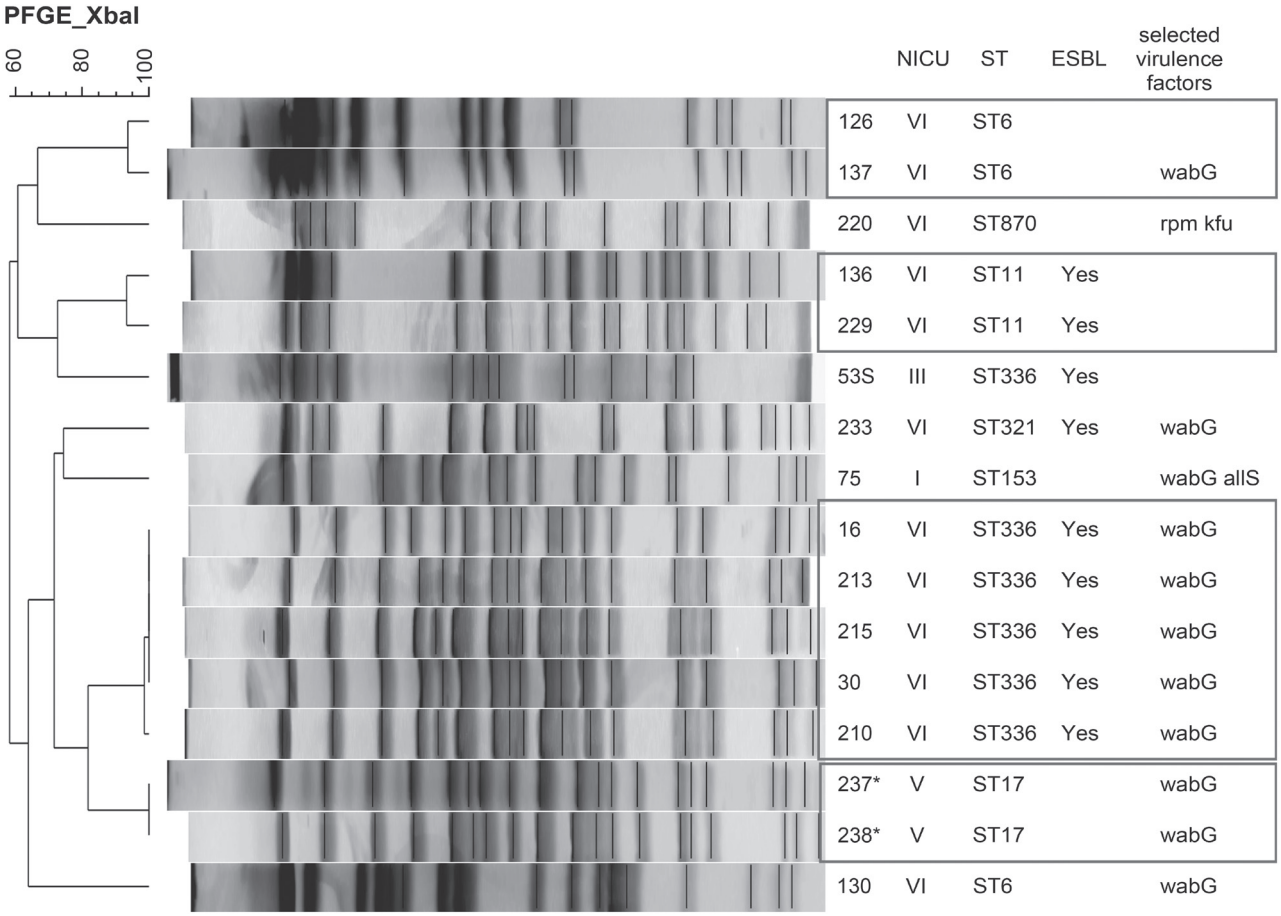

Fig. 2. Dendrogram of *K. pneumoniae* isolates. NICU was designated by Roman numerals. Detected clones were marked by frames. Asterisks indicate isolates derived from the same patient.

countries and *K. pneumoniae* and *E. coli* are prominent causative agents. In a study of 6215 infants admitted to the National Institute of Child Health and Human Development (NICHD) Neonatal Research Network (NRN) centers, 70% of first episode late-onset infections were caused by Gram-positive organisms, with coagulase-negative staphylococci accounting for 48% of the infections; however, the death rates were highest for infants infected with *E. coli. (*Karlowicz *et al*., 2000*)* Studies conducted by Makhoul *et al*. (2005) showed that mortality rate was about 4 times higher for infections caused by *E. coli* and 6 times higher for *K. pneumoniae* than for CoNS infections. Gram-negative bacilli (GNB) have been shown to be the non-dominant group of etiological risk factors for BSI, representing 20–30% of the infections in some studies (Graham *et al.*, 2006; Mitt *et al.*, 2014; Nagao, 2013). A study conducted by Cordero *et al.* (2004) showed that 20% of BSI episodes were caused by GNB, of which 15% were *Enterobacteriaceae*. Identification of these microorganisms in our study group was 15.2% and, importantly, infection with these etiological agents has been shown to be connected with high mortality rates in neonates (15%). Stoll *et al*. (2011) has described *E. coli* as the major causative pathogen of BSIs in preterm infants and the second most common cause of BSIs in term infants. Vergnano *et al*. (2011) indicated that *E. coli* was the third most common microorganism isolated from neonates and reported a prevalence of 13% in the UK, whereas in Germany the prevalence was 4.8% (Geffers *et al.*, 2008), which is about three times less than that observed in NICUs in the present study. Unfortunately, *E. coli* is frequently associated with severe infections and is the leading cause of sepsis-related mortality among VLBW infants. Indeed, *E. coli* accounted for 24.5% of EOI of neonates in the United States (Weston *et al.*, 2011) and 14.6% in Polish VLBW infants (Chmielarczyk *et al.*, 2014). In the present study, other Enterobacteriaceae family microorganisms such as *Klebsiella* spp. and *Enterobacter* spp. were markedly less common, similar to other studies (Cordero *et al.*, 2004; Geffers *et al.*, 2008; Lombardi *et al.*, 2014; Nagao, 2013; Vergnano *et al.*, 2011).

Crossing the skin barrier provides a direct route of invasion for bacteria; therefore, insertion of a CVC and the length of its duration *in situ* are risk factors for the development of a BSI. Lombardi *et al*. (2014) showed that in the neonatal pathology ward CVC infections reached 36.3% among Gram-negative bacteria, and

Klebsiella spp. were the most frequently isolated. This result is similar to our data.

E. coli and *Klebsiella* spp. isolated from NICUs in this study have different epidemiology to each other; hence, they require different surveillance and infection control. According to PFGE results, *E. coli* comprised different clones, while among the *K. pneumoniae* isolates, some showed high genetic similarity. Similar findings have been reported previously by other authors. (Castro *et al.*, 2010; Wojkowska-Mach *et al.*, 2013) Of the six NICUs we investigated, the majority of the *Enterobacteriaceae* isolates were from NICU VI, where *Klebsiella* dominated; this finding may be related to clonal spread of these bacteria. The *Klebsiella* clones detected in our study belong to four sequence types (ST): ST6, ST11, ST17 and ST336, of which ST11 and ST17 are known pathogens and colonizers widely distributed in Europe (Damjanova *et al.*, 2008; Oteo *et al.*, 2009).

The MLST technique showed that seven *E. coli* strains belonged to ST131, but according to the PFGE results, these strains had unique pulsotypes and came from three different centers; hence, they are assumed not to be clonally spread. It has been reported that strains belonging to the same ST do not always cluster in a single branch based on cluster analysis of PFGE patterns (Vimont *et al.*, 2008). ST131 is often reported in adults and recently also in children and neonates, and is probably transmitted between mothers and neonates (Denkel *et al.*, 2014). The spread of ESBL-producing ST131 *E. coli* in the community, especially during the neonatal period, is a cause for serious concern (Birgy *et al.*, 2013). Recently, a CTX-M-15 ESBL-positive *E. coli* ST131 clone, belonging to the B2 phylogenetic group and characterised by a particular antimicrobial resistance and high virulence potential, became a major public health problem especially in developing countries (Brisse *et al.*, 2012; Clermont *et al.*, 2009).

The microorganisms responsible for neonatal BSI have changed over time and vary from place to place. Prolonged use of broad-spectrum antibiotics in NICUs is associated with the current epidemic of MDR Gram-negative bacteria. Biedenbach *et al.* (2004) reported that the neonatal sepsis rate from *Klebsiella* spp. was higher in Latin America than in North America and was correlated with the use of extended-spectrum antibiotics. *Klebsiella* spp. and *E. coli* had the highest level of resistance to ampicillin, amoxicillin and aztreonam, which may have been caused by frequent administration of these drugs. Studies about antibiotic consumption conducted on the Polish NICUs have shown that beta-lactams were administred in more than 50% of infections (Rozanska *et al.*, 2012). In our study, higher levels of antibiotic resistance (and more ESBL-positive strains) were observed among *Klebsiella* strains, probably as a result of the epidemic clone detected in NICU VI.

The *E. coli* isolates studied here were more likely to posses the *ibe*A gene than those derived from urinary and respiratory tract infections (Chmielarczyk *et al.*, 2013). Soto *et al.* found that strains causing EOI harbored a higher frequency of the *ibe*A gene (Soto *et al.*, 2008). Among *Klebsiella* sp. only some of the isolates possessed virulence genes such as *rpm*A or *kfu*. None of the isolates possessed K1 or K2 serotypes. As the capsule is a major virulence factor for *K. pneumoniae* (Cortes *et al.*, 2002), information about the prevalence of the capsular types in such infections is an essential component of infection prevention and control (Pan *et al.*, 2013).

According to the results, contact isolation is required when a patient is colonized or infected by a microorganism which is transmitted by direct physical contact. The presented results have shown that reliable adherence to that principle by the personnel is necessary when *Klebsiella* spp. is highly level of endemic or in case of epidemic. However, data about *E. coli* showed that precautions should be different and regimen about hand hygiene is insufficient. In the case of *E. coli* surveillance on people who take care of a neonate including mother and people performing Kangaroo care, could be performed. Infection prevention should also require intensive education and preparing procedures about Kangaroo care, feeding and milk expression (including milk storage) (Guzman-Cottrill *et al.*, 2013).

Acknowledgements

The authors wish to thank the staff in NICUs for their help and interest in the study.

Funding

This work was supported by a grant from the Ministry of Science and Higher Education (DEC-2011/01/D/N27/00104). The sponsors provided the funding for the project only.

Literature

Biedenbach D.J., G. J. Moet and R. N. Jones. 2004. Occurrence and antimicrobial resistance pattern comparisons among bloodstream infection isolates from the SENTRY Antimicrobial Surveillance Program (1997–2002). *Diagn. Microbiol. Infect. Dis.* 50: 59–69.

Birgy A., P. Mariani-Kurkdjian, P. Bidet, C. Doit, N. Genel, C. Courroux, G. Arlet and E. Bingen. 2013. Characterization of extended-spectrum-beta-lactamase-producing *Escherichia coli* strains involved in maternal-fetal colonization: prevalence of *E. coli* ST131. *J. Clin. Microbiol.* 51: 1727–1732.

Brisse S., C. Fevre, V. Passet, S. Issenhuth-Jeanjean, R. Tournebize, L. Diancourt and P. Grimont. 2009. Virulent clones of *Klebsiella pneumoniae*: identification and evolutionary scenario based on genomic and phenotypic characterization. *PLoS One* 4: e4982.

Brisse S., L. Diancourt, C. Laouenan, M. Vigan, V. Caro, G. Arlet, L. Drieux, V. Leflon-Guibout, F. Mentre, V. Jarlier and others. 2012. Phylogenetic distribution of CTX-M- and non-extended-spectrum-beta-lactamase-producing *Escherichia coli* isolates: group B2 isolates, except clone ST131, rarely produce CTX-M enzymes. *J. Clin. Microbiol.* 50: 2974–2981.

Castro B., I. Montesinos, P. Fuster-Jorge, T. Delgado, M.A. Miguel-Gomez and A. Sierra. 2010. Epidemiology of Enterobacteriaceae causing bloodstream infections in neonatal intensive care unit patients. *Enferm. Infecc. Microbiol. Clin.* 28: 227–232.

Chmielarczyk A., M. Pobiega, J. Wojkowska-Mach, D. Romaniszyn, P. Adamski, P.B. Heczko and M. Bulanda. 2013. Molecular epidemiology, plasmid analysis, virulence, and resistance of *Escherichia coli* isolated from neonatal intensive care units in Poland. *Diagn. Microbiol. Infect. Dis.* 76: 542–545.

Chmielarczyk A., J. Wojkowska-Mach, D. Romaniszyn, P. Adamski, E. Helwich, R. Lauterbach, M. Pobiega, M. Borszewska-Kornacka, E. Gulczynska, A. Kordek and others. 2014. Mode of delivery and other risk factors for *Escherichia coli* infections in very low birth weight infants. *BMC Pediatr.* 14: 274.

Clermont O., S. Bonacorsi and E. Bingen. 2000. Rapid and simple determination of the Escherichia coli phylogenetic group. *Appl. Environ. Microbiol.* 66: 4555–4558.

Clermont O., H. Dhanji, M. Upton, T. Gibreel, A. Fox, D. Boyd, M.R. Mulvey, P. Nordmann, E. Ruppe, J.L.Sarthou and others. 2009. Rapid detection of the O25b-ST131 clone of *Escherichia coli* encompassing the CTX-M-15-producing strains. *J. Antimicrob. Chemother.* 64: 274–277.

Cordero L., R. Rau, D. Taylor and L.W. Ayers. 2004. Enteric gram-negative bacilli bloodstream infections: 17 years' experience in a neonatal intensive care unit. *Am. J. Infect. Control* 32: 189–195.

Cortes G., N. Borrell, B. de Astorza, C. Gomez, J. Sauleda and S. Alberti. 2002. Molecular analysis of the contribution of the capsular polysaccharide and the lipopolysaccharide O side chain to the virulence of *Klebsiella pneumoniae* in a murine model of pneumonia. *Infect. Immun.* 70: 2583–2590.

Damjanova I., A. Toth, J. Paszti, G. Hajbel-Vekony, M. Jakab, J. Berta, H. Milch and M. Fuzi. 2008. Expansion and countrywide dissemination of ST11, ST15 and ST147 ciprofloxacin-resistant CTX-M-15-type beta-lactamase-producing *Klebsiella pneumoniae* epidemic clones in Hungary in 2005--the new 'MRSAs'? *J. Antimicrob. Chemother.* 62: 978–985.

Denkel L.A., F. Schwab, A. Kola, R. Leistner, L. Garten, K. von Weizsäcker, C. Geffers, P. Gastmeier and B. Piening. 2014. The mother as most important risk factor for colonization of very low birth weight (VLBW) infants with extended-spectrum beta-lactamase-producing *Enterobacteriaceae* (ESBL-E). *J. Antimicrob. Chemother.* 69: 2230–2237.

Diancourt L., V. Passet, J. Verhoef, P.A. Grimont and S. Brisse. 2005. Multilocus sequence typing of *Klebsiella pneumoniae* nosocomial isolates. *J. Clin. Microbiol.* 43: 4178–4182.

Drieux L., F. Brossier, W. Sougakoff and V. Jarlier. 2008. Phenotypic detection of extended-spectrum beta-lactamase production in *Enterobacteriaceae*: review and bench guide. *Clin. Microbiol. Infect.* 14 Suppl 1: 90–103.

Fang C.T., S.Y. Lai, W.C. Yi, P.R. Hsueh, K.L. Liu and S.C. Chang. 2007. *Klebsiella pneumoniae* genotype K1: an emerging pathogen that causes septic ocular or central nervous system complications from pyogenic liver abscess. *Clin. Infect. Dis.* 45: 284–293.

Gastmeier P., C. Geffers, F. Schwab, J. Fitzner, M. Obladen and H. Ruden. 2004. Development of a surveillance system for nosocomial infections: the component for neonatal intensive care units in Germany. *J. Hosp. Infect.* 57: 126–131.

Geffers C., S. Baerwolff, F. Schwab and P. Gastmeier. 2008. Incidence of healthcare-associated infections in high-risk neonates: results from the German surveillance system for very-low-birth-weight infants. *J. Hosp. Infect.* 68: 214–221.

Graham P.L., M.D. Begg, E. Larson, P. Della-Latta, A. Allen and L. Saiman. 2006. Risk factors for late onset gram-negative sepsis in low birth weight infants hospitalized in the neonatal intensive care unit. *Pediatr. Infect. Dis. J.* 25: 113–117.

Guzman-Cottrill J.A., K.A. Ravin, K.A. Bryant, D.M. Zerr, L. Kociolek, J.D. Siegel and Society for Healthcare Epidemiology of America. 2013. Infection prevention and control in residential facilities for pediatric patients and their families. *Infect. Control Hosp. Epidemiol.* 34: 1003–1041.

Johnson J.R. and A.L. Stell. 2000. Extended virulence genotypes of *Escherichia coli* strains from patients with urosepsis in relation to phylogeny and host compromise. *J. Infect. Dis.* 181: 261–272.

Jung S.W., H.J. Chae, Y.J. Park, J.K. Yu, S.Y. Kim, H.K. Lee, J.H. Lee, J.M. Kahng, S.O. Lee, M.K. Lee and others. 2013. Microbiological and clinical characteristics of bacteraemia caused by the hypermucoviscosity phenotype of *Klebsiella pneumoniae* in Korea. *Epidemiol. Infect.* 141: 334–340.

Karlowicz M.G., E.S. Buescher and A.E. Surka. 2000. Fulminant late-onset sepsis in a neonatal intensive care unit, 1988–1997, and the impact of avoiding empiric vancomycin therapy. *Pediatrics* 106: 1387–1390.

Lombardi S., M. Scutell, V. Felice, E. Di Campli, M. Di Giulio and L. Cellini. 2014. Central vascular catheter infections in a Hospital of Central Italy. *New Microbiol.* 37: 41–50.

Lutsar I., C. Chazallon, F.I. Carducci, U. Trafojer, B. Abdelkader, V.M. de Cabre, S. Esposito, C. Giaquinto, P.T. Heath, M.L. Ilmoja and others. 2014. Current management of late onset neonatal bacterial sepsis in five European countries. *Eur. J. Pediatr.* 173: 997–1004.

Makhoul I.R., P. Sujov, T. Smolkin, A. Lusky, B. Reichman and Israel Neonatal Network. 2005. Pathogen-specific early mortality in very low birth weight infants with late-onset sepsis: a national survey. *Clin. Infect. Dis.* 40: 218–224.

Mitt P., T. Metsvaht, V. Adamson, K. Telling, P. Naaber, I. Lutsar and M. Maimets. 2014. Five-year prospective surveillance of nosocomial bloodstream infections in an Estonian paediatric intensive care unit. *J. Hosp. Infect.* 86: 95–99.

Monstein H.J., A. Ostholm-Balkhed, M.V. Nilsson, M. Nilsson, K. Dornbusch and L.E. Nilsson. 2007. Multiplex PCR amplification assay for the detection of blaSHV, blaTEM and blaCTX-M genes in *Enterobacteriaceae*. *APMIS* 115: 1400–1408.

Nagao M. 2013. A multicentre analysis of epidemiology of the nosocomial bloodstream infections in Japanese university hospitals. *Clin. Microbiol. Infect.* 19: 852–858.

Oteo J., O. Cuevas, I. Lopez-Rodriguez, A. Banderas-Florido, A. Vindel, M. Perez-Vazquez, V. Bautista, M. Arroyo, J. Garcia-Caballero, P. Marín-Casanova and others. 2009. Emergence of CTX-M-15-producing *Klebsiella pneumoniae* of multilocus sequence types 1, 11, 14, 17, 20, 35 and 36 as pathogens and colonizers in newborns and adults. *J. Antimicrob. Chemother.* 64: 524–528.

Ozkan H., M. Cetinkaya, N. Koksal, S. Celebi and M. Hacimustafaoglu. 2014. Culture-proven neonatal sepsis in preterm infants in a neonatal intensive care unit over a 7 year period: coagulase-negative *Staphylococcus* as the predominant pathogen. *Pediatr. Int.* 56: 60–66.

Pan Y.J., T.L. Lin, Y.H. Chen, C.R. Hsu, P.F. Hsieh, M.C. Wu and J.T. Wang. 2013. Capsular types of *Klebsiella pneumoniae* revisited by wzc sequencing. *PLoS One* 8: e80670.

Rozanska A., J. Wojkowska-Mach, M. Borszewska-Kornacka, A. Cmiel, J. Gadzinowski, E. Gulczynska, E. Helwich, A. Kordek, D. Pawlik, J. Szczapa and others. 2012. Antibiotic consumption and its costs of purchase in Polish neonatology networks units. *Przegl. Epidemiol.* 66: 513–519.

Soto S.M., J. Bosch, M.T. Jimenez de Anta and J. Vila. 2008. Comparative study of virulence traits of Escherichia coli clinical isolates causing early and late neonatal sepsis. *J. Clin. Microbiol.* 4: 1123–1125.

Stoll B.J., N. Hansen, A.A. Fanaroff, L.L. Wright, W.A. Carlo, R.A. Ehrenkranz, J.A. Lemons, E.F. Donovan, A.R. Stark, J.E. Tyson and others. 2002. Changes in pathogens causing early-onset sepsis in very-l ow-birth-weight infants. *N. Engl. J. Med.* 347: 240–247.

Stoll B.J., N.I. Hansen, P.J. Sanchez, R.G. Faix, B.B. Poindexter, K.P. Van Meurs, M.J. Bizzarro, R.N. Goldberg, I.D. Frantz, E.C. Hale and others. 2011. Early onset neonatal sepsis: the burden of group B Streptococcal and *E. coli* disease continues. *Pediatrics* 127: 817–826.

Turton J.F., H. Baklan, L.K. Siu, M.E. Kaufmann and T.L. Pitt. 2008. Evaluation of a multiplex PCR for detection of serotypes K1, K2 and K5 in *Klebsiella* sp. and comparison of isolates within these serotypes. *FEMS Microbiol. Lett.* 284: 247–252.

Vergnano S., E. Menson, N. Kennea, N. Embleton, A.B. Russell, T. Watts, M.J. Robinson, A. Collinson and P.T. Heath. 2011. Neonatal infections in England: the NeonIN surveillance network. *Arch. Dis. Child. Fetal Neonatal Ed.* 96: F9–F14.

Vimont S., B. Mnif, C. Fevre and S. Brisse. 2008. Comparison of PFGE and multilocus sequence typing for analysis of *Klebsiella pneumoniae* isolates. *J. Med. Microbiol.* 57: 1308–1310.

Watt S., P. Lanotte, L. Mereghetti, M. Moulin-Schouleur, B. Picard and R. Quentin. 2003. *Escherichia coli* strains from pregnant women and neonates: intraspecies genetic distribution and prevalence of virulence factors. *J. Clin. Microbiol.* 41: 1929–1935.

Weston E.J., T. Pondo, M.M. Lewis, P. Martell-Cleary, C. Morin, B. Jewell, P. Daily, M. Apostol, S. Petit, M. Farley and others. 2011. The burden of invasive early-onset neonatal sepsis in the United States, 2005–2008. *Pediatr. Infect. Dis. J.* 3: 937–941.

Wirth T., D. Falush, R. Lan, F. Colles, P. Mensa, L.H. Wieler, H. Karch, P.R. Reeves, M.C. Maiden, H. Ochman and others. 2006. Sex and virulence in *Escherichia coli*: an evolutionary perspective. *Mol. Microbiol.* 60: 1136–1151.

Wojkowska-Mach J., A. Chmielarczyk, M. Borszewska-Kornacka, J. Domanska, J. Gadzinowski, E. Gulczynska, M. Nowiczewski, E. Helwich, A. Kordek and others. 2013. *Enterobacteriaceae* infections of very low birth weight infants in Polish neonatal intensive care units: resistance and cross-transmission. *Pediatr. Infect. Dis. J.* 32: 594–598.

Wojkowska-Mach J., E. Gulczynska, M. Nowiczewski, M. Borszewska-Kornacka, J. Domanska, T.A. Merritt, E. Helwich, A. Kordek, D. Pawlik, J. Gadzinowski and others. 2014. Late-onset bloodstream infections of Very-Low-Birth-Weight infants: data from the Polish Neonatology Surveillance Network in 2009–2011. *BMC Infect. Dis.* 14: 339–2334–14–339.

Polish Journal of Microbiology
2015, Vol. 64, No 3, 227–239

ORIGINAL PAPER

Optimization of Culture Parameters for Maximum Polyhydroxybutyrate Production by Selected Bacterial Strains Isolated from Rhizospheric Soils

PRIYANKA LATHWAL, KIRAN NEHRA*, MANPREET SINGH, PRAGATI JAMDAGNI and JOGENDER S. RANA

Department of Biotechnology, Deenbandhu Chhotu Ram University of Science and Technology, Sonipat, Haryana, India

Submitted 6 July 2014, accepted 27 February 2015

Abstract

The enormous applications of conventional non-biodegradable plastics have led towards their increased usage and accumulation in the environment. This has become one of the major causes of global environmental concern in the present century. Polyhydroxybutyrate (PHB), a biodegradable plastic is known to have properties similar to conventional plastics, thus exhibiting a potential for replacing conventional non-degradable plastics. In the present study, a total of 303 different bacterial isolates were obtained from soil samples collected from the rhizospheric area of three crops, *viz*., wheat, mustard and sugarcane. All the isolates were screened for PHB (Poly-3-hydroxy butyric acid) production using Sudan Black staining method, and 194 isolates were found to be PHB positive. Based upon the amount of PHB produced, the isolates were divided into three categories: high, medium and low producers. Representative isolates from each category were selected for biochemical characterization; and for optimization of various culture parameters (carbon source, nitrogen source, C/N ratio, different pH, temperature and incubation time periods) for maximizing PHB accumulation. The highest PHB yield was obtained when the culture medium was supplemented with glucose as the carbon source, ammonium sulphate at a concentration of 1.0 g/l as the nitrogen source, and by maintaining the C/N ratio of the medium as 20:1. The physical growth parameters which supported maximum PHB accumulation included a pH of 7.0, and an incubation temperature of 30°C for a period of 48 h. A few isolates exhibited high PHB accumulation under optimized conditions, thus showing a potential for their industrial exploitation.

Key words: biochemical characterization, biodegradable plastic, culture parameters, optimization, PHB production

Introduction

Plastic materials have conquered our lives due to their desirable properties but their extensive uses have caused waste disposable problems for the environment. Improper disposal of plastics has threatened the natural environment worldwide. Conventional petrochemical plastics are recalcitrant to microbial degradation (Fiechter, 1990), and remain persistent in the soil for a long time, thus accumulating in the environment at a rapid rate of approximately 25 million tons per year. Thus, problems such as global environmental pollution and solid waste management associated with these petrochemical-based plastics have created much interest in the development of biodegradable plastics that retain the desirable properties of the conventional plastics. Such biopolymers form a safe alternative to petroleum-based polymers with a wide range of environmental advantages. Most of the biodegradable plastics are made from a compound called polyhydroxyalkanoate (PHA) (Lee, 1996). The family of PHAs includes several polymeric esters such as polyhydroxybutyrates, polyhydroxybutyrate co-hydroxyvalerates (PHBV), polyhydroxybutyrate co-hydroxyhexanoate (PHBHx), polyhydroxybutyrate co-hydroxyoctonoate (PHBO) *etc*. Poly 3-hydroxybutyric acid (PHB), the best known and the most common natural microbial PHA (Verlinden *et al*., 2007), is found to accumulate in a large number of microorganisms as reserve food material (Haywood *et al*., 1988; Peoples and Sinskey, 1989).

PHB is a thermoplastic polymer synthesized by a wide variety of bacteria (*Ralstonia eutropha, Azotobacter beijerinckia, Bacillus megaterium, Pseudomonas oleovorans*, various nitrogen fixing microorganisms found in root nodules of legume plant family, and many more) as intracellular compounds and energy storage materials when the nutritional elements are limited and the carbon source is in excess (Halami, 2008; Wang *et al*., 2009; Hyakutake *et al*., 2011; Rodriguez-Contreras *et al*., 2013). Usually lipid in nature, it is accumulated

* Corresponding author: Kiran Nehra, Dept. of Biotechnology, Deenbandhu Chhotu Ram University of Science and Technology, Sonepat, Haryana, India**; e-mail: nehrakiran@gmail.com**

as storage material in the form of mobile, amorphous, liquid granules, allowing microbial survival under stress conditions (Barnard and Sander, 1989; Sudesh *et al.*, 2000). Among terrestrial ecosystems, the rhizospheric soil layer influenced by plant roots, with its high microbial activity is a good habitat for PHB-producers. Indigenous microorganisms in the rhizosphere are adapted to changing conditions of the soil environment, and fluctuations in the concentration of nutrients exuded by plant roots. Bacteria capable of inclusion of storage substances have a competitive advantage over other bacteria, therefore, plants have been found to be colonized by numerous bacteria which are potentially able to accumulate polyhydroxybutyrate as energy and carbon sources.

A remarkable characteristic of P(3HB) is its biodegradability in different environments. Due to its similarity to conventional plastics in the physical properties, and having an additional advantage of being biodegradable; there is a great demand to replace the conventional plastics with that of the biodegradable plastics in order to safe guard our environment. However, the most important limitation of the widespread use and commercial production of PHB is the high cost of production compared to synthetic plastics (Sangkharak and Prasertsan, 2008). Isolation of novel high PHB producing strains, and improvement in the current PHB production strategies involving optimization of culture conditions could lead to cost reduction. Keeping these points in view, the present study was designed to isolate PHB producing bacteria from the rhizospheric soil of three different crops, and to optimize growth and culture conditions such as incubation time, temperature and pH; and medium constituents (carbon and nitrogen sources) for maximizing PHB production by them.

Experimental

Materials and Methods

Sample collection. For the isolation of PHB producing bacteria, rhizospheric soil samples were collected from three different crops, *viz*., wheat, mustard and sugarcane growing in 21 different districts of Haryana State in India, amounting to a total of 63 different soil samples (21 from each crop). Intact root systems along with adhered soil from all the three host plants were collected, and the samples were stored in plastic bags at low (4°C) temperature till further use. For further processing, the collected samples were air dried at room temperature, and then crushed with the help of pestle and mortar for further analysis.

Bacterial isolation from collected soil samples. For isolation of bacterial population, one gram of each collected soil sample was suspended in 10 ml of sterile distilled water, the suspension was shaken vigorously, serial dilutions were made and appropriate dilutions (10^{-4} to 10^{-6}) were plated on nutrient agar plates. After 48 hrs of incubation at 30°C, well- formed colonies were obtained on the plates. The total number of bacterial colony forming units (cfu) of each soil sample was enumerated, and the colonies were then studied for their morphological characteristics on the basis of their physical appearance (colour, size, shape and texture). Colonies showing remarkable differences in their morphology were selected and re-streaked on nutrient agar plates to obtain pure cultures.

Screening of isolates for PHB production using Sudan Black dye. All the representative pure isolates were screened for PHB production using the lipophilic stain Sudan Black B (Murray *et al*., 1994) on agar plates, and under light microscope.

Screening for PHB on solid agar. Individual bacterial isolates were streaked on nutrient agar plates (4–5 isolates on one plate), and the plates were incubated at 30°C for 24 hrs. Ethanolic solution of 0.3% (w/v in 70% ethanol) Sudan Black B was spread over the colonies and the plates were kept undisturbed for 30 minutes. The plates were then destained by washing with ethanol (96%) to remove excess stain from the colonies. The colonies that retained their black colour after destaining were attributed as PHB producing strains (Mohamed *et al*., 2012).

Screening for PHB production under light microscope. For microscopic studies, smears of respective colonies were prepared on glass slides, heat fixed and stained with a 0.3% (w/v in 70% ethanol) solution of Sudan Black B for 10 min. The colonies were decolorized by immersing the slides in xylene, and were then counterstained with safranin (5% w/v in sterile distilled water) for 10 sec. Bacterial cells appearing black under the microscope were considered PHB producing strains while others were marked as negative (Legat *et al*., 2010). All the positive isolates were assigned code numbers based on their source of isolation.

Quantification of PHB production and selection of isolates. PHB production was quantified by using the method of Law and Slepecky (1961) and the amount of PHB produced was calculated from the standard curve prepared by using commercial poly-β-hydroxybutyrate (Sigma-Aldrich). The PHB positive bacterial culture growth was pelleted at 10,000 rpm at 4°C for 10 min. The pellet was then washed with acetone and ethanol to remove unwanted materials, resuspended in equal volume of 4% sodium hypochlorite and incubated at room temperature for 30 min. The mixture was then centrifuged at 10,000 rpm for 10 min. to sediment the lipid granules. The supernatant was discarded, and the pellet was washed successively with acetone and etha-

nol. The pelleted polymer granules were dissolved in hot chloroform and filtered through Whatman No 1 filter paper (previously treated with hot chloroform). To the filtrate, 10 ml of hot concentrated H_2SO_4 was added, which converts the polymer to crotonic acid, turning it into a brown colored solution. The solution was cooled and absorbance was read at 235 nm against a concentrated H_2SO_4 blank on UV-VIS spectrophotometer (Soam *et al*., 2012). The quantity of PHB produced was determined by referring to the standard curve.

Preparation of standard curve: Pure PHB (Sigma, USA) was used to prepare the standard curve of PHB. Two gram of PHB was dissolved in 10 ml of concentrated H_2SO_4 and heated for 10 min to convert PHB into crotonic acid, which gave 200 mg/ml of crotonic acid. From the above stock, working solutions were prepared by diluting it to obtain different concentrations ranging between 10 mg/ml to 150 mg/ml. Absorbance of all the dilutions was read at 235 nm against a concentrated H_2SO_4 blank on UV-VIS spectrophotometer, and the standard graph was made by plotting the various concentrations on the x-axis and the respective optical densities on the y-axis. The standard curve was used for estimation of PHB yield of the bacterial isolates.

Selection of isolates: Based on the PHB yield, all the PHB isolates were divided into three categories, *viz*., high producers, medium producers and low producers. Representative isolates from each category (6, 1, and 1 each from high, medium and low producing categories, respectively, for isolates belonging to each of the three crops), amounting to a total of 24 isolates (8 isolates from the rhizospheric area of each of the three crops) were finally selected for further studies.

Morphological, physiological and biochemical characterization of selected isolates. The selected isolates were grown on nutrient agar plates and their colony morphology was recorded. The morphological characteristics of the representative bacterial isolates (from each soil sample) showing differences in their physical appearances were recorded under four major headings, *viz*., size, colour, texture and shape. All these isolates were also studied under the microscope with respect to their cellular morphology and Gram staining properties (Gram, 1884). Biochemical characteristics of the isolates were studied following the standard microbiological methods described by Williams *et al.* (1994). Identification of isolates was carried out on the basis of the results of morphological, cellular and biochemical characters studied. Molecular characterization of the isolates is underway.

Optimization of culture medium constituents and growth conditions for maximum PHB production. Growth conditions such as the presence of different nutrient sources in the media and other physical parameters play an important role in the production rate of PHB. Therefore, the effect of various media ingredients like different carbon and nitrogen sources; and of growth conditions such as pH, temperature, and incubation time on PHB production was determined for the selected isolates.

Optimization of different carbon sources. The effect of different carbon sources on PHB production was determined by raising the cultures of the selected isolates in 100 ml of minimal salt medium (MSM) (Suresh Kumar *et al*., 2004) supplemented with different carbon sources such as glucose, fructose, sucrose, maltose and arabinose at 2% concentration. Cultures were incubated at 30°C on a rotary shaker (150 rpm) for 48 hrs. After incubation, PHB produced by the isolates was quantified spectrophotometerically (as described earlier), and based on the yield, the best carbon source was determined.

Nitrogen source optimization. The selected isolates were inoculated in 100 ml of MSM broth containing the best carbon source and different nitrogen sources (ammonium sulphate, ammonium chloride, ammonium nitrate and yeast extract) at 1% concentration. After 48 h of incubation at 30°C, PHB yield was determined for all the isolates, and the best nitrogen source was selected on the basis of their yield. Further, the effect of different concentrations of the best nitrogen source on PHB production was also studied by determining the PHB yield upon growing the isolates in MSM supplemented with the best C-source and different concentrations (0.5, 1.0 and 1.5 g/l) of the best N-source.

Optimization of carbon to nitrogen ratio (C/N ratio). In addition to the determination of the best C and N sources, the effect of different C:N ratios on PHB production was also determined. For this, cultures were inoculated in MSM supplemented with different concentrations of the best C and N source (C/N ratio as 10:1, 15:1, 20:1 and 25:1). Cultures were incubated at 30°C on a rotary shaker (150 rpm) for 48 h. After incubation, PHB yield was quantified spectrophotometerically, and based on the yields the best C/N ratio was determined.

pH optimization. For pH optimization, cultures of the selected isolates were raised in MSM supplemented with the best C and N source having different pH, *viz*., 6.0, 7.0 and 8.0. Cultures were incubated at 30°C on a rotary shaker (150 rpm) for 48 hrs. After incubation, PHB yield was quantified spectrophotometerically, and the pH exhibiting maximum yield was determined.

Temperature optimization: The effect of different temperatures on PHB production was determined by inoculating the cultures in MSM supplemented with the best C and N source and then incubating at different temperatures *viz*., 25°C, 30°C, 35°C, 40°C, and 45°C. After 48 h of incubation at respective temperatures, PHB yield was quantified spectrophotometerically; based

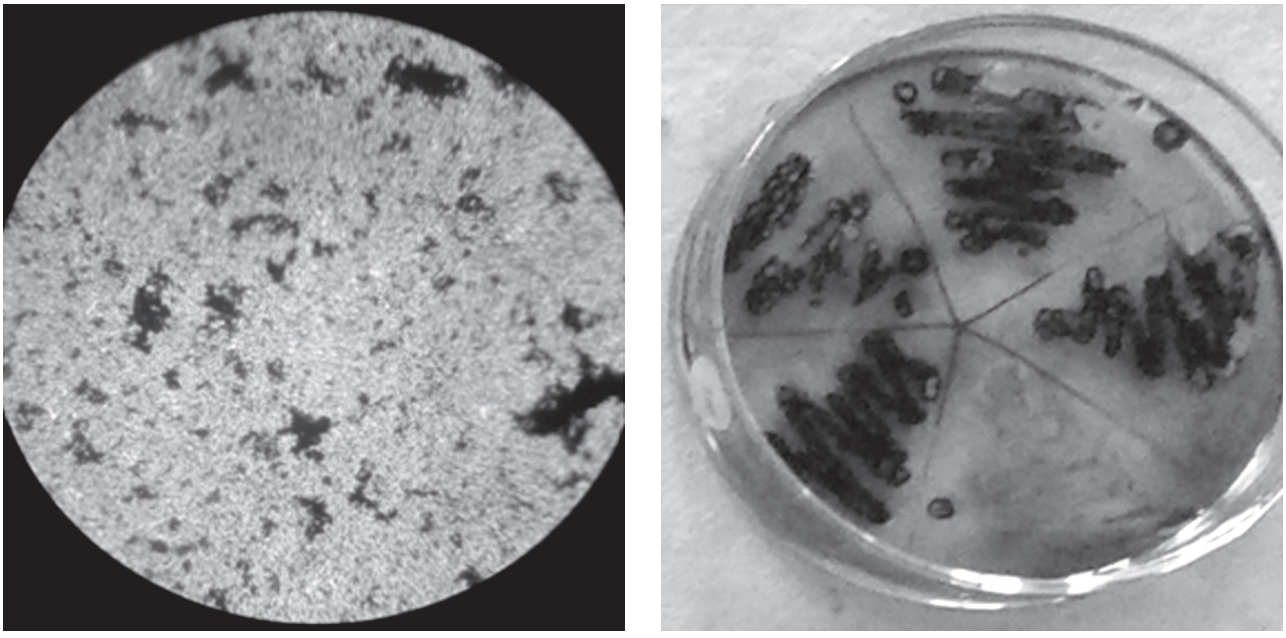

Fig. 1. Sudan Black screening of bacterial isolates, (a) Under the microscope, and (b) On nutrient agar plate

on the yields the optimum temperature for maximum PHB production was determined.

Optimization of incubation time. After the optimization of pH and temperature, the selected isolates were incubated for different time periods ranging from 12 to 72 hrs in optimized conditions. At each time point (12, 24, 36, 48, 60 and 72 h), cultures were tested for growth and PHB production and the PHB yield was recorded.

Results

Isolation and screening of PHB producing bacteria. For isolation of PHB producing bacteria, a total of 63 soil samples were collected from the rhizospheric area of three crops, *viz*., wheat, mustard and sugarcane belonging to 21 districts of Haryana State in India. The total bacterial population was isolated from each collected soil sample by making serial dilutions of the soil, and then plating appropriate dilutions on nutrient agar plates. Morphological studies of the isolates obtained revealed large diversity: on an average, 4–5 different types of colonies were obtained from each soil sample. Based upon the morphological differences in their colony characteristics (size, shape, colour and texture), a total of 303 different types of colonies (105 from wheat, 97 from mustard, and 101 from sugarcane) were picked up for further evaluation of PHB production using Sudan Black dye.

The screening was done by staining the isolates with Sudan Black B on petri plates as well as under the microscope. Out of a total of 303 isolates, 194 isolates (72 from wheat, 58 from mustard, and 64 from sugarcane rhizospheric soil) were found to be positive for PHB production; showing PHB granules which appeared as blue/ black droplets in the cells under the microscope, and as blue/black colonies when stained on plates with the Sudan Black stain, indicating PHB accumulation in the cells (Fig. 1 a, b). All the PHB positive isolates were given codes based upon the district and the crop (W for wheat, M for mustard, and S for sugarcane) represented by the soil sample.

Quantification of PHB production and selection of isolates. All the 194 Sudan Black B positive isolates were subjected to quantitative estimation of PHB production using the method described by Law and Slepecky (1961). By referring to the standard curve (Fig. 2), the PHB yield was calculated for all the 194 isolates, and it was found to vary between 6.5 mg/ml (MeS-4 isolate) to 132.58 mg/ml (KW-4 isolate) (Table I).

Based upon the amount of PHB produced, all the 194 PHB positive isolates were divided into three categories: (i) **High PHB producers**: having PHB yield above 80 mg/ml; (ii) **Medium PHB producers**: having PHB yield between 50–80 mg/ml; and (iii) **Low PHB producers**: having a PHB yield lower than 50 mg/ml. Out of a total of 194 isolates, 86 isolates were found to belong to the category of high producers, 81 isolates were medium producers, and 27 isolates were found to be low producers. Maximum number of high PHB producers were found to belong to wheat rhizosphere (39.53%), followed by those from the sugarcane rhizosphere (31.39%) and least from mustard rhizospheric soil (29.06%). The number of medium and low PHB producers was found to be almost similar in the bacterial strains isolated from the rhizospheric area of all the

Table I
PHB production by PHB positive bacterial isolates isolated from the rhizospheric soil of wheat, mustard and sugarcane crop.

Sr. No.	District	Wheat Crop		Mustard Crop		Sugarcane Crop	
		Strain	PHB Yield (mg/ml)	Strain	PHB Yield (mg/ml)	Strain	PHB Yield (mg/ml)
1	Ambala	AW-1	125.93	AM-2	110.31	AS-1	74.79
		AW-2	88.76	AM-4	68.09	AS-3	75.82
		AW-3	83.71			AS-4	105.88
						AS-5	28.40
2	Bhiwani	BW-1	90.98	BM-1	90.98	BS-1	60.00
		BW-3	70.57	BM-3	57.73	BS-3	42.37
				BM-4	94.12	BS-4	96.80
						BS-6	105.21
3	Faridabad	FW-2	47.11	FM-1	117.73	FS-1	116.55
		FW-3	55.52	FM-3	89.02	FS-3	90.82
		FW-5	90.31			FS-4	78.45
4	Fatehabad	FtW-2	78.35	FtM-3	108.97	FtS-1	98.71
		FtW-3	93.76	FtM-5	109.48	FtS-2	64.02
		FtW-5	94.95	FtM-7	58.09	FtS-5	89.12
		FtW-6	94.43	FtM-8	109.64		
5	Gurgaon	GW-2	61.29	GM-1	90.36	GS-2	56.65
		GW-4	65.82	GM-3	39.12	GS-3	68.51
				GM-4	94.95	GS-5	65.77
				GM-5	68.20		
6	Hisar	HW-3	98.51	HM-2	109.64	HS-1	69.12
		HW-4	92.01	HM-4	71.60	HS-2	65.26
						HS-4	47.27
						HS-7	59.07
7	Jind	JW-1	109.28	JM-2	92.78	JS-1	39.79
		JW-2	78.40	JM-3	94.79	JS-3	59.64
		JW-4	48.45			JS-4	70.98
		JW-5	64.18			JS-6	77.17
		JW-7	90.26				
8	Jhajjar	JhW-1	25.98	JhM-2	68.76	JhS-1	47.42
		JhW-2	58.09	JhM-3	68.09	JhS-3	97.11
		JhW-4	42.37			JhS-5	71.86
		JhW-5	70.57			JhS-6	89.12
		JhW-6	47.42			JhS-7	27.42
		JhW-8	57.94				
9	Kaithal	KW-1	80.21	KM-2	74.79	KS-1	126.44
		KW-3	79.18	KM-4	88.87	KS-3	126.24
		KW-4	132.58				
10	Karnal	KaW-1	72.11	KaM-1	61.75	KaS-2	57.84
		KaW-2	64.23	KaM-3	54.33	KaS-3	107.06
		KaW-4	61.60				
11	Kurukshetra	KuW-1	89.38	KuM-2	34.43	KuS-2	72.84
		KuW-2	37.58	KuM-3	33.97	KuS-3	94.18
		KuW-4	74.33	KuM-4	52.58	KuS-4	65.77
		KuW-5	62.73	KuM-6	74.85		

C.d. Table I.

Sr. No.	District	Wheat Crop		Mustard Crop		Sugarcane Crop	
		Strain	PHB Yield (mg/ml)	Strain	PHB Yield (mg/ml)	Strain	PHB Yield (mg/ml)
12	Mahendergarh	MW-2	70.77	MM-1	28.35	MS-4	21.91
		MW-3	77.06			MS-6	130.93
13	Mewat	MeW-1	63.45	MeM-1	73.35	MeS-3	7.17
		MeW-3	69.38	MeM-2	77.37	MeS-4	6.50
		MeW-4	82.22	MeM-3	108.76		
		MeW-5	90.26	MeM-4	77.27		
14	Palwal	PlW-1	71.19	PlM-2	30.41	PlS-2	70.36
		PlW-3	89.64	PlM-3	90.31	PlS-3	94.95
		PlW-4	94.43			PlS-4	89.69
15	Panchkula	PnW-2	95.46	PnM-2	70.67	PnS-1	60.46
		PnW-3	93.04	PnM-3	61.55	PnS-2	77.17
		PnW-4	114.43	PnM-6	52.11		
		PnW-5	47.63				
16	Panipat	PaW-2	87.32	PaM-1	71.60	PaS-2	72.01
		PaW-3	76.08	PaM-2	78.92	PaS-3	105.88
				PaM-3	90.98	PaS-4	37.99
				PaM-4	89.02		
17	Rewari	RW-2	109.48	RM-1	119.59	RS-1	105.21
		RW-3	93.92	RM-2	83.51	RS-3	40.57
		RW-5	52.06	RM-4	53.04		
		RW-6	52.94	RM-5	69.07		
		RW-7	37.84	RM-7	52.27		
		RW-8	52.68	RM-8	59.12		
18	Rohtak	RoW-1	126.19	RoM-1	108.76	RoS-4	120.62
		RoW-2	108.66	RoM-2	69.07	RoS-5	73.92
		RoW-4	110.26	RoM-3	80.41	RoS-6	89.43
19	Sirsa	SiW-1	104.59	SiM-1	68.71	SiS-1	85.77
		SiW-2	90.26	SiM-2	47.89	SiS-3	118.40
		SiW-3	75.93			SiS-4	91.03
		SiW-4	90.82			SiS-5	68.20
20	Sonipat	SW-1	94.18	SM-4	61.75	SS-1	94.18
		SW-3	94.02			SS-2	108.87
		SW-4	83.56			SS-4	94.18
		SW-5	70.15				
21	Yamunanagar	YW-5	38.35	YM-3	108.09	YS-2	92.47
		YW-6	18.92	YM-4	94.95	YS-3	58.76
		YW-8	57.73	YM-6	92.17	YS-5	69.07

three crops. However, bacterial strains isolated from the wheat and sugarcane rhizospheric soil showed a higher accumulation of PHB as compared to the strains isolated from the mustard rhizosphere. But still, the differences in the PHB yield were not significant enough to confirm any correlation between the PHB yield and the rhizospheric crop specificity of a bacterial isolate. One isolate each from the category of low and medium producers, and six from the category of high producers for each of the three different crops (constituting a total of 24 isolates: 8 from each crop) were selected (Table II) for characterization, and for optimization of medium constituents to maximize PHB production.

Morphological, physiological and biochemical characterization of selected isolates. The selected 24 isolates were subjected to morphological and bioche-

Table II
Bacterial isolates selected for optimization of medium constituents for maximum PHB production.

Category (On the basis of PHB yield)	Sr. No.	Strain	PHB Concentration (mg/ml)	Gram Staining	Shape	Identification (on the basis of biochemical characterization)
High PHB Producers	1.	AW-1	125.93	+	Diplococcus	*Micrococcus* sp.
(PHB Yield: Above 80 mg/ml)	2.	KW-4	132.58	+	Bacillus	*Bacillus* sp.
	3.	PnW-4	114.43	+	Coccus	*Micrococcus* sp.
	4.	RoW-1	126.19	+	Coccus	*Micrococcus* sp.
	5.	RoW-4	110.26	+	Coccus	*Micrococcus* sp.
	6.	SW-3	94.02	–	Coccus	*Acinetobacter* sp.
	7.	AM-2	110.31	+	Coccus	*Arthrobacter* sp.
	8.	FM-1	117.73	+	Coccus chains	*Micrococcus* sp.
	9.	FtM-8	109.64	–	Coccus	*Acinetobacter* sp.
	10.	HM-2	109.64	+	Coccus chains	*Micrococcus* sp.
	11.	RM-1	119.59	+	Coccus	*Arthrobacter* sp.
	12.	RoM-1	108.76	–	Coccus	*Acinetobacter* sp.
	13.	KS-1	126.44	+	Coccus	*Micrococcus* sp.
	14.	KS-3	126.24	+	Bacillus	*Geobacillus (Bacillus)*
	15.	MS-6	130.93	+	Coccus	*Arthrobacter* sp.
	16.	RoS-4	120.62	–	Coccus	*Acinetobacter* sp.
	17.	SiS-3	118.40	+	Coccus	*Staphylococcus* sp.
	18.	KaS-3	107.06	–	Bacillus	*Bacillus* sp.
Medium PHB Producers	19.	FtW-2	78.35	–	Coccus chains	*Acinetobacter* sp.
(PHB Yield: Between 50–80 mg/ml)	20.	PaM-2	78.92	+	Coccus	*Micrococcus* sp.
	21.	FS-4	78.45	+	Coccus	*Micrococcus* sp.
Low PHB Producers	22.	JW-4	48.45	–	Coccus	*Acinetobacter* sp.
(PHB Yield: Below 50 mg/ml)	23.	SiM-2	47.89	–	Coccus	*Acinetobacter* sp.
	24.	JhS-1	47.42	+	Coccus	*Streptococcus* sp.

mical characterization. Colony morphology was studied in terms of their size, shape, colour, texture and staining characteristics. Size varied from very small to large, while shapes swirled mainly between circular, ellipses and irregular. Colour varied from white to off-white to slightly yellowish. All types of colony textures were obtained such as raised, flat, convex, wrinkled, grainy, slimy *etc*. Gram staining revealed the presence of both Gram-positive and Gram-negative cells. However, a major section of the isolates was found to be Gram-positive in nature, with only eight Gram-negative isolates among the total 24 selected PHB positive isolates; and

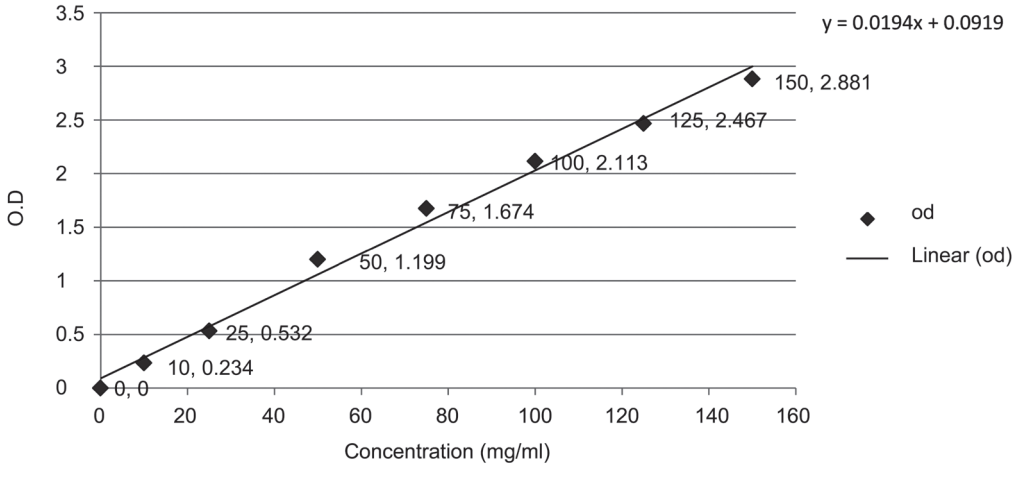

Fig. 2. PHB Standard Curve.

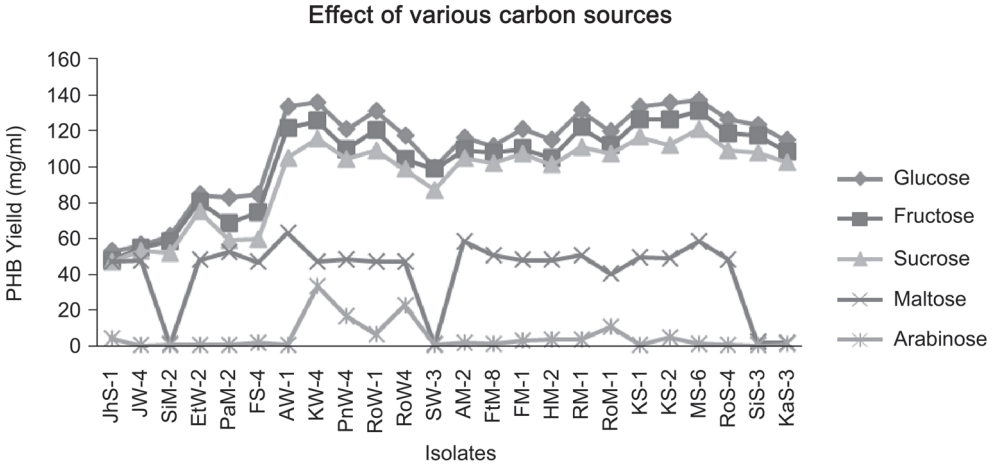

Fig. 3. Effect of various carbon sources on PHB production.

just 17 Gram-negatives among the total 194 PHB positive isolates obtained. Both coccus and bacillus forms were observed and cells could be seen in individual cell forms as well as in diplo- and chain forms (Table II).

All the PHB positive isolates were subjected to the standard biochemical tests and identification was carried out as per the details given in Bergey's Manual of Systematic Bacteriology (Williams *et al.*, 1994). On a preliminary basis, the isolates have been found to belong to six genera, namely *Micrococcus*, *Streptococcus*, *Staphylococcus*, *Bacillus*, *Acinetobacter* and *Arthrobacter.* The molecular identification of the isolates is underway.

Optimization of culture medium constituents and growth conditions for maximum PHB production. PHB accumulation by different bacteria is affected by the carbon (C) and nitrogen (N) sources being used for bacterial growth. The accumulation has been found to be enhanced if the bacterial cells are cultivated in the presence of an excess carbon source, and when their growth is impaired or restricted by lack of other nutrients, such as nitrogen, phosphorous and sulphur, or also dissolved oxygen (Reddy *et al.*, 2009). Therefore, it is important to find an optimum C and N source, and also to optimize their ratios for getting the maximum accumulation of PHB. In view of this, a total of twenty four isolates were selected for optimization of different medium constituents (carbon source, nitrogen source, and C/N ratio) for maximization of PHB production.

Effect of different carbon sources on PHB production. The selected isolates were grown in the presence of five carbon sources: glucose, fructose, sucrose, maltose, and arabinose. After incubation, the PHB produced by the isolates was quantified spectrophotometrically for selection of parameters showing highest PHB production. Figure 3 depicts the effect of different carbon sources on PHB yield. It was observed that different isolates utilize the various carbon sources differently. However, following a common trend, all of them showed maximum PHB accumulation when the minimal medium was supplemented with glucose, followed by supplementation with fructose and sucrose as C-sources. PHB yield was very low when maltose was used as the C-source; and with arabinose, none of the isolates could accumulate sufficient PHB. The mean PHB production values of all the 24 isolates were found to be 105.52 mg/ml, 102.52 mg/ml, 94.64 mg/ml, 41.89 mg/ml, and 5.23 mg/ml with glucose, fructose, sucrose, maltose and arabinose, respectively, as C-sources. Thus, among the different carbon sources tested to evaluate their effects on PHB yield, glucose was found to be the best carbon source, and least PHB production was obtained with arabinose. The isolate MS-6 recorded the highest PHB yield of 137.2 mg/ml, followed by KW-4, KS-3 and AW-1 with a PHB yield of 136.1, 135.6 and 133.7 mg/ml, respectively.

Effect of different nitrogen sources. PHB yields produced by the selected isolates when grown on different nitrogen sources in presence of the best carbon source (glucose) and four different nitrogen sources (ammonium sulphate, ammonium chloride, ammonium nitrate, and yeast extract) are presented in Fig. 4. Out of the four sources, ammonium sulphate was found to support highest PHB production; maximum PHB accumulation being observed by KS-3 (138.7 mg/ml), followed by AW-1 (138.2 mg/ml), MS-6 (137.9 mg/ml) and KW-4 (136.4 mg/ml). The mean PHB yields of all the 24 isolates was found to be 115.30 mg/ml, 81.32 mg/ml, 59.46 mg/ml and 25.93 mg/ml with ammonium sulphate, ammonium chloride, ammonium nitrate, and yeast extract, respectively.

The presence of high concentrations of nitrogen in the culture medium has been reported to be an inhibitor for the accumulation of PHB. Hence, the concentration of the best nitrogen source also needs to be optimized. Different concentrations (0.5, 1.0 and 1.5 g/l) of ammonium sulphate were therefore amended to the

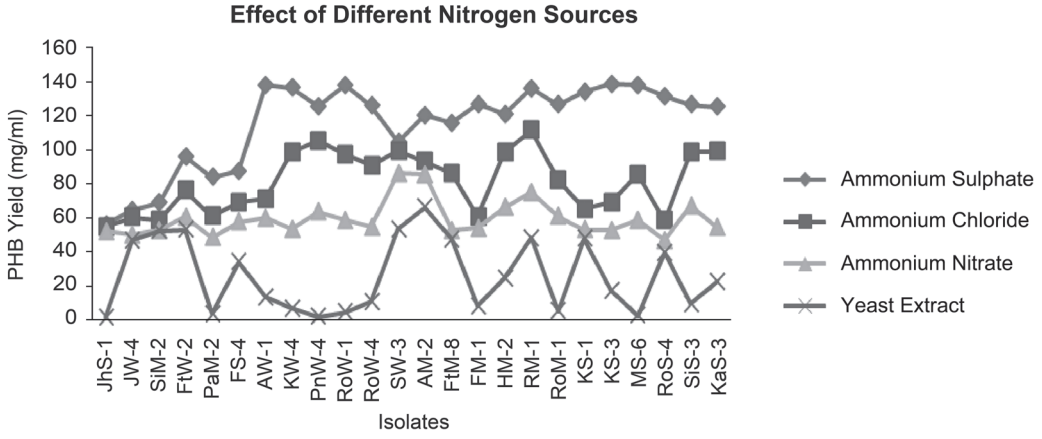

Fig. 4. Effect of different nitrogen sources on PHB production.

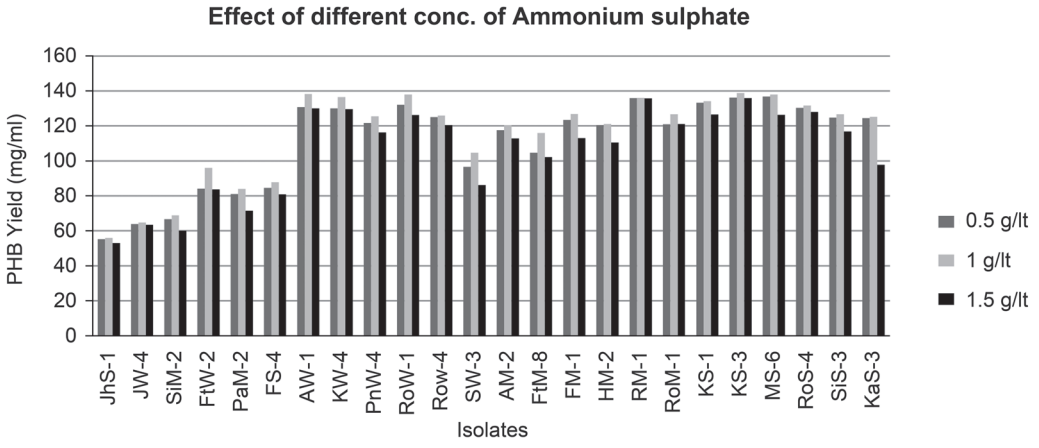

Fig. 5. Effect of different concentrations of ammonium sulphate on PHB production.

medium containing glucose as the best carbon source. From the studies, it was revealed that ammonium sulphate at 1.0 g/l was the optimum concentration for maximum PHB accumulation (Fig. 5). When ammonium sulphate concentration was increased from 0.5 to 1.00 g/l, the PHB accumulation also increased; but, concentrations above 1.0 g/l resulted into a decrease in PHB production by all the isolates.

Effect of relative concentration of carbon and nitrogen sources on PHB production. Under normal conditions, bacteria synthesize their cell materials like proteins and grow. But, in nutrient limiting conditions, bacteria may shift their protein synthesis to PHB synthesis for survival. To exploit this, the C:N ratios in the growth medium were adjusted to10:1, 15:1, 20:1 and 25:1 using glucose and ammonium sulphate as C and N sources, respectively; and the effect of these different concentrations on PHB production was studied (Fig. 6). As the carbon content was increased in the media keeping N as constant; up to a certain limit (*i.e.*, 20:1) PHB accumulation was found to increase, but thereafter (25:1) it showed a decline. This was probably due to the substrate inhibition.

The mean PHB yield with the four different C:N ratios (10:01, 15:01, 20:01 and 25:01) was found to be 107.74 mg/ml, 111.50 mg/ml, 119.86 mg/ml & 115.73 mg/ml, respectively, thus, showing that the C/N ratio 20:01 supported the maximum PHB productivity.

Effect of pH on PHB production. The effect of pH of the medium on PHB production was assessed, for which three different pH conditions (pH-6, pH-7 and pH-8) were maintained in the media prepared using the best carbon and nitrogen sources (Fig. 7). The results obtained revealed the mean PHB yields to be 3.76 mg/ml, 118.73 mg/ml and 100.56 mg/ml at pH 6.0, 7.0 and 8.0, respectively. Maximum PHB accumulation was observed for KS-3 and KW-4 (139.7 mg/ml by both), followed by MS-6 (137.3 mg/ml) and AW-1 (136.6 mg/ml) at pH 7.0. All the isolates were found to produce a very low PHB yield at pH 6. However, at pH 8.0, although the PHB yield was not too low, but still it was found to be less as compared to the accumulation at pH 7.0. It was thus concluded that out of the different media pH tested, pH 7.0 was optimum for PHB production.

Effect of incubation temperature on PHB production. Effect of varying the incubation temperature on

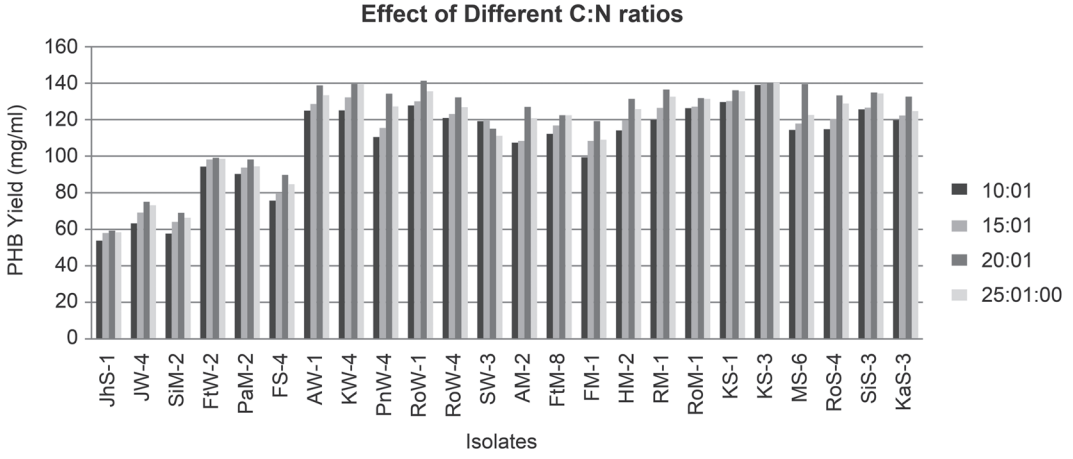

Fig. 6. Effect of different concentrations of carbon and nitrogen on PHB production.

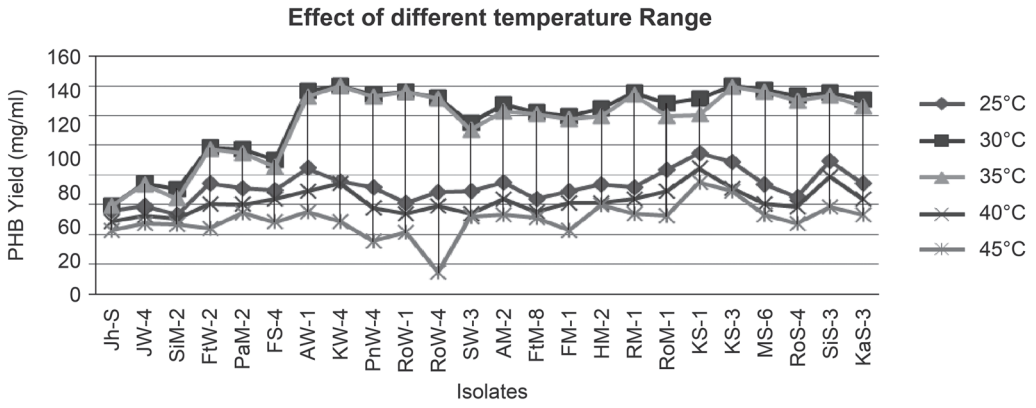

Fig. 7. Effect of incubation temperature on PHB production.

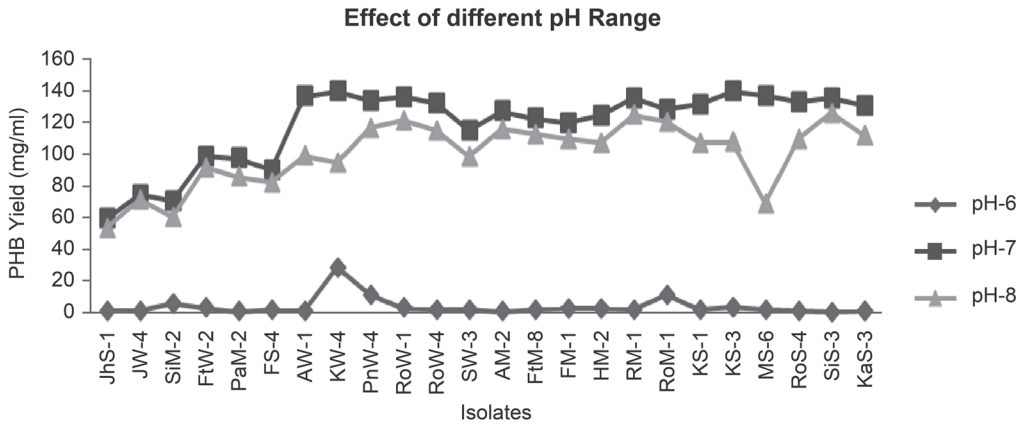

Fig. 8. Effect of pH on PHB production.

PHB production was studied by maintaining different temperature conditions (25°C, 30°C, 35°C, 40°C and 45°C) during incubation of the isolates inoculated in a medium prepared using the best carbon and nitrogen sources. The mean PHB yields of all the 24 isolates with these five different temperatures were found to be 72.47 mg/ml, 118.73 mg/ml, 115.81 mg/ml, 62.40 mg/ml and 50.12 mg/ml, respectively (Fig. 8). The incubation temperature of 30°C was found to be the optimum temperature for maximum PHB production by all the isolates. This was followed by the incubation temperature of 35°C at which the PHB yield was found to be only slightly less than the yield at 30°C. However, below 30°C and beyond 35°C, the PHB yield dropped significantly, suggesting that very low or very high temperatures do not support PHB accumulation.

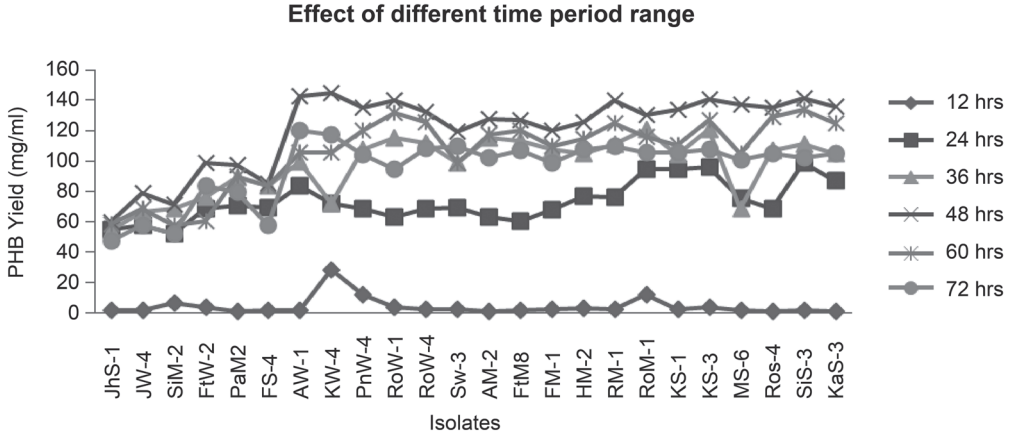

Fig. 9. Effect of incubation time on PHB production.

Effect of incubation time on PHB production. The effect of varying the growth incubation time of isolates on their PHB production was assessed by growing the isolates in a medium prepared using the best C and N sources for different lengths of time (12, 24, 36, 48, 60 and 72 h). The results revealed the mean PHB yields to be 04.08 mg/ml, 73.35 mg/ml, 97.21 mg/ml, 120.88 mg/ml, 105.72 mg/ml, 95.44 mg/ml, after 12, 24, 48, 60 and 72 h of incubation, respectively. It was observed that the PHB accumulation by different isolates increased up to 48 h of incubation, after which there was a decline in PHB production. Thus, an incubation period of 48 h was found to be optimum for maximum PHB production.

Discussion

Poly (β-hydroxybutyric acid) (PHB) is an intracellular microbial thermoplastic that is widely produced by many bacteria (Lee and Chang, 1995; Poirier *et al*., 1995; Braunegg *et al*., 1998). Due to its similarity in physical properties with synthetic plastics, it is possible to use PHB in place of conventional plastics. In certain applications, PHB can directly replace the traditional, nonbiodegradable polymers. Use of PHB, primarily as polymer blends, is therefore, becoming quite popular; as such blends greatly increase the spectrum of possible applications by expanding the range of available physical properties. But, the high production cost of PHB restricts its widespread use. However, if microorganisms capable of producing polyhydroxybutyrate are exploited for optimization of PHB production, this may reduce production cost and help in their large scale use for different applications. Plants are colonised by numerous bacteria which are capable of accumulating polyhydroxybutyrates as energy and carbon source; particularly the rhizosphere, which is characterised by temporal and spatial changes in nutrient availability, appears to be a good source for the isolation of PHB producers for biotechnological applications. Keeping this in view, the present study was designed to obtain PHB producing bacterial isolates from the rhizosperic soil of different crops, and to optimize the various culture conditions for maximizing PHB production by them.

Keeping this in view, in the present study, bacteria were isolated from soil samples collected from the rhizospheric area of three different crops on nutrient agar medium. Screening of the bacterial isolates for PHB production was done by using Sudan Black B dye. Sudan Black dye has been used as a screening measure for PHB production by several workers (Pal *et al*., 2009; Reddy *et al*., 2009; Bereka and Thawadi, 2012; Aly *et al*., 2013). Further, PHB production by different isolates was assessed by growing them in MSM supplemented with different sugars; and it was observed that the isolates produced maximum PHB by utilization of glucose as the sugar or C-source. Sujatha *et al*. (2005) reported that Luria Bertani broth supplemented with 2% glucose favours PHB accumulation due to higher C: N ratio. However, working with different carbon sources in MSM broth, Khanna and Srivastava (2005) observed higher PHB yield on fructose by *Alcaligenes eutrophus*. They reported that glucose and fructose, being monosaccharides were readily utilized by bacteria and, hence, support growth and subsequently PHB production, however, the complex molecules like starch and lactose were not utilized for effective PHB production. In our experiments also, the isolates did not produce PHB on maltose and arabinose indicating that the isolates do not possess enzymes involved in the degradation of arabinose and maltose into glucose. As the complexity of the carbon source increased, PHB yield was found to decrease. Similar conclusions were made by Joshi and Jayaswal (2010). To study the effect of N and to select the best N source for maximum PHB production, different nitrogen sources like ammonium sulphate, ammonium chloride and yeast extract were included in the mineral salts medium (1 g/l), with the best carbon source

(glucose, 2%). It is evident from our results that ammonium sulphate was the best supporter of PHB production. These results are in agreement with the results obtained by Khanna and Srivastava (2005) who also observed the highest PHB production (2.260 g/100 ml) by *R. eutropha* on MSM medium supplemented with ammonium sulphate. Mulchandani *et al.* (1989) and Raje and Srivastav (1998) also worked on the accumulation of PHB by *A. eutrophus* with different salts of ammonium. Similar to the results of the present study, they also obtained highest PHB yield in ammonium sulphate followed by ammonium chloride. Ammonium sulphate being a simple nitrogen source is probably more readily available than the other complex nitrogen sources.

PHB yield was also estimated by growing the isolates in MSM supplemented with different concentrations of the best nitrogen source, *i.e*., ammonium sulphate. It was found that ammonium sulphate at a concentration of 1.0 g/l supported the highest PHB production compared to other concentrations (0.5 and 1.5 g/l) tested. An observed decrease in PHB accumulation upon increasing the ammonium sulphate concentration beyond 1.0 g/l may be attributed to the absence of nitrogen stress condition required for accumulation of PHB. The results of the present study are in accordance with Belal (2013), Khanna and Srivastava (2005), and Shaaban *et al*., (2012) who have also reported maximum PHB accumulation at 1 % concentration of ammonium sulphate. PHB accumulation when assessed by using different C:N ratios maintained using the best carbon and nitrogen sources, it was found that C:N ratio as 20:1 resulted into maximum PHB production. Similar observations have been made by Belal (2013) and Panigrahi and Badveli (2013).

The results of PHB yields at different temperature conditions are in accordance with Grothe *et al*. (1999). They found that 33°C incubation temperature is optimum for PHB synthesis under fermentation condition. The data from our study also concluded that although 30°C was the optimum temperature for PHB production, but high PHB accumulation was also observed at 35°C. The influence of pH of culture media on PHB production was also optimized and highest production was obtained at pH range of 7.0. The obtained results (pH) were in agreement with Aslim *et al*. (2002) who also observed that the PHB in *Rhizobium* sp. strain produced was maximum at pH 7.0. Grothe *et al.* (1999) also reported that pH value ranging from 6.0–7.5 is optimum for PHB production. However, contrary to these, Nakata (1963) reported that PHB production occurs at pH 6.4 and that the lack of polymer accumulation at higher pH value can best be explained by an effect on the degenerative enzymes of polymer breakdown, so that the PHB is utilized at the rate almost equal to the rate of its synthesis.

During optimization studies related to the incubation period, the maximum PHB yield was found to be obtained after 48 h of incubation of the isolates in the medium under stationary conditions of growth and it was found to decrease thereafter. This reduction in PHB production after 48 h may be due to lack of micronutrients as well as increase in metabolites that might have negative effect on the PHB production (Flora *et al*., 2010). Studies conducted by Bonartseva *et al*. (1994) are also in consonance with these results wherein the maximal PHB accumulation was observed at 48 h. After 48 h, unfavorable conditions of the medium caused a decrease in PHB yield. This might be because the increase in medium viscosity accompanies exopolysaccharide production resulting in oxygen transfer limitation, causing a decrease in PHB synthesis (Stam *et al*., 1986). The yield decreased at 60 and 72 h; the decrease of PHB indicates that the bacteria use PHB as a source of carbon, causing unsuitable conditions due to inadequate nitrogen and carbon sources in the medium.

Conclusion. The major objective of the present study was to isolate effective polyhydroxybutyrate producing strains and to optimize their culture conditions so as to obtain the maximum PHB yield. According to the results of the present study, the optimum culture conditions for maximum PHB production by a wide range of soil bacteria include supplementation of the culture medium with glucose as C-source, ammonium sulphate at a concentration of 1.0 g/l with the C:N ratio maintained as 20:1 , pH as 7.0 and incubation at 30°C for 48 h. Four promising isolates, *viz.*, KW-4, KS-3, MS-6 and AW-1 were found to accumulate a high level of PHB at the optimized culture conditions; thus, showing a potential for their exploitation in industrial PHB production. The present study has thus provided useful data about the optimized conditions for PHB production that can be utilized for industrial production of PHB, a fast emerging alternative of non biodegradable plastics.

Acknowledgement

We wish to express our sincere gratitude to the University Grants Commission, New Delhi, for providing the financial support for carrying out this research.

Literature

Aly M.M., M.O. Albureikan, H.E.I. Rabey and S.A. Kabli. 2013. Effects of culture conditions on growth and poly-B-hydroxybutyric acid production by *Bacillus cereus* MM7 isolated from soil samples from Saudi Arabia. *Life Science Journal*. 10(4): 1884–1891.

Aslim B., Z.N. Yuksekdag and Y. Beyatli. 2002. Determination of PHB growth quantities of certain *Bacillus* species isolated from soil. *Turkish Electronic J. Biotechnol*. Special Issue: 24–30.

Barnard G.N. and J.K. Sander. 1989. The poly-b-hydroxybutyrate granule *in vivo*. A new insight based on NMR spectroscopy of whole cells. *J. Biol. Chem*. 264: 3286–3291.

Belal E.B. 2013. Production of poly-B-hydroxybutyric acid (PHB) by *Rhizobium elti* and *Pseudomonas stutzeri*. *Current Research Journal of Biological Sciences*. 5(6): 273–284.

Berekaa M. and A.M. Thawadi. 2012. Biosynthesis of polyhydroxybutyrate (PHB) biopolymer by *Bacillus megaterium* SW1-2: Application of Box-Behnken design for optimization of process parameters. *African J. Microbiol. Res*. 6(4): 838–845.

Bonartseva, G.A., V.L. Myshkina and E.D. Zagreba. 1994. Poly-b-hydroxybutyrate content in cells of various *Rhizobium* species during growth with different carbon and nitrogen sources. *Microbiol.* 63(1): 45–48.

Braunegg G., G. Lefebvre and K.F. Genser. 1998. Polyhydroxyalkanoates, biopolyesters from renewable resources: Physiological and Engineering Aspects. *J. Biotechnol*. 65: 127–161.

Fiechter A. 1990. Plastics from bacteria and for bacteria: Poly (beta-hydroxybutyrate) as natural, biocompatible and biodegradable polyesters. Springer-Verlag, New York, pp. 77–93.

Flora G.D., K. Bhatt and U. Tuteja. 2010. Optimization of culture conditions for poly b-hydroxybutyrate production from isolated *Bacillus* species. *J. Cell and Tissue Res.* 10(2): 2235–2242.

Gram C. 1884. The differential staining of Schizomycetes in tissue sections and in dried preparations. *Fortschitte der Medicin*. 2: 185–189.

Grothe, E., M. Moo-Young and Y. Chisti. 1999. Fermentation optimization for the production of poly-(B-hydroxybutyric acid) microbial thermoplastic. *Enzym. Microbial. Tech*. 25: 132–141.

Halami P.M. 2008. Production of polyhydroxyalkanoate from starch by the native isolates *Bacillus cereus* CFR06. *World J. Microbiol. Biotechnol*. 24(6): 805–812.

Haywood, G.W., A.J. Anderson, L. Chu and E.A. Dawes. 1988. Characterization of two 3-ketothiolases possessing differing substrate specificities in the polyhydroxyalkanoate synthesizing organism *Alcaligenes eutrophus*. *FEMS Microbiol. Lett*. 52: 91–96.

Hyakutake M., Y.Saito, S. Tomizawa, K. Mizuno and T. Tsuge. 2011. Polyhydroxyalkanoate (PHA) synthesis by class IV PHA synthases employing *Ralstonia eutropha* PH44 as host strain. 75(8): 1615–1617.

Joshi P.A. and S.R. Jaysawal. 2010. Isolation and characterization of poly-B-hydroxyalkanoate producing bacteria from sewage sample. *J. of Cell and Tissue Research*. 10(1): 2165–2168.

Khanna S. and A. K. and Srivastava. 2005. Statistical media optimization studies for growth and PHB production by *Ralstonia eutropha*. *Process of Biochemistry*. 4: 2173–2183.

Law J.H. and R.A. Slepecky. 1961. Assay of poly-β-hydroxybutyric acid. *J. Bacteriol*. 82: 33–36.

Lee S.Y. 1996. Bacterial polyhydroxyalkanoates. *Biotechnol. Bioeng.* 49: 1–14.

Lee S.Y. and H.N. Chang. 1995. Production of poly(hydroxyalkanoic acid). *Adv. Biochem. Eng. Biotechnol.* 52: 27–58.

Legat A., C. Gruber, K. Zangger, G. Wanner and H. Stanlotter. 2010. Identification of polyhydroxyalkanoates in *Halococcus* and other haloarchaeal species. *Appl. Microbiol. Biotechnol.* 87(3): 1119–1127.

Mohamed T., M. Shaaban, A. Turky and E.I. Mowafy. 2012. Production of some biopolymers by some selective Egyptian soil bacterial isolates. *J. Applied Sciences and Research*. 8(1): 94–105.

Mulchandani A., J.H.T. Luong and C. Groom. 1989 Substrate inhibition kinetics for microbial growth and synthesis of poly-β-hydroxybutyric acid by *Alcaligenes eutrophus* ATCC 17697. *Applied Microbial Biotechnology* 30: 11–17.

Murray R.G.E., R.N. Doetsch and C.F. Rainbow. 1994. Determinative and cytological light microscopy. In: Methods for General and Molecular Bacteriology. Eds., Gerhardt P., R.G.E. Murray, W.A. Wood and N.R. Kreig. Washington DC: American Society for Microbiol. Pp. 21–41.

Nakata H.M. 1963. Effect of pH on intermediates produced during growth and sporulation of *Bacillus cereus. J. Bacteriol*. 86: 577–581.

Pal A., A. Prabhu, A.A. Kumar, B. Rajagopal, K. Dadhe, V. Ponnamma and S. Shivakumar. 2009. Optimization of process parameters for maximum poly(-B-) hydroxybutyrate (PHB) production by *Bacillus thuringiensis* IAM12077. *Polish J. Microbiol*. 58(2): 149–154.

Panigrahi S. and U. Badveli. 2013. Screening, isolation and quantification of PHB-producing soil bacteria. *Int. J. of Engg. Sci. Innovation*. 2(9): 01–06.

Peoples O.P. and A.J. Sinskey. 1989. Poly-3-hydroxybutyrate (PHB) biosynthesis in *Alcaligenes eutrophus* H16. Identification and characterization of the PHB polymerase gene (*phbC*). *J. Biol. Chem*. 264: 15298–15303.

Poirier Y., C. Nawrath and C. Somerville. 1995. Production of polyhydroxyalkanoates, a family of biodegradable plastics and elastomers, in bacteria and plants. *Biotechnology* (NY) 13: 142–150.

Raje, P. and A.K. Srivastav. 1998. Updated mathematical model and fed batch strategies for poly-β-hydroxybutyrate (PHB) production by *Alcaligenes eutrophus*. *Bioresource Technology* 64: 185–192.

Reddy S.V., M. Thirumala and S.K. Mahmood. 2009. Production of PHB and P(3HB-co-3HV) biopolymers by *Bacillus megaterium* strain OU303A isolated from municipal sewage sludge. *World J. of Microbiol. and Biotechnol.* 25(3): 391–397.

Rodriguez-Contreras A., M. Koller, M.M. deSousa Dias, M. Calafell, G. Braunegg and M.S. Marques-Calvo. 2013. Novel poly [(R)-3-hydroxybutyrate]- producing bacterium isolated from a Bolivian hypersaline lake. *Food Technol. and Biotechnol*. 51(1): 123–130.

Sangkharak K. and P. Prasertsan. 2008. Nutrient optimization for production of polyhydroxyutyrate from halotolerant photosynthetic bacteria cultivated under aerobic-dark condition. *Electronic Journal of Biotechnology*. 11(3): 83–94.

Shaaban M.T., M. Attia, A.S. Turky and E.I. Mowafy. 2012. Production of some biopolymers by some selective Egyptian soil bacterial isolates. *J. Appl. Sci. Res*. 8(1): 94–105.

Soam A., A.K. Singh, R. Singh and S.K. Shahi. 2012. Optimization of culture conditions for bio-polymer producing *Bacillus mycoides* (WSS2) bacteria from sewage. *Current Discovery*. 1(1): 27–32.

Stam H., H.W. Verseveld, W.D.E. Van Vries and A.H. Stouthamer. 1986. Utilization of poly-β-hydroxy butyrate in free-living cultures of *Rhizobium* ORS571. *FEMS Microbiol. Lett.* 35: 215–220.

Sudesh K., H. Abe, and Y. Doi. 2000. Synthesis, structure and properties of polyhydroxyalkanoates: biological polyesters. *Prog Polym Sci.* 25: 1503–1555.

Sujatha K.A., Mahalakshmi and R. Shenbagarathai. 2005. Analysis of PCR products for PHB production in indigenous *Pseudomonas* sp. LDC-5. *Indian J. Biotechnol*. 4: 323–335.

Suresh Kumar M., S.N. Mudaliar, K.M.K. Reddy and J. Chakrabarti. 2004. Production of biodegradable plastics from activated sludge generated from a food processing industrial waste water. *Bioresource Technol*. 95: 327–330.

Verlinden R.A.J., D.J. Hill, M.A. Kenward, C.D. William and Radeckal. 2007. Bacterial synthesis of biodegradable polyhydroxyalkanoates. *J. Appl. Microbiol*. 102: 1437–1449.

Wang H.H., X.T. Li and G.Q. Chen. 2009 Production and characterization of homopolymer polyhydroxyheptanoate by a *fad*BA knockout mutant *Pseudomonas putida* KTOY06 derived from *P. putida* KT2442. *Process Biochemistry* 44(1): 106–111.

Williams S.T., M.E. Sharpe and J.G. Holt. 1994. Bergey's Manual of Systematic Bacteriology. 9th Eds. Williams and Wilkins, Baltimore, USA.

Polish Journal of Microbiology
2015, Vol. 64, No 3, 241–252

ORIGINAL PAPER

Phytoremediation of Polycyclic Aromatic Hydrocarbons in Soils Artificially Polluted Using Plant-Associated-Endophytic Bacteria and *Dactylis glomerata* as the Bioremediation Plant

ANNA GAŁĄZKA*[1] and RAFAŁ GAŁĄZKA[2]

[1] Institute of Soil Science and Plant Cultivation – State Research Institute, Department of Agricultural Microbiology, Puławy, Poland
[2] Institute of Soil Science and Plant Cultivation – State Research Institute, Department of Soil Science Erosion and Land Protection, Puławy, Poland

Submitted 5 August 2014, revised 16 January 2015, accepted 16 January 2015

Abstract

The reaction of soil microorganisms to the contamination of soil artificially polluted with polycyclic aromatic hydrocarbons (PAHs) was evaluated in pot experiments. The plant used in the tests was cock's foot (*Dactylis glomerata*). Three different soils artificially contaminated with PAHs were applied in the studies. Three selected PAHs (anthracene, phenanthrene, and pyrene) were used at the doses of 100, 500, and 1000 mg/kg d.m. of soil and diesel fuel at the doses of 100, 500, and 1000 mg/kg d.m. of soil. For evaluation of the synergistic effect of nitrogen fixing bacteria, the following strains were selected: associative *Azospirillum* spp. and *Pseudomonas stutzerii*. Additionally, in the bioremediation process, the inoculation of plants with a mixture of the bacterial strains in the amount of 1 ml suspension per 500 g of soil was used. Chamber pot-tests were carried out in controlled conditions during four weeks of plant growth period. The basic physical, microbiological and biochemical properties in contaminated soils were determined. The obtained results showed a statistically important increase in the physical properties of soils polluted with PAHs and diesel fuel compared with the control and also an important decrease in the content of PAHs and heavy metals in soils inoculated with *Azospirillum* spp. and *P. stutzeri* after cock's foot grass growth. The bioremediation processes were especially intensive in calcareous rendzina soil artificially polluted with PAHs.

Key words: *Azospirillum* spp., *Dactylis glomerata, Pseudomonas stutzeri,* diesel fuel phytoremediation, polycyclic aromatic hydrocarbons (PAHs)

Introduction

Persistent organic pollutants, including petroleum derivatives, are emitted to the environment mainly from anthropogenic sources and are characterized by high toxicity and power for bioaccumulation. More than 90% of global PAH's pollution that is coming from the combustion of organic matter is accumulated in the surface layer of soil (Anderson *et al*., 1993; Andreoni and Gianfreda, 2007). Biological degradation of petroleum derivatives by microorganisms and decline of metals often show a synergistic effect and is one of the most effective and most secure ways to remove them from the environment but the process is lengthy and multistage (Cerniglia, 1992). As a result of the metabolic activity of microorganisms, hydrocarbons are partially or completely turned into bacterial mass and stable, non-toxic end products. The effectiveness of the microbiological decomposition of PAHs in soil, requires the use of strains not only capable of catabolic degradation of pollutants and their usage as the only source of carbon and energy, but also a number of other features allowing adaptation to contaminated conditions and cometabolic degradation of organic compounds (Siciliano and Germida, 1998; Chauhan *et al*., 2008; Lee, 2013).

Phytoremediation, or use of plants and associated rhizosphere to decontaminate polluted sites, is considered today, as a realistic, low-cost alternative for treatment of extensive areas of pollution by organic chemicals (Dominguez-Rosado and Pitchel, 2004; Ma *et al*., 2010). This technology is based on the catabolic potential of root-associated microorganisms, which are supported by the organic substrates in root excretions and by a favorable micro-environment in the rhizosphere. Soils polluted by polycyclic aromatic hydrocarbons (PAHs) are suitable for treatment by phytoremediation, since several scientific studies, performed

* Corresponding author: A. Gałązka, Institute of Soil Science and Plant Cultivation – State Research Institute, Department of Agricultural Microbiology, Puławy, Poland; **e-mail: agalazka@iung.pulawy.pl**

with well-designed controls, have specifically shown higher rates of PAH biodegradation in whole soils planted with a variety of species. Biodegradation of PAHs in soils is often limited by the slow mass transfer of these hydrophobic compounds towards degrading microbes. This slow process may lead to bioavailability restrictions, even in the conditions of massive contamination often faced by bioremediation technologies. Little is known about bioavailability in phytoremediation systems. Specific bioavailability-promoting mechanisms, operating in soils with PAH-degrading populations, may be responsible for increased rates of pollutant transformation. These include an increased bacterial adherence to the pollutants, and production of biosurfactants by bacteria or by plants (Gunther *et al*., 1996; Huang *et al*., 2004).

There are many methods for removing PAH's contamination from natural environment. The elaboration of the most effective method of bioremediation is one of the most important problems related to the protection. Such methods make use of microorganisms inhabiting the natural environment or genetically changed microorganisms which utilize hydrocarbons as a only source of energy and carbon (Liste and Felgentreu, 2006; Liang *et al*., 2011).

The most important of the mentioned transformations are those that involve microbiological processes. The main organisms contributing to the degradation of hydrocarbons in the soil environment are bacteria and fungi. However, it is thought that the dominating role in this process is played by bacteria. Bacteria carrying out the degradation of hydrocarbons belong to the genera: *Alcaligenes*, *Arthrobacter*, *Bacillus*, *Micrococcus*, *Mycobacterium*, *Pseudomonas* (Gogoi *et al*., 2003; Liste and Felgentreu, 2006; Gałązka, 2008; Mahmoud *et al*., 2011; Abhilash *et al*., 2011; Gałązka *et al*., 2012; Tejeda-Agredano *et al*., 2013). The effectiveness of the bioremediation of soils contaminated with PAHs was also confirmed in experiments on soils contaminated with a mixture of PAH and heavy metals (Ciesielczuk *et al*., 2014). It is also known that the use in inoculated plants of a mixture of bacterial strains and in particular bacteria of the genus *Azospirillum* significantly improves plant growth (Naiman *et al*., 2009; Couilleror *et al*., 2013).

Evidence for biological nitrogen fixation in grasses was reported in many publications (Hung *et al*., 2004; Joner *et al*., 2007). Studies on long-term N-balance and 15N isotope dilution technique have shown that some plants may actually obtain up to 70% of their N requirements by nitrogen fixation. In this process both rhizosphere and endophytic diazotrophs seem to participate. Nitrogen fixing bacteria such as *Azospirillum* spp. and *Pseudomonas stutzeri* colonize the plant and its tissues. *Azospirillum* species belong to the facultative endophytic diazotrophs group which colonize the surface and the interior of roots, this kind of association being considered as the starting point of most ongoing BNF programs with non-legume plants worldwide (Muratova *et al*., 2003; Król *et al*., 2007). These bacteria are microaerophilic, nitrogen-fixing, Gram-negative rods and often associated with the roots of cereals and grasses (Muratova *et al*., 2003). However, obligate endophytes such as *Gluconacetobacter diazotrophicus* and *Herbaspirillum* spp. seem to be the promissory group in relation to nitrogen fixation associated with grasses. These bacteria have an advantage over root-associated diazotrophs, as *Beijerinckia* spp. and *Azotobacter* spp., they colonize the interior rather than the surface of plants, hence have better possibilities to exploit carbon substrates supplied by the plant (Steenhoudt *et al*., 2000). *Azospirillum* spp. and *P. stutzeri* are capable of creating permanent associations with the roots of most cereals and grasses, and use PAHs as the only carbon and energy source, as well as produce biosurfactants (Okon and Vanderleyden, 1997). Bacteria from the genus *Pseudomonas* are microorganisms that effectively decompose organic pollutants through cometabolism in natural water and soil environment. In the available literature, there is a lack of data on the participation of bacteria from the genus *Azospirillum* in the bioremediation processes. Free-living bacteria that fix nitrogen, namely *Azospirillum* spp. and *P. stutzeri*, may create permanent associations with the roots of most cereals and grasses used in plant production (Król *et al*., 2007; Gałązka *et al*., 2012).

Dactylis glomerata popularly called cock's foot grass is a very persistent plant in bioremediation studies. It does not require high temperatures for active growth, and is very winterhardy. It appreciates a high soil moisture content. *D. glomerata* can be grown successfully on a wide range of soils. This grass has an early spring growth, with a regrowth consisting mainly of leafy shoots. It is suitable for both cutting and grazing (Muratova *et al*., 2003).

The aim of the work was to estimate the effect of plant inoculation with the bacteria *Azospirillum* spp. and *P. stutzeri* on PAH degradation in soils artificially polluted with the use of cock's foot grass (*D. glomerata*) as a bioremediation plant.

Experimental

Materials and Methods

Soil samples and plant. Soil material, uptaken from the plough – humus horizon (0–20 cm) of arable land, distant from PAH emission sources, from various regions of Poland, was used for the studies

The selected soils are the most common in Lublin Province. The effect of soil (chernozem, calcareous rendzina, and lessives) pollution was studied, artificially polluted with polycyclic aromatic hydrocarbons (PAHs) and diesel fuel (DF) in the phytoremediation process. Agricultural areas from which the soil material for the studies was uptaken were distant from the sources of PAH emissions, and the content of Σ15 PAHs in the soils corresponded to the average content of those compounds in agriculturally used soils:

- charnozem generated from loess silty loam; Kułakowice near Hrubieszów
- calcareous rendzina light loamy sand; Mięćmierz near Kazimierz Dolny
- lessives generated from loess dusty loam, Las Stocki near Wąwolnica.

Plant used in the tests was cock's foot grass (*D. glomerata*), potting used about 50 seeds per pot.

Microorganisms – bacterial inoculants. Three bacterial strains were used in the study: (1) strain Aa1 isolated from endorhizosphere of barley (*Hordeum sativum*), identified by RFLP-PCR and 16S-23S rDNA methods as *Azospirillum amasoense*, (2) strain Ab2 isolated from endorhizosphere maize (*Zea mays* L.), identified by RFLP-PCR and 16S-23S rDNA methods as *Azospirillum brasilense*, (3) strain Ps, identified by RFLP-PCR and 16S-23S rDNA methods as *P. stutzeri*. This bacteria was isolated from the endorhizosphere grass *Leymus arenarius* (Król *et al*., 2007).

The physiological properties of *Azospirillum* spp. were determined with the use of BIOLOG test (Król *et al.*, 2007; Gałązka, 2008). Strains Aa1 and Ab2 have genes of the catabolic pathway of PAH degradation: catechol 2,3-dioxygenase (C2,3-DO), and naphtalene dioxygenase (NDO) (Gałązka, 2008). In the bioremediation process, plant inoculation with bacteria mixtures *Azospirillum* spp. and *P. stutzeri* was additionally applied on *D. glomerata* seeds inoculation in amount of 1 ml per 500 g of soil in proportion 1:1:1 for strains (Aa1:Ab2:Ps). An inoculum with approximate density of 0.5×10^7 cfu/ml was used for the experiments.

Bacteria strains (Aa1, Ab2) *Azospirillum* spp. and *P. stutzeri* (Ps), originated from the collection of the Department of Agricultural Microbiology, Institute of Soil Science and Plant Cultivation – State Research Institute in Puławy, Poland. Measuring the density of pure strains and tested by plating serial dilutions on nutrient agar plates. The plates were incubated in a thermostat at 28°C on PDA medium (*Azospirillum*) and Nfb medium for *P. stutzeri*. In order to verify the purity of the strains a single colony was viewed under a microscope.

Pot experiment. Pot-tests were carried out in controlled conditions in a climatic chamber during a four-week-long plant growth period with 16-hour lighting (light intensity 240 E/ms). Tests were carried out at the temperature of 24°C during the day and for 8 hours at night at the temperature of 18°C. In the pots, 500 g of air-dry, sieved soil were placed. Hydrocarbons were added as a solution in dichloromethane, reaching concentrations of 100, 500, and 1000 mg/kg d.m. of soil. Dichloromethane was also added to control soil for every pollution level, at the concentration equal to the polluted samples. Samples were left for 48 hours for the solvent to evaporate. Subsequently, the soil was thoroughly stirred and moistened to 60% of full water capacity. After soil moistening, in the pots pre-sprouted cock's foot grass seeds were sown (50 plants per pot). After the completion of the four-week plant growth cycle in the particular experiment combinations, basic physical properties of the soils were determined, as well as anthracene, phenanthrene, and pyrene content in artificially polluted soils and Σ15 PAHs in the case of soil pollution with diesel fuel.

Determination of physical and chemical properties of the soils. Basic physical properties of the soils were marked: soil texture (Casagrande'a method), pH (PN-ISO 10390:1997), total organic carbon (C_{org}-using the Tiurin's method) and total Kjeldahl nitrogen content (N_{total}-using flow spectrometry, wet sample mineralization).

Determination of biochemical and microbiological properties of soils. Soil microbial properties were evaluated on the basis of six parameters on different functional levels: three on the population level [total bacteria number (Wallace and Lockhead, 1950), total fungi number (Martin, 1950) and total number of microorganisms capable of degrading PAH (Jones and Edington, 1968)] and three on the activity level [dehydrogenase (Caside *et al*., 1964) and acid and alkaline phosphatase activities (Tabatabai and Bremner, 1969)]. Microorganisms were enumerated in triplicate using the plate-count techniques. Aqueous suspensions of the microbial population in 10 g of soil sample were serially diluted. Plates were inoculated at 28°C for 3 or 5 days prior to counting colony forming units (cfu). After the vegetation period the total number of microorganisms in the soil samples capable of degrading PAH as the sole source of carbon and energy was determined.

Determination of polycyclic aromatic hydrocarbons. For the experiment with artificial soil pollution the following compounds were chosen: anthracene, phenanthrene, and pyrene, which were applied in 100, 500, and 1000 mg/kg d.m. of soil doses and diesel fuel (Multi Motor Oil Jasol 12 SG/CE 5W/4 originating from Jasło Refinery, JSC, Poland) at the concentration of 100, 500, and 1000 mg/kg d.m. of soil. PAHs used in the soil samples were determined by HPLC: 20 µl of the extract was injected onto a reverse phase HPLC column (Li Chro CART® 250–4) using water and acetonitrile gradient with a flow rate of 1 ml/min.

PAHs in the samples were detected using UV (254 nm) absorbance detection and degradation was quantified against a negative control. The Σ15 PAHs were analysed, accepted for determination in environmental samples by the United States Environmental Protection Agency, excluding the most volatile hydrocarbons and those that rarely occur in soils.

Analysis of diesel fuel chemical composition was carried our according to the Decree by the Ministry of the Environment from September 9, 2002 concerning soil quality standards and ground quality standards. Determinations were made in chernozem, calcareous rendzina, and lessives with the highest doses of PAHs and diesel fuel. A dose of 1000 mg/kg PAHs, 1000 mg/kg of diesel fuel is equivalent to the border content of PAHs for soil used in agriculture and recreational areas. The scope of the applied PAH levels was equivalent to the content of these compounds that occur in soils in non-polluted areas, as well as from industrial areas (Kabata-Pendias *et al.*,1995).

Determination of heavy metals in soil samples. Microwave digestion of soil with the use of aqua regia in middle pressure (32 bars) digestion vessels coupled with ICP-MS (inductively coupled plasma mass spectrometry) technique was used for quantitative analysis of metals. Mars Xpress by CEM microwave digestion system was used for accelerated pressurized digestion of soil samples, 0.5 g of air dried soils was used with 10 ml of aqua regia prepared from Instra-analyzed grade nitric and hydrochloric acids by J.T. Baker. The setup of the digestion system was as follows: Power: 1600 W, temperature: 170°C, ramping time: 25 minutes, holding time: 20 minutes, cool down time: 20 minutes. Then the analyte was transferred to falcon vials and diluted to 50 ml with distilled water (0.05 μS/cm). The samples were additionally diluted 1:10 directly before the analysis. The same procedure was carried out for blank samples and to ensure quality control, for certified reference materials.

The quantitative analysis was conducted on Agilent 7500ce ICP-MS. This instrument is fitted with a micro mist nebulizer, Peltier cooled double pass spray chamber, peristaltic pump. Argon 5.0 (99.999% purity) was used as the carrier gas. The instrument was also fitted with a torch with "shield torch" system reducing so called "secondary discharge", off-axis ion lenses that prevent photons from entering the reaction cell and quadrupole, reaction/collision chamber with hydrogen 6.0 and helium 6.0 (purity 99.9999%) as reaction/collision gasses for the elimination of interferences. The vacuum system consisted of a rotary and turbomolecular pump. Quadrupol with hyperbolic rods is the mass separator that separates ions on the basis of their mass to charge (m/z) ratio. The detector has the ability to work in two modes: digital and analog that makes measurement through nine orders of magnitude possible. All determination were made in the presence of ^{45}Sc, ^{89}Y, ^{159}Tb as internal standards to minimize the matrix effect and ensure long term stability. The quantification limits were set at 0.01 mg/kg and the accuracy was 10%.

Statistical analysis. A randomized complete design in a factorial scheme was implemented with one plant. Three soils, two patterns of plants: (+) – inoculated, (–) – noninoculated and three replications. Analysis of variance procedure (one way ANOVA) for all treatments was conducted using the programme packet STATISTICA.PL (7) (Stat. Soft. Inc., 95% significance level). The difference between specific pairs of means was identified using Tukey test ($P < 0.05$).

Results and Discussion

Polycyclic aromatic hydrocarbons (PAHs) are compounds whose presence in contaminated soils and sediments poses a significant risk to the environment, and they have cytotoxic, mutagenic, and in some cases carcinogenic effects on human tissue (Parales *et al.*, 2002; Yu *et al.*, 2013).

The data concerning the effect of PAH's and diesel fuel on basic physical properties and biological indicators of the soil involving grass inoculation applied in the studies with bacteria *Azospirillum* spp. and *P. stutzeri* suspensions are presented in this work (Table I). It was found that soil pollution indeed contributed to a deterioration in the studied physical indicator. Statistically significant improvement was also found in the physical parameters and biological activity of the studied soils after grass inoculation with bacteria *Azospirillum* spp. and *P. stutzeri* during four-week plant growth. A statistically significant decrease in the content higher values of such parameters as: pH, total carbon was found in soils after bioaugmentation of plants with nitrogen fixing bacteria. The highest dehydrogenase activity and total number of bacteria were found in chernozem after growth of grasses inoculated with nitrogen fixing bacteria. Also soil contaminated with diesel fuel stimulated the enzymatic activity. Dehydrogenase, alkaline phosphatase and acidic phosphatase activities in chernozem and rendzina polluted with PAHs after the growth of plants was always higher after bioaugmentation of the plants. Relatively, the highest enzymatic activities and total number of bacteria were noted for samples inoculated with *Azospirillum* spp. and *P. stutzeri* – almost 20–40% more than for the control. The dehydrogenase activity appeared to be the most sensitive parameter of all six biological indexes tested. High applicability of this parameter for soil ecotoxicological testing was pointed out by other authors (Gogoi *et al.*, 2003; Parrish

Table I
Physical and biological properties of soils polluted with PAHs (1000 mg·kg^{-1}) and diesel fuel (PAHs (1000 mg·kg^{-1}).

PAHs/diesel fuel	pH	C_{total}%	N_{total}%	B+A	F	DEH	PHO Acid	PHO Alk
Chernozem								
Control	7.48	2.75	0.147	123	42	75	85	36
Non-inoculated grass								
Anthracene	7.25	2.52	0.121	54	36	54	38	15
Phenanthrene	7.15	2.58	0.113	48	28	48	41	21
Pyrene	7.13	2.55	0.128	37	21	52	45	18
Diesel fuel	7.02	2.84	0.135	124*	46	64	56	14
Grass inoculated with *Azospirillum* spp. and *Pseudomonas stutzeri*								
Anthracene	7.48*	2.78*	0.142*	110*	52	62	48	25
Phenanthrene	7.48*	2.85*	0.152*	144*	45	56	56	31*
Pyrene	7.35*	2.95*	0.148*	154*	48	78*	57*	36*
Diesel fuel	7.32*	2.96*	0.157*	174*	21*	88*	69*	42*
Calcareous rendzina								
Control	6.75	2.21	0.123	187	37	64	68	42
Grass non-inoculated								
Anthracene	6.64	1.78	0.107	74	23	42	36	26
Phenanthrene	6.72	1.73	0.105	56	31	38	42	28
Pyrene	6.52	1.77	0.110	53	28	36	39	31
Diesel fuel	6.31	1.88	0.092	197*	42	45	31	27
Grass inoculated with *Azospirillum* spp. and *Pseudomonas stutzeri*								
Anthracene	6.88*	2.22*	0.134*	98	21*	56	45	36*
Phenanthrene	6.82*	2.21*	0.144*	237*	18*	58	56*	41*
Pyrene	6.85*	2.23*	0.138*	186*	24	66*	43*	33*
Diesel fuel	6.89*	2.32*	0.146*	245*	16*	56	58*	28
Lessives								
Control	5.37	1.21	0.097	42	18	32	46	26
Grass non-inoculated								
Anthracene	5.22	1.32	0.094	34	14	12	15	15
Phenanthrene	4.84	1.33	0.085	24	16	14	21	10
Pyrene	4.67	1.22	0.084	26	12	7	18	8
Diesel fuel	4.52	1.27	0.092	87*	8*	23	16	12
Grass inoculated with *Azospirillum* spp. and *Pseudomonas stutzeri*								
Anthracene	5.75*	1.56*	0.099	56	8	34	32	18
Phenanthrene	5.75*	1.63*	0.112*	78*	5*	24	37	15
Pyrene	5.78*	1.62*	0.108	69*	6*	26	25	10
Diesel fuel	5.82*	1.45*	0.115*	120*	5*	42	34	15

* statistically significant decrease in the content ($P \leq 0.05$) in comparison with the control in the particular soils;
data is an arithmetic mean (n = 6) control –soil non-polluted with PAHs and diesel fuel – with no plant
pH – using the potentiometric method
C_{total} – using the Tiurin's method
N_{total} – using flow spectrometry, wet sample mineralisation
B+A – total number of bacteria and Actinomycetes (10^7 cfu·g^{-1} d.m. of soil)
F– total number of fungi (10^4 cfu·g^{-1} d.m. of soil)
DEH – dehydrogenase activity (μg·g^{-1} d.m. of soil)
PHO Acid – acid phosphatase activity (μg·g^{-1} d.m. of soil)
PHO Alk – alkaline phosphatase activity (μg·g^{-1} d.m. of soil)

et al., 2005; Gałązka *et al*., 2012). Muratova *et al*. (2003) contaminated soil with 5 g/kg of diesel oil and observed that the activity of soil dehydrogenase increased immediately after oil introduction. *Azospirillum* spp. and *Pseudomonas* spp. are predominant plant growth-promoting rhizobacteria extensively used as phytostimultory crop inoculants, but mixed inocula involving more than two strains are not very common. The cooperation

of *Azospirillum* and *Pseudomonas* bacterial strains with fungi of the genus Glomus has a significant effect on promoting the growth and yield of maize (Couillerot *et al*., 2013). According to Gunther *et al*. (1996), pyrene had an inhibitive effect on alfalfa growth and the residual concentrations of pyrene in the rhizosphere soil were lower than those in the non-rhizosphere soil. The rhizospheric bacterial counts were 30–50% higher than those in the non-rhizosphere soil, respectively. The effectiveness of the bioremediation of high molecular weight polycyclic aromatic hydrocarbons by *Bacillus thuringiensis* strain NA2 was presented in a work by Maiti *et al*. (2012).

A wide range of different soil microorganisms are able to metabolise, co-metabolize and utilize PAHs as a sole source of carbon and energy. The aerobic catabolism of one-cyclic and two-, three-cyclic aromatic hydrocarbons by bacteria has been extensively studied. Naphthalene has often been selected as a model compound for the study of PAH degradation because of its high aqueous solubility and the ease of isolation of microbes capable of its degradation. Since the first report of a biochemical pathway for naphthalene oxidation by *Pseudomonas* species in 1964 by Davis and Evans, extensive studies have rigorously defined the metabolic pathway genes, and the enzymes involved. In the last decade a number of bacteria that metabolise larger PAHs molecules have been isolated. These include *Azoarcus evansii*, various *Mycobacterium* species and several *Pseudomonas* species (Walton *et al*., 1994; Parrish *et al*., 2005; Pizzul *et al*., 2007).

The presented results are a consequence of research initiated to obtain an answer to the question of the possibility of using the bacterial strains *Azospirillum* spp. and *P. stutzeri* in bioremediation processes, and at the same time to supplement missing data in this field of science. A positive effect of the bacteria *Azospirillum* spp. and *P. stutzeri* on PAH degradation was found in soils artificially polluted with PAHs. The bioremediation process in aged polluted soil was more intense perhaps because in that environment, numerous autochthonous groups of microorganisms capable of pollution degradation are situated and the introduced strains additionally increased the effect (Walton *et al*., 1994; Parrish *et al*., 2005).

Phytoremediation occurs the most intensely in the rhizosphere, so the depth to which the roots grow is one of the most important factors that limit the process (Muratova *et al*., 2003; Hung *et al*., 2004; Gałązka *et al*., 2012). The studies conducted so far demonstrate that the most effective phytoremediation of soil polluted with hydrocarbons is obtained with the sowing of monocotyledonous plants, including grasses (Leigh *et al*., 2002). Good results are given also by legumes, which may be related to root secretions rich in nitrogen compounds (Liste and Felgentreu, 2006; Ouvrard *et al*., 2013).

In order to establish the effect of plant inoculation on the degree of PAH's degradation in the polluted soils, chromatographic determinations of aromatic hydrocarbons were carried out. In the soils artificially polluted with PAHs, a significant degree of anthracene, phenanthrene, and pyrene degradation was noted (dose 1000 mg/kg) after plant inoculation with the bacteria *Azospirillum* spp. and *P. stutzeri*, particularly visible in the case of calcareous chernozem and rendzina pollution (Fig. 1a). The bioremediation process occurred most efficiently in rendzina soil, especially in degradation degree of anthracene, phenanthrene, and pyrene in the three applied doses (100, 500, and 1000 mg/kg) during four-week long grasses growth inoculated and non-inoculated with *Azospirillum* spp. and *P. stutzeri* (Fig. 1b). With the highest PAH doses (1000 mg/kg), a decrease in the content of anthracene in the soil took place – from 96% with no plant inoculation to 24% with inoculation, phenanthrene from 56 to 22%, and pyrene from 42 to 18%.

In the root area of plants, an increased bioremediation rate of organic pollutants is observed in comparison with non-rhizospheric soil (Liste and Aleksander, 2000). This is related first of all to the metabolic activity

Fig. 1a.

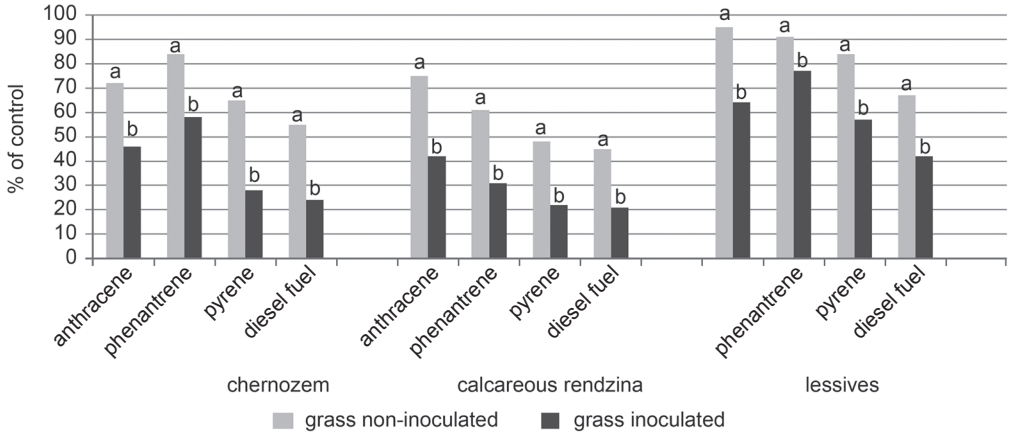

Fig. 1b.

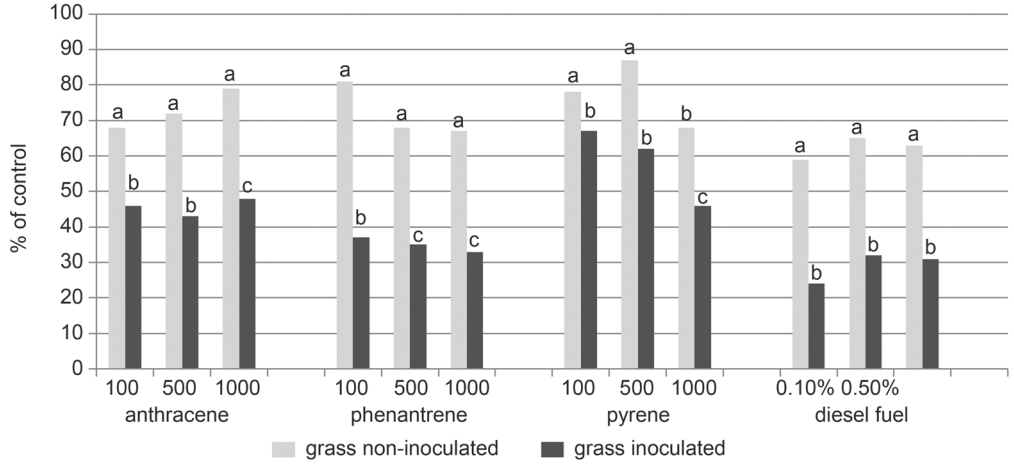

Fig. 1. Degree of PAHs degradation: a) in soils artificially polluted with anthracene, phenanthrene, and pyrene (doses in soil 1000 mg/kg) and diesel fuel (doses in soil 1000 mg/kg); b) in calcareous rendzina artificially polluted with PAHs.

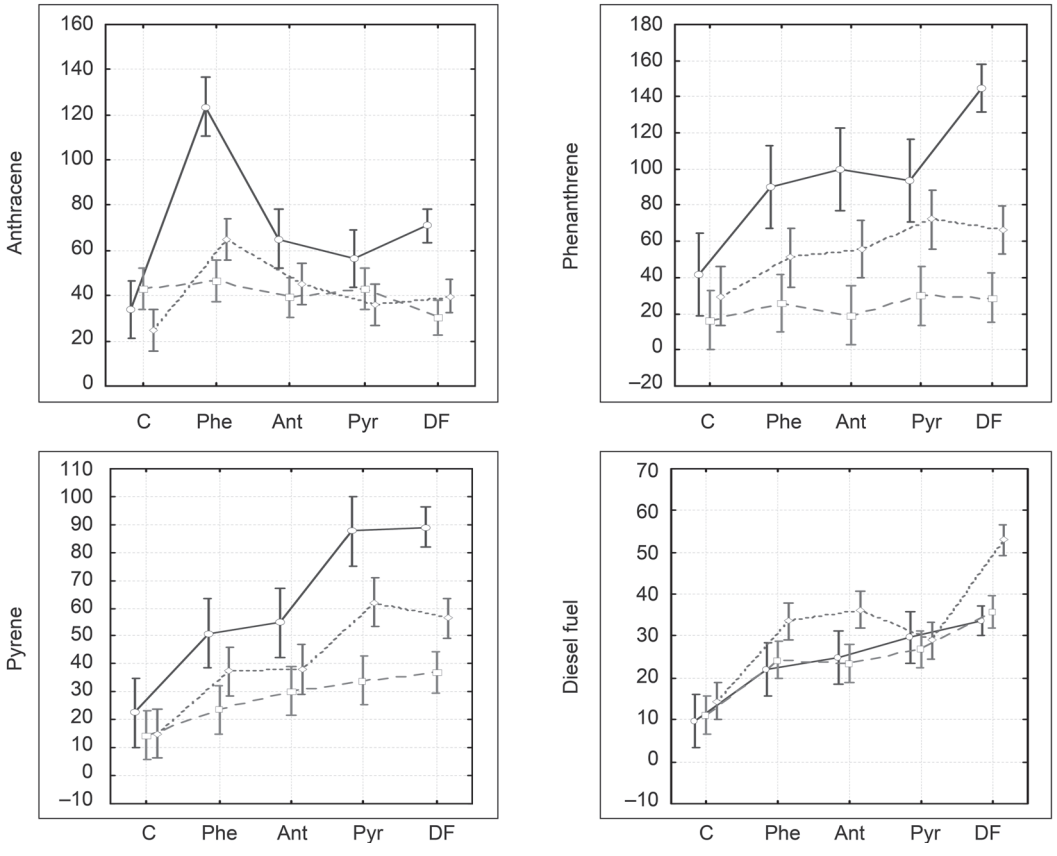

Fig. 2. The total number of microorganisms capable of degrading PAH (doses in soil 1000 mg/kg) and diesel fuel (doses in soil 1000 mg/kg) as a sole source of carbon and energy [10^4 cfu/g d.m. of soil] – two-way analysis of variance.
C – control; Phe – phenantrene; Ant – anthracene; Pyr – pyrene; DF – diesel fuel ——— chernozem – – – – rendzina ----- lesives

of microflora, which populates the rhizosphere in great numbers. It turns out that of significant importance are also microorganisms directly connected with the plant that live inside root, stem, and leaf tissues. Examples of such microorganisms are strains of *Azospirillum* spp. and *P. stutzeri*. The total number of microorganisms capable of degrading PAHs as a sole source of carbon and energy was found in in each of the studied soils (Fig. 2). The tested soils showed a large number of microorganisms capable of degrading anthracene, phenanthrene, pyrene, and diesel fuel (10^4 cfu/g d.m. of soil). The analysis of variance indicate the statistical important differences of total number of microorganism able to degrade anthracene, phenanthrene

and pyrene in different soils. The highest total number of microorganisms able to degrade diesel fuel was observed in chernozem after grown of cock's food grass. Bacteria are mayor players in the degradation of PAHs, bioremediation is an increasingly popular option for reclamation of oil-contaminated sites. Many bacteria that utilize a polycyclic aromatic hydrocarbon as the source of carbon and energy have been isolated (Pizzul *et al.*, 2007).

A number of different metabolic pathways have been established for the bacterial degradation of PAHs. The genes coding for the enzymes involved in the degradation of alkanes (*alk*), naphthalene (*nah*), benzoate *via* ortho cleavage of catechol (in bacteria) or prothocatechuate (in fungi) by the β-ketoadipate pathway have been extensively characterized. Evaluation of the effect of contaminants on soil microflora strongly depended on the applied parameters. A more detailed discussion of the results regarding the effect of PAH's on soil microorganisms is given elsewhere (Johnsen *et al.*, 2007; Ahammed *et al.*, 2012). In contrast to inorganic compounds, microorganisms can degrade and even mineralize organic compounds in association with plants. Hence the discovery of effective pathways for degradation and mineralization of organic compounds may play an important role in the future. So far, bacteria capable of degrading certain kinds of organic pollutant, such as PAHs have been isolated from a range of sites and the pathways and encoding genes have also been well studied. But most of these bacteria cannot survive in the near-starvation conditions found in soils, including the rhizosphere (Joner *et al.*, 2007). Compared with physical and chemical remediation, phytoremediation has several advantages: it preserves the natural properties of soil; it acquires energy mainly from sunlight; high levels of microbial biomass in the rhizosphere can be achieved; it is low in cost; and it has the potential to be rapid. Although with these advantages, some plants show very low tolerance to soil contaminants, which limits the degradation efficiency to an insufficient level for meaningful soil remediation. As described above, although rhizobacteria may play an important role in the degradation and mineralization of organic compounds, the metabolic efficiency can be very low. Possible causes may be the small microbial biomass or the low solubility and bioavailability under high toxic pressure (Liste and Aleksander, 2000).

Grasses, thanks to a well-developed and dense root system, became an adequate habitat for the applied in the inoculation entophytic bacteria capable of using PAHs as the only source of carbon and energy (Leigh *et al.*, 2002). A statistically significant ($P \leq 0.05$) decrease in aromatic carbon content was obtained in the polluted soils. It cannot be unambiguously stated, however, that the entire amount of PAHs per soil pollution was used by the bacteria in the bioremediation process. In the conducted studies with the use of non-inoculated plants, a decrease in PAH content in the soil was also observed, but it was significantly smaller than in the inoculated combinations. The degree of degradation of the particular aromatic hydrocarbons in the soils polluted with the highest diesel fuel doses (1000 mg/kg) is presented in Fig. 3. The highest degree of their degradation was found in calcareous rendzina (Fig. 3b). Equally intensive was the degradation of those hydrocarbons in chernozem (Fig. 3a), whilst it was significantly weaker in lessives (Fig. 3c).

Liste and Felgentreu (2006) found a decrease in gasoline hydrocarbon content to 68.7% and PAHs to 59% at mustard growth during a 90-day-long bioremediation process with natural plant rhizosphere microflora. In the present studies, with significantly higher soil pollution (1000 mg/kg) at non-inoculated and inoculated maize growth in calcareous rendzina the following results were obtained: decrease in the anthracene content in the soil from 95% with no plant inoculation to 42% with inoculation, phenanthrene from 72% to 36%, whilst pyrene from 58 to 27%. Gałązka *et al.*

Fig. 2a.

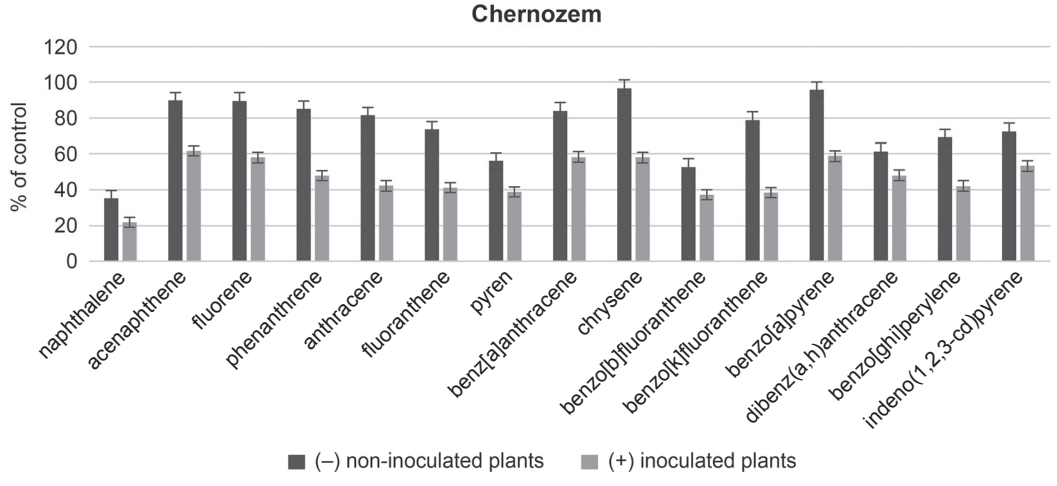

Fig. 2b.

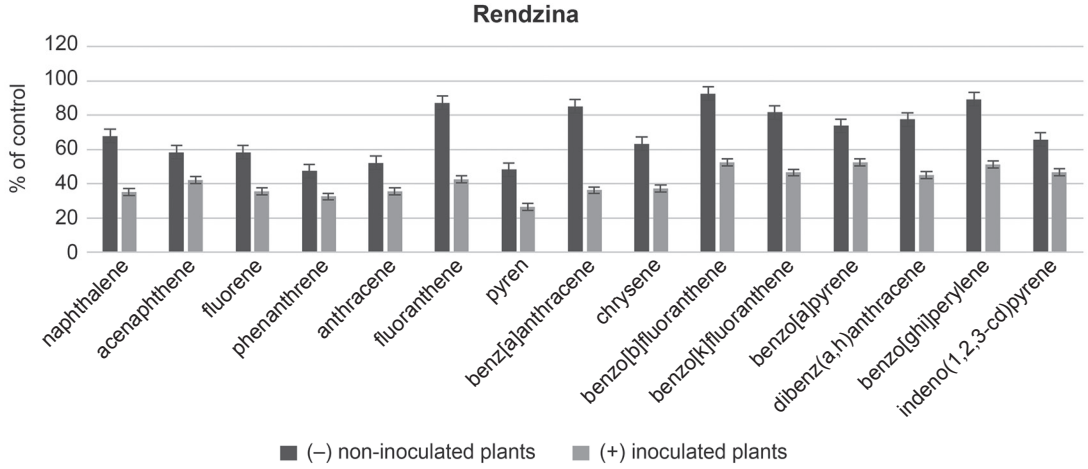

Fig. 2c.

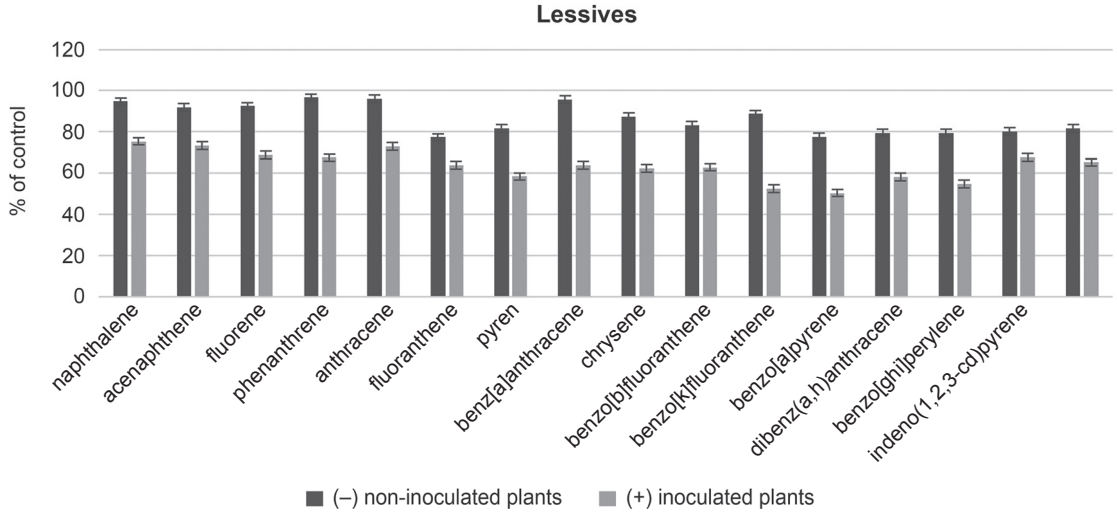

Fig 3. The PAHs content in in soils polluted with 1000 mg/kg diesel fuel.
a) chernozem, b) calcareous rendzina, c) lessives.

(2012) found the degradation degree with the highest PAHs and diesel fuel doses in soils artificially polluted during four-week long meadow fescue growth inoculated and non-inoculated with nitrogen fixing bacteria a decrease in the content of Σ15PAHs in the soil took place – from 65% with no plant inoculation to 15% with inoculation. A decrease in hydrocarbon content was noted at meadow fescue growth from 80–91% (non-inoculated plant) to 18–56% (inoculated plant), whilst it was significantly weaker in lessives.

A plant is capable – through the root system – of absorbing various organic compounds depending on their relative lipophilicity (Kang and Xing, 2006). Compounds uptaken by the plant may accumulate in the root or become permanently built into its structure, for example lignin, which is an example of pollution phytostabilisation (Siciliano and Germida, 1998). However, a significant part of the absorbed organic compound undergoes only translocation along the vascular bundles of the plant and is transpirated through the leaves. This process decreases pollution concentration in the soil but it is not advantageous to the environment because it causes atmosphere pollution. Moreover, the presence of plants in the soil intensifies humification (Liste and Aleksander, 2000; Smith *et al.*, 2006), as the organic compounds of the pollutant are built into humus components. Immobilised in such a way do not pose a significant threat to the environment, but this does not solve the problem of pollution, either. Much better results are obtained during bioaugmentation processes with the use of soil microorganisms capable of pollution degradation (Johnsen *et al.*, 2007).

After 30 days of experiment concentrations of PAH's in soils decreased almost 10–60% comparing to control. In other hand content of heavy metals in soils was also lower. The content of heavy metals determined by ICP-MS methods confirmed the statistically significant decrease in their levels if inoculated plants were used (decline in chernozem and rendzina by 20–45% and lessives 15–23%) (Table II). Through the root system

Table II
Degree of PAHs degradation in soils polluted with 1000 mg·kg^{-1} diesel fuel: calcareous rendzina, chernozem, lessives, brown soil aged polluted with crude oil

	Factors of the experiment					
	chernozem		calcareous rendzina		lessives	
	I–	I+	I–	I+	I–	I+
PAHs [% of control]						
naphthalene	35.2 ± 1.2^a	21.8 ± 2.1^a	67.9 ± 1.5^b	35.2 ± 0.5^a	94.8 ± 2.1^b	75.4 ± 1.2^a
acenaphthene	89.8 ± 0.5^b	61.7 ± 1.6^b	58.3 ± 1.3^a	42.2 ± 0.2^a	91.9 ± 1.0^b	73.8 ± 0.7^a
fluorene	89.6 ± 1.5^b	58.1 ± 1.8^a	58.4 ± 0.8^a	35.7 ± 0.2^c	92.5 ± 1.0^b	68.8 ± 0.5^a
phenanthrene	85.1 ± 0.5^b	47.9 ± 1.1^a	47.4 ± 1.1^a	32.5 ± 1.1^c	96.5 ± 0.5^b	67.5 ± 1.1^a
anthracene	81.5 ± 1.2^b	42.3 ± 2.2^a	52.2 ± 0.2^a	35.4 ± 0.8^c	96.1 ± 1.2^b	72.9 ± 0.7^a
fluoranthene	73.5 ± 2.2^b	41.2 ± 2.3^a	87.2 ± 0.5^b	42.6 ± 2.5^a	77.3 ± 0.5^b	63.9 ± 0.4^a
pyren	56.1 ± 1.5^a	38.9 ± 0.4^c	48.2 ± 0.7^a	26.4 ± 1.4^c	81.7 ± 1.1^b	58.4 ± 1.2^a
benz[a]anthracene	84.0 ± 2.5^b	58.4 ± 0.7^a	85.1 ± 0.8^b	38.6 ± 1.3^c	95.6 ± 0.4^b	63.8 ± 0.3^a
chrysene	96.7 ± 1.2^b	58.1 ± 1.5^a	63.4 ± 1.1^a	37.4 ± 1.1^c	87.5 ± 0.3^b	62.4 ± 0.6^c
benzo[b]fluoranthene	52.8 ± 1.3^a	37.3 ± 0.8^a	92.5 ± 1.2^b	52.6 ± 0.2^a	83.3 ± 1.2^b	62.9 ± 0.5^a
benzo[k]fluoranthene	78.9 ± 1.9^b	38.4 ± 1.2^a	81.7 ± 0.7^b	46.5 ± 0.1^c	88.7 ± 1.2^b	52.4 ± 0.4^c
benzo[a]pyrene	95.8 ± 1.2^b	58.9 ± 1.8^a	73.9 ± 0.4^b	52.4 ± 0.3^a	77.6 ± 0.5^a	50.4 ± 0.9^c
dibenz(a, h)anthracene	61.5 ± 1.2^a	48.1 ± 2.2^a	77.6 ± 1.2^a	45.1 ± 1.2^a	79.5 ± 0.4^b	58.3 ± 0.3^c
benzo[ghi]perylene	69.1 ± 0.8^b	42.2 ± 0.5^a	89.2 ± 1.1^b	51.4 ± 0.4^a	80.2 ± 0.5^b	54.8 ± 1.2^a
indeno(1, 2, 3–cd)pyrene	72.6 ± 1.7^a	53.5 ± 1.2^a	65.7 ± 0.5^b	46.8 ± 0.7^a	81.7 ± 1.0^b	67.7 ± 1.1^a
Heavy metal [mg·kg^{-1}]						
Cr	16.4 ± 0.2^a	14.5 ± 0.4^a	15.8 ± 0.5^a	11.5 ± 0.1^b	17.4 ± 0.3^a	16.2 ± 0.2^a
Pb	24.2 ± 1.2^a	11.4 ± 0.8^b	22.4 ± 0.7^a	15.4 ± 0.5^b	21.4 ± 0.7^a	18.4 ± 0.2^a
Cu	11.4 ± 0.4^a	7.4 ± 0.4^b	10.7 ± 0.2^a	8.6 ± 0.3^b	11.6 ± 0.1^a	8.4 ± 0.4^a
Zn	62.4 ± 0.2^a	45.5 ± 0.5^b	58.7 ± 0.5^a	32.5 ± 0.4^b	60.4 ± 0.2^a	55.2 ± 0.3^a
Ni	16.5 ± 0.4^a	9.4 ± 0.2^b	15.7 ± 0.3^a	8.4 ± 0.5^b	14.2 ± 0.2^a	10.4 ± 0.6^c
Co	5.4 ± 0.2^a	3.4 ± 0.3^b	6.2 ± 0.4^a	4.2 ± 0.5^b	6.1 ± 0.6^a	3.1 ± 0.4^b
Cd	0.298 ± 0.02^a	0.098 ± 0.01^b	0.242 ± 0.02^a	0.075 ± 0.01^b	0.187 ± 0.02^a	0.142 ± 0.02^a
Sn	1.2 ± 0.02^a	0.4 ± 0.02^b	1.7 ± 0.01^a	0.3 ± 0.02^b	1.9 ± 0.02^a	0.7 ± 0.01^b
Pb	24.6 ± 0.3^a	11.4 ± 0.2^b	22.6 ± 0.2^a	14.5 ± 0.1^b	28.4 ± 0.2^a	18.7 ± 0.1^b

values marked with different letters (a, b, c) are statistically significantly different ($P < 0.05$)
I+ inoculated plants; I– non inoculated plants

heavy metals were accumulated in the plant tissues. The results obtained show that *D. glomerata* is not only a good bioremediation plant but also effective in soils polluted with heavy metals. Lower concentrations of PAH's and heavy metals were observed in chernozem and rendzina after inoculation grass with *Azospirillum* spp. and *P. stutzeri*.

As described, applied coupling decreased the pollution of the soil environment with PAHs and metals which means it was simultaneously beneficial for the growth of plants in contamination conditions. Under the influence of synergistic reaction of nitrogen fixing bacteria the toxic effect of PAH's content and heavy metals on chosen plant species and their rhizosphere was reduced and the processes of PAH's degradation in soils increased. To conclude, the application of grass inoculation with *Azospirillum* spp. and *P. stutzeri* had a positive effect on the degradation processes of polycyclic aromatic hydrocarbons in soils artificially polluted with PAHs. A detailed understanding of all the mechanisms responsible for physiological and biological interactions during hydrocarbons degradation may be useful for the application of these bacteria in field studies on bioremediation of oil contaminated sites. Therefore, the present inoculation of plants with *Azospirillum* spp. and *P. stutzeri* was effective in promoting the phytoremediation of freshly added PAH's into the soil.

Literature

Abhilash P.C., S. Srivastava and N. Singh. 2011. Comparative bioremediation potential of four rhizospheric microbial species against lindane. *Chemosphere* 82 (1): 56–63.

Ahammed G.J., S. Zhang, K. Shi, Y.-H. Zhou, and J.Q. Yu. 2012. Brassinosteroid improves seed germination and early development of tomato seedling under phenanthrene stress. *Plant Growth Regul* 68: 87–96.

Anderson T.A., E.A. Guthire and B.T. Walton. 1993. Bioremediation in the rhizosphere: plant roots and associated microbes clean contaminates soil. *Environ. Sci. Technol.* 27: 2630–2636.

Andreoni V. and L. Gianfreda. 2007. Bioremediation and monitoring of aromatic-polluted habitats. *Appl. Microbiol. Biotechnol*. 76: 287–308.

Caside L., D. Klein and T. Santoro. 1964. Soil dehydrogenase activity. *Soil Sci*. 98: 371–376.

Cerniglia C. 1992. Biodegradation of polycyclic aromatic hydrocarbons. *Biodegradation* 3: 351–368.

Chauhan A., Fazlurrahman, J.G. Oakeshott and R.K. Jain. 2008. Bacterial metabolism of polycyclic aromatic hydrocarbons: strategies for bioremediation. *Indian J. Microbiol*. 48: 95–113.

Ciesielczuk T., G. Kusza, J. Poluszyńska and K. Kochanowska. 2014. Pollution of Flooded arable soils with heavy metals and polycyclic aromatic hydrocarbons (PAHs). *Water Air Soil Pollut.* 225(10): 2145.

Couillerot O., A. Ramírez-Trujillo, V. Walker, A. von Felten, J. Jansa, M. Maurhofer, G. Défago, C. Prigent-Combaret, G. Comte, J. Caballero-Mellado and Y. Moënne-Loccoz. 2013. Comparison of prominent *Azospirillum* strains in *Azospirillum-Pseudomonas-Glomus* consortia for promotion of maize growth. *Appl. Microbiol. Biotechnol*. 97(10): 4639–4649.

Dominiguez-Rosado E., and J. Pichtel. 2004. Phytoremediation of soil contaminated with used motor oil: II. Greenhouse studies. *Environ. Engin. Sci.* 21(2): 169–180.

Gałązka A. 2008. PhD Thesis (Assessment of bacteria *Azospirillum* spp. and *Pseudomonas stutzeri* usefulness for the bioremediation of soils polluted with aromatic hydrocarbons). IUNG – PIB Puławy, Poland (in Polish).

Gałązka A., Król M. and A. Perzyński. 2012. The efficiency of rhizosphere bioremediation with *Azospirillum* sp. and *Pseudomonas stutzeri* in soils freshly contaminated with PAHs and diesel fuel. *Pol. J. Environ. Stud.* 21(2): 345–353.

Gogoi B.K., N.N. Dutta, P. Goswami and T.R.K. Mohan. 2003. A case study of bioremediation of petroleum-hydrocarbon contaminated soil at a crude oil spill. *Adv. Environ. Res.* 7: 757–782.

Günther T., U. Dornberger and W. Fritsche. 1996. Effects of ryegrass on biodegradation of hydrocarbons in soil. *Chemosphere*. 33: 203–215.

Huang X.D., Y. El-Alawi, D.M. Penrose, B.R. Glick and B.M. Greenberg. 2004. Responses of three grass species to creosote during phytoremediation. *Environ. Poll.* 130: 453–463.

Johnsen A.R., S. Schmidt, T.K. Hybholt, S. Henriksen, C.S. Jacobsen and O. Andersen. 2007. Strong impact on the Polycyclic aromatic hydrocarbon (PAH) – degrading community of a PAH-polluted soilbut marginal effect on PAH degradation when priming with bioremediated soil dominated by Mycobacterium. *Appl. Environ. Microbiol.* 73(5): 1474–1480.

Joner E.J., A. Johannes, A.P. Loibne, M.A. de la Cruz, O.H. Szolar, J.M. Portal and C. Leyval. 2007. Rhizosphere effects on microbial community structure and dissipation and toxicity of polycyclic aromatic hydrocarbons (PAHs) in spiked soil. *Environ. Sci. Technol.* 35: 2773–2777.

Jones J.G. and M.A. Edington. 1968. An ecological survey of hydrocarbon – oxidazing microorganisms. *J. Gen. Microbiology* 52: 381–390.

Kabata-Pendias A., M. Piotrowska, T. Motowicka-Terelak, B. Maliszewska-Kordybach, K. Filipiak, A. Krakowiak and Cz. Pietruch. 1995. Fundamentals of the assessment of chemical soil pollution; heavy metals, sulphur, and PAHs. Bibl. Monitoringu Środowiska Warszawa (in Polish).

Kang S.H. and B.S. Xing. 2006. Phenanthrene sorption to sequentially extracted soil humic acids and humins. *Environ. Sci. Technol.* 39: 134–140.

Król M.J., A. Perzyński and A. Leśniak. 2007. *Pseudomonas stutzeri* – bacteria colonizing the plants endoryzoshere (in Polish). *Postępy Nauk Rol*. 1: 81–91.

Lee J.H. 2013. An overview of phytoremediation as a potentially promising technology for environmental pollution control. *Biotechnol. Bioproc. Eng.* 18: 431–439.

Leigh M.B., J.S. Fletcher, X. Fu and F.J. Schmitz. 2002. Root turnover: an important substrate of microbial substrates in rhizosphere remediation of recalcitrant contaminants. *Environ. Sci. Tech.* 36: 1579–1583.

Liang Meng L., M. Qiao and H. Peter. 2011. Phytoremediation efficiency of a PAH-contaminated industrial soil using ryegrass, white clover, and celery as mono- and mixed cultures. *H. Arp. J. Soils Sediments* 11:482–490.

Liste H.H. and M. Aleksander. 2000. Accumulation of phenanthrene and pyrene in rhizosphere soil. *Chemosphere* 40: 11–14.

Liste H.H. and D. Felgentreu. 2006. Crop growth, culturable bacteria, and degradation of petrol hydrocarbons (PHCs) in a long-term contaminated field soil. *Appl. Soil Ecol*. 31: 43–52.

Ma B., H. Chen, Y. He, H. Wang and J. Xu. 2010. Evaluation of toxicity risk of polycyclic aromatic hydrocarbons (PAHs) in crops rhizosphere of contaminated field with sequential extraction. *J. Soils Sediments* 10:955–963.

Mahmoud H.M., P. Suleman, N.A. Sorkhoh, S. Salamah and S.R. Samir. 2011. The potential of established turf cover for cleaning oily desert soil using rhizosphere technology. *Int. J. Phytoremediat.* 13(2): 156–67.

Martin J.P. 1950. Use of acid, rose bengal and streptomycin in the plate method for estimating soil fungi. *Soil Science*, 69: 215–232.

Muratova A., T. Hubner, S. Tischer, O. Turkovskaya, M. Moder and P. Kuschk. 2003. Plant-rhizosphere-microflora association during phytoremediation of PAH-contaminated soil. *Int. J. Phytoremediat.* 5(2):137–151.

Naiman A.D., A. Latrónico and I.E. García de Salamone. 2009. Inoculation of wheat with *Azospirillum brasilense* and *Pseudomonas fluorescens*: Impact on the production and culturable rhizosphere microflora. *Eur. J. Soil Biol.* 45: 44–51.

Okon, Y. and J. Vanderleyden. 1997. Root-Associated *Azospirillum* species can stimulate plant. *ASM News* 63: 366–370.

Order by the Minister of the Environment on soil quality standards and ground quality standards. 2002. Dz.U. Nr 165 poz. 1359 (in Polish). http://isap.sejm.gov.pl/DetailsServlet?id=WDU20021651359, 2015.08.22.

Ouvrard S., E.D. Chenot, J.F. Masfaraud and Ch. Schwartz. 2013. Long-term assessment of natural attenuation: statistical approach on soils with aged PAH contamination. *Biodegradation* 24: 539–548.

Parales R.E., N.C. Bruce, A. Schmid and L.P. Wackett. 2002. Biodegradation, Biotransformation, and Biocatalysis (B3). *Appl. Environ. Microbiol.* 68(10): 4699–4709.

Parrish Z.D., M.K. Banks and A.P. Schwab. 2005. Assessment of contaminant lability during phytoremediation of polycyclic aromatic hydrocarbon impacted soil. *Environ. Poll.* 137: 187–197.

Pizzul L., M. del Pilar Castillo and J. Stenström. 2007. Effect of rapeseed oil on the degradation of polycyclic aromatic hydrocarbons in soil by *Rhodococcus wratislaviensis*. *Int. Biodet. Biodegr.* 59: 111–118.

Siciliano S.D. and J.J. Germida. 1998. Mechanisms of phytoremediation: Biochemical and ecological interactions between plants and bacteria. *Environ. Rev*. 6: 65–79.

Smith M.J., T.H. Flowers, H.J. Duncan and J. Alder. 2006. Effects of polycyclic aromatic hydrocarbons on germination and subsequent growth of grasses and legumes in freshly contaminated soil and soil with aged PAHs residues. *Environ. Poll*. 141: 519–525.

Steenhoudt O. and J. Vanderleyden. 2000. *Azospirillum*, a free-living nitrogen-fixing bacterium closely associated with grasses: genetic, biochemical and ecological aspects, *FEMS Microbiol. Rev*. 24: 487–506.

Tabatabai M. A. and J.M. Bremner. 1969. Use of p-nitrophenyl phosphate for assay of soil phosphatase activity. *Soil Biol. Biochem.* 1: 301–307.

Tejeda-Agredano M.C., S. Gallego, J. Vila, M. Grifoll, J.J. Ortega-Calvo and M. Cantos. 2013. Influence of the sunflower rhizosphere on the biodegradation of PAHs in soil. *Soil Biol. Biochem.* 57: 830–840.

Wallace R. and A. Lockhead. 1950. Qualitative studies of soil microorganisms. Aminoacid requirements of rhizosphere bacteria. *Can. J. Research. section C* 28: 1–6.

Walton B.T., A.M. Hoylman, M.M. Perez, T.A. Anderson, T.R. Johnson, E.A. Guthrie and R.F. Christman. 1994. Bioremediation through Rhizosphere Technology, pp. 82–92. *In*: Anderson T.A. and J.R. Coats (eds). Am. Chem. Soc. Washington.

Yu W., S. Kuang and L. Zhao. 2013. Uptake, accumulation and translocation of polycyclic aromatic hydrocarbons by winter wheat cultured on oily sludge-amended soil. *Chin. J. Geochem.* 32: 295–302.

Polish Journal of Microbiology
2015, Vol. 64, No 3, 253–263

ORIGINAL PAPER

Characteristics of Newly Isolated *Geobacillus* sp. ZY-10 Degrading Hydrocarbons in Crude Oil

YUMEI SUN, ZHANGUO NING, FAN YANG and XIANZHEN LI*

School of Biological Engineering, Dalian Polytechnic University, Dalian, PR China

Submitted 13 October 2014, revised 18 February 2015, accepted 18 February 2015

Abstract

An obligately thermophilic strain ZY-10 was isolated from the crude oil in a high-temperature oilfield, which was capable of degrading heavy crude oil. Phenotypic and phylogenetic analysis demonstrated that the isolate should be grouped in the genus *Geobacillus*, which shared the highest similarity (99%) of the 16S rDNA sequence to *Geobacillus stearothermophilus*. However, the major cellular fatty acid iso-15:0 (28.55%), iso-16:0 (24.93%), iso-17:0 (23.53%) and the characteristics including indole production, tolerance to NaN_3 and carbohydrate fermentation showed some difference from the recognized species in the genus *Geobacillus*. The isolate could use tridecane, hexadecane, octacosane and hexatridecane as sole carbon source for cell growth, and the digesting rate of long-chain alkane was lower than that of short-chain alkane. When the isolate was cultured in the heavy crude oil supplement with inorganic salts and trace yeast extract, the concentration of short-chain alkane was significantly increased and the content of long-chain alkane was decreased, suggesting that the larger hydrocarbon components in crude oil were degraded into shorter-chain alkane. Strain ZY-10 would be useful for improving the mobility of crude oil and upgrading heavy crude oil *in situ*.

Key words: *Geobacillus* sp., biodegradation, crude oil, hydrocarbon, thermophilic

Introduction

Most oil reservoirs have become depleted and marginal after recovery of crude oil for hundred years, although more than 40% crude oil is still reserved in those reservoirs (Brown, 2010; Sen, 2008). It is not economically attractive to recover the residual crude oil by conventional means due to the high percentage of heavy crude oil, which is highly viscous and cannot easily flow to production wells under normal reservoir conditions (Hao and Lu, 2009; Hasanuzzaman *et al.*, 2007). It will be beneficial to the recovery of heavy crude oil if asphaltene and long-chain alkane in highly paraffinic crude could be converted into the transportable fluid portion (C7-C15) by suitable methods (Leon and Kumar, 2005). In fact, the microbial cracking of long-chain paraffin can promote the mobility of heavy crude oil and lower the cloud point (Etoumi, 2007; Gudiña *et al.*, 2012). Therefore, it is significant to find a microbial strain capable of upgrading the heavy crude oil *in situ* (Sood and Lal, 2008).

Some microbes were isolated for hydrocarbon degradation, which can degrade n-alkane C18-C20 into shorter chains (Gudiña *et al.*, 2012), or convert the heavy hydrocarbon fraction into C15-C20 hydrocarbon (Etoumi, 2007). Recently, much more attention was paid to the genus *Geobacillus* due to its tolerance to high temperature (Nazina *et al.*, 2001). Some *Geobacillus* species were found to be able to use hydrocarbon as carbon and energy source for cell growth. *G. stearothermophilus* KTCC-B7S grew well when pentadecane (C15), hexadecane (C16) and heptadecane (C17) was used as sole carbon source (Sorkhoh *et al.*, 1993) and *Geobacillus uzenensis* could utilize C10-C16 alkane, methane--naphthenic and naphthenic-aromatic oil (Nazina *et al.*, 2001). *G. stearothermophilus* DSM 22 utilizes only C10 and C11 alkane (Nazina *et al.*, 2001). Nine *Geobacillus* strains were isolated for degrading long-chain alkane from a volcano island (Meintanis *et al.*, 2006). *Geobacillus thermodenitrificans* NG80-2 also could utilize long--chain alkane (C15-C36) (Feng *et al.*, 2007) and *Geobacillus kaustophilus* TFRI NSM could degrade alkane from C14 to C32 (Sood and Lal, 2008). The capability of microbes degrading and utilizing hydrocarbon in crude oil varies with the used *Geobacillus* species (Kohr, 2011).

In searching for microbes improving the mobility of crude oil and upgrading heavy crude oil *in situ*, we isolated *Geobacillus* sp. strain ZY-10 from crude oil, which

* Corresponding author: Xianzhen Li, School of Biological Engineering, Dalian Polytechnic University, Dalian, PR China; **e-mail: xianzhen@mail.com**

can grow well on heavy crude oil. It has been found that the long-chain hydrocarbon component in the heavy crude oil could be degraded into shorter-chain alkane. In this paper, we describe the isolation and some properties of this hydrocarbon-degrading strain.

Experimental

Materials and Methods

Isolation of hydrocarbon-degrading strain and culture condition. Approximately 2 g crude oil sample, collected from the Liaohe oilfield in the northeast of China, was suspended in 50 ml sterile water containing 0.15 g Tween-80 and 10 glass beads in diameter of 0.5 cm and shaken at 60°C and 120 rev/min. After the crude oil was completely emulsified, an aliquot of 10 ml emulsified crude oil was inoculated into 100 ml nutrient broth and incubated at 60°C and 120 rev/min for 2 days. The liquid culture was transferred into fresh nutrient broth at 10% inoculum and incubated in the same conditions for another 2 days. After five cycles of such transformation and incubation for bacterial enrichment, a 10-fold serial dilution of the enriched culture with sterile saline was spread on the selective medium plates. All plates were incubated at 60°C for 48 h. Colonies with different colony characteristics were selected from the selective medium plates and incubated in 100 ml of the liquid selective medium without agar at 60°C and 120 rev/min for 5 days. The extracellular surface activity and the residual crude oil in the culture supernatant were analyzed. One strain producing maximal surface activity and degrading most crude oil was selected. To ensure strain purity, the obtained isolate was streaked on nutrient broth agar plates and a single colony was chosen for further study. The purified isolate was stored at –80°C in nutrient broth mixed with sterile glycerol at a final concentration of 16% (v/v). For routine use, it was preserved on a nutrient broth agar slant at 5°C.

The nutrient broth consisted of (per liter) 5 g NaCl, 5 g beef extract and 10 g peptone. The selective medium plates were composed of (per liter) 4.112 g $NaNO_3$, 3.4 g KH_2PO_4, 1.5 g Na_2HPO_4, 0.2 g $MgSO_4 \cdot 7H_2O$, 0.2 g yeast extract, 1.0 g crude oil and 2 g agar.

Morphological, physiological and biochemical characterization. The morphology of colony and cell were determined after culturing on nutrient broth agar plate at 60°C for 24 h. Cell morphology was observed using transmission electron microscope (JEM-1200 EX, Japan) and phase-contrast microscope (Leica DM4000B, Germany). When transmission electron microscopy was used, the specimen was prepared by fixing cells with 5% (w/v) glutaraldehyde and 1% (w/v) osmium tetroxide, and ultrathin sections of the sample embedded in epoxy resin were prepared with an ultramicrotome, stained with uranyl acetate and lead citrate. The motility of cells was determined by phase-contrast microscopy using the hanging-drop technique (Murray *et al.*, 1994). The spore formation was examined after the cells were cultured in the nutrient broth supplemented with 5 mg/l manganous sulfate monohydrate. Gram-staining was performed using the Hucker method (Murray *et al.*, 1994).

The oxidase, catalase, urease, denitrification and Voges-Proskauer reaction were tested as described by Smibert and Krieg (1994). The hydrolysis of starch, casein and gelatin and H_2S production were examined by the methods described elsewhere (Li *et al.*, 2003). Medium containing (per liter) 5 g beef extract, 10 g peptone, 3 g NaCl, 2 g $NaHPO_4 \cdot 12H_2O$, 5 g of various carbohydrates and 0.04 g bromothymol blue was used for testing carbohydrate fermentation. The isolate was incubated on the Simmons Agar plate with citrate, formate and acetate respectively for examining the capacity of utilizing citrate, formate and acetate.

Cell growth was measured by OD_{600nm} after it static incubation for 24 h in nutrient broth. The growth optimum was determined at 40, 50, 60, 70, 75, 80°C and pH 7.0, or pH 4.0, 5.0, 6.0, 7.0, 8.0, 9.0, 10.0 and 60°C. Halotolerance was tested in nutrient broth with 0, 0.5, 1.5, 2.5, 3.0 and 3.5% (w/v) NaCl at 60°C and pH 7.0.

Phylogenetic analysis. Genomic DNA was extracted from the cells growing on the nutrient broth agar plate for 24 h. Amplification and determination of 16S rDNA gene sequence were performed by Takara Bio. Co. (Dalian, China). To avoid misreading as a result of PCR error, the PCR fragment was sequenced twice. The 16S rDNA sequences of the closely related strains to the isolate ZY-10 were retrieved by comparing with those available strains in the GenBank/EMBL databases using the BLAST program (Altschul *et al.*, 1990) and at Ribosomal Database Project-II (Cole *et al.*, 2003). The MegAlign program in DNASTAR software package (Dnastar Inc., USA) were used for similarity analysis with the sequences of closely related strains (Hagström *et al.*, 2002). The sequences of closely related strains were aligned using CLUSTAL X program and corrected manually. The phylogenetic analyses were performed using the PHYLIP software package as described previously (Li *et al.*, 2003). The statistical signification of the groups obtained was assessed by bootstrapping using the programs Seqboot, Dnadist, Neighbor and Consense in the Phylip software package.

Cellular fatty acid analysis. The isolate was cultured on a nutrient broth agar plate for 24 h, and the sample for fatty acid analysis was prepared according to the protocol described by Sasser (1990). Briefly, 40 mg cells were mixed with 1 ml reagent containing 45 g sodium

hydroxide in 300 ml aqueous methanol (methanol: distilled water, 1:1, v/v) and saponified at 100°C for 30 min. After methylation in 2 ml acidified methanol (6 mol/l hydrochloric acid and methanol, 13:11, v/v) at 80°C for 10 min, cellular fatty acids methyl esters were extracted with methyltert-butyl ether (1:1) and washed with 3 ml sodium hydroxide (1.2 %). Identification of the cellular fatty acid composition was carried out using the Sherlock Microbial Identification System (Tighe *et al*., 2000).

Biodegradation of heavy crude oil by strain ZY-10. After static cultivation in LB medium at 60°C for 24 h, the cells in 6 ml broth were harvested by centrifugation at 3500 g for 20 min. After being washed twice with sterile saline, the cells were resuspended in 6 ml sterile saline and inoculated into mineral salt fermentation medium (60 ml) supplemented with 0.6 g crude oil in 100 ml conical flask and incubated statically at 60°C for 15 days.

The mineral salt fermentation medium contained (per liter) 4.112 g $NaNO_3$, 3.4 g KH_2PO_4, 1.5 g Na_2HPO_4, 0.2 g $MgSO_4 \cdot 7H_2O$ and 0.2 g yeast extract, giving 1.05% salinity.

Utilization of n-alkanes as sole carbon source by strain ZY-10. An aliquot of 6 ml resuspended cells was inoculated into 60 ml mineral salt fermentation medium in 100 ml conical flask, in which 2% tridecane, 2% hexadecane, 0.2% octacosane or 0.2% hexatriacontane were used as sole carbon source. During the static cultivation at 60°C, the tridecane and hexadecane remaining in the culture were measured within 15 days and octacosane and hexatriacontane remaining in the culture were measured within 25 days.

Analysis of fractions in the crude oil. The residual crude oil in the liquid culture was extracted three times with 20 ml chloroform, and the combined organic phase was dehydrated with 12 g anhydrous sodium sulfate for 24 h. The oil sample was dissolved in petroleum ether after removing chloroform and left for 24 h at room temperature to precipitate asphaltene. The residual oil was further separated into saturated hydrocarbons, aromatic hydrocarbons and non-hydrocarbons by adsorption chromatography (Hao and Lu, 2009; Giger and Blumer, 1974). The net weight of the oil components was determined respectively after the solvent was volatilized. The fraction of aromatic hydrocarbon dissolved in cyclohexane was determined by scanning in the range of 200–400 nm (White *et al.*, 1993).

The saturated hydrocarbon fraction in heavy crude oil was analyzed by Agilent GC6890 equipped with flame ionization detector and methyl polysiloxane capillary column OV-1 (30 m × 0.32 mm × 0.3 μm). Split injections were conducted with nitrogen as carrier. Injector and detector temperature was at 300°C. The oven temperature was set to 80°C for 2 min, raised to 200°C at a rate of 5°C/min for 2 min, then raised to 280°C at a rate of 8°C/min for 30 min. The residual n-alkanes in the culture were analyzed by the same method as the saturated hydrocarbon fraction in heavy crude oil.

Statistical analysis. All the experiments were carried out in triplicate unless otherwise stated. Results were expressed as Means ± standard deviation of three replicates.

Results and Discussion

Isolation of *Geobacillus* sp. strain ZY-10 degrading heavy crude oil. Fifty colonies in total with legible zone were grown out on selective medium plates after incubation at 60°C for 48 h, suggesting that those strains could use crude oil for cell growth. About eight kinds of colonies with different colony characteristics were observed. After incubation in liquid selective medium, one colony degrading most crude oil and producing maximal surface activity was obtained, and designated as ZY-10.

Morphology of isolate ZY-10. The colony growing on the nutrient broth agar plate was smooth, convex, circular and cream-colored with entire margins and 2–3 mm in diameter after incubation at 60°C for 24 h. The vegetative cells were motile, Gram-negative, rod-shaped, usually 7–9 μm long and 0.7–0.9 μm wide. Capsule (Fig. 1A) and oval spore (Fig. 1B) with 1.0–1.5 μm in size were located terminally or subterminally, which was not swollen beyond the cell size. The length of cells in liquid culture was increased with extending culture time or after 12 h incubation at the salinity up to 2.5%, and a floccules suspension appeared in the culture at the same time. The longer cells showed straight or flexuous thread shape (Fig. 1C), which was not found at earlier incubation or lower salinity.

Physiological and biochemical characterization. Physiological and biochemical characteristics of the isolate are shown in Table I. Strain ZY-10 was facultatively anaerobic and could grow in the range of 0–3.0% NaCl. Acid was produced from glucose, D-xylose, maltose, fructose, ribose, trehalose, melibiose, palatinose, cellobiose, sucrose and mannitol, but not from glycerol, lactose, galactose, rhamnose, sorbitol, inositol, inulin, raffinose and L-arabinose. The taxonomic properties of the strain ZY-10 are consistent with the distinguishing key characteristics of the genus *Geobactillus* (Coorevits *et al.*, 2011; Nazina *et al.*, 2001) including Gram-positive rod-shaped cells, endospore formation, motile by peritrichous flagella, facultatively anaerobe, obligately thermophilic within the range of 37–75°C for growth, and utilization of n-alkanes. Therefore, strain ZY-10 should be assigned to the genus *Geobacillus*.

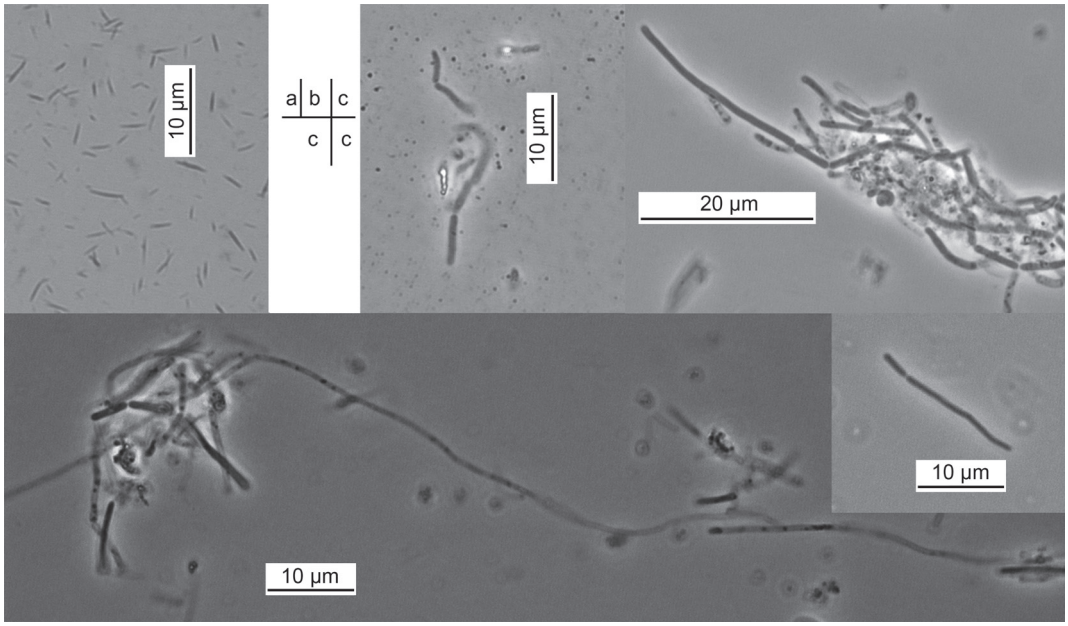

Fig. 1. Micrograph (100 × magnification) of capsule (a), endospore (b), rod and thread shaped cell (c) of strain Y-10 under light microscope (a) and phase-contrast microscope (b, c).

Strain ZY-10 could grow in the temperature range of 50–75°C and optimal growth occurred at 60°C. Such growth temperature is suitable for use in high temperature oil reservoirs (Sood and Lal, 2008). At high temperature, some long-chain n-alkanes are in liquid state and their mass transfer on interphase is improved, which is more desirable for microbial uptake of hydrocarbon (Feitkenhauer *et al.*, 2003). The oxygen concentration would affect the biodegradation of n-alkane. *Rhodococcus ruber* Z25 can degrade greatly the C6-C16 of n-alkane under aerobic condition but the C35-C45 of n-alkane under anaerobic condition (Zheng *et al.*, 2012). The results of cell growth of strain ZY-10 in crude oil at the facultatively anaerobic culture suggested that the isolate could degrade n-alkane under micro-aerobic environment, which is close to

Table I
Characteristics of the isolate *Geobacillus* sp. ZY-10

Characteristics	Reaction	Characteristics	Reaction
Cell width (µm)	0.7–0.9	Acid production from	
Cell length (µm)	7.0–9.0	Glucose	+
Gram stain	+	Glycerol	–
Motility	+	Mannitol	+
Endospore formation	+	Maltose	+
Denitrification	+	Sucrose	+
Methyl red test	+	D-Xylose	+
V.P	–	L-Arabinose	–
Indole production	+	Utilization of:	
Urease	+	Asculum	+
Oxidase	+	n-Alkanes	+
Catalase	–	Formate	–
Hydrolysis of:		Acetate	+
Gelatin	–	Citrate	+
Casein	–	Growth in NaCl range (%, w/v)	0–3
Starch	+	pH range for cell growth	5–10
Growth at 0.02 % NaN_3	+	Temperature for cell growth (°C)	50–75
Aerobic or facultatively anaerobic	+		

Symbol: "+" positive; "–" negative.

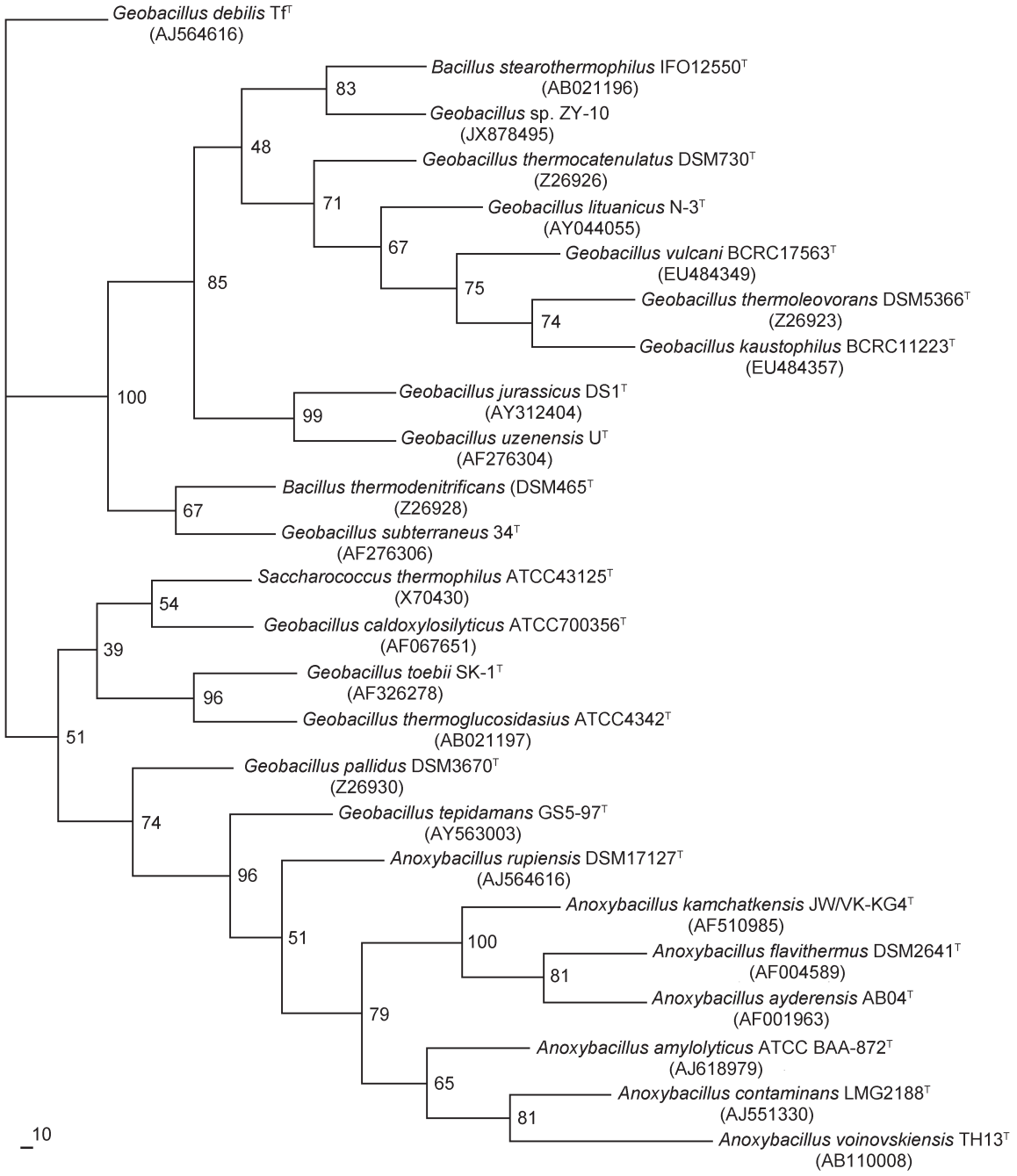

Fig. 2. Phylogenetic position of strain ZY-10 among species of the genus *Geobacillus*. The bootstrap values are shown at branch points.

the hydrocarbon biodegradation *in situ* in reservoirs with lower oxygen concentration. In addition, strain ZY-10 was able to produce bioemulsifier efficiently emulsifying paraffin (data not shown), which could selectively emulsify hydrocarbons with different chain--length resulting in improvement of the microbial accessing and utilizing hydrocarbon (Muligan *et al.*, 2001; Wang, 2011).

Phylogenetic analysis. The 16S rDNA gene sequence of strain ZY-10 was 1460 bp (accession JX878495, GenBank). The sequence similarity compared with the available reference sequences showed that strain ZY-10 was most similar to the species in the genus *Geobacillus*. Its sequence similarity is 93–98.8% with all other sequences in the genus *Geobacillus* except *Geobacillus debilis* with similarity less than 93%. The highest sequence similarity of 16S rDNA is 99% to that of the type strain of *G. stearothermophilus* (former name *Bacillus stearothermophilus*), and high sequence similarities (more than 98%) are to that of the other *Geobacillus* species including *Geobacillus subterraneus*, *Geobacillus thermocatenulatus*, *Geobacillus vulcani*, *Geobacillus lituanicus*, *Geobacillus thermoleovorans*, *Geobacillus uzenensis* and *Geobacillus jurassicus*. The phylogenetic tree constructed by neighbour-joining method on the basis of the 16S rDNA gene sequence was shown in Fig. 2.

Table II
Cellular fatty acid profiles (%) of *Geobacillus*. sp. ZY-10 and closely related *Geobacillus* species (Caccamo *et al.*, 2000; Nazina *et al.*, 2001)

Fatty acid	ZY-10	1	2	3	4	5	6
anteisoC13:0			5.1				
isoC14:0	1.15		0.1	1.3	1.0		2.9
C14:0	0.28		1.5	0.6	1.4		
C15:0			0.5	1.3	2.1	0.4	1.4
isoC15:0	28.55	16.6	39.8	25.5	22.6	20.7	37.8
anteisoC15:0	2.19	2.2	6.4	0.6	1.3	2.0	2.3
C16:0	4.63		6.2	8.3	11.2	3.7	1.7
isoC16:0	24.93	14.6	9.2	31.8	21.0	16.6	29.2
isoC17:0	23.53	21	17.1	21.0	18.5	36.7	18.5
C17:0				2.3	1.3	0.4	0.4
anteisoC17:0	9.04	11.4	13.3	3.1	4.6	18.7	5.8
isoC18:0	0.88			1.3	0.9	0.6	
C18:0	0.81	13		2.2	3.4		
C18:1 ω9c	3.07			0.7	1.2		

Species: 1, *G. vulcani*; 2, *G. stearothermophilus*; 3, *G. thermocatenulatus*; 4, *G. thermoleovorans*; 5, *G. uzenensis*; 6, *G. subterrane* (Caccamo *et al.*, 2000; Nazina *et al.*, 2001).

Phylogenetic analysis based on 16S rDNA gene sequences also supported that strain ZY-10 was clear affiliated to the genus *Geobacillus*. The sequence similarity between strain ZY-10 and *Geobacillus* species was about 98.0%, which were in accordance with the proposal of 93% or 95% 16S rDNA gene sequence similarity as a cut-off value for delineating genera (Fox *et al.*, 1992; Wagner-Döbler *et al.*, 2004). Strain ZY-10 showed the highest level of similarity to *B. stearothermophilus* with 99% homology and higher similarity to *B. thermodenitrificans* with 97.7% homology, whereas both the species have been incorporated in the genus *Geobacillus* (Nazina *et al.*, 2001), giving further evidence that the new strain should be a member of the genus *Geobacillus*. As shown in the phylogenetic tree (Fig. 2), the isolate was clearly clustered into the clade of the genus *Geobacillus* and the closest species was *B. stearothermophilus* (*G. stearothermophilus*).

Cellular fatty acids analysis. The iso-branched saturated acids including iso-15:0, iso-16:0 and iso-17:0 was the main fatty acids in the genus *Geobacillus* species which was over 60% of the total cellular fatty acids (Nazina *et al.*, 2001). As shown in Table II, the major fatty acids of strain ZY-10 were iso-branched saturated acids including iso-15:0, iso-16:0 and iso-17:0, the content of which was 28.55%, 24.93%, 23.53% respectively, accounted for about 77% of the total fatty acid. Strain ZY-10 exhibited the same major fatty acids profile as the genus *Geobacillus* species, the major fatty acids content of which is close to that of *G. stearothermophilus*, suggesting that the strain ZY-10 should be a member of the genus *Geobacillus*. The dendrogram of fatty acid similarity was derived from the cluster analysis by Euclidian distance based on the fatty acid profile (Fig. 3). It summarizes the relatedness of the fatty acid composition of some thermophilic strains closely related to strain ZY-10. As shown in Fig. 3, strain ZY-10 belonged to the same cluster with *G. thermoleovorans* and *G. thermocatenulatus*, but did not cluster closely with *G. stearothermophilus*.

Identification of strain ZY-10 as a new member of the genus *Geobacillus*. As shown in Table I, strain ZY-10 could be distinguished from its nearest apparent phylogenetic neighbor *Geobacillus* spp. in a number of important characteristics, including acid production from glycerol, mannitol, D-xylose and L-arabinose, the ability to hydrolyze gelatine, casein and starch, indole production and tests in oxidase, catalase and urease. Especially the capacity of growth in nutrient broth supplemented with 0.02% sodium azide can distinguish strain ZY-10 from *G. stearothermophilus*, because this closest species is sensitive to sodium azide (White *et al.*, 1993). The content of C18:1ω9c is 3.07% in strain ZY-10 that is higher than that in other strains, especially the species in the genus *Geobacillus*. The content of unsaturated fatty acids is higher in the alkalotolerant strains like *Bacillus firmus* and *Bacillus alcalophilus* than that in any other strains (Kaneda, 1991). The growth ability at pH 10.0 was correlated with the character of lipids in the cell membranes for strain ZY-10. Therefore, it appears that strain ZY-10 represents a new member of the genus *Geobacillus*.

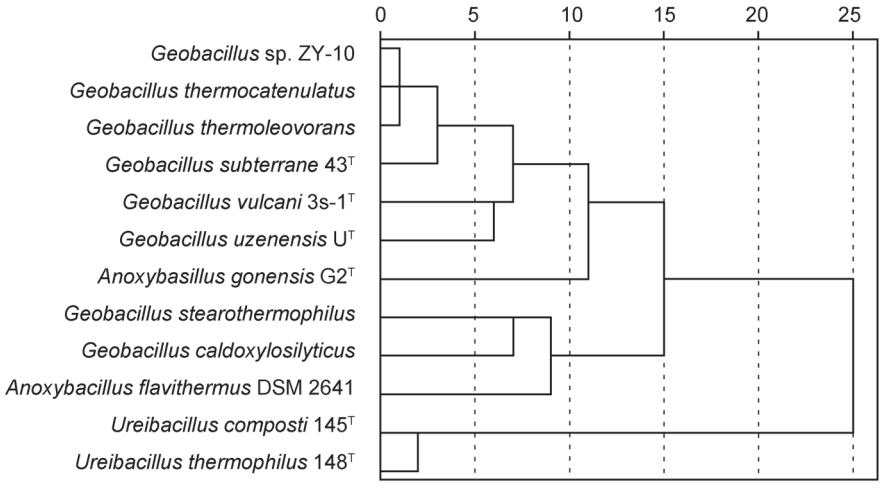

Fig. 3. Dendrogram of fatty acid similarities (Euclidian distance) based on data for strains related with strain ZY-10 in fatty acid composition.

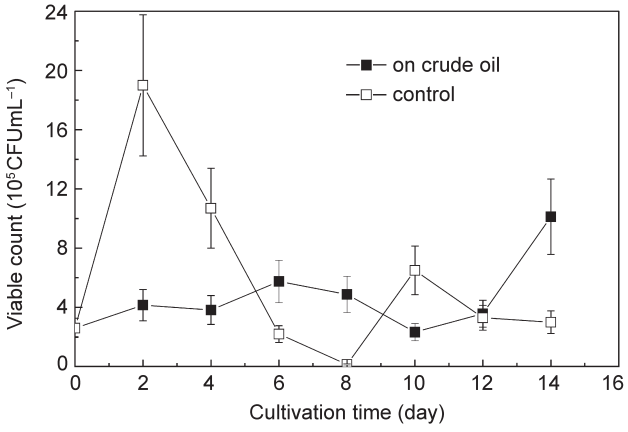

Fig. 4. Cell growth of strain ZY-10 with crude oil as carbon source in the mineral salt fermentation medium at 60°C.

Cell growth on crude oil. The cell growth in medium with crude oil as sole carbon source is shown in Fig. 4. Strain ZY-10 grew slowly at the beginning of the cultivation and rapidly grew after incubation for 12 days. For the control without crude oil as carbon source, the viable count increased rapidly at the earlier period of cultivation, and after that it decreased (Fig. 4).

Some components in crude oil are toxic to strain ZY-10 or the solubility of crude oil in water is too low. With the extension of culture time, the cells gradually adapted to the crude oil and utilized it to produce metabolites that could improve the dissolution of crude oil in water. Therefore, the growth rate of strain ZY-10 was intensified by utilizing crude oil and its metabolites. Therefore the cells grew quickly at the earlier stage of cultivation in the control without toxicity from crude oil, but cell growth declined in the following incubation because of a lack of a carbon source for cell growth. The viable cell count was determined as close to zero on the 8th day, presumably due to cells' autolysis. However, after that strain ZY-10 showed a secondary growth speculatively by utilizing the autolysate from autolyzed cells.

Variation of fraction content in the crude oil treated by strain ZY-10. As shown in Fig. 5, the content of saturated hydrocarbon, aromatic hydrocarbon and asphaltenes decreased and non-hydrocarbon content increased in the crude oil treated by strain ZY-10. The data in Fig. 5 demonstrates that strain ZY-10 could utilize saturated hydrocarbon, aromatic hydrocarbon and asphaltenes to produce non-hydrocarbon such as alcohol, aldehyde, ketone and carboxylic acid by oxidizing hydrocarbons and asphaltenes in the process of culturing. It is similar to metabolism of aromatic hydrocarbon, asphaltenes and non-hydrocarbon in crude oil M851 by strain BNL-4–23 (Premuzic and Lin, 1999).

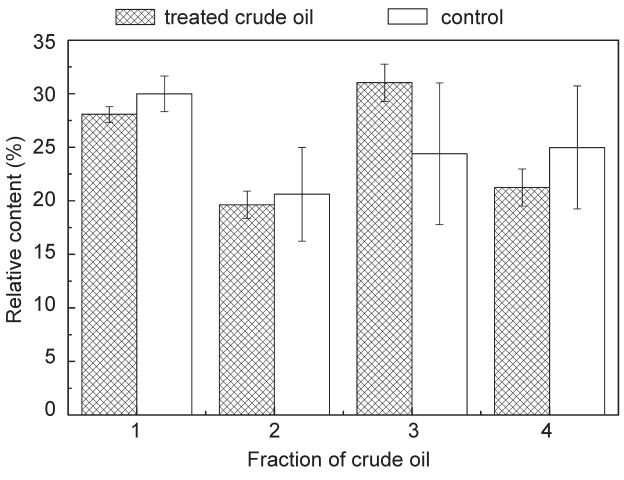

Fig. 5. Content of fraction in the crude oil after treatment with strain ZY-10.

Symbol: 1 – saturated hydrocarbon; 2 – aromatic hydrocarbon; 3 – non-hydrocarbon; 4 – asphaltenes.

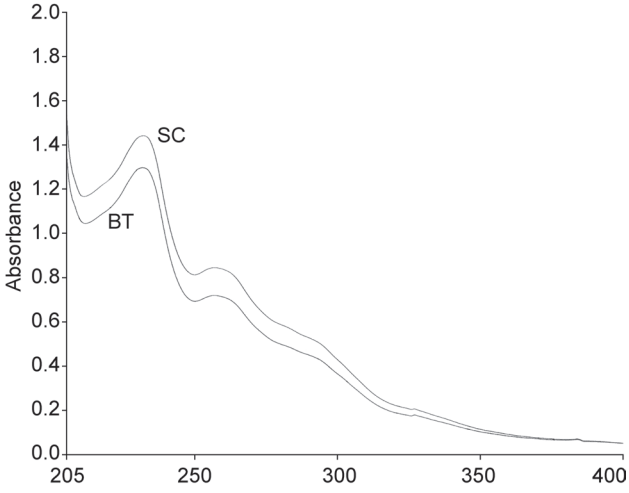

Fig. 6. Changes in absorption spectra (200–400 nm) of crude oil after treatment with strain ZY-10.
Symbol SC – sterile control; BT – sample treated by strain ZY-10.

It is known that aromatic hydrocarbon has a maximum absorption at 205–240 nm. For naphthalene, acenaphthene, six hydrogenated pyrene, phenathrene and pyrene, the maximum absorption is at 211 nm, 218 nm, 225 nm, both 243 and 280 nm, 232 and 265 and 323 nm respectively. The aromatic hydrocarbons with more than four aromatic rings show the strongest absorbance at more than 350 nm, and at longer wave length when dissolved in cyclohexane (Halasinski *et al.*, 2005; Mille *et al.*, 1991). The absorbance of crude oil untreated and treated by strain ZY-10 was scanned in the wave length range of 200–400 nm and their absorption spectra are shown in Fig. 6. The absorbance of the treated crude oil decreased by comparing with the crude oil without inoculation of strain ZY-10 in the ultraviolet region. This demonstrated that the content of aromatic hydrocarbon fraction in the crude oil decreased when the crude oil was treated by strain ZY-10. It can be inferred that strain ZY-10 could utilize and/or degrade aromatic hydrocarbons with less than three aromatic rings but not with more than four aromatic rings in the tested crude oil.

Biodegradation of saturated alkane fraction in heavy crude oil by strain ZY-10. In the heavy crude oil incubated with strain ZY-10 for 15 days, the alkane with retention time of 10–25 min increased and the alkane with retention time of 25–60 min decreased when compared with the control sample of the sterilized crude oil untreated by strain ZY-10 (Fig. 7). The retention time of tridecane, hexadecane, eicosane, octacosane and hexatriacontane was at 12.9 min, 20.6 min, 30.7 min, 41.2 min and 69.7 min respectively on the gas chromatogram.

Crude oil is a complex mixture of hydrocarbon and other organic compounds, and the saturated hydrocarbon composition in the crude oil affects the bacterial degradation of alkane (Hao *et al.*, 2004). The saturated hydrocarbons in heavy crude oil used in this study were mainly n-alkanes with chain length more than 16. As shown in Fig. 8, the analysis of alkane with chain length less than C36 in the crude oil showed that the content of C13-C16, C8-C13 and C16-C20 alkane increased by 155%, 117% and 106% respectively, and the content of C20-C28 alkane decreased by 2% at the same time, while there was nearly no change in the content of C28-C36 alkane. The content of tridecane, hexadecaneand hexatriacontane significantly increased to 3–4 times of the control, and the content of eicosane and octacosane visibly decreased in the heavy crude oil treated by strain ZY-10. The results revealed that the rate of producing tridecane, hexadecane and hexatriacontane was faster than the rate of degrading or utilizing those three alkanes by strain ZY-10 when crude oil was used as carbon source. Although it is difficult to utilize larger compounds, strain ZY-10 could

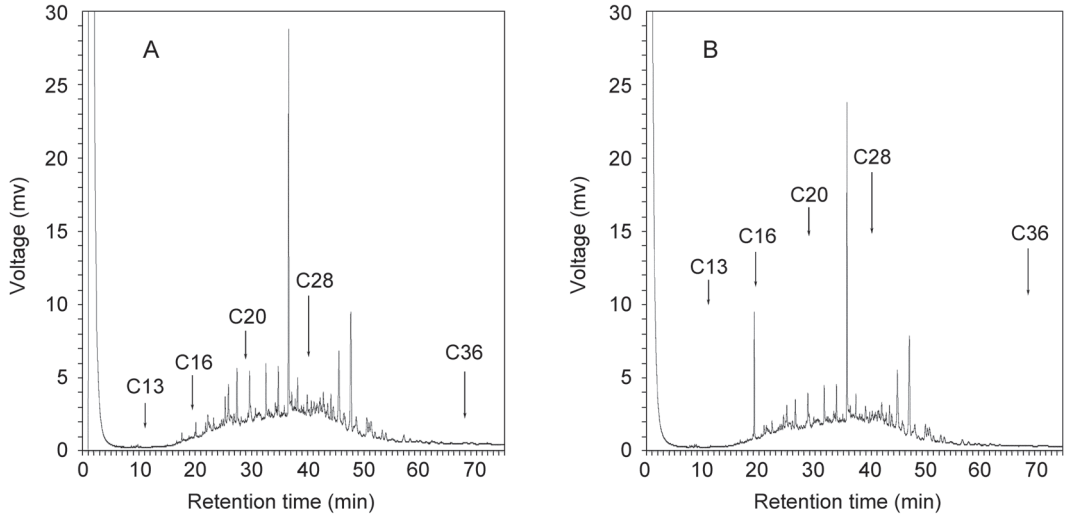

Fig. 7. Gas chromatography of the saturated hydrocarbon fraction in sterile crude oil (A) and crude oil treated by strain ZY-10 (B).

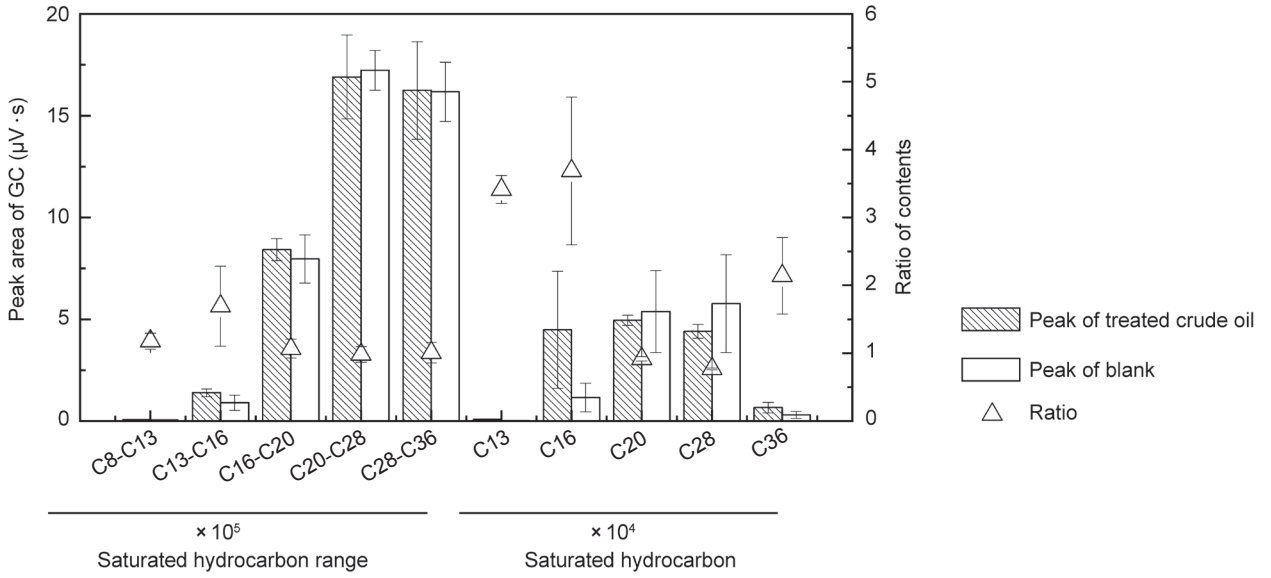

Fig. 8. Alkanes in crude oil treated and untreated by cultivating strain ZY-10, in which the clear column is the untreated crude oil and the filled column is the treated crude oil by strain ZY-10, and clear triangle is the ratio of alkane in treated sample to that in sterile control in crude oil fermentation.

produce short-chain alkane by degrading hydrocarbon and other large molecular compounds.

According to the experimental results described above, the short-chain n-alkane (tridecane and hexadecane) in soluble state was known to be utilized more easily than the long-chain n-alkane (octacosane and hexatriacontane) in insoluble state by strain ZY-10. The long-chain n-alkane might be degraded slowly before being utilized for cell growth. The cultivation of strain ZY-10 in the heavy crude oil could result in a significant increase in the content of C13-C16 alkane (tridecane and hexadecane) and an increase in the content of C8-C13 and C16-C20 alkane, but in a decrease in the content of C20-C28 alkane. Premuzic and Lin (1999) reported that the content of long-chain n-alkane decreased and the content of short-chain n-alkane increased in crude oil when treated with strain BNL-4-23. The degradation of crude oil by thermophilic strain TH-2 also displayed similar results (Hao *et al.*, 2004). The bacteria that can increase the content of C10-C20 n-alkane in crude oil have received much attention in recent years because the increasing content of short--chain alkane as a solvent in crude oil is beneficial to crude oil recovery. It can be concluded that strain ZY-10 is able to convert heavy crude oil, such as long-chain n-alkane, macromolecular aromatic hydrocarbon and larger hydrocarbon, into short-chain n-alkanes. The oxidization of hydrocarbons in heavy crude oil by strain ZY-10 was limited consequently under static cultivation because of the low oxygen concentration. However, this assumption needs to be verified experimentally. The specificity of the emulsifier should be examined further to clarify the relationship between the characteristic of the emulsifier and the preferential degradation of alkane by strain ZY-10.

Utilization and biodegradation of n-alkane (C13, C16, C28 or C36) by strain ZY-10. When tridecane, hexadecane, octacosane and hexatriacontane were used as sole carbon source respectively, the growth and residual n-alkanes were determined (Fig. 9). Tridecane and hexadecane could be utilized within 15 days and

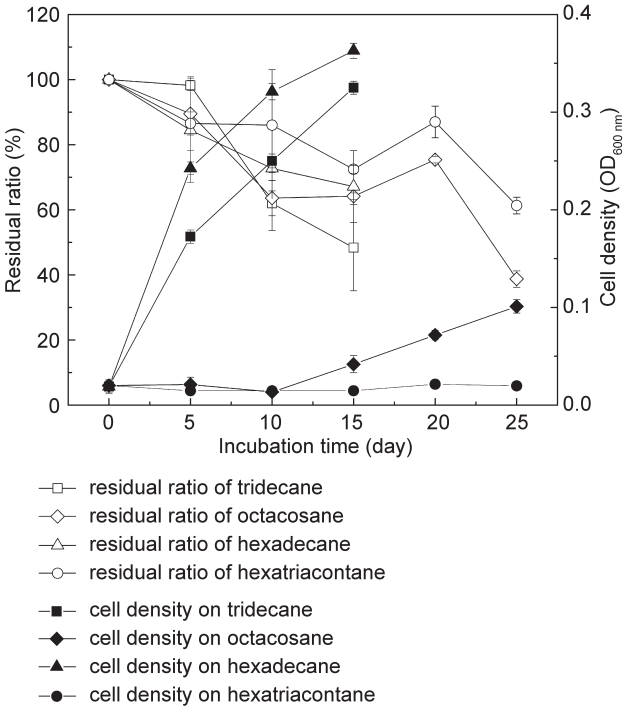

Fig. 9. Cell growth of strain ZY-10 and residual n-alkane when tridecane (■, □), hexadecane (▲, Δ), octacosane (♦, ◊), hexatriacontane (●, ○) were used respectively as sole carbon source.

octacosane was utilized within 25 days. As shown in Fig. 9, cell growth of strain ZY-10 was fast and there was no lag phase in the growth curve when tridecane and hexadecane were used as carbon source. However, a long lag phase was observed when strain ZY-10 was incubated in the medium with octacosane and hexatriacontane as carbon source, in which the lag phase in octacosane was longer than that in hexatriacontane. Moreover, the viable cell content decreased in the first five day culture following a long lag phase in the growth curve when hexatriacontane was used as carbon source. The cell density cultivated in tridecane or hexadecane was much more than that in octacosane or hexatriacontane.

The results shown in Fig. 9 indicate that a high ratio of alkane remained when the longer alkane was utilized (in comparison between tridecane and hexadecane, between octacosane and hexatriacontane). We can conclude that strain ZY-10 prefers to utilize the shorter-chain n-alkanes (tridecane and hexadecane), but might first absorb longer-chain n-alkanes (octacosane and hexatriacontane) on the cell surface and then slowly convert them into the easier-used compounds (including short-chain n-alkanes). Most bacterial cells prefer to use n-alkanes with chain length from 10 to 20 (Wentzel *et al.*, 2007). For example, *G. stearothermophilus* MH-1 could degrade alkane in the range of C12-C31, and C12-C20 alkane was degraded much easily (Liu *et al.*, 2009).

It can be concluded that strain ZY-10 as a thermophilic bacterium capable of degrading hydrocarbons has a potential to improve the mobility of crude oil and upgrade heavy crude oil *in situ*.

Acknowledgements

Financial support provided by Natural and Scientific Funding of China (31371742), Special Funding for Agroscientific or Marine Research in Public Interest (201303095, 201405003), Program for Science and Technology Department of Dalian (2013B11NC078) are greatly acknowledged.

Literature

Altschul S.F., W. Gish, W. Miller, E.W. Myers and D.J. Lipman. 1990. Basic local alignment search tool. *J. Mol. Biol.* 215: 403–410.

Brown, L.R. 2010. Microbial enhanced oil recovery (MEOR). *Curr. Opin. Microbiol.* 13: 316–320.

Caccamo D., C. Gugliandolo, E. Stackebrandt and T.L. Maugeri. 2000. *Bacillus vulcani* sp. nov., a novel thermophilic species isolated from a shallow marine hydrothermal vent. *Int. J. Syst. Evol. Microbiol.* 50: 2009–2012.

Cole J.R., B. Chai, T.L. Marsh, R.J. Farris, Q. Wang, S. Kulam, S. Chandra, D. McGarrell, T.M. Schmidt and G.M. Garrity. 2003. The Ribosomal Database Project (RDP-II): previewing a new autoaligner that allows regular updates and the new prokaryotic taxonomy. *Nucleic Acids Res.* 31: 442–443.

Coorevits A., A.E. Dinsdale, G. Halket, L. Lebbe, P. De Vos, A. Van Landschoot and N.A. Logan. 2011. Taxonomic revision of the genus *Geobacillus*: emendation of *Geobacillus*, *G. stearothermophilus*, *G. jurassicus*, *G. toebii*, *G. thermodenitrificans* and *G. thermoglucosidans* (nom. corrig., formerly 'thermoglucosidasius'); transfer of *Bacillus thermantarcticus* to the genus as *G. thermantarcticus* comb. nov.; proposal of *Caldibacillus debilis* gen. nov., comb. nov.; transfer of *G. tepidamans* to *Anoxybacillus* as *A. tepidamans* comb. nov.; and proposal of *Anoxybacillus caldiproteolyticus* sp. nov. *Syst. Appl. Microbiol.* 34: 419–423.

Etoumi A. 2007. Microbial treatment of waxy crude oils for mitigation of wax precipitation. *J. Petrol. Sci. Eng.* 55: 111–121.

Feitkenhauer H., R. Müller and H. Märkl. 2003. Degradation of polycyclic aromatic hydrocarbons and long chain alkanesat 60–70 °C by thermus and *Bacillus* spp. *Biodegradation.* 14: 367–372.

Feng L., W. Wang, J. Cheng, Y. Ren, G. Zhao, C. Gao, Y. Tang, X. Liu, W. Han, X. Peng and others. 2007. Genome and proteome of long-chain alkane degrading *Geobacillus thermodenitrificans* NG80-2 isolated from a deep-subsurface oil reservoir. *Proc. Natl. Acad. Sci. U. S. A.* 104: 5602–5607.

Fox G.E., J.D. Wisotzkey and P. Jurtshuk. 1992. How close is close: 16S rRNA sequence identity may not be sufficient to guarantee species identity. *Int. J. Syst. Bacteriol.* 42:166–170.

Giger W. and M. Blumer. 1974. Polycyclic aromatic hydrocarboms in the environment isolation and characterization by chromatography, visible, ultraviolet, and mass spectrometry [J]. *Anal. Chem.* 46:1663–1671

Gudiña E.J., J.F.B. Pereira, L.R. Rodrigues, J.A.P. Coutinho and J.A. Teixeira. 2012. Isolation and study of microorganisms from oil samples for application in microbial enhanced oil recovery. *Int. Biodeterior. Biodegrad.* 68: 56–64.

Hagström Å., T. Pommier, F. Rohwer, K. Simu, W. Stolte, D. Svensson and U.L. Zweifel. 2002. Use of 16S ribosomal DNA for delineation of marine bacterioplankton species. *Appl. Environ. Microbiol.* 68: 3628–3633.

Halasinski T.M., F. Salama and L.J. Allamandola. 2005. Investigation of the ultraviolet, visible, and near-infrared absorption spectra of hydrogenated polycyclic aromatic hydrocarbons and their cations. *Ap. J.* 628: 555–566

Hao R. and A. Lu. 2009. Biodegradation of heavy oils by halophilic bacterium. *Prog. Nat. Sci.* 19: 997–1001.

Hao R., A. Lu and Y. Zeng. 2004. Effect on crude oil by thermophilic bacterium. *J. Petrol. Sci. Eng.* 43: 247–258.

Hasanuzzaman M., A. Ueno, H. Ito, Y. Ito, Y. Yamamoto, I. Yumoto and H. Okuyama. 2007. Degradation of long-chain n-alkanes (C36 and C40) by *Pseudomonas aeruginosa* strain WatG. *Int. Biodeterior. Biodegrad.* 59: 40–43.

Kaneda T. 1991. Iso- and anteiso-fatty acids in bacteria: biosynthesis, function, and taxonomic significance. *Microbiol. Mol. Biol. R.* 55: 288–302.

Kohr W.J. 2011. Microbial enhanced oil recovery methods, U.S. Patent 2011/0067856. filed Aug. 26, 2010, and issued Mar. 24, 2011.

Leon V. and M. Kumar. 2005. Biological upgrading of heavy crude oil. *Biotechnol. Bioprocess Eng.* 10(6):471–481

Li X., C. Zhao, Q. An and D. Zhang. 2003. Substrate induction of isomaltulose synthase in a newly isolated *Klebsiella* sp. LX3. *J. Appl. Microbiol.* 95: 521–527.

Liu Y.C., T.T. Zhou, J. Zhang, L. Xu, Z.H. Zhang, Q.R. Shen and B. Shen. 2009. Molecular characterization of the *alk*B gene in the thermophilic *Geobacillus* sp. strain MH-1. *Res. Microbiol.* 160: 560–566.

Mille G., M. Almallah, M. Bianchi, F. Wambeke and J.C. Bertrand. 1991. Effect of salinity on petroleum biodegradation. *Fresenius J. Anal. Chem.* 339: 788–791

Meintanis C., K.I. Chalkou, K.A. Kormas and A.D. Karagouni. 2006. Biodegradation of crude oil by thermophilic bacteria isolated from a volcano island. *Biodegradation* 17: 3–9.

Muligan C.N., R.N. Yong, B.F. Gibbs. 2001. Surfactant-enhanced remediation of contaminated soil: a review. *Eng. Geol.* 60: 371–380.

Murray R.G.E., R.N. Doetsch and C.F. Robinow. 1994. Determinative and cytological light microscopy, pp. 22–41. In: Gerhardt, P., R.G.E. Murray, W.A. Wood and N.R. Krieg (eds.). Methods for General and Molecular Bacteriology. American Society for Microbiology, Washington D.C.

Nazina T.N., T.P. Toruova, A.B. Poltaraus, E.V. Novikova, A.A. Grigoryan, A.E. Ivanova, A.M. Lyseko, V.V. Petrunyaka, G.A. Osipov, S.S. Belyaev and others. 2001. Taxonomic study of aerobic thermophilic bacilli: descriptions of *Geobacillus subterraneus* gen. nov., sp. nov. and *Geobacillus uzenensis* sp. nov. from petroleum reservoirs and transfer of *Bacillus stearothermophilus*, *Bacillus thermocatenulatus*, *Bacillus*, *Bacillus kaustophilus*, *Bacillus thermoglucosidasius* and *Bacillus thermodenitrificans* to *Geobacillus* as the new combinations *G. stearothermophilus*, *G. thermocatenulatus*, *G. thermoleovorans*, *G. kaustophilus*, *G. thermoglucosidasius* and *G. thermodenitrificans*. *Int. J. S yst. Evol. Microbiol.* 51: 433–446.

Premuzic E.T. and M.S. Lin. 1999. Induced biochemical conversions of heavy crude oils. *J. Petrol. Sci. Eng.* 22: 171–180.

Sasser M. 1990. Identification of bacteria by gas chromatography of cellular fatty acids, MIDI Technical Note 101. Newark, DE: MIDI Inc.

Sen R. 2008. Biotechnology in petroleum recovery: the microbial EOR. *Prog. Energy Combust. Sci.* 34: 714–724.

Smibert R.M. and N.R. Krieg. 1994. Phenotypic characterization. pp. 607–654 In: Gerhardt P., R.G..E. Murray, W.A. Wood and N.R. Krieg (eds). *Methods for General and Molecular Bacteriology.* ASM Press, Washington, D.C.

Sood N. and B. Lal 2008. Isolation and characterization of a potential paraffin-wax degrading thermophilic bacterial strain *Geobacillus kaustophilus* TERI NSM for application in oil wells with paraffin deposition problems. *Chemosphere* 70: 1445–1451.

Sorkhoh N.A., A.S. Ibrahim, M.A. Ghannoum and S.S. Radwan. 1993. High-temperature hydrocarbon degradation by *Bacillus stearothermophilus* from oil-polluted Kuwaiti desert. *Appl. Microbiol. Biotechnol.* 39: 123–126.

Tighe S.W., P. de Lajudie, K. Dipietro, K. Lindstrom, G. Nick, and B.D.W. Jarvis. 2000. Analysis of cellular fatty acids and phenotypic relationships of *Agrobacterium*, *Bradyrhizobium*, *Mesorhizobium*, *Rhizobium* and *Sinorhizobium* species using the Sherlock Microbial Identification System. *Int. J. Syst. Evol. Microbiol.* 50: 787–801.

Wagner-Döbler I., H. Rheims, A. Felske, A. El-Ghezal, D. Flade-Schröder, H. Laatsch, S. Lang, R. Pukall and B.J. Tindall. 2004. *Oceanibulbus indolifex* gen. nov., sp. nov., a North Sea alphaproteobacterium that produces bioactive metabolites. *Int. J. Syst. Evol. Microbiol.* 54: 1177–1184.

Wang X.B., C.Q. Chi, Y. Nie, Y.Q. Tang, Y. Tan, G.. Wu and X.L. Wu. 2011. Degradation of petroleum hydrocarbons (C6-C40) and crude oil by a novel *Dietzia* strain. *Bioresour. Technol.* 102: 7755–7761.

Wentzel A., T.E. Ellingsen, H.K. Kotlar, S.B. Zotchev and M. Throne-Holst. 2007. Bacterial metabolism of long-chain n-alkanes. *Appl. Microbiol. Biotechnol.* 76: 1209–1221.

White D., R.J. Sharp and F.G. Priest. 1993. A polyphasic taxonomic study of thermophilic bacilli from a wide geographical area. *Antonie Van Leeuwenhoek* 64: 357–386.

Zheng C., L. Yu, L. Huang, J. Xiu and Z. Huang. 2012. Investigation of a hydrocarbon-degrading strain, *Rhodococcus ruber* Z25, for the potential of microbial enhanced oil recovery. *J. Petrol. Sci. Eng.* 81: 49–56.

Polish Journal of Microbiology
2015, Vol. 64, No 3, 265–271

ORIGINAL PAPER

Evaluation of Two Lactic Acid Bacteria Starter Cultures for the Fermentation of Natural Black Table Olives (*Olea europaea* L cv Kalamon)

MARINA PAPADELLI[1]*, GEORGIA ZOUMPOPOULOU[2], MARINA GEORGALAKI[2], RANIA ANASTASIOU[2], EUGENIA MANOLOPOULOU[2], IOANNA LYTRA[1], KONSTANTINOS PAPADIMITRIOU[2] and EFFIE TSAKALIDOU[2]

[1] Technological Educational Institute of Peloponnese, Department of Food Technology, Kalamata, Greece
[2] Agricultural University of Athens, Department of Food Science and Human Nutrition, Athens, Greece

Submitted 2 January 2015, revised 22 February 2015, accepted 5 March 2015

Abstract

The production of Greek-style natural black table olives remains an empirical process relying on spontaneous fermentation despite its economic significance. For this reason producers often resort to increased NaCl concentration of the brine to secure quality of the product. In this study we employ two lactic acid bacteria *Leuconostoc mesenteroides* subsp. *mesenteroides* Lm139 and *Lactobacillus pentosus* DSM 16366 as starters in separate laboratory low salinity fermentations of "Kalamon" cultivar olives, processed according to the Greek-style method. *L. mesenteroides* subsp. *mesenteroides* Lm139 was previously isolated from Kalamon olives laboratory spontaneous fermentations, while *L. pentosus* DSM 16366 was isolated from fermenting green olives prepared according to the Spanish-style method. Spontaneous olives fermentation was also performed as a control. Microbiological and physicochemical analyses of the brines revealed that the use of the starters had a significant effect on the olives fermentation, leading to a faster acidification due to the more efficient consumption of soluble sugars in the brines. The final pH value reached by each starter culture used indicates a successful lactic fermentation. The production of lactic acid by the starters and the concomitant drop of the pH value proved to inhibit enterobacteria in a shorter period of time compared to the spontaneous fermentation. Concluding, the use of either of the two lactic acid bacteria as starters in Greek-style Kalamon olives fermentation could lead to a more controllable fermentation at lower salinities. The resulting product could be of higher quality with extended shelf-life while being at the same time safer for the consumer.

Key words: fermentation, Greek-style olives, Kalamon olives, lactic acid bacteria

Introduction

For thousands of years, table olives have been a basic component of the Mediterranean diet. They have high nutritional value, being rich in energy, minerals and vitamins, and they possess antioxidant properties. The estimated Greek production of table olives for the period 2011/12 was about 130,000 tons, the 2nd (after Spain) in the EU which corresponds to the 17.5% of the total EU production (International Olive Council, 2012a; 2012b).

"Kalamata type table olives" is a very well known type of Greek-style natural black olives, mainly due to the excellent characteristics of the raw material used, which is the Greek olive cultivar "Kalamon". The processing method for their production remains artisanal and empirical despite its economic importance. According to the common practice applied by the producers, the "Kalamon" olives are placed in brine of high salt concentration (usually 6–10% w/v NaCl, but very often even higher, 10–14% w/v NaCl) and they are spontaneously fermented in brine by a mixed population of indigenous microorganisms, mainly yeasts and lactic acid bacteria (LAB). In the final step of the preparation, fermented black olives are size graded before being packed also in brine solution (Balatsouras, 1967; 1990; Garrido-Fernández *et al*., 1997).

The use of high salinity brine ensures the inhibition of spoilage microbiota and the growth of pathogens in the brines, but it also leads to a slow extraction of soluble components from the olives to the brine. This means a slower removal of bitterness but also a longer fermentation period of olives, lasting even 10 or more months. Furthermore, in such a high salinity (> 8% NaCl in equilibrium), yeasts dominate over LAB which are prevented to grow and thus cannot assist in the fermentation process (Arroyo-López *et al*., 2008). When yeasts are dominant the product has a milder

* Corresponding author: M. Papadelli, Technological Educational Institute of Peloponnese, Department of Food Technology, Antikalamos, 24-100 Kalamata, Greece; **e-mail: m.papad@teikal.gr**

taste and a shorter shelf life (Garrido-Fernández *et al*., 1997; Panagou *et al*., 2008). More precisely, an incomplete yeast fermentation, leading to the remaining of residual sugars in the brine even after a long fermentation period, may result in future undesirable secondary fermentations during the storage of the olives. Furthermore, yeasts may cause gas pocket formation, softening of the olive tissue, package bulging, clouding of the brines and production of off flavors and odours (Tofalo *et al*., 2012). Finally, the olives produced by fermentation in high salinity brines are usually shrunk with high salt content and with a remaining bitterness.

In order to reduce the above mentioned negative consequences of the high salt content and yeast domination, a more active role of LAB in olives fermentation is required. For this purpose, during this study, laboratory fermentations using specific LAB strains as starter cultures were performed in the presence of low salt concentration (5% w/v NaCl).

Experimental

Materials and Methods

Olive fermentation. The experimental olive fermentations were carried out with olives *Olea europaea* L. cv. "Kalamon", kindly provided by a table olive producer from Petalidi village in Messinia area, Peloponnese. The olive fruits were collected during November 2009, transported within 24 h to the laboratory, and washed with tap water in order to remove the dust and the impurities. The olives were once cut and left in tap water at room temperature for 24 hours. After that period, nine lidded plastic fermentation vessels were set up, each of them containing 1,200 g of olives and 800 ml of brine (5% w/v NaCl). All fermentation vessels remained at 22°C for 48 h prior the inoculation.

Three sets of fermentations (B1, B2, B3) were performed and each set was repeated three times. In fermentation B1, no inoculation was applied and a spontaneous fermentation was leaded by the indigenous microbiota. In fermentation B2, the vessels were inoculated with the *Lactobacillus pentosus* DSM 16366 strain (Delgado *et al*., 2005), which was purchased from the DSMZ collection (Germany). In fermentation B3 the vessels were inoculated with a wild strain of *L. mesenteroides* subsp. *mesenteroides* (Lm139) isolated from a spontaneous Kalamon olives fermentation. In both fermentations B2 and B3, the inocula were taken from overnight cultures in MRS broth supplied with 5% w/v NaCl, for a better adaptation of the bacteria to the salinity in the cover brine. The cells were collected by centrifugation at 10 000 × g at 4°C, resuspended in 0.9% w/v NaCl and inoculated to 10^6 cfu × $ml^{-1}$of cover brine solution.

All fermentation vessels were incubated at 22°C for 70 d. During that period, the salt concentration of the brine was periodically monitored and adjusted to the initial level of 5%. Brine samples were collected at day 0 (the sample was taken about 30 min after the inoculation), 3, 5, 7, 10, 13, 17, 21, 30, 40 and 70 d of fermentation, for microbiological and physicochemical analyses.

Microbiological analysis. Samples (brine or olives) were serially diluted with a factor of 10 in saline solution (0.9% w/v) and plated in triplicate on selective agar media (Biokar Diagnostics Beauvais, France) in order to enumerate the following microbial groups: (i) LAB on double layer of de Man-Rogosa-Sharp (MRS) pH 5.6, modified by the addition of 500 μg ml^{-1} cyclohexamide, incubated at 30°C for 48 h, (ii) yeasts and moulds on Yeast Extract Glucose Chloramphenicol (YGC) incubated at 25°C for 72 h and, (iii) enterobacteria on double layer of Violet Red Blue Lactose (VRBL) incubated at 30°C for 24 h. The same microbial groups were enumerated in fresh (raw) olive fruits before their immersion in tap water, by dilution of 10 g of olives in 90 ml of saline solution (0.9% w/v), decimal dilutions in the same saline solution and plating on the above mentioned selective agar media.

Physicochemical analyses. The pH of the brine samples was measured using a Metrohm model 827 pH meter (Herisau, Switzerland). Titratable acidity of the brines was determined by titration with 0.1 N NaOH up to pH 8.2 and the result was expressed as % of lactic acid (w/v).

Total phenolics in the brine as well as in the fruit flesh were quantified by the Folin-Ciocalteau assay (Singleton and Rossi, 1965) with the adaptations for the olive fruit applied by Marsilio *et al*. (2005).

Organic acids (lactic, succinic, malic, acetic, citric and tartaric) as well as sugars (glucose, sucrose and fructose) and sugar alcohols (mannitol) in the brine were determined by HPLC (LC 1150 HPLC Pump, GBC Scientific Equipment, Dandenong, Victoria, Australia). One ml of the brine sample was overnight precipitated with $HClO_4$ (final concentration 6.4%) at 4°C, centrifuged (12000 × g for 1 h at 4 °C) and the supernatant was filtered (0.2 μm filters). A 20-μl sample of the filtrate was injected into an Aminex HPX-87H column (300 by 7.8 mm; Bio-Rad, Hercules, CA, USA) connected to a refractive index detector (model LC 1240; GBC Scientific Equipment). Elution was performed at 65°C with 4.5 mM H_2SO_4 at a flow rate of 0.5 ml min^{-1}. Data acquisition and processing were performed by the Win Chrom™ Chromatography Data Acquisition Software v. 1.32 (GBC Scientific Equipment). The quantification analysis of the above organic acids and sugars was performed from standard curves, which were prepared from different concentrations of the respective reference substances analyzed under the same conditions.

Statistical analysis. Differences among means of measurements were assessed with the analysis of variance (ANOVA). Post-hoc analysis was performed with the Tukey's test for $p < 0.05$.

Results and Discussion

The aim of this study was to evaluate the potential of the wild strain *L. mesenteroides* subsp. *mesenteroides* Lm139, isolated from the brine of Kalamon olives laboratory spontaneous fermentation, as a starter in Kalamon table olives fermentation, in low salinity brines. The choice of this autochthonous LAB strain was based on its tolerance to 1% w/v oleuropein – the bitter glucoside found in olives – and to high salt concentration (10% w/v NaCl), as well as to its ability to hydrolyse the oleuropein, as it produces the β-glucosidase enzyme (data not shown). *Lactobacillus pentosus* DSM 16366, isolated from fermenting green olives of "Azeiteria" cultivar prepared according to Spanish style (Delgado *et al*., 2005), was also examined as an alternative starter culture. This strain is considered to be a strain with technological interest which could be used as a starter for table olives, since it produces the bacteriocin plantaricin S in environmental conditions resembling green olives fermentation (Delgado *et al*., 2005). It has been additionally successfully used in experimental green olives Spanish-type fermentation by Peres *et al.* (2008).

Evolution of microbial populations during fermentation. Microbiological analysis of fresh/raw Kalamon olives used in the experimental fermentations, after washing and before their placement in tap water, resulted in the following microbial populations: LAB < 10 cfu g^{-1}, yeasts and moulds 1.3×10^3 cfu g^{-1} and enterobacteria < 10 cfu g^{-1}.

The population dynamics of the three microbial groups (LAB, yeasts/moulds, enterobacteria) examined in the brines of the three olive fermentations is presented in Fig. 1. All three microbial groups exhibited

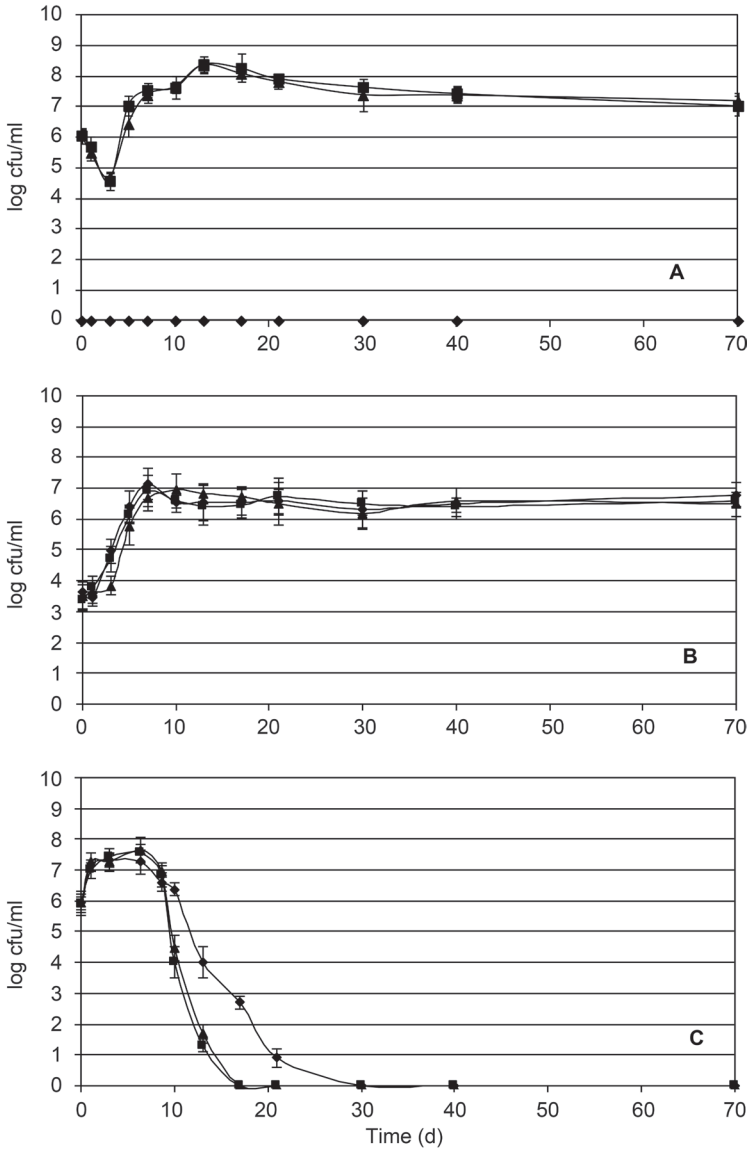

Fig. 1. Population dynamics of lactic acid bacteria (A), yeasts/moulds (B) and enterobacteria (C) in brines, during the 70 days of cv. Kalamon olives fermentation.
(♦): spontaneous fermentation B1, (■): fermentation B2, inoculated with *L. pentosus* DSM 16366, and (▲): fermentation B3, inoculated with *L. mesenteroides* subsp. *mesenteroides* Lm139. Data reported are means from three repetitions ± standard deviation.

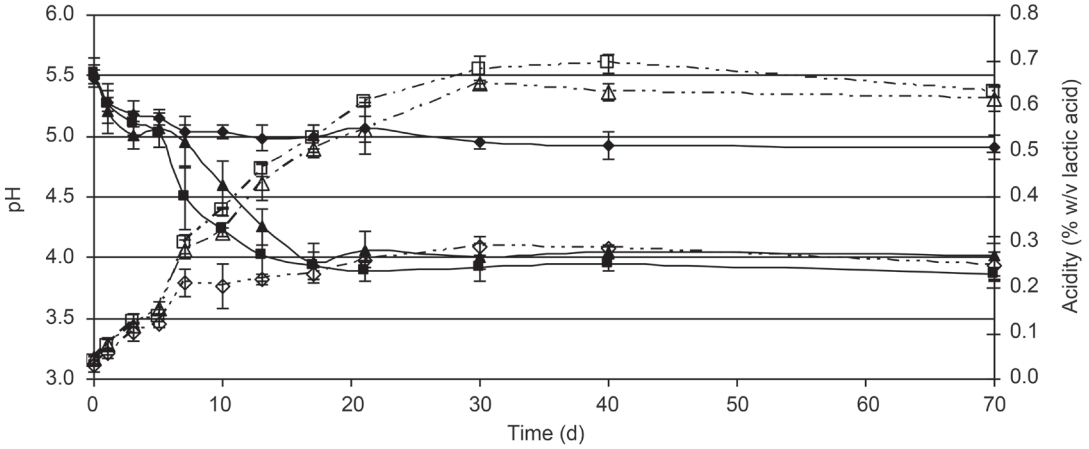

Fig. 2. Changes in pH (solid symbols) and titratable acidity (empty symbols, dashed lines) of brines, during the 70 days of cv. Kalamon olives fermentations.

(♦): spontaneous fermentation B1, (■): fermentation B2, inoculated with *L. pentosus* DSM 16366, and (▲): fermentation B3, inoculated with *L. mesenteroides* subsp. *mesenteroides* Lm139. Data reported are means from three repetitions ± standard deviations.

growth in the inoculated fermentation brines (B2 and B3 inoculated with *L. pentosus* DSM 16366 and *L. mesenteroides* subsp. *mesenteroides* Lm139, respectively). In contrast, in the brines of the non-inoculated spontaneous fermentation B1, LAB were not detected at all throughout the fermentation period of 70 d (Fig. 1a).The growth profile of LAB in brines B2 and B3 revealed that after a 3-day initial phase of adaptation, LAB managed to recover, and their population increased by 2 logs on day 13, compared to the initial inoculum in the brines (Tukey's test, $p < 0.05$). Afterwards, the population plateaued for several days followed by a slow decrease that reached an approximately 1 log reduction at day 70 in comparison to the population observed at day 13. No significant differences were observed among the growth patterns of the yeast populations in fermentations B1, B2 and B3 (Fig. 1b). In the spontaneous fermentation B1, growth of yeasts and moulds was not stimulated by the absence of competition from the LAB population and enterobacteria were eliminated after 30 d, while in fermentations B2 and B3 the use of the starter cultures influenced the population of enterobacteria that disappeared much earlier, on day 13 and 17, respectively (Fig. 1c).

Physicochemical changes during fermentation. Figure 2 presents changes in pH and titratable acidity of brines in the three olive fermentations. In the spontaneous fermentation B1, the pH value of the brine dropped only to 4.9 (from the initial value of 5.5) at the end of the experiment (day 70), when the acidity reached only the value of 0.25% (w/v) lactic acid. On the contrary, in fermentations B2 and B3, the pH dropped within the first 17 days to the values of 3.9 and 4.0 respectively and remained almost constant until the day 70. The corresponding values of the brines' acidity at the end of the experiment were 0.63% for B2 and 0.62% for B3 (day 70). Our findings suggest that the use of LAB starter cultures had a significant effect on the acidification of the brines. The amount of acid produced and the final pH value in fermentations B1 may not contribute enough to the preservation of the product. The higher acidity and the lower pH values of fermentations B2 and B3 are sufficient to inhibit the growth of spoilage microorganisms and thus they may provide an extended shelf life to the product. This could also be supported by the faster disappearance of enterobacteria in the latter fermentations as discussed above.

In the three fermentations, the phenolic content of the olives declines because of the diffusion of the compounds to the brine, and as a consequence the brines' phenolic concentration increases (data not shown). The phenolic content of the fresh olives used for all fermentations corresponded to about 20 mg gallic acid $\times$ g olive^{-1}.

The concentration levels of organic acids in the brine during the fermentation process are presented in Fig. 3. The major organic acid detected during fermentations B2 and B3 was lactic acid (ranging from 99 mM in B3 to 118 mM in B2, after 70 d of fermentation), produced probably by the LAB growing in the brine. In the spontaneous fermentation B1, lactic acid was detected in traces throughout the 70 days. This result is in accordance with the absence of LAB observed in this fermentation (Fig. 1a).

The acidification of the inoculated brines was not only due to the production of lactic acid, but also due to the production of acetic acid. In fermentations B2 and B3, acetic acid was detected in lower concentrations compared to lactic acid, ranging from 18 mM in B3 to 22 mM in B2 after 70 days of fermentation. The presence of acetic acid in the brines of both B2 and B3 could be attributed to a shift from homo- to hetero-

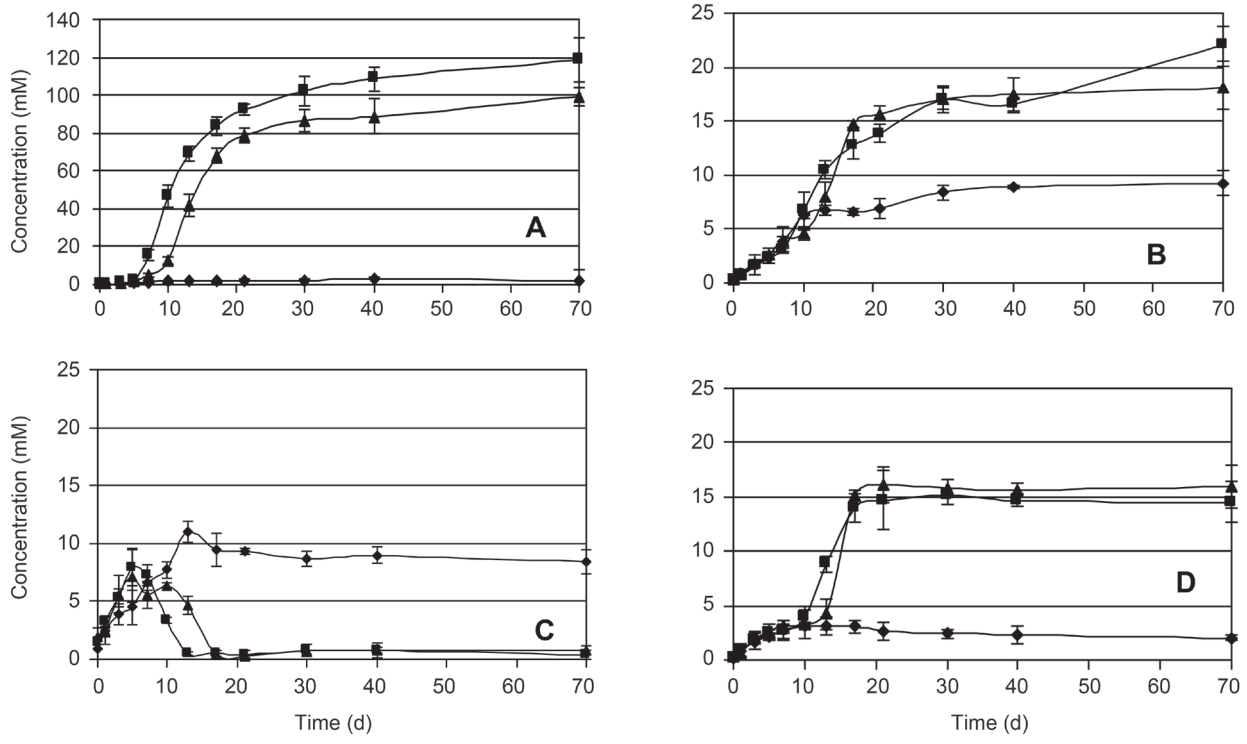

Fig. 3. Changes in the concentration (mM) of lactic acid (A), acetic acid (B), tartaric acid (C) and succinic acid (D) in brines, during the 70 days of cv. Kalamon olives fermentation.

(♦): spontaneous fermentation B1, (■): fermentation B2, inoculated with *L. pentosus* DSM 16366, and (▲): fermentation B3, inoculated with *L. mesenteroides* subsp. *mesenteroides* Lm139. Data reported are means from three repetitions ± standard deviations.

fermentative metabolism of *L. pentosus* and *L. mesenteroides* subsp. *mesenteroides*. In the non-inoculated brine B1, the presence of acetic acid remained lower (9 mM at day 70) compared to fermentations B2 and B3. Succinic acid was not detected in brine B1, while the evolution of its concentration in fermentations B2 and B3 was found to be similar to that of the acetic acid. Low concentration of tartaric acid was also detected in both inoculated samples during the first 10 days of fermentation; the concentration observed reached 7.9 mM and 7.3 mM at day 5 for fermentations B2 and B3, respectively. It was further decreased to almost zero on day 13 for both samples. On the contrary, in spontaneous fermentation B1, tartaric acid was constantly detected in the brine till the end of the fermentation (8.4 mM on day 70). The tartaric acid is referred as an acid found in olives and the observed increase of its concentration in the brines during the first days of fermentation is attributed to its extraction from the olives (Vlachov, 1976). It could be assumed that in fermentations B2 and B3 the microorganisms may have metabolised the acid.

Finally, HPLC analysis revealed either absence or presence in traces for malic and citric acid, in all three samples, during the entire process of fermentation (data not shown). This finding is in agreement with results reported by other authors (Tassou *et al*., 2002; Panagou *et al*., 2008; Tofalo *et al*., 2012), who detected malic acid at low amounts at the beginning of the process that decreased at the end of the fermentation period. According to the literature, the gradual decrease in the concentration of these two organic acids in brines observed during the fermentation of green olives is attributed to the microbial degradation of malic acid to lactic acid and CO_2, as well as to the citric acid metabolism to acetic and succinic acid (Montano *et al*., 1993). However, in the current study, the absence of both acids from the brines even at day 0, *i.e.* after two days of incubation of olives in the brine, means that these two acids were not extracted from the olives at all.

Soluble sugars extracted from olive fruits into the brine are the substrates for microbial fermentation, leading to the production of acids responsible for the low pH, but also to the production of secondary metabolites responsible for the organoleptic characteristics of the final product. In order to investigate the availability of sugars for the accomplishment of the microbial fermentation as well as the evaluation of their consumption, HPLC analysis of glucose, mannitol, sucrose and fructose was performed. The choice of these sugars was based on the fact that, according to the literature, they are the main sugars present in olives, although their concentration depends on the variety, ripeness and cultivation conditions (Kailis and Harris, 2007).

Figure 4 presents the changes of glucose and mannitol concentration in the brine during fermentations B1, B2 and B3. The concentration of glucose gradually

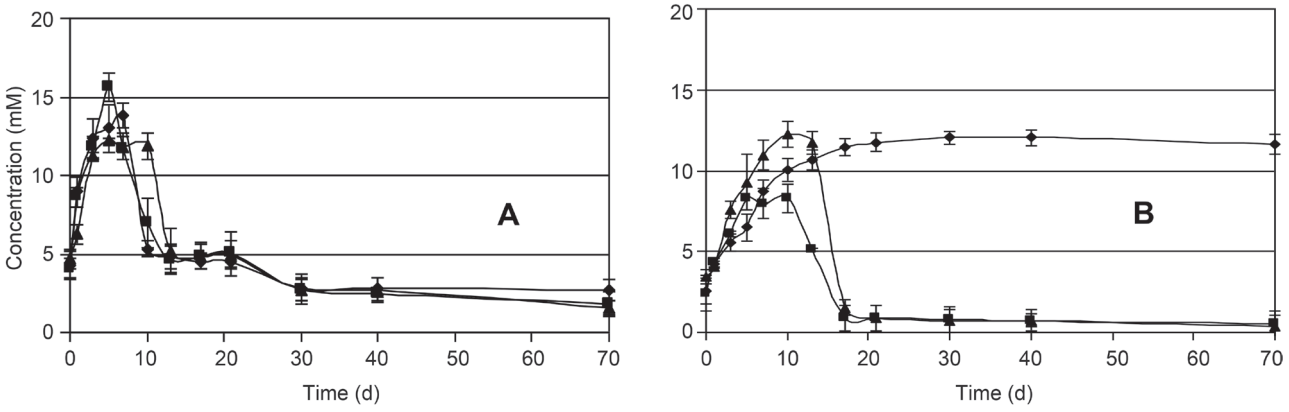

Fig. 4. Changes in the concentration (mM) of glucose (A) and mannitol (B) in brines, during the 70 days of cv. Kalamon olives fermentation.

(♦): spontaneous fermentation B1, (■): fermentation B2, inoculated with *L. pentosus* DSM 16366, and (▲): fermentation B3, inoculated with *L. mesenteroides* subsp. *mesenteroides* Lm139. Data reported are means from three repetitions ± standard deviations.

increased in all brines during the first 5–7 days, due to its diffusion from the olives to the brine, and then gradually decreased probably due to its consumption by the microorganisms. In fermentations B2 and B3 this decrease was observed earlier (at day 7) compared to fermentation B1 (at day 10). A clear difference between inoculated and non-inoculated samples was observed in the mannitol consumption which took place only in fermentations B2 and B3. Fructose was not detected at all and sucrose was detected only in traces in all three samples on day 30 and remained at the same level till the end of the fermentation period (data not shown). These two sugars were not obviously extracted from the olives, as they were not detected in the water where the olives remained for 24 h before being placed in the brine nor in the brines where the olives remained for 48 h before the addition of the starters (data not shown).

The comparison of the results obtained by monitoring of the two controlled olive fermentations B2 and B3 with the respective one corresponding to the spontaneous olive fermentation B1 revealed that in both cases of starters, a lactic acid fermentation was achieved by LAB. This can be supported by the growth of this microbial group solely in fermentations B2 and B3 as well as by the high lactic acid production in both inoculated samples, which led to a faster pH drop. The final pH value reached by each starter culture used (around 4.0) indicates a successful lactic fermentation that can be considered as an extra technological hurdle (Garrido-Fernández *et al.*, 1997; Sánchez-Gómez *et al.*, 2006; Hurtado *et al.*, 2008).

The production of lactic acid in fermentations B2 and B3 as well as the concomitant drop of the pH value, led to the inhibition of enterobacteria in a shorter period of time compared to the spontaneous fermentation B1, as indicated by the microbiological analysis. It is already known that Gram-negative bacteria, mainly enterobacteria, dominate (10^7–10^8 cfu ml^{-1}) during the first days of olive fermentation process, till LAB or yeasts or both start to emerge. Then the Gram-negative bacteria disappear because of the increase of acidity due to the acid produced by the fermentation process (Garrido-Fernández *et al.*, 1997; Sánchez-Gómez *et al.*, 2006; Hurtado *et al.*, 2008). Apart from the role of enterobacteria as spoilage microorganisms in table olives, their absence is also considered as an indicator of olives' safety and suitability for consumption.

On the contrary, the pH and the acidity values achieved as well as the absence of lactic acid in the brine of the spontaneous fermentation B1, indicate the absence of lactic fermentation and the domination of yeasts, which was confirmed by the microbiological analysis. This observation is in accordance with previous studies referring that LAB and yeasts compete for the fermentation of natural olives and that yeasts can be very often exclusively responsible for the fermentation (Balatsouras, 1990; Garrido-Fernández *et al.*, 1997; Sánchez-Gómez *et al.*, 2000; Brenes, 2004; Aponte *et al.*, 2010). Tassou *et al.* (2002) reported that only yeasts were able to grow in naturally black olives (cv. Conservolea) when the NaCl concentration was 8%.

The lactic acid fermentation accomplished in inoculated samples B2 and B3 obviously led to a faster consumption of sugars effused from the olive fruits into the brines and thus, the risk of undesirable secondary fermentations during the storage of the olives was minimized. On the contrary, the delay in the sugar consumption observed in fermentation B1 could be attributed to the limited fermentation activity due to the absence of LAB.

Fermentation of olives with each of the starters in brines of lower salt concentration compared to those traditionally used by the producers is important because it allows the production of Kalamata table olives with

low salt content. Furthermore, from an environmental point of view, there is an interest in reducing the NaCl content of brines which are extremely difficult to treat as waste (Hurtado *et al*., 2012).

Concluding, the use of the LAB *L. pentosus* DSM 16366 and *L. mesenteroides* subsp. *mesenteroides* Lm139 as starter cultures in Kalamon olives fermentation in low salinity brine could lead to the production of olives of a constant quality, which will not depend on the indigenous microbiota that is influenced by the year and cultivation region. Such a practice could lead to a more controllable fermentation resulting in a product of high and constant quality being safer for the consumers and having a longer lifetime. As far as we know this is the first study considering the use of LAB as starter cultures during Kalamon olives fermentation, and more particularly the use of autochthonous LAB strains isolated from a spontaneous fermentation of the respective olive cultivar.

Acknowledgements

This study was funded by the "John S. Latsis Public Benefit Foundation" in the frame of "Scientific Projects 2009" program.

Literature

Aponte M., V. Ventorino, G. Blaiotta, G. Volpe, V. Farina, G. Avellone, C.M. Lanza and G. Moschetti. 2010. Study of green Sicilian table olive fermentations through microbiological, chemical and sensory analyses. *Food Microbiol.* 27: 162–170.

Arroyo-López F.N., A. Querol, J. Bautista-Gallego and A. Garrido-Fernández. 2008. Role of yeasts in table olive production. *Int. J. Food Microbiol.* 128: 189–196.

Balatsouras G.D. 1967. Processing the naturally ripe (black) olives, pp. 491–550. In: Proceedings of the *International Olive Oil Seminar*. Perugia-Spoleto. Italy.

Balatsouras G.D. 1990. Edible olive cultivars, chemical composition of fruit, harvesting, transportation, processing, sorting and packaging, styles of black olives, deterioration, quality standards, chemical analysis, nutritional and biological value of the end product. Proceedings of the *International Seminar*" Olio d'oliva e olive da tavola: tecnologia e qualità"(Istituto Sperimentale per la Elaiotecnica), pp. 291–330. Pescara. Italy.

Brenes M. 2004. Olive fermentation and processing: scientific and technological challenges. *J. Food Sci.* 69: 33–34.

Delgado A., D. Brito, C. Peres, F. Noé-Arroyo and A. Garrido-Fernández. 2005. Bacteriocin production by *Lactobacillus pentosus* B96 can be expressed as a function of temperature and NaCl concentration. *Food Microbiol.* 22: 521–528.

Garrido-Fernández A., M.J. Fernández and M.R. Adams. 1997. Naturally black olives type, pp. 289–367. In: Garrido-Fernández A., M.J. Fernández and M.R. Adams (eds). *Table olives: Production and processing*. Chapman and Hall, London, UK.

Hurtado A., C. Reguant, B. Esteve-Zarzoso, A. Bordons and N. Rozès. 2008. Microbial population dynamics during the processing of Arbequina table olives. *Food Res. Int.* 41: 738–744.

Hurtado A., C. Reguant, A. Bordons and N. Rozès. 2012. Lactic acid bacteria from fermented table olives. *Food Microbiol.* 31: 1–8.

International Olive Council (IOC). 2012a. World Table Olive Figures. *http://www.internationaloliveoil.org/estaticos/view/132-world-table-olive-figures*, 2015.01.02.

International Olive Council (IOC). 2012b. The world market in figures. In: International Olive Council (ed). *Olivae* 117–2012: 28–34.

Kailis S. and D. Harris. 2007. The olive tree *Olea europaea*, pp. 17–66. In: Kailis S. and D. Harris (eds). *Producing Table olives*. Landlinks Press, Collingwood, USA.

Marsilio V., L. Seghetti, E. Iannucci, F. Russi, B. Lanza and M. Felicioni. 2005. Use of a lactic acid bacteria starter culture during green olive (*Olea europaea* L cv Ascolana tenera) processing. *J. Sci. Food Agr.* 85: 1084–1090.

Montano A., A.H. Sanchez and A. De Castro. 1993. Controlled fermentation of Spanish-type green olives. *J. Food Sci.* 58: 842–844.

Panagou E.Z., U. Schillinger, C.M.A.P. Franz and G.J. Nychas. 2008. Microbiological and biochemical profile of cv. *Conservolea* naturally black olives during controlled fermentation with selected strains of lactic acid bacteria. *Food Microbiol.* 25: 328–358.

Peres C., L. Catulo, D. Britoa and C. Pintadoa. 2008. *Lactobacillus pentosus* DSM 16366 starter added to brine as freeze-dried and as culture in the nutritive media for Spanish style green olive production. *Grasas Aceites* 59: 234–238.

Sánchez-Gómez A.H., A. de Castro, L. Rejano and A. Montaño. 2000. Comparative study on chemical changes in olive juice and brine during green olive fermentation. *J. Agr. Food Chem.* 48: 5975–5980.

Sánchez-Gómez A.H., P. García and L. Rejano. 2006. Trends in table olives production, elaboration of table olives. *Grasas Aceites.* 57: 86–94.

Singleton V.L. and J.A. Rossi. 1965. Colorimetry of total phenolics with phosphomolybdic-phosphotungstic acid reagents. *Am. J. Enol. Viticult.* 16: 144–158.

Tassou C.C., E.Z. Panagou and K.Z. Katsaboxakis. 2002. Microbiological and physicochemical changes of naturally black olives fermented at different temperatures and NaCl levels in the brines. *Food Microbiol.* 19: 605–615.

Tofalo R., M. Schirone, G. Perpetuini, G. Angelozzi, G. Suzzi and A. Corsetti. 2012. Microbiological and chemical profiles of naturally fermented table olives and brines from different Italian cultivars. *A. Van Leeuw.* 102: 121–131.

Vlachov G. 1976. Gli acidi organici delle olive: il rapporto malico/citrico quelle indice de maturazione. *Ann. Inst. Sper. Elaiotecn.* 2: 93–112.

Polish Journal of Microbiology
2015, Vol. 64, No 3, 273–278

ORIGINAL PAPER

Activity of Natural Polyether Ionophores: Monensin and Salinomycin against Clinical *Staphylococcus epidermidis* Strains

JOANNA STEFAŃSKA[1]*, KAROLINA STĘPIEŃ[1], ADAM HUCZYŃSKI[2] and STEFAN TYSKI[1, 3]

[1] Department of Pharmaceutical Microbiology, Medical University of Warsaw, Poland
[2] Faculty of Chemistry, Adam Mickiewicz University, Poznań, Poland
[3] Department of Antibiotics and Microbiology, National Medicines Institute, Warsaw, Poland

Submitted 15 December 2014, revised 16 February 2015, accepted 17 February 2015

Abstract

Staphylococcus epidermidis, a coagulase-negative *Staphylococcus*, is the most important pathogen responsible for chronic nosocomial infections. These bacteria produce extracellular slime and form biofilms on various biotic and abiotic surfaces. Bacterial biofilms are very resistant to standard antimicrobial therapy and difficult to eradicate, so it is important to search for new more effective anti-biofilm agents, for example in the group of natural substances. The aim of the study was to examine the activity of two ionophores-salinomycin and monensin against clinical *S. epidermidis* strains, using MIC/MBC method and biofilm formation inhibition assay. Bacterial strains were tested also for slime production using Congo Red Agar. Both tested ionophore antibiotics showed the highest activity against planktonic bacteria of clinical as well as standard *S. epidermidis* strains and effectively inhibited the formation of bacterial biofilm.

Key words: *Staphylococcus epidermidis*, bacterial biofilm, Congo Red Agar, ionophores

Introduction

Staphylococcus epidermidis belonging to coagulase-negative staphylococci, the regular component of human skin and mucous membranes, is a major cause of chronic nosocomial infections associated with implanted medical devices, *i.e.* vascular line, artificial heart valves, catheters, bone implants (Arciola *et al.*, 2005; Montanaro *et al.*, 2011). Multi-drug resistance strains, the most common reasons of nosocomial postoperative wound and bloodstream infections, create serious problems. *S. epidermidis* produce extracellular slime and are able to adhere to various surfaces (biotic and abiotic), as well as form biofilms (Christensen *et al.*, 1982; Götz, 2002; Mack *et al.*, 2006). Slime production and formation of biofilms have been considered as important *S. epidermidis* virulence factor in the development of biomaterials-related infections (Pascual, 2002; Podbielska *et al.*, 2010). Biofilms are multicellular, three-dimensional structures composed of aggregates of microorganisms cells and the extracellular matrix, comprising polysaccharides, proteins, nucleic acids and water (Costerton *et al.*, 1999). Bacteria in biofilm form are very difficult to eradicate and more resistant to the host immune response and standard antimicrobial agents, such as antibiotics, antiseptics and disinfectant than planktonic form (Bridier *et al.*, 2011; Gomes *et al.*, 2014; Høiby *et al.*, 2010). Due to the problems in the treatment of biofilm-related infections, it is very urgent and important to search for new more effective anti-biofilm agents, *e.g.* in the group of natural substances.

Natural polyether ionophores, such as salinomycin (SAL) and monensin (MON), have been objects of great interest, because of their antibacterial (Rutkowski and Brzezinski, 2013), antifungal (Oz *et al.*, 1997), antiparasitic (Adovelande and Schrével, 1996; Kevin *et al.*, 2009) as well as antiviral (Johnson *et al.*, 1982) activities. Furthermore, salinomycin and monensin are commonly used in veterinary medicine as a non-hormonal growth promoting (Callaway *et al.*, 2003) and coccidiostatic agents (Butaye *et al.*, 2003; Rutkowski and Brzezinski, 2013).

Recently, it has been found that this class of compounds might be also important as chemotherapeutic agents, especially against the proliferation of various cancer cells, including those displaying multi-drug resistance and against cancer stem cells (CSCs). It has been found that salinomycin and monensin exhibit

* Corresponding author: J. Stefańska, Department of Pharmaceutical Microbiology, Medical University of Warsaw, Warsaw, Poland; **e-mail: jstefanska@wum.edu.pl**

high antimicrobial activity against Gram-positive bacteria, including mycobacteria and some filamentous fungi (Huczyński, 2012; Łowicki and Huczyński, 2013).

Polyether skeletons of the pseudo-cyclic structure of polyether ionophores are able to form complexes with metal cations and facilitate their transport across cellular membranes, disrupting the Na^+/K^+ ion balance across cell membranes, which finally leads to death of a cell. Monensin and salinomycin derivatives such as esters and amides are also active against the strains of Gram-positive bacteria, including hospital *S. aureus* strains, *i.e.* methicillin-susceptible (MSSA) and methicillin-resistant *S. aureus* (MRSA) and *S. epidermidis* (MRSE) strains (Antoszczak *et al*., 2014; Łowicki *et al*., 2009).

In this study antimicrobial activity of monensin and salinomycim against planktonic cells of clinical *S. epidermidis* strains as well as inhibition of bacterial biofilm formation by ionophores were investigated.

Experimental

Materials and Methods

Chemicals. Salinomycin was prepared conveniently by isolation of its sodium salt from commercially available veterinary premix – SACOX® following acidic extraction using the procedure described previously (Huczyński *et al*., 2012). The spectroscopic data of salinomycin were in agreement with previously published assignments (Huczyński *et al*., 2012). Monensin was purchased from Sigma-Aldrich.

Bacterial strains. Twelve clinical *S. epidermidis* strains and two reference strains: *S. epidermidis* ATCC 12228 and *S. epidermidis* ATCC 35984 were used in this study.

The clinical strains were isolated from blood of hospitalised patients. S. *epidermidis* ATCC 12228 was used in biofilm assay as a negative control (low biofilm-producer), *S. epidermidis* ATCC 35984 was used as positive control (high biofilm-producer).

Microorganisms were obtained from the collection of Department of Pharmaceutical Microbiology, Medical University of Warsaw, Poland.

Evaluation of minimal inhibitory concentration (MIC) and minimal bactericidal concentration (MBC) of tested compounds. The minimal concentrations of monensin, salinomycin and the reference antibacterial agent – ciprofloxacin (CIP), inhibiting growth of bacterial strains were determined by reference broth dilution methods using 96-well microtitre plates (Medlab Products), according to Clinical and Laboratory Standards Institute recommendation (CLSI, 2012a). Concentrations of tested compounds in Mueller-Hinton liquid medium (Beckton Dickinson) ranged from 0.0625 to 256 $\mu g \times ml^{-1}$. The final inoculum of all microorganisms studied was about 10^5 CFU/ml (colony forming units per ml). MICs values were estimated after 18 h incubation at 35°C. MBC values (99.9 % cells killing of the final inoculums) of the compounds were determined by subculturing 10 µl of suspension from each negative (no visible growth) well from the MIC assay, onto TSA plates (CLSI, 1999). The plates were incubated for 24 hours at 37°C.

Detection of slime-production on Congo Red Agar. All *S. epidermidis* strains were tested for slime production on Congo Red Agar (CRA) according to Podbielska *et al*. (2010). The CRA medium was composed of 37 g/l BHI agar (bioMérieux) supplemented with 0.8 g/l of Congo red (Sigma) and 50 g/l sucrose (POCh). Bacteria from one colony were cultured on medium in two replicates. Plates were incubated for 24 h at 37°C and for 24 h at 20°C in the dark. After incubation the color of bacterial colonies was assessed.

***S. epidermidis* biofilm formation – MTT assay.** *S. epidermidis* stains were cultured in Tryptone Soy Broth (BTL) supplemented with 0.5% glucose (POCh) for 24 h at 37°C. Bacterial culture was diluted 1:1 in fresh TSB-glucose to obtain a final concentration of approximately 10^7 CFU/ml. This suspension was transferred to wells of 96-well microdilution plates (Karell-Medlab, Italy). The medium TSB-glucose without bacteria was a negative control.

The plates were incubated for 24 h at 37°C. After incubation, the contents of each well were removed and wells were washed with sterile phosphate buffered saline (PBS). Adherent bacteria in wells were stained with 3-(4,5-dimethyl-2-thiazolyl)-2,5 diphenyl-2H-tetrazolium bromide (MTT, Sigma; 0.5% in PBS). The plates were incubated for 2 hours at 37°C. Adherent bacterial cells, which usually formed biofilm on wells surface, were uniformly stained with MTT. After incubation the solution was removed and bacterial biofilm was solubilized in DMSO (Merck) with glycine buffer (pH 10.2) and incubated for 15 minutes at room temperature. The absorbance was measured at 554 nm using spectrophotometer (Power Wave XS, BioTek). The experiments were performed in four replicates.

Biofilm inhibition assay. Inhibition of bacterial biofilm formation was screened using modified method, described previously (Nagender *et al*., 2013). All tested *S. epidermidis* strains were cultured overnight in Tryptone Soy Broth supplemented with 0.5% glucose. The solutions of tested compounds in TSB-glucose medium were mixed (1:1) with the bacterial inocula (10^7 CFU/ml) in sterile 96-well polystyrene microtitre plates and incubated at 37°C for 24 h. The final concentrations of the tested compounds ranged from 1 to 32 µg/ml.

The negative control was TSB-glucose medium, whereas the positive control was bacterial culture without tested compounds in TSB-glucose. After incubation

medium was discarded from the wells and wells were washed twice with sterile phosphate buffered saline (PBS) to remove the non-adherent bacteria. Alive bacterial cells in each well of the microdilution plate were stained with MTT in PBS buffer for 2 hours at 37°C. After incubation, the solution was removed and the bacterial biofilm was solubilised in DMSO with glycine buffer and mixed for 15 minutes at room temperature. Biofilm absorbance was measured at 554 nm using a spectrophotometer.

The biofilm-inhibition results were interpreted from dose (concentrations)-response graphs. All the experiments were carried out in quadruplicate.

Results

The antibiotic susceptibility of the bacterial strains was determined by the standard CLSI disk diffusion method (CLSI, 2012b) and automated manner by Vitek 2 system (bioMérieux). All clinical strains were resistant to methicillin (MRSE). Ten strains were also resistant to ciprofloxacin and two – to moxifloxacin. Eleven isolates presented MLS_B phenotype (10 – constitutive and 1-inducible). Nine strains were resistant to gentamicin, four – to tetracycline and rifampicin, one – to fosfomycin and fusidic acid. All strains were susceptible to vancomycin and linezolid.

The activities of tested compounds (salinomycin, monensin and reference antibacterial agent-ciprofloxacin) against planktonic (free-swimming) of clinical and standard *S. epidermidis* strains are listed in Table I. The salinomycin MIC values for planktonic cells ranged from 0.5 $\mu g \times ml^{-1}$ to 2.0 $\mu g \times ml^{-1}$, MBC values ranged from 4.0 to 32 $\mu g \times ml^{-1}$. Monensin was found to be active against tested strains, with MIC values ranging from 0.5 to 2.0 $\mu g \times ml^{-1}$ and MBC values ranged from 4 to 16 $\mu g \times ml^{-1}$. For the standard antimicrobial agent-ciprofloxacin MIC values ranged from 0.125 to 64 $\mu g \times ml^{-1}$ and MBC values ranged from 0.5 to > 256 $\mu g \times ml^{-1}$.

Slime production by the tested *S. epidermidis* strains was assessed on the basis of the color of bacterial colonies on Congo Red Agar. A black or brick-brown color of colonies were interpreted as slime-positive producing in contrast with red or pinkish-red colonies which were interpreted as slime-negative producing (Fig. 1).

The level of biofilm formation by *S. epidermidis* strains were tested using MTT-method. The absorbance levels (A_{554}) were assumed by the authors in order to classify the analyzed clinical strains into 2 groups: high biofilm-producers (absorbance $A_{554} \geq 1.5$; strains: 433/11, 439/11, 519/12, 526/12, 528/12, 531/12) and low biofilm-producers (absorbance $A_{554} < 1.5$; strains 430/11, 431/11, 432/11, 434/11, 517/12, 523/12).

At the phenotypic evaluation of the ability of the strains for biofilm formation, correlation between the color of bacterial colony on Congo Red Agar and the level of biofilm production in MTT-test (the average of value absorbance) was observed. Six slime-positive on CRA medium strains (black or brown colonies) were high biofilm-producers, six slime-negative isolate (brick-red or pinkish-red colonies), were low biofilm producers.

Table I
In vitro activity of salinomycin and monensin in comparision to reference ciprofloxacin against planktonic cells of *S. epidermidis* strains

S. epidermidis strains	SAL		MON		Ref*	
	MIC $\mu g \times ml^{-1}$	MBC $\mu g \times ml^{-1}$	MIC $\mu g \times ml^{-1}$	MBC $\mu g \times ml^{-1}$	MIC $\mu g \times ml^{-1}$	MBC $\mu g \times ml^{-1}$
430/11	1	16	1	8	0.5	4
431/11	2	32	2	16	4	32
432/11	2	32	2	16	64	256
433/11	1	8	0.5	4	64	256
434/11	1	8	1	8	64	>256
439/11	1	4	0.5	4	64	>256
517/12	0.5	4	0.5	2	32	256
519/12	1	8	1	8	0.5	4
523/12	2	32	2	16	64	>256
526/12	2	16	2	8	4	32
528/12	2	16	2	8	32	256
531/12	2	32	2	8	8	64
ATCC 12228	1	8	1	8	0.25	1
ATCC 35984	2	32	2	8	0.125	0.5

SAL – salinomycin, MON – monensin, Ref*– ciprofloxacin, MIC – minimal inhibitory concentration, MBC – minimal bactericidal concentration

Fig. 1. Detection of slime production on Congo Red Agar: A. Black colonies of a slime-producing clinical *S. epidermidis* 519/12 strain. B. Red colonies of a non-slime producing clinical *S. epidermidis* 523/12 strain.

The tested ionophore antibiotics (salinomycin and monensin) were further studied for their ability to inhibit the formation of biofilms by clinical and standard *S. epidermidis* strains.

The biofilm formation by most of the clinical *S. epidermidis* strains (9 of 12) was reduced in the range from 70% to above 90% by monensin and from 60% to above 90% by salinomycin in concentration 4 μg × ml^{-1} (2 × MIC for planktonic cells). The same concentration of reference antibacterial drug – ciprofloxacin, caused inhibition of biofilm formation in 60% by 5 clinical isolates. The graphs shows the effect of tested ionophores (salinomycin and monensin) and standard antimicrobial drug (ciprofloxacin) on biofilm formation by reference *S. epidermidis* ATCC 12228 and selected low-biofilm producing clinical *S. epidermidis* strains (Fig. 2–4). The standard deviation values were very low, is they are sometimes invisible in the figures.

Discussion

The results revealed that monensin and salinomycin show high antibacterial activities against planktonic cells of methicillin-resistant *S. epidermidis* clinical strains, even higher than the activity of the reference antibacterial drug – ciprofloxacin. The values of the minimal inhibitory concentration of both ionophore substances ranged from 0.5 μg × ml^{-1} to 2.0 μg × ml^{-1}, minimal bactericidal concentration values ranged from 4 μg × ml^{-1} to 16 μg × ml^{-1} (for monensin) and 4.0 μg × ml^{-1} to 32 μg × ml^{-1} (for salinomycin). The obtained results are in agreement with the literature data concerning antibacterial activity of ionophores against Gram-positive bacteria (Antoszczak *et al.*, 2014; Łowicki *et al.*, 2012; Łowicki *et al.*, 2009). There was no previous data concerning the influence of the tested ionophore antibiotics, salinomycin and monensin on staphylococcal bio-

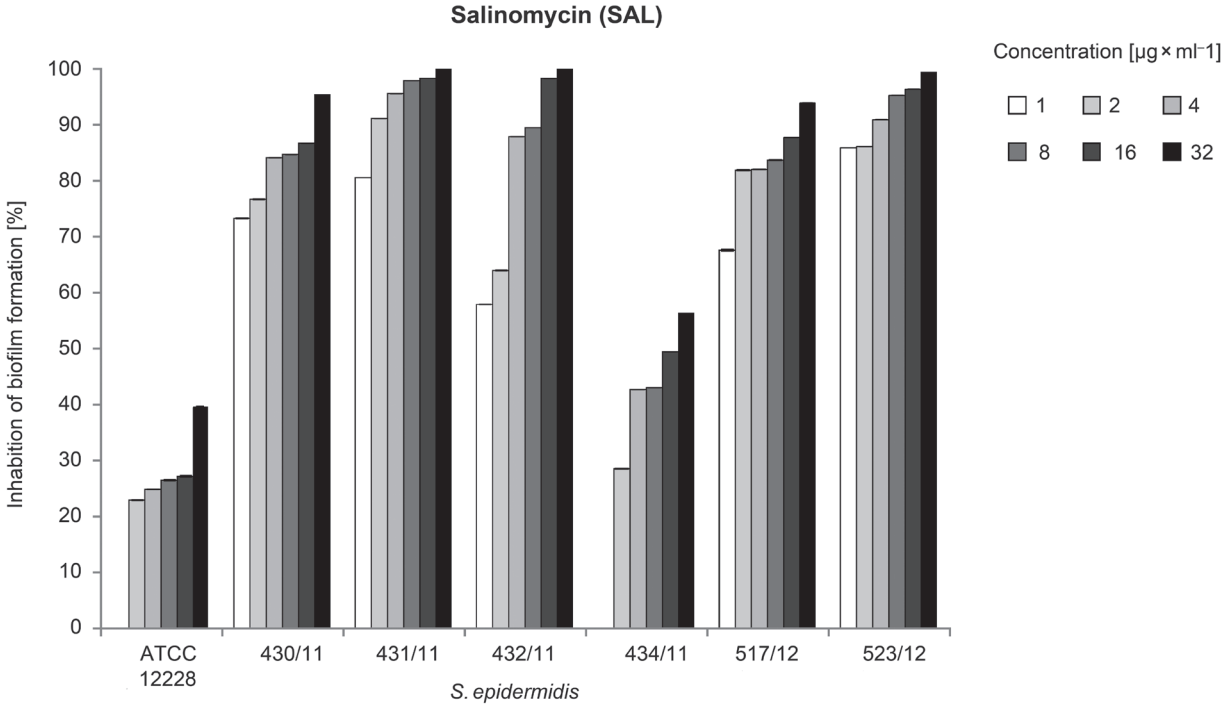

Fig. 2. Effect of the salinomycin on biofilm formation by standard and selected low-biofilm producing clinical *S. epidermidis* strains. All presented results are means from experiments performed in quadruplicate ± S.D.

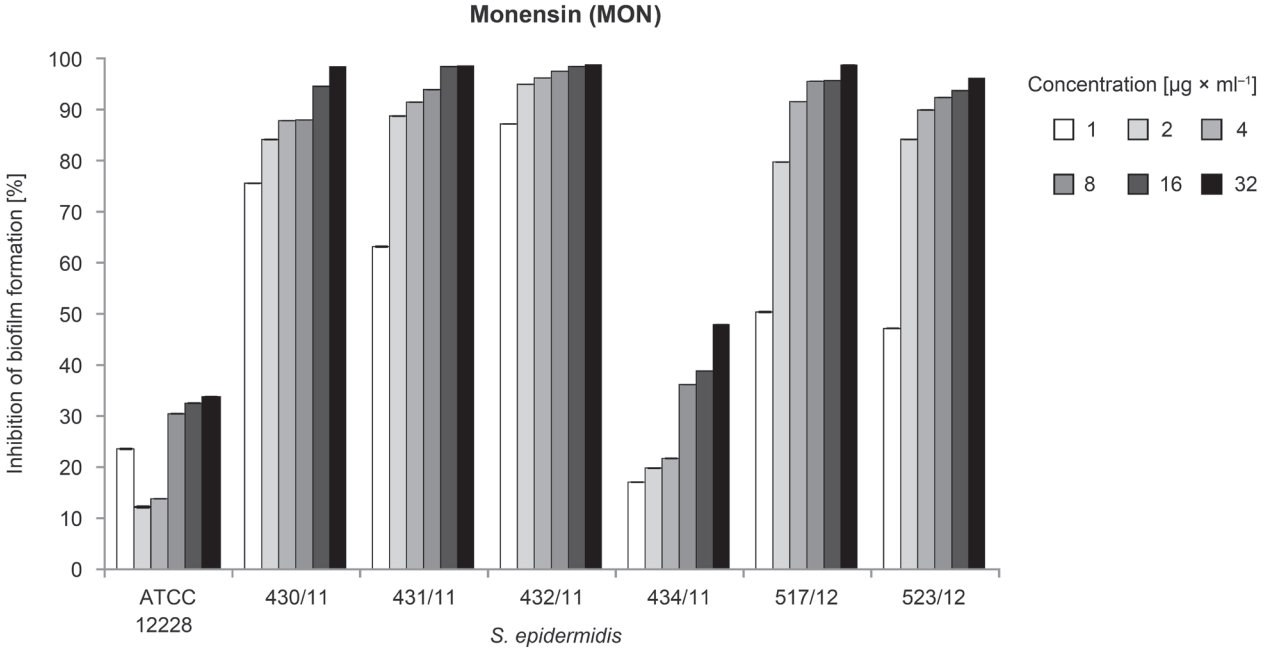

Fig. 3. Effect of monensin on biofilm formation by standard and selected low-biofilm producing clinical *S. epidermidis* strains. All presented results are means from experiments performed in quadruplicate ± S.D.

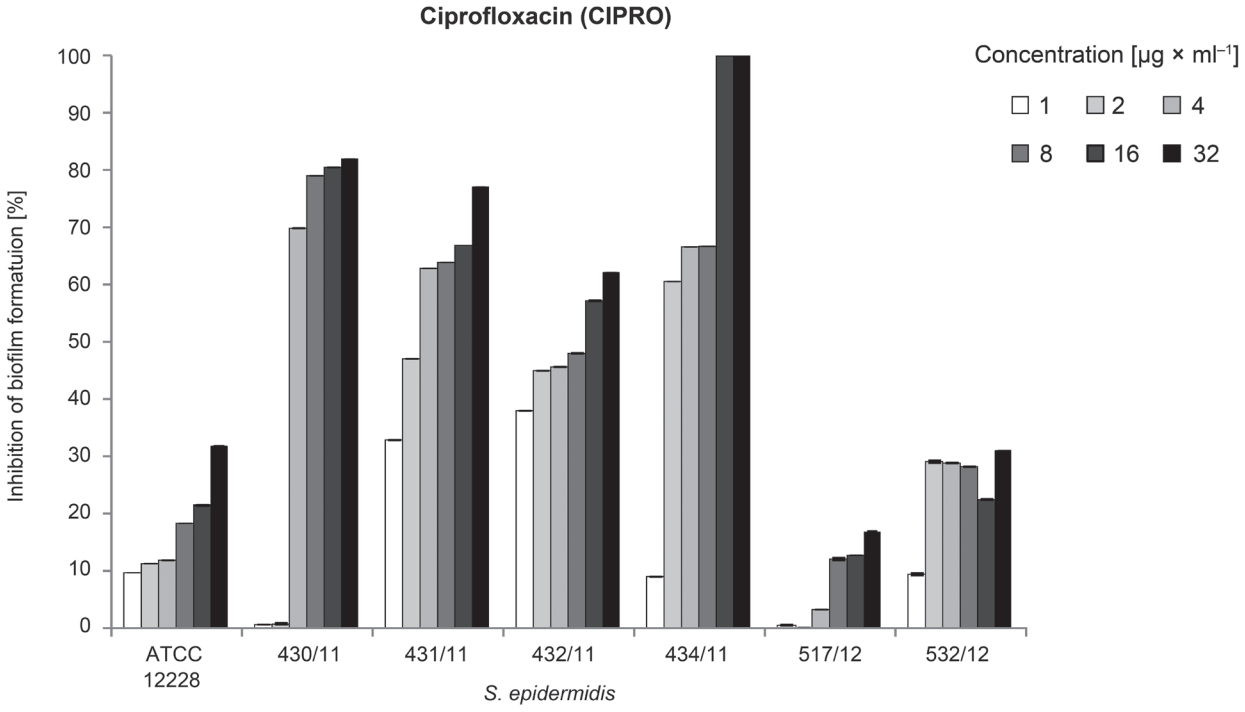

Fig. 4. Effect of ciprofloxacin on biofilm formation by standard and selected low-biofilm producing clinical *S. epidermidis* strains. All presented results are means from experiments performed in quadruplicate ± S.D

film formation. Charlebois *et al.* (2014) in their study showed the inhibitory effect of antibiotics and anticoccidials (*i.e.* monensin, narasin and salinomycin) on *Clostridium perfringens* biofilm formation. In this study both tested ionophores – monensin and salinomycin, exhibited high biofilm forming inhibitory activity against the clinical *S. epidermidis* strains, regardless of the level on which the biofilm was formed. The tested compounds showed potent antimicrobial activity when compared to standard drug-ciprofloxacin.

Conclusion. In this study two ionophore antibiotics were examined against methicillin-resistant *S. epidermidis* strains isolated from blood samples. The results

revealed that monensin and salinomycin show high antibacterial activities against planktonic cells of staphylococcal strains, even higher than the activity of the reference antibacterial drug-ciprofloxacin. In biofilm inhibitory test for most of *S. epidermidis* strains salinomycin and monensin at concentration 4 $\mu g \times ml^{-1}$ inhibited the biofilm formation at above 70%.

The presented study demonstrated that both tested ionophore antibiotics-monensin and salinomycin, possess significant antimicrobial activity against planktonic cells and showed a significant effect on biofilm formation by methicillin-resistant clinical *S. epidermidis* strains.

Acknowledgments

Research subject carried out with the use of CePT infrastructure financed by the European Union – the European Regional Development Fund within the Operational Programme "Innovative economy for 2007–2013".

Literature

Adovelande J. and J. Schrével. 1996. Carboxylic ionophores in malaria chemotherapy: the effects of monensin and nigericin on *Plasmodium falciparum in vitro* and *Plasmodium vinckei petteri in vivo*. *Life Sci*. 59: PL309-PL315

Antoszczak M., E. Maj, J. Stefańska, J. Wietrzyk, J. Janczak and B. Brzezinski. 2014: Synthesis, antiproliferative and antibacterial activity of new amides of salinomycin. *Bioorg. Med. Chem. Lett.* 24: 1724–1729.

Arciola CR., D. Campoccia, S. Gamberini, M.E. Donnati, V. Pirini, L. Visai, P. Spaziale and L. Montanaro. 2005. Antibiotic resistance in expolysaccharide-forming *Staphylococcus epidermidis* clinical isolated from orthopedic implant infections. *Biomaterial*. 26: 6530–6535.

Bridier A., R. Brandet, V. Thomas and F. Dubois-Brissonnet. 2011. Resistance of bacterial biofilms to desinfectants: a review. *Biofouling*. 27: 1017–1032.

Butaye P., L.A. Devriese and F. Haesebrouck. 2003. Antimicrobial growth promoters used in animal feed: effects of less well known antibiotics on Gram-positive bacteria. *Clin. Microbiol. Rev*. 16: 175–188

Callaway T.R., T.S Edrington., J.L. Rychlik, K.J. Genovese, T.L. Poole, Y.S. Jung, K.M. Bischoff, R.C. Anderson and D.J. Nisbet. 2003. Ionophores: their use as ruminant growth promotants and impact on food safety. *Curr. Issues Intest. Microbiol*. 4: 43–51.

Charlebois A., M. Jacques and M. Archmbault. 2014. Biofilm formation of *Clostridium perfringens* and its exposure to low-dose antimicrobials. *Front. Microbiol*. 5: 183.

Christensen G.D, W.A. Simpson, A.L. Bisno, E.H. and Beachey. 1982. Adherence of slime-producing strains of *Staphylococcus epidermidis* to smooth surfaces. *Infection and Immunity* 37: 318–326.

Clinical and Laboratory Standards Institute. 2012a. Methods for dilution antimicrobial susceptibility tests for bacteria that grow aerobically. Approved Standard M07-A9. CLSI CLSI, Wayne, Pennsylvania, USA.

Clinical and Laboratory Standards Institute. 2012b. Performance standards for antimicrobial disk susceptibility tests. Approved Standard M07-A11. CLSI, Pennsylvania, USA.

Clinical and Laboratory Standards Institute. 1999. Methods for determining bactericidal activity of antimicrobial agents. Approved Guideline M26-A. CLSI, Wayne, Pennsylvania, USA.

Costerton J.W., P.S. Stewart and E.P. Greenberg. 1999. Bacterial biofilms: a common cause of persistent infections. *Science* 284: 1318–1322.

Gomes F., P. Teixeira and R. Oliveira. 2014. Mini-review: *Staphylococcus epidermidis* as the most frequent cause of nosocomial infections: old and new fighting strategies. *Biofouling*. 30:131–141.

Götz F. 2002. *Staphylococcus* and biofilms. *Mol. Microbiol*. 43: 1367–137.

Høiby N., T. Bjarnsholt, M. Givskov, S. Molin and O. Ciofu. 2010. Antibiotic resistance of bacterial biofilms. *Int. J. Antimicrob. Agents.* 35: 322–332.

Huczyński A. 2012: Salinomycyn – a new cancer drug candidate. *Chem. Biol. Drug. Des.* 79: 235–238.

Huczyński, A., J. Janczak, J. Stefańska, M. Antoszczak and B. Brzezinski. 2012. Synthesis and antimicrobial activity of amide derivatives of polyether antibiotic-salinomycin. *Bioorg. Med. Chem. Lett.* 22: 4697–4702.

Johnson D.C. and P.G. Spea. 1982. Monensin inhibits the processing of herpes simplex virus glycoproteins, their transport to the cell surface, and the egress of virions from infected cells. *J. Virol.* 43: 1102–1112

Kevin D.A. II, D.A.F. Meujo and M.T. Hamann. 2009. Polyether ionophores: broad spectrum and promising biologically active molecules for the control of drug-resistant bacteria and parasites. *Expert Opin. Drug. Discov*. 4: 109–146

Łowicki D., A. Huczyński, J. Stefańska and B. Brzezinski. 2009. Synthesis, structural and antimicrobial studies of new N-allylamide of monensin A and its complexes with monovalent cations. *Tetrahedron* 65: 7730–7740.

Łowicki D., A. Huczyński, J. Stefańska and B. Brzezinski. 2010. Structural characterization and antibacterial activity against clinical isolates of *Staphylococcus* of N-phenylamide of monensin A and its 1:1 complexes with monovalent cations. *Eur. J. Med. Chem*. 45:4050–4057.

Łowicki D. and A. Huczyński. 2013. Structure and antimicrobial properties of monensin A and its derivatives: summary of the achievements. *Bio. Med. Res. Int*. 2013: Article ID 742149.

Mack D., H. Rohde, L.G. Harris, A.P. Davies, M.A. Horstkotte and J.K. Knobloch. 2006. Biofilm formation in medical device-related infection. *Int. J. Artif. Organs*. 29:343–359.

Montanaro L., P. Speziale, D. Campoccia, S. Ravaioli, I. Cangini, G. Pietrocola, S. Giannini and C.R. Arciola. 2011. Scenery of *Staphylococcus* implant infections in orthopedics. *Future Microbiol*. 6: 1329–1349.

Nagender P., G. Malla Reddy, R. Naresh Kuma, Y. Poornachandra, C. Ganesh Kumar and B. Narsaiah. 2014. Synthesis, cytotoxicity, antimicrobial and anti-biofilm activities of novel pyrazolo[3,4-b] pyridine and pyrimidine functionalized 1,2,3-triazole derivatives. *Bioorg. Med. Chem. Lett.* 24:2905–2908.

Oz H.S., W.T. Hughes and J.E. Rehg. 1997. Efficacy of lasalocid against murine *Pneumocystis carinii* pneumonitis. *Antimicrob. Agents Chemother*. 41: 191–192

Pascual A. 2002. Pathogenesis of catheter-related infection; lessons for new design. *Clin. Microbiol. Infect*. 8:256–264.

Podbielska A., H. Gałkowska, E. Stelmach, G. Młynarczyk and W.L. Olszewski. 2010. Slime production by *Staphylococcus aureus* and *Staphylococcus epidermidis* strains isolates from patients with diabetic foot ulcers. *Arch. Immunol. Ther. Exp*. 58: 321–324.

Rutkowski J. and B. Brzezinski. 2013. Structures and properties of naturally occurring polyether antibiotics. *BioMed. Res. Int*. 2013: Article ID 162513.

Polish Journal of Microbiology
2015, Vol. 64, No 3, 279–283

SHORT COMMUNICATION

Chaperone DnaJ Influences the Formation of Biofilm by *Escherichia coli*

ANNA M. GRUDNIAK*, JOLANTA WŁODKOWSKA and KRYSTYNA I. WOLSKA

Department of Bacterial Genetics, Institute of Microbiology, Faculty of Biology, University of Warsaw, Poland

Submitted 11 February 2015, Revised 16 July 2015, Accepted 17 July 2015

Abstract

DnaJ chaperone, a member of the so called DnaK-DnaJ-GrpE chaperone machine plays an important role in cell physiology. The ability of *Escherichia coli* Δ*dnaJ* mutant to form biofilm was studied. It was shown that this mutant is impaired in biofilm development when exposed to 42°C for 2 h. The impairment in biofilm development was observed when the heat shock was applied either at the onset of biofilm formation or 2 h later. The biofilm formed was thinner and its structure was changed as compared to wild-type strain. This defect could be complemented by the introduction of a wild-type gene on a low-copy plasmid.

Key words: *Escherichia coli*, chaperone DnaJ, biofilm

In natural habitats the majority of microbes form a structured biofilm ecosystem in which bacterial communities are embedded in an extracellular polymeric matrix which stabilizes biofilm structure and mediates bacterial adhesion (Flemming and Wingender, 2010). Bacterial biofilms can develop on various surfaces (Donlan, 2002) including every niche of the human body (Karatan and Watnick, 2009). Bacteria, including pathogens, when living in a biofilm, exhibit increased resistance to antimicrobials which creates a big medical problem (Hoiby *et al*., 2010). The formation of an *E. coli* biofilm requires several factors including fimbriae, adhesins, polysaccharides, lipopolysaccharides, small signaling and quorum sensing molecules (Beloin *et al*., 2008). Biofilms formed by pathogenic strains cause several food and water-born diseases such as diarrhea, urinary tract infections and chronic bacterial prostatitis (McFarlane and Dillon, 2007).

DnaJ chaperone is a prototypical member of the Hsp40 family and functions as a cochaperone of DnaK (Hsp70). It contains distinct domains involved in the regulation of the activity of Hsp70 and the binding of several substrates with different conformational properties – folded, partially (un)folded and unfolded (Walsh *et al*., 2004). The main function of DnaJ and DnaK is assistance in the folding of newly synthesized or unfolded polypeptides. The interaction of DnaJ with the hydrophobic motifs of the substrate proteins modifies their structure and function, this being crucial for DnaJ-mediated transfer of substrates to Hsp70 and modulation of its ATPase activity (Cuéllar *et al*., 2013). The two-chaperone system is sufficiently versatile to act on the entire proteome and every protein is predicted to contain multiple DnaK and DnaJ-binding sites (Srinivasan *et al*., 2012). Recently it was demonstrated that DnaJ together with DnaK and Trigger Factor (TF) are strongly involved in protein translocation by their targeting to Sec and twin-arginine translocation (Tat) pathways (Castanié-Cornet *et al*., 2014).

The involvement of DnaK chaperone in bacterial biofilm formation is the subject of several papers (*e.g.* van der Veen and Abee, 2010) but there is only one publication describing an indirect effect of DnaJ on the development of *Pseudomonas putida* biofilms (Dubern *et al*., 2005). Therefore we decided to determine the importance of DnaJ for *E. coli* biofilm development by studying the ability of a *dnaJ* null mutant to form a biofilm. We also checked the effect of DnaJ on biofilm structure as well as cell viability and motility.

E. coli Δ*dnaJ* strain (KW69) used in this study is a derivative of *E. coli* MC1061 (Casadaban and Cohen, 1980) in which *dnaJ* gene is replaced by Kan^R cassette. To complement *dnaJ* deletion defect KW87 strain was constructed. Wild type *dnaJ* allel was introduced in pJW14 plasmid containing the replication origin of pACYC184 and carrying a chloramphenicol resistance determinant. The details of strain and plasmid genotypes and genetic manipulation procedures were described previously (Wolska *et al*., 2000). Strains were grown in LB medium supplemented with kanamycin to

* Corresponding author: A.M. Grudniak, Institute of Microbiology, University of Warsaw, Warsaw, Poland; **e-mail: grudam@biol.uw.edu.pl**

final concentration of 100 µg/ml and glucose to final concentration 0.4%. When necessary the medium was solidified with 1.5% agar and supplemented with chloramphenicol to final concentration 20 µg/ml. To study bacterial motility LB medium solidified with 0.3% or 0.5% agar was used. The cultures of all strains were subjected to heat shock by transient elevation of temperature from 30°C to 42°C for 2 h, control cultures were incubated constantly at 30°C.

To determine the ability of MC1061, KW69 and KW87 strains to form a biofilm the following incubation protocol was used. Overnight cultures were diluted 100-fold in LB medium with 0.4% glucose, incubated in polystyrene microtiter plates at 30°C for 2 h, subjected to heat shock at 42°C for 2 h and incubated further at 30°C for additional 20 h. The control cultures were incubated at 30°C for 24 h. The amount of biofilm formed was determined after staining with crystal violet according to the procedure described by O'Toole and Kotler (1998). The absorbance at 570 nm was measured using microtiter plate reader (Sunrise, Tecan, Switzerland). To study the viability of cells biofilms formed in the condition described above were dried (by 20 min at 37°C) and than 100 µl of BacTiter-Glo™ Reagent was added to each microplate well. After incubation for 5 min the luminescence was measured in Microplate Luminometr GloMax-Multi® Detection system (Promega, Madison, USA), using integration time 5 sec. The results are presented as a number of RLU (Relative Luminescence Units) (Hall *et al.*, 1998; Lundin and Thore, 1975; https://pl.promega.com/resources/protocols/technical-bulletins/101/bactiter-glo-microbial-cell-viability-assay-protocol/).

Bacterial motility was estimated according to the protocol described by Lippolis *et al.* (2014). Each experiment was performed 3 times. The photographs were taken at a fixed distance between the plates and camera.

SCLM (Confocal Laser Scanning Microscopy) was used to quantify biofilm development on the glass bottom of microscope dishes (WillCo Wells BV, the Netherlands, diameter 40 mm, thickness of a glass bottom 0.16–0.19 mm). The details of procedures were described previously by Raczkowska *et al.* (2011). SCLM was conducted using a Nikon Eclipse Ti (A1) microscope equipped with a ×60, 1.4 NA oil immersion phase-contrast lens. An argon laser with a maximum emission line at 488 nm was used as the excitation source. Horizontal optical thin sections were collected at 4.0-µm intervals from the outer surface of the biofilm to the bottom of the glass plate. These images were captured by NIS-ELEMENTS interactive software and three-dimensional reconstructions (3D) were created.

The data presented in Figure 1 show that Δ*dnaJ* mutant strain is impaired in biofilm formation only in cultures transiently incubated at elevated temperature.

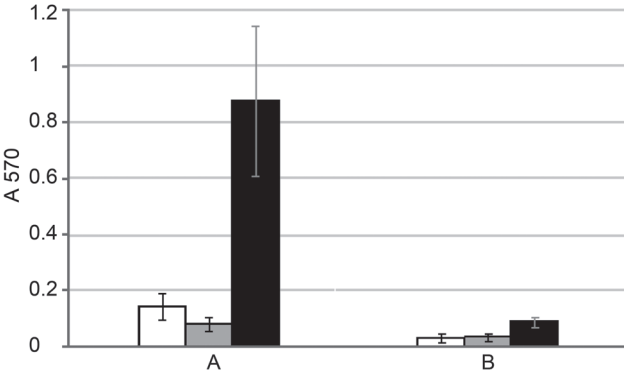

Fig. 1. The amount of biofilm formed by wild-type (white bars), Δ*dnaJ* (grey bars) and complemented strains (black bars). Heat shock condition (A), and control condition (B).

The amount of biofilm formed was diminished nearly 2-fold. It should be noted that raising the temperature for 2 h did not influence growth of Δ*dnaJ*, this effect is not observed until 3 h incubation at restrictive temperature (Paciorek *et al.*, 1997). Complemented strain KW79 formed a 6.2-fold and 2.7-fold thicker biofilm than that formed by the wild type strain incubated with or without heat shock, respectively. It was also noted that the elevation of temperature is a factor severely inducing biofilm formation in all strains tested. This observation is consistent with the literature data mentioning that bacterial biofilm development can be considered a multicellular adaptation to physical stress (de la Fuente-Núñez *et al.*, 2013).

The micrographs presented in Fig. 2 clearly demonstrate that the biofilm formed by Δ*dnaJ* mutant subjected to heat shock is much thinner than that formed by control MC1061 strain. Moreover no bulges were seen which suggests the lack of sites indicating the position of the future mushroom-shape structures characteristic for mature biofilms of many bacterial species. BactoTiterGlo™ assay was applied to determine the number of viable cells. The intensity of the signal is proportional to the amount of ATP in the sample and therefore to the number of metabolically active cells. It was demonstrated that the number of living cells in the biofilm is not significantly influenced by the lack of DnaJ chaperone either after heat shock or in control cultures (Tab. I).

Table I
The effect of DnaJ protein on cell viability in biofilm

Strain	Heat shock	RLU × 10^5
MC1061	+	6.5
	–	2.9
KW69	+	8.0
	–	3.9
KW87	+	16.5
	–	4.5

RLU – Relative Luminescence Unitsf

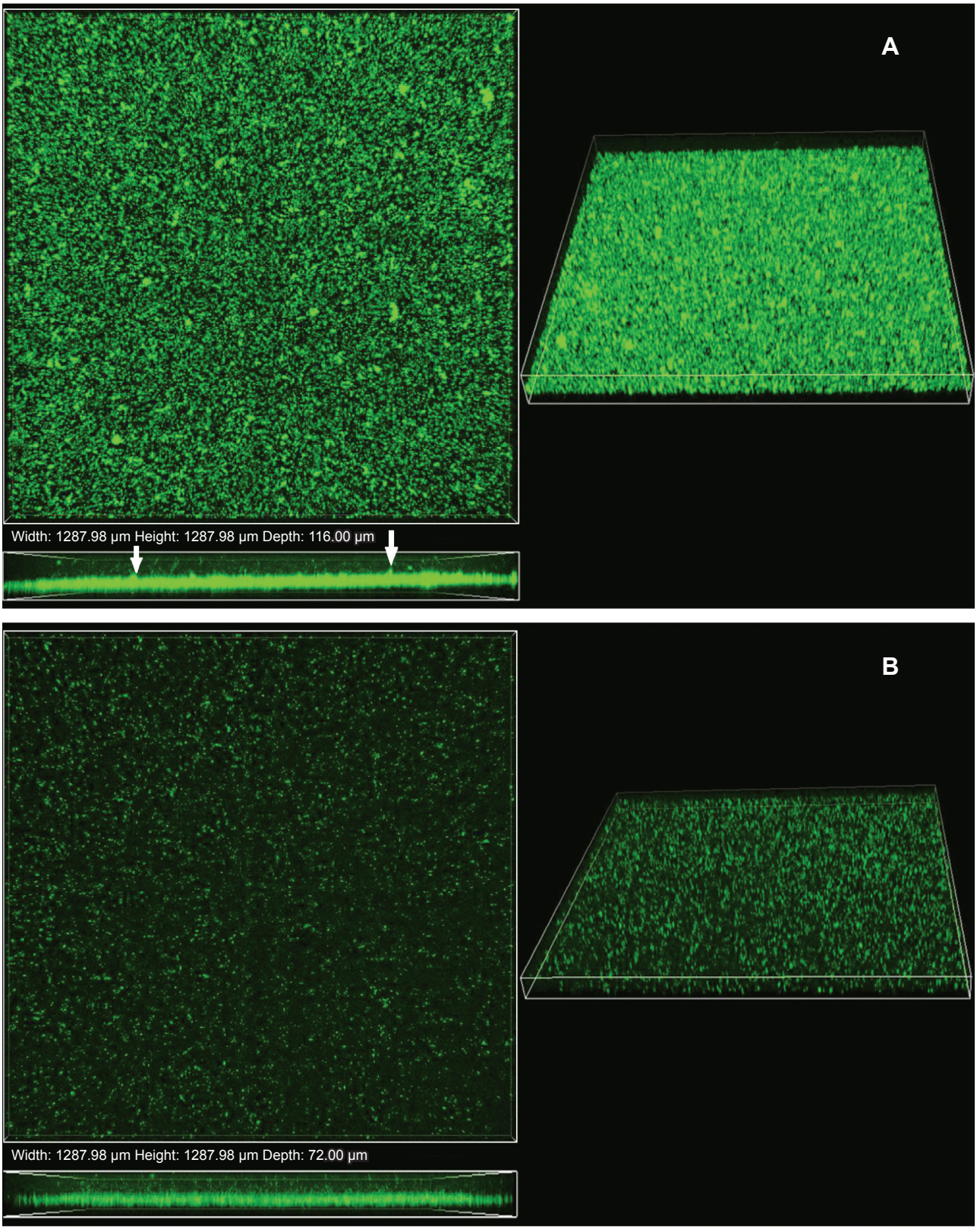

Fig. 2. Micrographs of *E. coli* biofilm after heat shock. Wild-type strain, control (A); Δ*dnaJ* mutant (B). White arrows indicate the bulges in biofilm layer.

We also observed that in all strains tested heat shock resulted in the elevation of RLU what was consistent with the induction of biofilm formation. In complemented KW87 strain the increase of copy number of *dnaJ* gene leads to an increase in the number of living cells in biofilm in comparison to wild type strain.

The involvement of DnaJ chaperone in *Pseudomonas putida* PCL1445 biofilm formation and degradation was

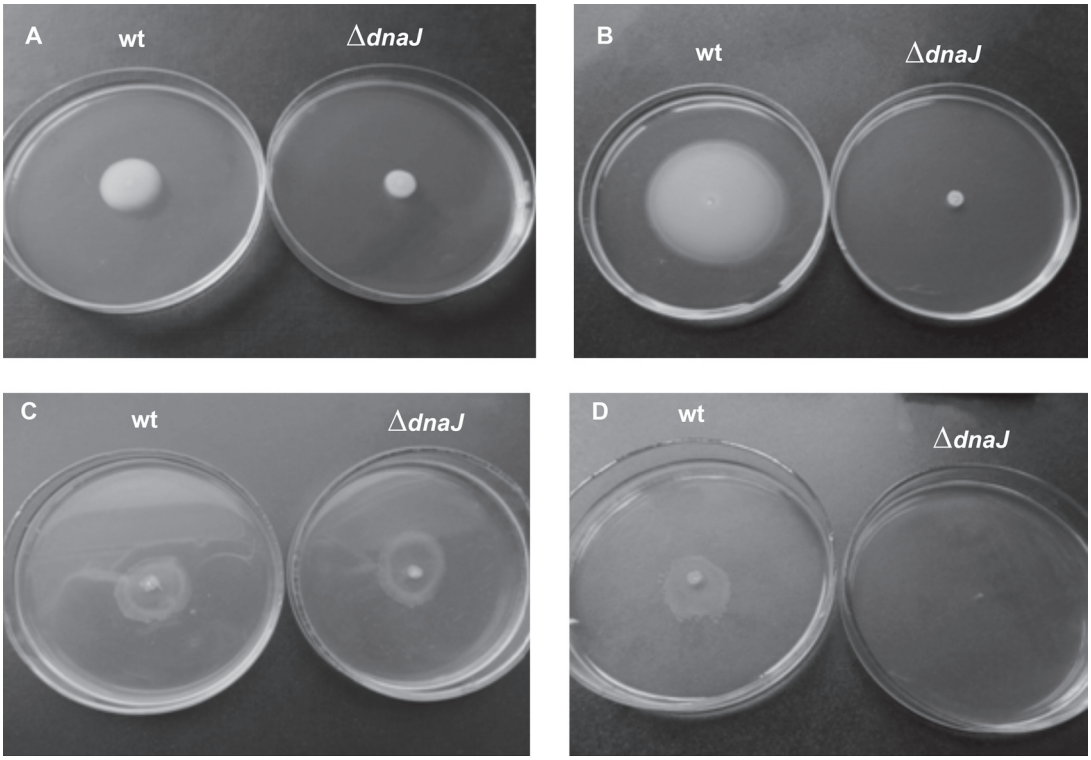

Fig. 3. Swimming and swarming motility. Swimming motility, control (A); swimming motility after heat shock (B); swarming motility, control (C); swarming motility, heat shock (D).

concluded by its involvement in the regulation of two cyclic lipopeptides, putisolvin I and II (Dubern *et al.*, 2005). On the contrary, the role of partner chaperone DnaK in formation of *Staphylococcus aureus* and *Streptococcus mutans* biofilm has been well proven (Singh *et al.*, 2012; Lemos *et al.*, 2007). The role of DnaJ protein in formation of biofilm by *E. coli* has not been studied until now so the results of our experiments demonstrating that DnaJ chaperone is involved in biofilm development in this species have the virtue of originality.

The inhibition of biofilm was seen when the heat shock was applied after 2 h from the onset of biofilm formation or just at the beginning of experiment (data not shown), which suggests that extracellular matrix formation can be inhibited, for example by a defect in polysaccharide secretion. However, the early stages of biofilm development – such as adhesion utilizing type I pili, curli and conjugative pili and colonization of the surfaces cannot be excluded. Bacterial swimming motility is a factor severely influencing adhesion (Verstraeten *et al.*, 2008). Swarming motility is a factor positively influencing biofilm formation (Verstraeten *et al.*, 2008). Therefore the ability of Δ*dnaJ* mutant to move in swimming and swarming fashion was checked. The inhibition of both types of motility as compared to wild type strain was demonstrated (Fig. 3).

The introduction of wild-type *dnaJ* gene at low-copy plasmid led not only to the complementation of Δ*dnaJ* defect but even to substantial enhancement of biofilm formation. It was proved that the phenotype of strains overexpressing DnaJ chaperone differed from wild-type strains *e.g.* they increased survival in the presence of bactericidal antibiotics and suppressed all known *dnaJ cbpA djlA* triple mutant phenotypes (Genevaux *et al.*, 2007). However, the enhancement of biofilm formation is most likely due to the overexpression of *dnaJ*, as indicated by other research referring to the altered phenotype of such strains.

It is well known that DnaJ is important for many cellular functions, such as protein release and transport (Mayhew and Hartl, 1996), membrane lipid composition (Sieńczyk *et al.*, 2004) and cell division (McCarthy and Walker, 1994), to mention only a few. We have demonstrated that biofilm formation by *E. coli* is another function influenced by this chaperone.

Literature

Beloin C., A. Roux and J.-M. Ghigo. 2008. *Escherichia coli* biofilms. *Curr. Topics Microbiol. Immunol.* 322: 249–289.

Casadaban M. and S.S. Cohen. 1980. Analysis of gene control signals by DNA fusion and cloning in *Escherichia coli*. *J. Molec. Biol.* 138: 179–207.

Castanié-Cornet M.P., N. Bruel and P. Genevaux. 2014. Chaperone networking facilitates protein targeting to the bacterial cytoplasmic membrane. *Biochim. Biophys. Acta* 1843: 1442–1456.

Cuéllar J., J. Perales-Calvo, A. Muga, J. M. Valpuesta and F. Moro. 2013. Structural insights into the chaperone activity of the 40-kDa heat shock protein DnaJ: binding and remodeling of a native substrate. *J. Biol. Chem*. 288: 15065–15074.

de la Fuente-Núñez C., F. Reffeuville, L. Fernández and R.E. Hancock. 2013. Bacterial biofilm development as a multicellular adaptation: antibiotic resistance and new therapeutic strategies. *Curr. Opin. Microbiol*. 16: 580–589.

Donlan R.M. and J.W. Costerton. 2002. Biofilms: survival mechanisms of clinically relevant microorganisms. *Clin. Microbiol. Rev.* 15: 167–193.

Dubern J.F., E.L. Lagendijk, B.J. Lugtenberg and G.V. Bloemberg. 2005. The heat shock genes *dnaK*, *dnaJ* and *grpE* are involved in regulation of putisolvin biosynthesis in *Pseudomonas putida* PCL1445. *J. Bacteriol* 187: 5967–5976.

Flemming H.-C. and J. Wingender. 2010. The biofilm matrix. *Nat. Rev. Microbiol*. 8: 623–633.

Genevaux P., C. Georgeopoulos and W.L. Kelly. 2007. The Hsp70 chaperone machines in *Escherichia coli*; a paradigm for the repartition of chaperone functions. *Mol. Microbiol*. 66: 840–857.

Hall M.P., M.G. Gruber, R.R. Hannah, M.L. Jennes-Clough and K.V. Wood. 1998. Stabilization of firefly luciferase using directed evolution. pp. 392–395. In: Roda A., M. Pazzagli, L.J. Kricka and P.E. Stanley (eds). *Bioluminescence and Chemiluminescence, Perspectives for the 21st Century*. John Wiley & Sons, New York.

Hoiby N., T. Bjarnsholt, M. Givskov, S. Molin and O. Ciofu. 2010. Antibiotic resistance of bacterial biofilms. *Int. J. Antimicrob. Agents* 35: 322–332.

Karatan E. and P. Watnick. 2009. Signals, regulatory networks, and materials that build and break bacterial biofilms. *Microbiol. Mol. Biol. Rev*. 73: 310–347.

Lemos J.A., Y. Luzardo and R.A. Burne. 2007. Physiologic effects of forced down-regulation of *dnaK* and *groEL* expression in *Streptococcus mutants*. *J. Bacteriol*. 189: 1582–1588.

Lippolis J.D., B.W. Brunelle, T.A. Reinhardt, R.E. Sacco, B.J. Nonnecke, B. Dogan, K. Simpson and Y.H. Schukken. 2014. Proteomic analysis reveals protein expression diffrences in *Escherichia coli* strains associated with persistent versus transient mastitis. *J. Proteomics* 108: 373–381.

Lundin A. and A. Thore. 1975. Analytical information obtained by evaluation of the time course of firefly bioluminescence in the assay of ATP. *Anal. Biochem*. 66: 47–63.

Mayhew M. and F.U. Hartl. 1996. Molecular chaperone proteins, pp. 217–261. In: Neidhard N.C., R. Curtiss III, J.L. Ingraham, E.C.C. Lin, K.B. Low, B. Magasanik, W.S. Reznikoff, M. Riley, M. Schaechter and H.E. Umbarger (eds). *Escherichia coli and Salmonella, Cellular and Molecular Biology.* ASM Press, Washington, D.C.

McCarthy J. and G.C. Walker. 1994. DnaK mutants defective in ATPase activity are defective in negative regulation of the heat shock response: expression of the mutant DnaK proteins results in filamentation. *J. Bacteriol*. 76: 764–780.

McFarlane S. and J.F. Dillon. 2007. Microbial biofilms in the human gastrointestinal tract. *J. Appl. Microbiol*. 192: 1187–1196.

O'Toole G.A. and R. Kotler. 1998. Initiation of biofilm formation in *Pseudomonas fluorescens* WCS365 proceeds *via* multiple, convergent signaling pathways; a genetic analysis. *Mol. Microbiol*. 28: 449–461.

Paciorek J., K. Kardyś, B. Łobacz and K.I. Wolska. 1997. *Escherichia coli* defects caused by null mutations in *dnaK* and *dnaJ* genes. *Acta Microbiol. Polon*. 46: 7–17.

Raczkowska A., S. Karolina, M. Brzóstkowska, A. Łasińskaand K. Brzostek. 2011. Pleiotropic effects of a *Yersinia enterocolitica ompR* mutation on adherent-invasive abilities and biofilm formation. *FEMS Microbiol. Lett*. 321: 43–49.

Sieńczyk J., A. Skłodowska, A. Grudniak and K.I. Wolska. 2004. Influence of DnaK and DnaJ chaperones on *Escherichia coli* membrane lipid composition. *Pol. J. Microbiol*. 53: 121–123.

Singh V.K., M. Syring, A. Singh, K. Singhal, A. Dalecki and T. Johansson. 2012. An insight into the significance of DnaK heat shock system in *Staphylococcus aureus*. *Int. J. Med. Microbiol*. 302: 242–252.

Srinivasan S.R., A.T. Gilles, L. Chang, A.D. Thompson and J.E. Gestwicki. 2012. Molecular chaperones DnaK and DnaJ share predicted binding sites on most proteins in the *E. coli* proteome. *Mol. Biosyst*. 8: 2323–2333.

van der Veen S. and T. Abee. 2010. HrcA and DnaK are important for static and continuous-flow biofilm formation and disinfectant resistance in *Listeria monocytogenes*. *Microbiology* 156: 3782–3790.

Verstraeten N., K. Braeken, B. Debkumari, M. Fauvarat, J. Fransaer, J. Vermant and J. Michiels. 2008. Living on a surface: swarming and biofilm formation. *Trends Microbiol*. 16: 496–506.

Walsh P., D. Bursać, Y.C. Law, D. Cyr and T. Lithgow. 2004. The J-protein family: modulating protein assembly, disassembly and translocation. *EMBO Rep*. 5: 567–571.

Wolska K.I., E. Bugajska, D. Jurkiewicz, M. Kuć and A. Jóźwik. 2000. Antibiotic susceptibility of *Escherichia coli dnaK* and *dnaJ* mutants. *Microb. Drug Res*. 6: 119–126.

Polish Journal of Microbiology
2015, Vol. 64, No 3, 285–288

SHORT COMMUNICATION

Characterization of Extended-Spectrum-β-Lactamases Produced by *Escherichia coli* Strains Isolated from Dogs in Poland

MAGDALENA RZEWUSKA[1]*, ILONA STEFAŃSKA[2], MAGDALENA KIZERWETTER-ŚWIDA[1], DOROTA CHROBAK-CHMIEL[2], PAULINA SZCZYGIELSKA[1], MONIKA LEŚNIAK[3] and MARIAN BINEK[1]

[1] Department of Preclinical Sciences, Faculty of Veterinary Medicine, Warsaw University of Life Sciences, Warsaw, Poland
[2] Department of Fermentation Technology, Institute of Agricultural and Food Biotechnology, Warsaw, Poland
[3] Department of Regenerative Medicine, Military Institute of Hygiene and Epidemiology, Warsaw, Poland

Submitted 25 March 2015, accepted 8 April 2015

Abstract

Escherichia coli is a common cause of infections in companion animals. In recent years the increasing prevalence of resistance to β-lactams, including extended-spectrum cephalosporins, antimicrobials frequently used in small animal veterinary practice, was observed in canine isolates of *E. coli*. The aim of this study was to detect and to characterize extended-spectrum β-lactamases (ESBLs) produced by *E. coli* isolated from diseased dogs in Poland. Four isolates out of 119 studied (3.4%) were ESBL-positive. They harbored the $bla_{SHV\text{-}12}$, $bla_{CTX\text{-}M\text{-}15}$, and $bla_{TEM\text{-}116}$ genes. This study provides the first report of the occurrence of ESBL-producing *E. coli* in dogs in Poland.

Key words: *Escherichia coli*, extended-spectrum β-lactamases, dog infections, multidrug resistance

Escherichia coli is an important opportunistic pathogen, causing in dogs mainly extraintestinal infections including those of urinary, respiratory and reproductive tracts. The antimicrobial resistance of *E. coli* occurring in companion animals, especially the multidrug resistance, becomes an emerging problem in veterinary medicine. The increasing percentage of multidrug resistant (MDR) *E. coli* isolation from dogs and cats in Poland, between 2007 and 2013, has been reported by Rzewuska *et al*. (2015). The increase in the prevalence of resistance to β-lactams, such as aminopenicillins and extended-spectrum cephalosporins, was also observed in canine *E. coli* isolates. The β-lactam resistance in *Enterobacteriaceae* is associated mainly with production of enzymes hydrolyzing these antibiotics, among which the extended-spectrum β-lactamases (ESBLs), plasmidic AmpC β-lactamases and carbapenemases are the most important resistance mechanisms (Rubin and Pitout, 2014). ESBLs mediate resistance to penicillins, cephalosporins and monobactams, but they are sensitive to β-lactam inhibitors. The presence of ESBL-producing *E. coli* in clinical specimens from dogs has been reported previously in some countries, such as the United States (O'Keefe *et al*., 2010; Shaheen *et al*., 2011), the Netherlands (Dierikx *et al*., 2012; Hordijk *et al*., 2013), Germany (Schmiedel *et al*., 2014), Italy (Carattoli *et al*., 2005) and Korea (So *et al*., 2012). However, detailed information about properties of ESBLs occurring in canine *E. coli* and their geographic distribution are still limited. To our knowledge, there are no published data regarding the occurrence of ESBLs in canine *E. coli* in Poland.

The aim of the study was to detect and to characterize ESBLs in *E. coli* isolated from diseased dogs in Poland.

E. coli isolates (n = 119) investigated in this study were obtained from clinical samples collected from diseased dogs. The isolates were identified using standard microbiological diagnostic techniques. Antimicrobial susceptibility was determined by the disk diffusion method, as described previously (Rzewuska *et al*., 2015). *E. coli* ATCC 25922 was used as a quality control.

The phenotypic test using ceftazidime and ceftazidime/clavulanic acid disks (Becton Dickinson) was performed according to the Clinical and Laboratory Standards Institute guidelines (CLSI, 2013) to detect ESBLs production.

The presence of bla_{TEM}, bla_{SHV}, $bla_{CTX\text{-}M\text{-}1\ \text{group}}$ and $bla_{CTX\text{-}M\text{-}9\ \text{group}}$ genes was studied by PCR to determine the genotype of ESBL-positive isolates. In addition,

* Corresponding author: M. Rzewuska, Department of Preclinical Sciences, Faculty of Veterinary Medicine, Warsaw University of Life Sciences, Warsaw, Poland; **e-mail: magdalena_rzewuska@sggw.pl**

Table I
Primers used to detect genes encoding β-lactamases in the study

Target gene	Primer sequence (5'-3')	Amplicon size (bp)	Literature
bla_{TEM}	F-ATTCTTGAAGACGAAAGGGC	1150	Briñas *et al.*, 2005
	R-ACGCTCAGTGGAACGAAAAC		
bla_{SHV}	F-CACTCAAGGATGTATTGTG	885	Briñas *et al.*, 2005
	R-TTAGCGTTGCCAGTGCTCG		
$bla_{CTX\text{-}M\text{-}1\ group}$	F-GTTACAATGTGTGAGAAGCAG	1049	Costa *et al.*, 2008
	R-CCGTTTCCGCTATTACAAAC		
$bla_{CTX\text{-}M\text{-}9\ group}$	F-GTGACAAAGAGAGTGCAACGG	857	Coque *et al.*, 2002
	R ATGATTCTCGCCGCTGAAGCC		
$bla_{CMY\text{-}2}$	F-GATTCCTTGGACTCTTCAG	1807	Briñas *et al.*, 2005
	R-TAAAACCAGGTTCCCAGATAGC		

those isolates were screened for the $bla_{CMY\text{-}2}$ gene, as the activity of β-lactamase CMY-2 could mask the ESBL-positive phenotype (Thomson, 2010). The PCR assays were performed using primers (Genomed, Poland) and reaction conditions described previously (Table I). DNA was isolated using Genomic Mini kit (A&A Biotechnology, Poland) according to the manufacturer's recommendations. In order to identify the type of genes detected, the obtained amplicons were purified with the GeneJET™ PCR Purification Kit (Thermo-Scientific) according to the manufacturer's recommendations, and sequenced using the same primers and a 3730 *xl* DNA Analyzer (Applied Biosystems, USA). Sequencing files were evaluated using the Chromas Lite version 2.33 program (Technelysium Pty Ltd., Australia). Subsequently, the nucleotide sequences were compared to the sequences in the GenBank database using BLAST (http://blast.ncbi.nlm.nih.gov). Additionally, the bla_{TEM} nucleotide sequences were translated into protein sequences, and then aligned with the reference sequence of TEM-1 β-lactamase (GenBank Accession Number J01749) by MEGA version 5.0. On the basis of the amino acid substitutions found and the TEM mutation table (http://www.lahey.org/Studies/temtable.asp), the type of TEM β-lactamase was determined for each bla_{TEM} gene detected.

ESBL-producing *E. coli* was detected among the studied isolates, and this is the first report on the presence of this bacterium in dogs in Poland. The ESBL-positive phenotype was found in four *E. coli* isolates from extraintestinal infections in dogs. Characteristics of these isolates are presented in Table II. Genes of three different ESBLs were detected and identified, as $bla_{SHV\text{-}12}$, $bla_{CTX\text{-}M\text{-}15}$, and $bla_{TEM\text{-}116}$. The fourth gene whose presence was assayed, $bla_{CMY\text{-}2}$ encoding a plasmidic class C β-lactamase CMY-2, was not found in any of those isolates.

In the present study all ESBL-producing *E. coli* isolates were classified as MDR bacteria, showing resistance to at least three antimicrobial classes (Table III). Multidrug resistance has been also observed in ESBL-positive *E. coli* of various origin in other studies (Schmiedel *et al.*, 2014; Shaheen *et al.*, 2011).

The occurrence of ESBL-producing *E. coli* in dogs, ranging from 1% to 33.3%, has been reported previously (Dierikx *et al.*, 2012; Ewers *et al.*, 2010; Hordijk *et al.*, 2013; Huber *et al.*, 2013; O'Keefe *et al.*, 2010; Schmiedel *et al.*, 2014; Shaheen *et al.*, 2011; So *et al.*, 2012). Ewers *et al.* (2010) reported that ESBL-producing *E. coli* was isolated from 10.7% of clinical samples collected from dogs. The high prevalence (33.3%) of these bacteria isolated from rectal swabs of hospitalized dogs in Korea was reported by So *et al.* (2012). In our study, only 3.4% (4/119 isolates) of studied *E. coli* isolates were ESBL-positive. These findings correspond with the observations of Shaheen *et al.* (2011) in the

Table II
Characteristics of ESBLs produced by *E. coli* isolates obtained from dogs

Strain designation	Clinical sample	ESBL type		
		bla_{SHV}	bla_{TEM}	bla_{CTX}
1062/09/D	pharyngeal swab	–	TEM-116	CTX-M-15
1370/06/D	ear canal swab	–	TEM-116	CTX-M-15
1945/06/D	nasal swab	SHV-12	TEM-116	–
2017/11/D	soft tissue (liver)	–	TEM-116	CTX-M-15

Table III
Antimicrobial susceptibility of ESBL-producing *E. coli* strains isolated from dogs

Antimicrobial	1062/09/D	1370/06/D	1945/06/D	2017/11/D
Amoxicillin	R	R	R	R
Amoxicillin/clavulanic acid	R	R	R	R
Cefuroxime	R	R	R	R
Cefotaxime	R	R	R	R
Cefovecin	R	R	R	R
Ciprofloxacin	R	R	S	R
Enrofloxacin	R	R	S	R
Marbofloxacin	R	R	S	R
Tetracycline	R	R	R	R
Gentamicin	S	S	R	R
Nitrofurantoin	R	R	R	R
Colistin	S	S	R	R
Florfenicol	S	S	R	R
Trimethoprim/Sulfamethoxazole	S	R	R	R

R – resistant, S – susceptible

United States and Huber *et al*. (2013) in Switzerland, where the frequency of ESBL-producing *E. coli* isolation from dogs, mainly from urinary tract infections, was 3% and 3.3%, respectively.

Three different types of ESBLs were found in the studied *E. coli* isolates (Table II). The β-lactamase CTX-M-15, detected in three isolates, belongs to the CTX-M-1 group and represents the most frequently reported ESBL type in *E. coli* isolates of canine and feline origin (Ewers *et al*., 2010; Huber *et al*., 2013; O'Keefe *et al*., 2010; Schmiedel *et al*., 2014; Shaheen *et al*., 2011). The other ESBL, SHV-12, detected in one of the studied isolates, has rarely been found in *E. coli* isolated from dogs (Carattoli *et al*., 2005; Ewers *et al*., 2010; O'Keefe *et al*., 2010). Furthermore, in all ESBL-positive isolates the gene encoding the TEM-116 β-lactamase was detected. This enzyme is TEM-1 derivative with ESBL activity, and occurs in various species of *Enterobacteriaceae* isolated from humans (Dhara *et al*., 2013). This is only the second report of TEM-116 β-lactamase in *E. coli* of canine origin, the first being that of Ewers *et al*. (2010).

In this study ESBL-producing *E. coli* strains were isolated from diseased dogs with extraintestinal infections. However, they have also been detected in faecal samples of healthy dogs and cats (Belas *et al*., 2014; Hordijk *et al*., 2013), and it seems that companion animals could be asymptomatic carriers of these bacteria.

The β-lactams are antimicrobial drugs commonly used in small animal veterinary practice (Murphy *et al*., 2012). The β-lactamases, which mediate the β-lactam resistance, are most often encoding by genes grouped in cassettes and located on mobile genetic elements, such as plasmids and transposons, so they may be extensively transmitted between different bacteria. Therefore inappropriate usage of β-lactams may contribute to the development of broad-spectrum resistance and to the dissemination of multiresistant strains among humans and animals. Our study showed that dogs in Poland can be a potential reservoir of ESBL-positive *E. coli*, though the prevalence of these bacteria in clinical specimen was relatively low. The results suggest that the ESBL production is probably not a main mechanism of resistance to β-lactams in the studied *E. coli* population. However, the further investigation should explain a role of other resistance mechanisms in *E. coli* of canine origin.

Acknowledgements

The authors thank Barbara Chojnacka and Alicja Grzechnik for excellent technical assistance.

Literature

Belas A., A.S. Salazar, L.T. Gama, N. Couto and C. Pomba. 2014. Risk factors for faecal colonisation with *Escherichia coli* producing extended-spectrum and plasmid-mediated AmpC β-lactamases in dogs. *Vet. Rec*. 175: 202.

Briñas L., M. Lantero, I. de Diego, M. Alvarez, M. Zarazaga and C. Torres. 2005. Mechanisms of resistance to expanded-spectrum cephalosporins in *Escherichia coli* isolates recovered in a Spanish hospital. *J. Antimicrob. Chemother*. 56: 1107–1110.

Carattoli A., S. Lovari, A. Franco, G. Cordaro, P. Di Matteo and A. Battisti. 2005. Extended-spectrum beta-lactamases in *Escherichia coli* isolated from dogs and cats in Rome, Italy, from 2001 to 2003. *Antimicrob. Agents Chemother*. 49: 833–835.

CLSI. 2013. Performance Standards for Antimicrobial Disk and Dilution Susceptibility Tests for Bacteria Isolated From Animals; Second Informational Supplement. *CLSI document VET01-S2*. Clinical and Laboratory Standards Institute, Wayne, PA.

Coque T.M., A. Oliver, J.C. Pérez-Díaz, F. Baquero and R. Cantón. 2002. Genes encoding TEM-4, SHV-2 and CTX-M-10 extended-spectrum β-Lactamases are carried by multiple *Klebsiella*

pneumoniae clones in a single hospital (Madrid, 1989 to 2000). *Antimicrob. Agents Chemother*. 46: 500–510.

Costa D., P. Poeta, Y. Sáenz, A.C. Coelho, M. Matos, L. Vinué, J. Rodrigues and C. Torres. 2008. Prevalence of antimicrobial resistance and resistance genes in faecal *Escherichia coli* isolates recovered from healthy pets. *Vet. Microbiol*. 127:97–105.

Dhara L., A. Tripathi and A. Pal. 2013. Molecular characterization and *in silico* analysis of naturally occurring TEM beta-lactamase variants among pathogenic *Enterobacteriaceae* infecting Indian patients. *Biomed Res Int*. 2013: Article ID 783540.

Dierikx C.M., E. van Duijkeren, A.H. Schoormans, A. van Essen-Zandbergen, K. Veldman, A. Kant, X.W. Huijsdens, K. van der Zwaluw, J.A. Wagenaar and D.J. Mevius. 2012. Occurrence and characteristics of extended-spectrum-β-lactamase-and AmpC-producing clinical isolates derived from companion animals and horses. *J. Antimicrob. Chemother.* 67: 1368–1374.

Ewers C., M. Grobbel, I. Stamm, P.A. Kopp, I. Diehl, T. Semmler, A. Fruth, J. Beutlich, B. Guerra, L.H. Wieler and others. 2010. Emergence of human pandemic O25:H4-ST131 CTX-M-15 extended-spectrum-beta-lactamase-producing *Escherichia coli* among companion animals. *J. Antimicrob. Chemother*. 65: 651–660.

Hordijk J., A. Schoormans, M. Kwakernaak, B. Duim, E. Broens, C. Dierikx, D. Mevius and J.A. Wagenaar. 2013. High prevalence of fecal carriage of extended spectrum β-lactamase/AmpC-producing *Enterobacteriaceae* in cats and dogs. *Front. Microbiol*. 4: 242.

Huber H., C. Zweifel, M.M. Wittenbrink and R. Stephan. 2013. ESBL-producing uropathogenic *Escherichia coli* isolated from dogs and cats in Switzerland. *Vet. Microbiol.* 162: 992–996.

Murphy C.P., R.J. Reid-Smith, P. Boerlin, J.S. Weese, J.F. Prescott, N. Janecko and S.A. McEwen. 2012. Out-patient antimicrobial drug use in dogs and cats for new disease events from community companion animal practices in Ontario. *Can. Vet. J.* 53: 291–298.

O'Keefe A., T.A. Hutton, D.M. Schifferli and S.C. Rankin. 2010. First detection of CTX-M and SHV extended-spectrum beta-lactamases in *Escherichia coli* urinary tract isolates from dogs and cats in the United States. *Antimicrob. Agents Chemother*. 54: 3489–3492.

Rubin J.E. and J.D.D. Pitout. 2014. Extended-spectrum β-lactamase, carbapenemase and AmpC producing *Enterobacteriaceae* in companion animals. *Vet. Microbiol*. 170: 10–18.

Rzewuska M, M. Czopowicz, M. Kizerwetter-Świda, D. Chrobak, B. Błaszczak and M. Binek. 2015. Multidrug resistance in *Escherichia coli* strains isolated from infections in dogs and cats in Poland (2007–2013) *The Scientific World Journal* 2015: Article ID 408205.

Schmiedel J., L. Falgenhauer, E. Domann, R. Bauerfeind, E. Prenger-Berninghoff, C. Imirzalioglu and T. Chakraborty. 2014. Multiresistant extended-spectrum β-lactamase-producing *Enterobacteriaceae* from humans, companion animals and horses in central Hesse, Germany. *BMC Microbiol*. 14: 187.

Shaheen B.W., R. Nayak, S.L. Foley, O. Kweon, J. Deck, M. Park, F. Rafii and D.M. Boothe. 2011. Molecular characterization of resistance to extended-spectrum cephalosporins in clinical *Escherichia coli* isolates from companion animals in the United States. *Antimicrob. Agents Chemother*. 55: 5666–5675.

So J.H., J. Kim, I.K. Bae, S.H. Jeong, S.H. Kim, S.K. Lim, Y.H. Park and K. Lee. 2012. Dissemination of multidrug-resistant *Escherichia coli* in Korean veterinary hospitals. *Diagn. Microbiol. Infect. Dis*. 73: 195–199.

Thomson K.S. 2010. Extended-Spectrum-β-Lactamase, AmpC and Carbapenemase Issues. *J. Clin. Microbiol*. 48: 1019–1025.

Polish Journal of Microbiology
2015, Vol. 64, No 3, 289–293

SHORT COMMUNICATION

Epidemiological Analysis of *Mycobacterium tuberculosis* Strains Isolated from Patients of Small Communities Living in the South-East of Poland

ANNA ŻACZEK[1], IWONA SZWAJA[2], MONIKA SKIBA[2], ANNA BRZOSTEK[3], CZESŁAW PUCHALSKI[1], KAROLINA LEWANDOWSKA[3, 4] and JAROSŁAW DZIADEK[1, 3]*

[1] Faculty of Biology and Agriculture, University of Rzeszow, Rzeszów, Poland
[2] Independent Public Health Care Facility "Sanatorium", Gorno, Poland
[3] Institute of Medical Biology, Polish Academy of Sciences, Łódź, Polamd
[4] Faculty of Biotechnology and Food Sciences, Lodz University of Technology, Łódź, Poland

Submitted 25 March 2015, accepted 8 April 2015

Abstract

The diversity of *Mycobacterium tuberculosis* clinical isolates, collected from a single hospital, was analyzed by ligation-mediated PCR techniques: FLiP and FLAP, and hybridization technique, IS*6110*-RFLP. The isolated strains were divided in terms of location (3 towns of Podkarpackie voivodeship differing in population size) and relationship (8 members of 4 families, each represented by 2 patients). Within each family identical DNA profiles, as well as drug resistance patterns were identified indicating a great chance of transmission of strains within the same family. Identical, or very similar patterns were also shared by strains isolated from unrelated patients living in a very small town (1 200 inhabitants) or hospitalized in the same place and time.

Key words: *Mycobacterium tuberculosis*, FLAP, FLiP, IS*6110*-RFLP, spoligotyping

Despite the fact that *Mycobacterium tuberculosis* (*Mtb*) is known as a causative agent of tuberculosis (TB) since 1882 (when it was first discovered), it remains a major threat to the public health all over the world. It is estimated that even one third of the world's population is infected with *Mtb* strains. According to World Health Organization, in 2012 around 8.6 million new tuberculosis cases and 1.3 million deaths caused by TB were registered worldwide (WHO Report, 2012). In Poland, in spite of observed decrement in the number of new cases, the incidence of TB is still considerably higher than in western European countries (19.6 vs 13.5 in 2012) (WHO Report, 2012). As reported in 2014, significant differences in morbidity between distinct regions of Poland were observed, varying from 10.6 (lubuskie) up to 30.2 (lubelskie) (Korzeniewska-Koseła, 2014); the incidence for the Podkarpackie voivodeship was 19.8 (Statistical Bulletin, Ministry of Health, 2013).

The frequency of *Mtb* transmission depends, among others, on population size. It is expected that transmission occurs more frequently in large populations in urban areas rather than in small towns or rural regions. Therefore, the prevalence of TB occurring among the inhabitants of the big cities is significantly higher than among the rural population (20.2 vs. 18.6 ratio) (Korzeniewska-Koseła, 2014). Additionally, the number of epidemiologically unrelated *Mtb* strains present within a large population is supposed to be much higher than in a small, local community.

The aim of this study was to analyze the diversity of *Mtb* strains isolated in 2012 and collected from 3 distinct towns of Podkarpackie region in Poland differing in population size (1 200, 30 000 and 60 000 inhabitants). Moreover, the epidemiological patterns of strains isolated within a few families of the same region were also identified.

The modern epidemiology of TB is based on molecular methods, which mainly focus on the diversity in number and localization of various repetitive DNA elements (Valcheva *et al*., 2008; Moström *et al*., 2002; Zozio *et al*., 2005). The most common techniques are spoligotyping, MIRU-VNTR typing and reference method IS6110-RFLP, which are indispensable for typing of large collections of strains (van Embden *et al*., 1993; Barnes and Cave, 2003; Crawford, 2003; Kremer *et al*., 2005; Supply *et al*., 2006; Covan *et al*., 2005). However, for an initial analysis of a limited number of strains or as a secondary methods, less laborious and cheaper

* Corresponding author: J. Dziadek, Institute of Medical Biology, Polish Academy of Sciences Łódź, Poland; **e-mail: jdziadek@toya.net.pl or jdziadek@cbm.pan.pl**

methods could be applied, for instance ligation-mediated PCR methods, LM-PCR, which appeared to be highly discriminative (Masny and Płucienniczak, 2003; Krawczyk *et al*., 2006; Krawczyk *et al*., 2011, Zaczek *et al*., 2013a; 2013b; 2013c).

In the present study, *Mtb* clinical isolates were compared by means of two LM-PCR methods: FLiP (Reisig, 2005) and FLAP (Zaczek *et al*., 2014a; 2014b) and the obtained results were verified by the "gold" epidemiological standard IS*6110*-RFLP hybridization technique.

The 21 *Mtb* strains used in this analysis were isolated in 2012 from patients in the Podkarpackie voivodeship and hospitalized in the Independent Public Health Care Facility "Sanatorium" in Gorno. All strains were tested for susceptibility to isoniazid, rifampicin, pyrazinamide and ethambutol (Janowiec, 1988). The research material was sputum collected from patients of Polish nationality who were diagnosed with pulmonary tuberculosis. All patients, besides one, were newly detected cases. Detailed epidemiological data collected in course of community interviews, based on surveys, and from medical records are shown in the table (Table I). Genomic DNA was extracted and purified from all the isolates using the protocol proposed by van Embden (van Embden *et al*., 1993) and recommended for the standard IS*6110*-RFLP methods. The concentration of DNA was measured with NanoDrop ND-1000 spectrophotometer. Subsequently, isolates were characterized by IS*6110*-RFLP typing using internationally standardized protocol (van Embden *et al*., 1993). The FLAP method was performed as described previously (Zaczek *et al*., 2014a; 2014b) and the FLiP analysis was performed as originally described by Reisig (Reisig *et al*., 2005). The fingerprint patterns obtained by these three methods were compared visually with one another and strains were considered identical if their DNA profiles, obtained by all three methods, were the same.

The subject of the research were *Mtb* strains divided into two groups: first was comprised of the isolates taken from 13 unrelated patients living in 3 locations (A, B and C) in the Podkarpackie region, whereas the other consisted of 8 strains isolated from members of four families, each represented by two patients. From the location A, which counts over 60 000 inhabitants – 4 strains were analyzed, from the location B with 1 200 inhabitants – 2 strains were examined and from the location C with population 35 000 – 7 strains were analyzed, which represent 20%, 100% and 46% of all strains isolated in these cities in 2012, respectively.

The analysis of epidemiological patterns indicated that strains isolated in the location A represent identical banding patterns obtained by LM-PCR methods. However, banding profiles obtained with IS*6110*-RFLP proved that only three of these strains are identical, whereas the RFLP-IS*6110* pattern of the fourth strain

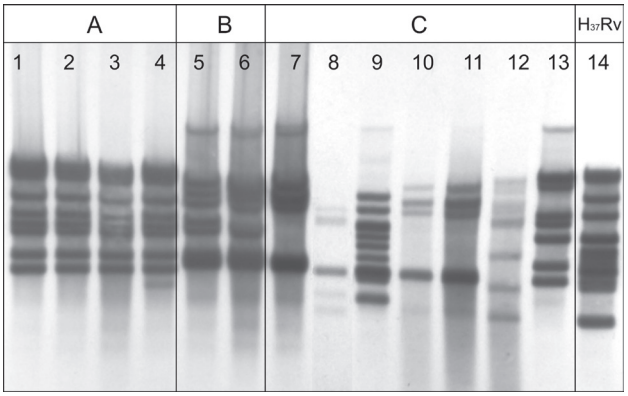

Fig. 1. DNA profiles obtained with IS*6110*-RFLP method. Line 1 to 4 – strains number 1, 2, 3, 4 from location A, line 5, 6 – strains number 9 and 10 from location B, line 7 to 13 – strains 13, 14, 15, 16, 17, 18, 19 from location C, line 14 – $H_{37}Rv$.

revealed one additional band suggesting a transposition of the mobile element (Fig. 1). Furthermore, this slightly different strain appeared to be sensitive to isoniazid (INH), while others were INH-resistant. In the case of 3 strains, due to their identical profiles obtained with three methods and the same drug resistance phenotype, it may be suspected that patients were in a close relationship or had accidental contact and there is a high probability of transmission of strains between them or a common source of infection.

Strains from location B were sensitive to all tested antimicobacterial drugs and identical in terms of DNA profiles obtained by the FLAP method. However, the DNA profiles obtained with FLiP and IS*6110*-RFLP methods (Fig. 1, lines 5 and 6) were slightly different (one additional band in strain number 9) what makes the direct transmission of these strains unlikely. On the other hand, the relationship between strains is clear and the common source of infection cannot be excluded. Among 7 strains analyzed from patients from the location C only two strains (Fig. 1, lines 10 and 11) showed the same molecular patterns obtained with three methods used, which indicates their great molecular affinity. However, some differences were observed in patterns of drug resistance. Strain 16 proved to be sensitive to the drugs used in the treatment of tuberculosis, while strain 17 showed resistance to streptomycin (SM) and INH. It is noteworthy that patients 16 and 17 live in the neighborhood, in the distance of approx. 500 m and on this basis, the transmission of strains between patients can be assumed as possible. Patient 17 could get infected by patient 16 or alternatively both patients could be infected from a common, unknown source. Other strains isolated from patients from this town showed different DNA profiles by means of all the methods used, confirming separate sources of infection and no transmission between patients. Out of 8 strains, isolated from patients who were members of 4 families,

Table I
Epidemiological data about strains based on surveys and from medical records.

Location/Family	Sample No	Sex/ Relationship	Age	AFB	Culture	Drug resistance				Drugs administered in treatment	Other Drugs	Comorbidities
						SM 4.0	INH 0.2	RFP 40.0	ETB 2.0			
A	1	F	31	+	+++	R	R	S	S	RFZ, PZA, EMB, SM, INH, Tarivid	Pyralgin, Gasec, Thiocodin, Hepatil, Allupol, Encorton	cholelithiasis, nephro-lithiasis of left kidney
	2	M	30	+	+	R	R	S	S	RMZ, PZA, EMB, Tarivid	Kalipoz, Nifuroksazyd, Insulatard, Novo-Rapid	diabetes type 1, alcohol dependence syndrome
	3	M	53	+++	+++	R	R	S	S	RMZ, PZA, EMB, SM	Pyralgin, Liv52, Acard, Kalipoz, Thiocodin, Contix, Allupol, Biodacyna	cardiorespiratory distress, alcoholism, nicotinism
	4	M	48	+	++	R	S	S	S	RMZ, PZA, EMB, INH	Hemofer, Liv52, Thiocodin, Exacyl, Pyralgina Cyclonamina	anemia
B	9	M	34	+	++	S	S	S	S	RMZ, PZA, EMB, SM	–	alcoholism, nicotinism
	10	M	22	+	$+^{10}$	S	S	S	S	RMZ, PZA, EMB	Cyclonamina, Pyralgin, Allupol	–
C	13	M	30	++	+++	S	S	S	S	RMP, PZA, SM	Cyclonamina, Exacyl, Thiocodin	fibro-infiltrative lesions of left lobe, alcoholism
	14	M	61	+	+++	S	S	S	S	RMP, PZA, SM	Pyralgin, Cyclonamina, 5%glukoza	fibro-infiltrative lesions of left lobe, cholelithiasis, drug-induced gastritis, nicotinism
	15	M	50	+	+++	S	R	S	S	RMF, PZA, SM, EMB, RMZ	Hemofer, Acard, Pyralgin	toxic liver damage, thrombosis of left leg, TB miliaris
	16	F	28	++	+++	S	S	S	S	RMZ,PZA, EMB	Contix, Nifuroxazyl, Allupol, Loperamid, PWE, Metronidazol	anemia, nicotinism
	17	F	50	+++	+++	R	R	S	S	SM, RMZ, PZA, EMB	PWE, Paracetamol, Biotrakson	secondary anemia, haemorrage into alvoli, nicotinism
	18	M	60	+	+++	S	S	S	S	SM, RMZ, PZA, EMB	Allupol, Promazin, Oxodil	manic-depressive disorder, nephrolithiasis, thyroid lumps, nicotinism
	19	M	52	(–)	$+^{12}$	S	S	S	S	SM, RMZ, PZA, EMB	Hemofer, Prol. Ac., Folicum, Allupol	nicotinism
D	7	M/ friend	53	+	++	S	S	S	S	PZA, EMB, Refalin, Tarivid	Gasec, Pyralgina, Allupol, Hepatil	alcohol-induced liver damage, chronic gastritis
	8	M/ brother	52	+	+++	S	S	S	S	RMZ, PZA, EMB, SM	Pyralgin, Liv52, Acard, Kalipoz, Thiocodin, Contix, Allupol, Biodacyna	cardiorespiratory distress, alcoholism, nicotinism
E	32	M/son	61	+++	+++	S	S	S	S	RMZ, PZA, EMB, SM	Allupol, Amlopin Alermed, Contix, Loperamid	hypertension, alcoholism, nicotinism
	33	M/ father	40	+	+++	S	S	S	S	RMZ, PZA, EMB, SM	Ketokonazol, Flukonazol, Paracetamol	mitral regurge, pulmonary embolism, alcoholism, nicotinism
F	6	M/ brother	61	+	+	S	S	S	S	RMZ, PZA, EMB, INH	Zafiron, Acenol, Hemofer	chronic obturative pulmo-nary disease, secondary anemia, pneumonia, alcoholism, nicotinism
	23	M/ brother	51	+	+	S	S	S	S	RMZ, PZA, EMB, SM	Hemofer, Folicum, Flegamina	fibro-infiltrative TB of left lobe
G	30	K/ mother	54	+	+	S	S	S	S	RMZ, PZA, EMB, SM	Kalipoz, Poltram, Bisocard	infiltrative TB of lungs, alcoholism, nicotinism
	31	M/son	31	+	+	S	S	S	S	RMZ, PZA, EMB	Contix, Estazdom, Allupol	secondary anemia, alcoholism, nicotinism

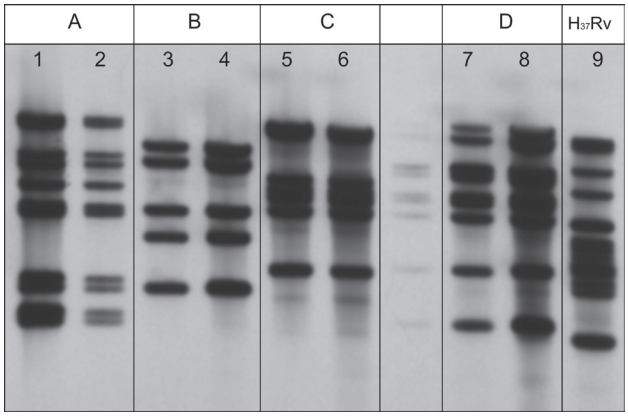

Fig. 2. DNA profiles obtained with IS*6110*-RFLP method. Line 1 and 2 – strains number 7 and 8 from family D, line 3, 4 – strains number 32 and 33 from family E, line 5, 6 – strains 6 and 23 from family F, line 7 and 8 – strains 30 and 31 from family D, line 9 – $H_{37}Rv$.

4 epidemiological groups corresponding to 4 analyzed families were distinguished. Within each family identical DNA profiles, as well as drug resistance patterns were identified (Fig. 2, Table I). This indicates a great chance of transmission of strains within the same family. A similar situation was observed in a small town, where the contact with infected persons is very likely.

Properly conducted tuberculosis supervision includes, apart from identification of the source of infection, tracking the ways of transmission of strains in the environment. It is known that the best way of tuberculosis prevention and its surveillance are primarily: detection of sputum positive Tuberculosis patient, integration of antituberculous treatment and examination of all the people around the patient in order to detect or exclude the contagion (Kozińska *et al*., 2011). Molecular methods used in the epidemiology of tuberculosis allow for prompt recognitions of specific strains and monitor the transmission of the disease. However, those methods should be supported by socio-demographic data that are substantial for identification of epidemiological groups in which mycobacteria could be transmitted. These include *i.a.*: a degree of kinship of people diagnosed with mycobacteria, the social status of the subjects, comorbidities, place of residence, *etc.* The transmission of strains is greater when the contact is more direct, primarily in close proximity to the patient (family, closed groups, small communities, prisons, health centers). However, even identical molecular formulas of strains may not constitute sufficient evidence that the source of infection is a person from the immediate surroundings. In this report, the molecular part of epidemiological investigations was based on 3 different methods. It should be noted that only data obtained by means of several methods of strains differentiation accompanied by detailed social history may show the actual transmission of individual strains. On the other hand, if different molecular patterns are obtained with the aforementioned methods, it allows for unambiguous interpretation of the results and the exclusion of transmission of strains between patients from whom they were isolated.

Analysis of the strains was used to assess the degree of TB spreading among subjects and point to the likelihood of strain transmission among patients. In all studied cases of families a high probability of transmission was observed. Also, the analysis of strains from patients residing in a small town (1 200 inhabitants) indicated a direct transmission between patients or a common source. On the other hand, out of 7 strains from location C only 2 were epidemiologically linked. In numerous community contacts a potential source of infection can be random and more unrelated *Mtb* strains might be present. The tested strains of location A accounted for 20% of all registered cases of tuberculosis in this town in 2012, and this was probably not a very representative group, and patients could come from a single place, *e.g.* from one surgery. More general conclusions about the level of transmission of *Mtb* strains require performing a molecular analysis of strains isolated over a number of years.

Acknowledgments

This work was supported by the Operational Programme Development of Eastern Poland.

Literature

Barnes P.F and M.D. Cave. Molecular epidemiology of tuberculosis. 2003. *N. Engl. J. Med*. 349: 1149–1156.

Covan L.S., L. Diem, T. Monson, P. Wand, D. Temporado, T.V. Oemig and J.T. Crawford. 2005. Evaluation of a two-step approach for large-scale, prospective genotyping of *Mycobacterium tuberculosis* isolates in the United States. *J. Clin. Microbiol*. 43: 688–695.

Crawford J.T. 2003. Genotyping in contact investigations: a CDC perspective. *Int. J. Tuberc. Lung Dis*. 7: 8453–57.

Janowiec M. 1988. Microbiology and serology (in Polish). National Institute of Medical Publishing.

Korzeniewska-Koseła M. 2014. Tuberculosis in Poland in 2012 (in Polish). *Przegl. Epidemiol*. 68: 389–393.

Kozińska M., Z. Zwolska and E. Augustynowicz-Kopeć. 2011. Transmission of drug-resistant tuberculosis among closely related (in Polish). Postępy Nauk Medycznych 10: 824–830.

Krawczyk B., A. Samet, J. Leibner, A. Sledzinska and J. Kur. 2006. Evaluation of a PCR melting profile technique for bacterial strain differentiation. *J. Clin. Microbiol.* 44: 2327–2332.

Krawczyk B., J. Leibner-Ciszak, K. Stojowska and J. Kur. 2011. The new LM-PCR/shifter method for the genotyping of microorganisms based on the use of a class IIS restriction enzyme and ligation mediated PCR. *J. Microbiol. Biotechnol.* 21: 1336–1344.

Kremer K., C. Arnold, A. Cataldi, M.C. Gutiérrez, W.H. Haas, S. Panaiotov, R.A. Skuce, P. Supply, A.G. van der Zanden and D. van Soolingen. 2005. Discriminatory power and reproducibility of novel DNA typing methods for *Mycobacterium tuberculosis* complex strains. *J. Clin. Microbiol.* 43: 5628–5638.

Masny A. and A. Plucienniczak. 2003. Ligation mediated PCR performed at low denaturation temperatures-PCR melting profiles. *Nucleic Acids Res*. 31(18):e114.

Moström P., M. Gordon , C. Sola, M. Ridell and N. Rastogi. 2002. Methods used in the molecular epidemiology of tuberculosis. *Clin. Microbiol. Infect*. 8: 694–704.

Reisig F., K. Kremer, B. Amthor, D. van Soolingen and W.H. Haas. 2005. Fast ligation-mediated PCR, a fast and reliable method for IS*6110*-based typing of *Mycobacterium tuberculosis* complex. *J. Clin. Microbiol.* 43: 5622–5627.

Statistical bulletin. 2013**.** Ministry of Health. http://www.csioz.gov.pl/publikacja.php?id=6, 1.08.2015.

Supply P., C. Allix, S. Lesjean, M. Cardoso-Oelemann, S. Rusch-Gerdes, E. Willery and others. 2006. Proposal for standardization of optimized mycobacterial interspersed repetitive unit-variable-number tandem repeat typing of *M. tuberculosis. J. Clin. Microbiol.* 44: 4498–4510.

Valcheva V., I. Mokrousov, N. Rastogi, O. Narvskaya and N. Markova. 2008. Molecular characterization of *Mycobacterium tuberculosis* isolates from different regions of Bulgaria. *J. Clin. Microbiol*. 46: 1014–1018.

van Embden J.D., M.D. Cave, J.T. Crawford, J.W. Dale, K.D. Eisenach, B. Gicquel, P. Hermans, C. Martin, R. McAdam and T.M. Shinnick. 1993. Strain identification of *Mycobacterium tuberculosis* by DNA fingerprinting: recommendations for a standardized methodology. *J. Clin. Microbiol.* 31: 406–409.

World Health Organization, Global Tuberculosis Report. 2012.

Zaczek A., A. Brzostek, A. Gorna, A. Sajduda, A. Wojtasik and J. Dziadek. 2013a. Application of FLiP method for differentiation of *Mycobacterium tuberculosis* strains in comparison to commonly used methods, spoligotyping and MIRU-VNTR typing. *Pol. J. Microbiol.* 62: 73–76.

Zaczek A., M. Ziolkiewicz, A. Wojtasik, J. Dziadek and A. Sajduda. 2013b. IS*6110*-based differentiation of *Mycobacterium tuberculosis* strains. *Pol. J. Microbiol*. 62: 201–204.

Zaczek A., A. Brzostek, A. Wojtasik, J. Dziadek and A. Sajduda. 2013c. Genotyping of clinical *Mycobacterium tuberculosis* isolates based on IS*6110* and MIRU-VNTR polymorphisms. *Biomed. Res. Int*. 2013: 865197.

Zaczek A., A. Brzostek, A. Kuroń, A. Wojtasik, A. Sajduda and J. Dziadek. 2014a. Development of a new ligation-mediated PCR method for the differentiation of Mycobacterium tuberculosis strains. *Int. J. Tuberc. Lung Dis.* 18: 302–309.

Zaczek A., A. Brzostek, A. Wojtasik, A. Sajduda and J. Dziadek. 2014b. Comparison of ligation-mediated PCR methods in differentiation of *Mycobacterium tuberculosis* strains. *Biomed. Res. Int.* 2014: 782071.

Zozio T., C. Allix, S. Gunal, Z. Saribas, A. Alp, R. Durmaz, M. Fauville-Dufaux, N. Rastogi and C. Sola. 2005. Genotyping of *Mycobacterium tuberculosis* clinical isolates in two cities of Turkey: description of a new family of genotypes that is phylogeographically specific for Asia Minor. *BMC Microbiol*. 5: 44.

Polish Journal of Microbiology
2015, Vol. 64, No 3, 295–298

SHORT COMMUNICATION

Relapsing Bacteraemia due to *Corynebacterium striatum* in a Patient with Peripheral Arterial Disease

ANTEA TOPIĆ[1]*, ROK ČIVLJAK[1,2], IVA BUTIĆ[3], MARIJA GUŽVINEC[3] and ILIJA KUZMAN[1, 2]

[1] Department of Acute Respiratory Diseases, University Hospital for Infectious Diseases "Dr. Fran Mihaljević", Zagreb, Croatia
[2] University of Zagreb School of Medicine, Zagreb, Croatia
[3] Department of Microbiology, University Hospital for Infectious Diseases "Dr. Fran Mihaljević", Zagreb, Croatia

Submitted 28 December 2014, revised 11 April 2015, accepted 13 April 2015

Abstract

We describe the first reported case of *Corynebacterium striatum* (*C. striatum*) relapsing bacteraemia in a patient with peripheral arterial disease and proven *Corynebacterium* species colonization of a chronic foot ulcer, focusing on the difficulties in the management of the patient. We conclude that the optimal duration of the antibiotic treatment for relapsing *C. striatum* bacteraemia from a chronic ulcer should be 6 weeks together with surgical treatment.

Key words: *Corynebacterium striatum*, antibiotic treatment, peripheral arterial disease, relapsing bacteraemia, skin infection

Corynebacterium species other than *Corynebacterium diphteriae* are part of the normal flora of human skin and mucous membranes (Coyle and Lipsky, 1990). *Corynebacterium striatum* (*C. striatum*), a Gram-positive bacillus, was traditionally regarded to be a colonizer or a contaminant (Watkins *et al*., 1993). The first published case of *C. striatum* infection was in 1980 in an immunocompromised patient with pleuropulmonary lesions (Bowstead and Santiago, 1980). Since then, the frequency of *C. striatum* community acquired and nosocomial infections has increased significantly. Reported cases of *C. striatum* infections include a wide variety of different types of infections: bacteraemia (Dall *et al.*, 1989; Martin *et al.*, 2003; Tumbarello *et al*., 1994; Watkins *et al*., 1993), endocarditis (Marull and Casares, 2008; Mashavi *et al.*, 2006; Fernandez Guerrero *et al.*, 2013; Tran *et al*., 2012), central catheter infection (Martinez-Martinez *et al.*, 1997; Chen *et al*., 2012), meningitis (Hoy *et al.*, 1997; Weiss *et al.*, 1996), pleuropneumonia (Cowling and Hall, 1993; Martinez-Martinez *et al*., 1994; Renom *et al*., 2014; Severo *et al.*, 2014), osteomyelitis (Fernandez-Ayala *et al.*, 2001), arthritis (Cone *et al.,* 1998; Scholle, 2007; Westblade *et al*., 2014), and intrauterine infection (Martinez-Martinez *et al.*, 1997). Person to person transmission in intensive care units (Brandenburg *et al.*, 1996; Iaria *et al*., 2007; Leonard *et al*., 1994) and a number of skin infection cases like pyogenic granuloma, infected ischemic ulcer, breast abscess and a skin ulcer in an HIV patient (Bottone *et al*., 2010; Peiris *et al*., 1994; Stone *et al*., 1997; Watkins *et al*., 1993) have also been described. Although *C. striatum* has been linked to chronic ulcer infection and bacteraemia (Martin *et al.*, 2003; Martinez-Martinez *et al*., 1997), to the best of our knowledge, no patient with relapsing bacteraemia after appropriate antibiotic treatment has been reported. We present a case of a 61-y-old man with *C. striatum* relapsing bacteraemia, peripheral arterial disease and proven *Corynebacterium* species colonization of chronic foot ulcer, focusing on the difficulties in the management of the patient.

A 61-y-old man was admitted to the University Hospital for Infectious Diseases, Zagreb, Croatia in November of 2013 because of fever and a painless ulcer of his right foot stump. He had been sick for 14 d with fever and oral clindamycin was prescribed, but without effect. His medical history was remarkable for coronary heart disease (1 y earlier the patient underwent PCA stent insertion and was treated with beta-blocker, ACE-inhibitor, statin and antiplatelet drugs) and 10 y severe peripheral arterial disease with development of gangrene of right foot which resulted in amputation (at the level of the Chopart's joint). During the 6-months

* Corresponding author: A. Topic, Department of Acute Respiratory Diseases, University Hospital for Infectious Diseases "Dr. Fran Mihaljević", Zagreb, Croatia; **e-mail: antea.topic@gmail.com**

prior to the admission of the patient, the ulceration formed with sporadic non-purulent secretion followed by debridement, antibiotic treatment (oral clindamycin) and hyperbaric oxygen treatment with consecutive good healing. The patient was a heavy smoker.

On admission the patient was febrile (38°C), but in good general condition with blood pressure of 130/80 mmHg, pulse 90/min and respirations 18/min. On examination a 1.5 cm ulcer was present above his right foot stump with no surrounding erythema, tenderness or purulent drainage. Right inguinal lymph nodes were enlarged up to 2 cm, painless and elastic. The pulse of his dorsal artery of the foot was faint. Meningeal signs were negative, the patient had no signs of pharyngitis or oral mucosal ulcers, but his oral cavity was in poor condition. His chest and cardiac examination were unremarkable. The abdomen was soft and painless, the liver was palpable 2 cm below the right costal margin, while the spleen was not palpable.

Laboratory tests revealed an increased erythrocyte sedimentation rate (70 mm/h), C-reactive protein was 141.8 mg/l and the total white blood count was 9.0×10^9/l with mature neutrophilia. The red blood cell count was 4.49×10^{12}/l, haemoglobin was 131 g/l and the platelet count 133×10^9/l. The levels of sodium, potassium, chloride, urea nitrogen, creatinin, glucose, total proteins (albumin and globulin), total bilirubin, aminotransferases, lactate dehydrogenase and alkaline phosphatase were normal; only the level of gamma glutamyl transferase was increased at 184 IU/l. Routine coagulation tests were normal with no signs of disseminated intravascular coagulation, but the level of fibrinogen was 8.0 g/l. Urinalysis revealed no abnormalities. The serologic HIV test was negative. Chest X-ray and electrocardiogram were normal. Abdominal ultrasound examination revealed a mild hepatomegaly and small gallstones without inflammation of the gallbladder. Radiographs of the right leg showed no findings of osteomyelitis. Both transthoracic and transesophageal echocardiograms were normal.

Gram-stained smear of scrapings of the ulcerative lesion showed a presence of Gram-positive bacilli without polymorphonuclear leucocytes and the culture revealed *Corynebacterium* species. Four separate sets of blood culture taken at different times on admission grew *C. striatum* susceptible to vancomycin, imipenem, penicillin and amoxicillin-clavulanic acid. The strain was identified using the commercial system of cultivation BacT/ALERT (bioMerieux, France) and identification system VITEK 2 (bioMerieux, France). Upon identification, the strain was confirmed by an in house method of sequence analysis of the internal fragment of the 16S rRNA gene (Savini *et al.*, 2013), using no control, but comparing the final sequence to the one in the PubMed database. Antibiotic susceptibility was determined using E-test (bioMerieux, France) for penicillin, amoxicillin-clavulanic acid, clindamycin, imipenem and vancomycin following the recommendations of the European Committee for Antimicrobial Susceptibility Testing (EUCAST). E-test values revealed that all isolates were resistant only to clindamycin. The MIC_s were as follows: penicillin 0.12 mg/l, amoxicillin-clavulanic acid 0.19 mg/l, vancomycin 0,5 mg/l, imipenem 0.032 mg/l and clindamycin > 256 mg/l.

The initial antibiotic treatment with intravenous amoxicillin-clavulanic acid was continued for 15 d after the diagnosis was established. Defervescence occurred 1 d after the initiation of the treatment and surveillance cultures were negative on day 8. Seven days after the amoxicillin-clavulanic acid treatment ended (during which the patient developed a mild *Clostridium difficile* diarrhoea and was treated with oral metronidazole) recurrence of the fever occurred and two sets of repeated blood culture were positive for *C. striatum* of identical antibiotic susceptibility. Based on the clinical presentation and positive blood culture, intravenous vancomycin was started and after clinical improvement of the patient, was continued for 15 d. The patient fully recovered and was discharged from the hospital with instructions of taking oral amoxicillin-clavulanic acid for another 4 weeks. During these 4 weeks, the patient also underwent surgical treatment (debridement) of the ulcer, which finally resulted in the healing of the ulcer of the right foot. During a 3 month follow up no fever was noted.

C. striatum, a coryneform bacteria usually considered a contaminant, is a non-sporulating, non-acid-fast pleomorphic gram-positive rod that is aerobic and facultatively anaerobic (Coyle and Lipsky, 1990). It was until recently that *C. diphteriae* was considered to be the only pathogen of the coryneform species. Today, besides *C. striatum*, other well known pathogens of the species include *Corynebacterium jeikeium*, *Corynebacterium urealyticum*, and *Corynebacterium amycolatum* (Funke *et al.*, 1997). Most cases of *C. striatum* infection occurred either in immunocompromised patients or patients whose skin barrier integrity was broken, rather than in previously healthy persons, because of *C. striatum*'s low adhesive properties and low pathogenicity. Neither toxin nor other virulence factors explain the transmission from contamination to infection (Watkins *et al.*, 1993). The number of reported cases of diseases generated by *C. striatum* in the past few decades, and especially in the last couple of years, has been on the rise due to the improvement of microbiological techniques and the survival of patients with underlying diseases. *C. striatum* bacteraemia is a rare event and is scarcely documented in literature (Chen *et al.*, 2012; Dall *et al.*, 1989; Martin *et al.*, 2003; Martinez-Martinez *et al.*, 1997; Tumbarello *et al.*, 1994; Watkins *et al.*, 1993). Associated

conditions include diabetes, cirrhosis, chronic renal failure, trauma, surgery and malignancy.

The case we have described is the first reported case of a relapsing bacteraemia in a patient with a proven source of infection (in this instance a chronic foot ulcer) despite appropriate treatment. Several factors promoted the risk of *C. striatum* infection; the presence of a foot ulcer as a result of a compromised peripheral arterial circulation, age, and previous antibiotic treatment. As has previously described (Leonard *et al.*, 1994), we also presume that, in our patient, selective pressure due to a prior antibiotic consumption favoured the overgrowth of *C. striatum*.

Corynebacteria are common skin and culture media contaminants, and discrimination between colonization and infection is, in some cases, difficult. In our case, the presence of four consecutive blood cultures positive only for. *C. striatum* suggests that this microorganism was the likely pathogen. Although the *C. species* cultivated from the foot ulcer was not identified to species level, because it was regarded as a contaminant, the skin-circulation route is most likely. Some authors (Martin *et al.*, 2003) have demonstrated by molecular techniques (PCR) identical strains of *C. striatum* from the skin and the bloodstream in a patient with peripheral arterial disease, confirming the entry of the bacterium trough the skin to the circulation. In our case, as a colonizer of the patient's skin, *C. striatum* established a *de novo* bacteraemia despite antibiotic treatment. Probable causes of the relapsing bacteraemia are a (too) short antibacterial treatment, choice of antibiotics, and vasculopathy.

The optimal duration of antibiotic treatment for. *C. striatum* bacteraemia is not known (Fernandez-Roblas *et al.*, 2009; Martinez-Martinez *et al*., 1996), but the clinical course of the infection in the presented patient (recurrence of fever and bacteraemia) suggests a need for a prolonged antibiotic treatment (we recommend 6 weeks) together with surgical treatment. If aggressive debridement is performed earlier, we presume that much shorter course of antibiotic treatment may be sufficient.

In conclusion, this case highlights the growing importance of *C. striatum* as a serious pathogen and the fact that consecutive positive blood cultures for corynebacteria, and *C. striatum* in particular, should never be overlooked.

Literature

Bottone E.J., M. Fabbri and A. Ashraf. 2010. *Corynebacterium striatum*: Chronic infection of a cutaneous ulcer in a patient with AIDS. *Rev. Infect.* 1: 104–109.

Bowstead T.T. and S.M. Santiago. 1980. Pleuropulmonary infection due to *Corynebacterium striatum*. *Br. J. Dis. Chest.* 74: 198–200.

Brandenburg A.H., A.Van Belkum, C. Van Pelt, H.A. Bruining, J.W. Mouton and H.A. Verbrugh. 1996. Patient-to-patient spread of a single strain of *Corynebacterium striatum* causing infections in a surgical intensive care unit. *J. Clin. Microbiol.* 34: 2089–2094.

Chen F.-L., P.-R. Hsueh, S.-O. Teng, T.-Y. Ou and W.-S. Lee. 2012. *Corynebacterium striatum* bacteremia associated with central venous catheter infection. *J. Microbiol. Immunol. Infect.* 45: 255–258.

Cone L.A., N. Curry, M.A. Wuestoff, S.J. O'Connell and J.F. Feller. 1998. Septic synovitis and arthritis due to *Corynebacterium striatum* following an accidental scalpel injury. *Clin. Infect. Dis.* 27: 1532–1533.

Cowling P. and L. Hall. 1993. Corynebacterium striatum: a clinically significant isolate from sputum in chronic obstructive airways disease. *J. Infect.* 26: 335–336.

Coyle M.B. and B.A. Lipsky. 1990. Coryneform bacteria in infectious diseases: clinical and laboratory aspects. *Clin. Microbiol. Rev.* 3: 227–246.

Dall L., W.G. Barnes and D. Hurford. 1989. Septicaemia in a granulocytopenic patient caused by *Corynebacterium striatum*. *Postgrad. Med. J.* 65: 247–248.

Fernandez-Ayala M., D.N. Nan and M.C. Farinas. 2001. Vertebral osteomyelitis due to *Corynebacterium striatum*. *Am. J. Med.* 111: 167.

Fernandez-Roblas R., H. Adames, N.Z.

Martin-De-Hijas, D.G. Almeida, I. Gadea and J. Esteban. 2009. *In vitro* activity of tigecycline and 10 other antimicrobials against clinical isolates of the genus *Corynebacterium*. *Int. J. Antimicrob. Agents* 33: 453–455.

Fernandez Guerrero M.L., I. Robles, C. Nogales Mdel and D. Nuevo. 2013. *Corynebacterium striatum*: an emerging nosocomial drug-resistant endocardial pathogen. *J. Heart Valve Dis.* 22: 428–430.

Funke G., A. Von Graevenitz, J.E. 3rd Clarridge and K.A. Bernard. 1997. Clinical microbiology of coryneform bacteria. *Clin. Microbiol. Rev.* 10: 125–159.

Hoy C.M., K. Kerr and J.H. Livingston. 1997. Cerebrospinal fluid-shunt infection due to *Corynebacterium striatum*. *Clin. Infect. Dis.* 25: 1486–1487.

Iaria C., G. Stassi, G.B. Costa, C. Biondo, E. Gerace, A. Noto, S.G. Spinella, A. David and A. Cascio. 2007. Outbreak of multiresistant *Corynebacterium striatum* infection in an Italian general intensive care unit. *J. Hosp. Infect.* 67: 102–104.

Leonard R.B., D.J. Nowowiejski, J.J. Warren, D.J. Finn and M.B. Coyle. 1994. Molecular evidence of person-to-person transmission of a pigmented strain of *Corynebacterium striatum* in intensive care units. *J. Clin. Microbiol.* 32: 164–169.

Martin M.C., O. Melon, M.M. Celada, J. Alvarez, F.J. Mendez and F. Vazquez. 2003. Septicaemia due to *Corynebacterium striatum*: molecular confirmation of entry via the skin. *J. Med. Microbiol.* 52: 599–602.

Martinez-Martinez L., A. Pascual, K. Bernard and A.I. Suarez. 1996. Antimicrobial susceptibility pattern of *Corynebacterium striatum*. *Antimicrob. Agents Chemother.* 40: 2671–2672.

Martinez-Martinez L., A.I. Suarez, M.C. Ortega and R. Rodriguez-Jimenez. 1994. Fatal pulmonary infection caused by *Corynebacterium striatum*. *Clin. Infect. Dis.* 19: 806–807.

Martinez-Martinez L., A.I. Suarez, J. Rodriguez-Bano, K. Bernard and M.A. Muniain. 1997. Clinical significance of *Corynebacterium striatum* isolated from human samples. *Clin. Microbiol. Infect.* 3: 634–639.

Marull J. and P.A. Casares. 2008. Nosocomial valve endocarditis due to *Corynebacterium striatum*: a case report. *Cases J.* 1: 388.

Mashavi M., E. Soifer, D. Harpaz and Y. Beigel. 2006. First report of prosthetic mitral valve endocarditis due to *Corynebacterium striatum*: Successful medical treatment. Case report and literature review. *J. Infect.* 52: e139–141.

Peiris V., S. Fraser, C. Knowles, S. Norris and C. Bennett. 1994. Isolation of *Corynebacterium striatum* from three hospital patients. *Eur. J. Clin. Microbiol. Infect. Dis.* 13: 36–38.

Renom F., M. Gomila, M. Garau, M.D.C. Gallegos, D. Guerrero, J. Lalucat and J.B. Soriano. 2014. Respiratory infection by *Corynebacterium striatum*: epidemiological and clinical determinants. *New Microbes New. Infect.* 2: 106–114.

Savini V., G. Gherardi, M. Favaro, C. Fontana, R. Marrollo, A.V. Argentieri, G. Dicuonzo, P. Fazii and D. D'antonio. 2013. About a bloodstream *Corynebacterium striatum* isolate. *Folia Microbiol.* (*Praha*) 58: 451–453.

Scholle D. 2007. A spontaneous joint infection with *Corynebacterium striatum*. *J. Clin. Microbiol.* 45: 656–658.

Severo C.B., L.S. Guazzelli, M.B. Barra, B. Hochhegger and L.C. Severo. 2014. Multiple pulmonary nodules caused by *Corynebacterium striatum* in an immunocompetent patient. *Rev. Inst. Med. Trop São Paulo* 56: 89–91.

Stone N., P. Gillett and S. Burge. 1997. Breast abscess due to *Corynebacterium striatum*. *Br. J. Dermatol.* 137: 623–625.

Tran T.T., S. Jaijakul, C.T. Lewis, L. Diaz, D. Panesso, H.B. Kaplan, B.E. Murray, A. Wanger and C.A. Arias. 2012. Native valve endocarditis caused by *Corynebacterium striatum* with heterogeneous high-level daptomycin resistance: collateral damage from daptomycin therapy? *Antimicrob. Agents Chemother.* 56: 3461–3464.

Tumbarello M., E. Tacconelli, A. Del Forno, S. Caponera and R. Cauda. 1994. *Corynebacterium striatum* bacteremia in a patient with AIDS. *Clin. Infect. Dis.* 18: 1007–1008.

Watkins D.A., A. Chahine, R.J. Creger, M.R. Jacobs and H.M. Lazarus. 1993. *Corynebacterium striatum*: a diphtheroid with pathogenic potential. *Clin. Infect. Dis.* 17: 21–25.

Weiss K., A.C. Labbe and M. Laverdiere. 1996. *Corynebacterium striatum* meningitis: case report and review of an increasingly important *Corynebacterium* species. *Clin. Infect. Dis.* 23: 1246–1248.

Westblade L.F., F. Shams, S. Duong, O. Tariq, A. Bulbin, D. Klirsfeld, W. Zhen, S. Sakaria, B.A. Ford, C.-A.D. Burnham and C.C. Ginocchio. 2014. Septic arthritis of a native knee joint due to *Corynebacterium striatum*. *J. Clin. Microbiol.* 52: 1786–1788.

Polish Journal of Microbiology
2015, Vol. 64, No 3, 299–305

SHORT COMMUNICATION

N-Substituted *N′*-(2-alkylthio-4-chloro-5-methylbenzenesulfonyl)guanidines – Antibacterial, Cytotoxic Activities and Some Structure-Activity Relationships

BEATA ŻOŁNOWSKA[1], JAROSŁAW SŁAWIŃSKI[1]*, ALEKSANDRA GRZONEK[1], ANNA KĘDZIA[2], EWA KWAPISZ[2] and ANNA KAWIAK[3, 4]

[1] Department of Organic Chemistry, Medical University of Gdańsk, Gdańsk, Poland
[2] Department of Oral Microbiology, Medical University of Gdańsk, Gdańsk, Poland
[3] Department of Biotechnology, Intercollegiate Faculty of Biotechnology, University of Gdańsk and Medical University of Gdańsk, Gdańsk, Poland
[4] Department of Human Physiology, Medical University of Gdańsk, Gdańsk, Poland

Submitted 29 September 2014, revised 23 December 2014, accepted 16 February 2015

Abstract

A series of *N*-substituted *N′*-(2-alkylthio-4-chloro-5-methylbenzenesulfonyl)guanidine derivatives bearing sulfonamide moiety have been screened *in vitro* for antibacterial activity against isolates from patients with infections of oral cavity, respiratory tract and intestinal tract. The majority of compounds exhibited good antibacterial potency. 1-[4-Chloro-5-methyl-2-(4-trifluoromethylbenzylthio)benzenesulfonyl]-3-(3-sulfamoylphenyl)guanidine (13) showed very strong activity, with MIC ≤6.2 μg/ml against eleven bacteria strains belonged to Gram-positive anaerobes and aerobes. Furthermore, compound 13 exhibited promising activity toward highly resistant microorganisms such as methicillin-resistant *Staphylococcus aureus* and *Enterococcus faecalis*. It was found that *Parvimonas micra*, *Finegoldia magna*, *Peptostreptococcus anaerobius*, *Propionibacterium acnes* showed the highest susceptibility toward the investigated guanidines.

Key words: 2-mercaptobenzenesulfonamide, antibacterial activity, polar surface area, sulfonylguanidine, theoretical calculations

Symbiotic relationship of bacteria and humans has beneficial influence on host health by modifying the composition of intestinal microbiota or by direct impact on the host such as modulating the immune response. Unfortunately, many pathogenic bacteria cause various diseases, for example, acute otitis media, sinusitis, pneumonia, bronchitis, sexually transmitted diseases, endocarditis, sepsis, septicemia, as well as infections of skin, soft tissue, surgical wound, urinary tract and gastrointestinal tract (Chu *et al.*, 1996). The use of antibiotics has revolutionized the treatment of these infections, improving health of uncountable number of patients of worldwide (Mishra *et al.*, 2012). However, the use of millions of tonnes of antibiotics over the past 75 years had made almost all pathogenic bacteria resistant to antibiotics commonly used to treat them (Laxminarayan *et al.*, 2013). Antibacterial resistance can be developed through several mechanisms, including alteration by mutations of the antibiotic target, changes in cell permeability or efflux, and horizontal transfer of resistance genes (Rodríguez-Rojas *et al.*, 2013). These bacterial evolutionary processes resulting in reduction of the options of treating bacterial infections in public health, especially in medical interventions such as surgery, transplantation, and chemotherapy. Other consequences of bacterial resistance including illness prolongation, higher rates of mortality in patients and increasing of costs of treatment for resistant infections (Laxminarayan *et al.*, 2013). The most problematic microorganisms that have developed multidrug resistance are methicillin-resistant *Staphylococcus aureus* (MRSA), penicillin-resistant *Streptococcus pneumoniae* (PRSP), vancomycin-resistant *Enterococcus* (VRE) (Eells *et al.*, 2013; Baquero *et al.*, 1991; Steed *et al.*, 2011). A growing number of resistant bacteria impel researchers to develop new antibacterial agents that target the broadest spectrum of bacteria.

Sulfonamides has played important role in treatment of antibacterial infections since over 70 years ego (Connor, 1998). This class of sulfa drugs are mainly used to treat gastrointestinal, upper respiratory tract and urinary tract infections. They are popular due to good tolerance by patients, ease of administration, wide spectrum of antibacterial activity and relatively low costs

* Corresponding author: J. Sławiński, Department of Organic Chemistry, Medical University of Gdańsk, Gdańsk, Poland; **e-mail: jaroslaw@gumed.edu.pl**

(Connor, 1998; Gadad *et al*., 2000). Sulfonamide derivatives as the structural analogues of *p*-aminobenzoic acid, inhibit the 6-hydroxymethyl-7,8-dihydropteroate synthase and limit of folic acid synthesis in prokaryotes, that is essential to cell growth (Brown, 1962).

Our previous studies concerning synthetic antibacterials (Sławiński *et al*., 2013) and bioactive properties of sulfonamides prompted us to search the new antimicrobials in our library of *N*-sulfonamide substituted *N′*-(2-alkylthio-4-chloro-5-methylbenzenesulfonyl) guanidines. The guanidine derivatives containing sulfonamide group exhibited anticancer activity and abilities to inhibition of human carbonic anhydrase (hCA) (Żołnowska *et al*., 2014).

In the present study, the *N*-substituted *N′*-(2-alkylthio-4-chloro-5-methylbenzenesulfonyl)guanidines containing sulfonamide moiety **1**–**29** were investigated for their antibacterial activity against various genera of bacteria isolated from patients with infections of the oral cavity, respiratory tract and intestinal tract. Their activities, as given by the minimal inhibitory concentration (MIC) values are shown in Table I. The guanidine derivatives were synthesized by methods established in our previous paper (Żołnowska *et al*., 2014) and the structure of each of those compounds (**1**–**29**) was displayed in Table I.

Antibacterial susceptibility tests were performed against 28 strains of anaerobic and 28 strains of aerobic bacteria, obtained from Laboratory of Department of Oral Microbiology, Medical University of Gdańsk, Poland. The strains of bacteria were isolated from patients with infections of the oral cavity: gingivitis, periodontal diseases, corrosive ulcers, stomatitis (swabs, paper point), respiratory tract (sputum, swabs), intestinal tract (stool). The samples were quickly (1 h) sent to the laboratory and inoculated onto agar and incubated under aerobic or anaerobic conditions at 37°C for 48 h (aerobic) and 10–14 days (anaerobic bacteria). The aerobic bacteria were identified according to established procedures. The identification of anaerobic bacteria was based according to physiological, morphological and biochemical reactions (API 20A) (Holdeman *et al.*, 1977; Forbes *et al*., 2007). Analysis of conversion glucose into C1 to C6 fatty acids, lactic, fumaric and succinic acids involved the use of gas chromatography. The ability of the strains to produce fluorescence was observed at a spectrum of ultraviolet radiation (UV). The investigated anaerobes belonged to the following genera: *Peptostreptococcus* (1 strain), *Parvimonas* (2), *Bifidobacterium* (1), *Finegoldia* (3), *Actinomyces* (2), *Propionibacterium* (3), *Prevotella* (5), *Porphyromonas* (2), *Fusobacterium* (4), *Bacteroides* (4), *Parabacteroids* (1) and reference strains *Bacteroides fragilis* ATCC 25285, *Bacteroides vulgatus* ATCC 8482, *Parabacteroides distasonis* ATCC 8503, *Fusobacterium nucleatum* ATCC 25586, *Peptostreptococcus anaerobius* ATCC 27337, *Finegoldia magna* ATCC 25285, *Propionibacterium acnes* ATCC 11827. As a reference substance, metronidazole (Fluka) was applied.

Aerobic bacteria were as follows: *Staphylococcus* (8), *Enterococcus* (3), *Corynebacterium* (2), *Klebsiella* (2), *Acinetobacter* (2), *Escherichia* (2), *Citrobacter* (2), *Pseudomonas* (5), S*erratia* (2) and reference strains *S. aureus* ATCC 25923, *E. faecalis* ATCC 29212, *Klebsiella pneumoniae* ATCC 13883, *Acinetobacter baumannii* ATCC 19606, *Escherichia coli* ATCC 25922. Amikacin (Fluka) was used as a reference compound.

The minimal inhibitory concentration (MIC) was defined as the lowest compound concentration which inhibited growth of bacteria. The susceptibility of the anaerobic bacteria was determined by means of the plate dilution technique in Brucella agar supplemented with 5% sheep blood, menadione and hemin (CLSI, 2007). The compounds were dissolved in 1 ml of DMSO immediately before the experiment. Further dilutions were performed in sterile distilled water. The following concentrations of the compounds were used: 200, 100, 50, 25, 12.5, and 6.2 μg/ml. The inoculum containing 10^5 CFU/spot was applied to agar plates with Steers replicator. The inoculated agar plates and compound-free ones were incubated in anaerobic jars for 48 h at 37°C in 10% CO_2, 10% H_2, 80% N_2 atmosphere with palladium catalyst and indicator of anaerobiosis.

The susceptibility of the aerobic bacteria was determined by means of agar dilution technique with Mueller-Hinton agar (CLSI, 2006). The compounds were dissolved in 1 ml of DMSO immediately before the experiment. Further dilutions were performed in sterile distilled water. The following concentrations of the derivatives were used: 200, 100, 50, 25, 12.5, and 6.2 μg/ml. The inoculum containing 10^5 CFU/spot was applied to the agar plates with Steers replicator. The inoculated agar plates and compound-free ones were incubated for 24 h at 37°C in aerobic conditions.

P.an. – Peptostreptococcus anaerobius; P.m. – Parvimonas micra; B.b. – Bifidobacterium breve; F.m. – Finegoldia magna; A.o. – Actinomyces odontolyticus; P.ac. – Propionibacterium acnes; P.g. – Propionibacterium granulosum; P.as. – Porphyromonas asaccharolytica; B.v. – Bacteroides vulgatus; F.n. – Fusobacterium nucleatum; S.a. – Staphylococcus aureus MSSA; MRSA – methicillin-resistant *Staphylococcus aureus; S.e. – Staphylococcus epidermidis; E.f.-Enterococcus faecalis; C.x. – Corynebacterium xerosis;*

[a] the strains that were not sensitive (MIC ≥ 200 μg/ml) were not presented in table; [b] compounds **4**, **11**, **15**, **16**, **23**, **25**, **26**, **28** and **29** were inactive; [c] no. of tested strains; * – MIC ≥ 200 μg/ml; NT – not tested; M – metronidazole; A – amikacin

Table I
Antibacterial activity of compounds 1–29[a, b] against anaerobes and aerobes.

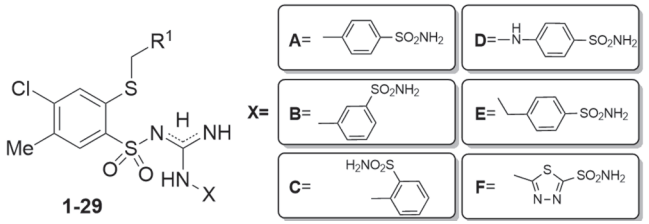

Comp	R^1	X
1		A
2		B
3		D
4		E
5		F

Comp	R^1	X
6		A
7		B
8		C
9		D
10		E
11		F

Comp	R^1	X
12		A
13		B
14		D
15		E
16		F

Comp	R^1	X
17		A
18		B
19		C
20		D
21		E
22		F

Comp	R^1	X
23	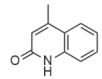	B
24		C
25		D
26		E

Comp	R^1	X
27	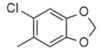	A
28		D
29		E

Compd	Minimal inhibitory concentration (MIC) in μg/ml														
	Gram-positive anaerobes							Gram-negative anaerobes			Gram-positive aerobes				
	P. an. (1)[c]	*P. m.* (2)	*B.b.* (1)	*F.m.* (3)	*A.o.* (2)	*P.ac.* (1)	*P.g.* (2)	*P.as.* (2)	*B.v.* (1)	F.n. (2)	S.a. (4)[c]	MRSA (2)	S.e. (2)	E.f. (3)	C.x. (2)
1	≤6.2	≤6.2; ≤6.2	*	≤6.2; ≤6.2; ≤6.2	NT	*	*; *	100; *	50	*; *	*; *; *; *	*; *	*; *	*; *; *	*; *
2	≤6.2	25; 25	*	≤6.2; ≤6.2; ≤6.2	NT	50	100; *	100; *	100	*; *	50; 50; 100; 100	25; 25	50; 50	12.5; 25; 50	50; 100
3	25	50; *	*	50; 50; 100	NT	50	50; 100	*; *	*	*; *	≤6.2; 12.5; 25; 25	100; *	25; 50	≤6.2; 100; *	12.5; 25
5	100	50; 100	*	50; 50; 100	NT	50	100; *	100; *	*	*; *	≤6.2; 25; 25; 50	50; 50	12.5; 50	50; 50; 50	≤6.2; 25
6	25	25; 50	*	25; 25; 50	NT	50	*; *	25; 50	*	*; *	*; *; *; *	*; *	*; *	*; *; *	*; *
7	≤6.2	25; 50	*	≤6.2; ≤6.2; ≤6.2	NT	12.5	25; 50	50; 100	100	*; *	≤6.2; 12.5; 25; 50	25; 50	25; 50	≤6.2; 25; 50	*; *
8	≤6.2	12.5; 12.5	50	≤6.2; ≤6.2; ≤6.2	NT	≤6.2	50; 50	25; 50	100	*; *	≤6.2; 50; *; *	100; *	50; 100	≤6.2; ≤6.2; 50	≤6.2; 12.5
9	≤6.2	25; 50	*	12.5; 50; 50	NT	12.5	50; 100	50; 50	*	*; *	50; 100; 100; *	*; *	50; 100	50; *; *	25; 50
10	*	25; 25	NT	12.5; 25; 25	25; 25	100	*; *	*;*	*	*; *	*; *; *; *	NT	*; *	*; *; *	≤6.2; 6.2
12	*	25; 25	NT	25; 25; 50	25; 50	≤6.2	*; *	*;*	*	*; *	*; *; *; *	NT	*; *	*; *; *	25; 50
13	≤6.2	≤6.2; ≤6.2	*	≤6.2; ≤6.2; ≤6.2	NT	≤6.2	25; 50	*; *	100	*; *	≤6.2; ≤6.2; 12.5; 12.5	50; 100	25; 100	≤6.2; ≤6.2; 100	50; 100
14	≤6.2	12.5; 25	*	25; 50; 50	NT	≤6.2	25; 50	25; 25	100	50; *	50; 50; 50; 50	*; *	50; 100	50; * ;*	≤6.2; 12.5
17	*	25; 25	NT	≤6.2; 12.5; 25	12.5; 25	≤6.2	*; *	*; *	*	*; *	*; *; *; *	NT	*; *	*; *; *	25; 50
18	*	25; 25	NT	12.5; 12.5; 50	12.5; 25	≤6.2	*; *	*; *	*	*; *	*; *; *; *	*; *	*; *	*; *; *	*; *
19	*	≤6.2; ≤6.2	NT	≤6.2; ≤6.2; 25	≤6.2; ≤6.2	≤6.2	*; *	*; *	*	*; *	*; *; *; *	*; *	*; *	*; *; *	*; *
20	25	100; 100	*	50; *; *	NT	12.5	50; 100	50; 100	50	*; *	*; *; *; *	*; *	*; *	*; *; *	12.5; 100
21	≤6.2	≤6.2; 12.5	NT	≤6.2; 12.5; 50	25; 25	≤6.2	*; *	*; *	*	*; *	*;*; *; *	NT	*; *	*; *; *	25; 50
22	*	≤6.2; 12.5	NT	≤6.2; 12.5; 12.5	50; 50	50	*; *	*; *	*	*; *	25; 50; 100; *	NT	25; *	25; 25; 25	25; 50
24	50	≤6.2; 50	≤6.2	25; 50; 50	NT	50	100; *	100; *	100	100; *	*; *; *; *	*; *	*; *	*; *; *	*; *
27	25	100; *	*	12.5; 100; *	NT	50	*; *	*; *	50	*; *	*; *; *; *	*; *	*; *	*; *; *	*; *
M	1.6	0.8; 0.8	100	≤0.4; ≤0.4; ≤0.4	3.1; 6.2	≥100	≥100; ≥100	≤0.4; ≤0.4	≤0.4	≤0.4; ≤0.4	–	–	–	–	–
A	–	–	–	–	–	–	–	–	–	–	≤6.2; ≤6.2; ≤6.2; ≤6.2	*; *	≤6.2; 12.5	25; 25; 50	50; 50

Generally, tested guanidines showed auspicious antibacterial activity. *N*-Substituted *N′*-[4-chloro-5-methyl-2-(3- and 4-trifluoromethylbenzylthio)benzenesulfonyl] as well as *N′*-[4-chloro-5-methyl-2-(naphthalen-1-ylmethylthio)benzenesulfonyl]guanidines presented the most active antibacterial agents in anaerobic conditions (Table I). Among them, compounds **8** (R^1 = = 3-CF_3Ph) and **14** (R^1 = 4-CF_3Ph) appeared as the promising agents inhibiting the broadest spectrum of anaerobic strains at range of concentration 6.2–100 μg/ml. On the other hand, **13** (R^1 = 4-CF_3Ph) and **19** (R^1 = = 1-naphthyl) showed the very strong antibacterial activity against the largest number of bacterial strains with MIC ≤ 6.2 μg/ml.

The results of our studies indicated that aerobic bacterium were less susceptible toward tested guanidines than anaerobic ones. The most potent compounds **2**, **5** and **13** belonged to *N*-substituted *N′*-[4-chloro-5-methyl-2-(benzylthio / 3- and 4-trifluoromethylbenzylthio)benzenesulfonyl]guanidines and were active against thirteen aerobic bacterial strains (Table I). It should be pointed out that only **13** exhibited the highest potential as antibacterial agent with relatively wide range of actions.

Among the screened microorganisms the highest susceptibility against tested guanidines demonstrated *P. micra*, *F. magna*, *P. acnes* and *P. anaerobius*. It is known that *P. micra, F. magna*, and *P. anaerobius* are the most commonly found Gram-positive anaerobic cocci (GPAC) in clinical material (Veloo *et al*., 2011). Additionally, microbiologists are interested in *F. magna* because it has one of the highest resistance rates of the GPAC and is capable of producing several virulence factors. The most promising compounds **1** and **13** inhibited simultaneously the growth of three important GPAC with MIC ≤ 6.2 μg/ml. Other relatively sensitive to investigated guanidines strains belonged to *P. acnes*, which is associated mostly with acne vulgaris but also is found to be the causative agent in discitis, endophthalmitis, or infections of the bones and joints, mouth, eye and central nervous system (Perry and Lambert, 2006; Perry and Lambert, 2011). Surprisingly, methicilin-resistant *S. aureus* (MRSA), one of the most problematic pathogens in hospitals and healthcare facilities were susceptible toward compounds **2**, **5**, **7** and **13** (MIC; 25–100 μg/ml), while *Enterococcus faecalis*, known as multidrug resistant bacteria, were sensitive towards **2**, **5**, **7–8**, **13** and **22** (MIC; 6.2–100 μg/ml). From the point of view of resistance of MRSA and enterococci to numerous antibiotics such as the beta-lactams, aminoglycosides, macrolides and lincosamides, the active guanidines seem to be the promising leads in searching for new antibiotics.

It is significant that several tested compounds more effectively inhibited the growth of *B. breve* (two compd), *P. acnes* (18 compd), *P. granulosum* (7 compd), MRSA (6 compd), *E. faecalis* (5 compd), and *C. xerosis* (11 compd) than reference metronidazole (anaerobes) and amikacin (aerobes) (Table I).

From the obtained results of antibacterial assay some observations concerning the structure-activity relationships (SAR) can be noticed:

1. Antibacterial activity against GPAC depended on structural nature of R^1 and X groups. Comparing the structural properties of **13** (R^1 = 4-CF_3Ph, X = 3-sulfamoylphenyl) to other compounds with 3-sulfamoylphenyl group as the substituent of guanidine moiety, it should be seen that presence of phenyl (**2**, R^1 = Ph) or 4-trifluoromethylphenyl (**7**, R^1 = 3-CF_3Ph) slightly reduced the activity against only *P. micra*. The presence of 1-naphthyl group as R^1 in compound **18** decreased antibacterial activity (MIC; 12.5–50 μg/ml) against *P. micra* and *F. magna* and made the compound inactive against *P. anaerobius*. In the series of 3-(4-sulfamoylphenyl)guanidines (X = A) exchanging of phenyl substituent (**1**, R^1 = Ph, MIC ≤ 6.2 μg/ml) into 3- or 4-trifluoromethylphenyl (**6**, **12**) or expanded aromatic fragments (**17**, **27**) decreased activity against GPAC at different degrees (MIC; 12.5–200 μg/ml). For **12** and **17** these modifications caused loss of the activity against *P. anaerobius*.

2. Compounds **17–22** containing as R^1 the 1-naphthyl group exhibited strong antibacterial activity against bacterium *P. acens*. As can be seen guanidines with either phenyl, 6-chlorobenzo[*d*][1,3]dioxol-5-yl or 2-oxo-1,2-dihydroquinolin-4-yl group showed the significant lower activity (MIC; 50–200 μg/ml) then **17–22**.

3. Significant bioactivity against the staphylococci was observed for some guanidine derivatives containing phenyl or 3-/4-trifluoromethylphenyl groups as R^1. The relatively highest antibacterial activity in this series had compounds with 3-sulfamoylphenyl (**2**, **7**, **13**) and 4-sulfamoylphenylamino (**3**, **9**, **14**) substituents at guanidine fragment. It was also found that for active **5** (R^1 = Ph, X = 2-sulfamoyl-1,3,4-thiadiazol-5-yl, MIC; 6.2–50 μg/ml) exchange of phenyl to 1-naphthyl group decreased antibacterial effect against staphylococci (**22**, MIC; 25–200 μg/ml), while substitution with the remaining substituents R^1 resulted in loss of bioactivity. The relationship between the structure of guanidine and their antibacterial activity against *E. faecalis* were the same as for staphylococci.

4. Considering the very strong activity of **10** (R^1 = 3-CF_3Ph, X = E) against *C. xerosis* it should be noted that to maintain a good activity of compound, only naphthyl group was acceptable, other modification at substituent R^1 caused loss of this effect.

In order to explain some differences in biological activity of investigated guanidines, molecular descriptors, such as polar surface area (PSA), molecular surface

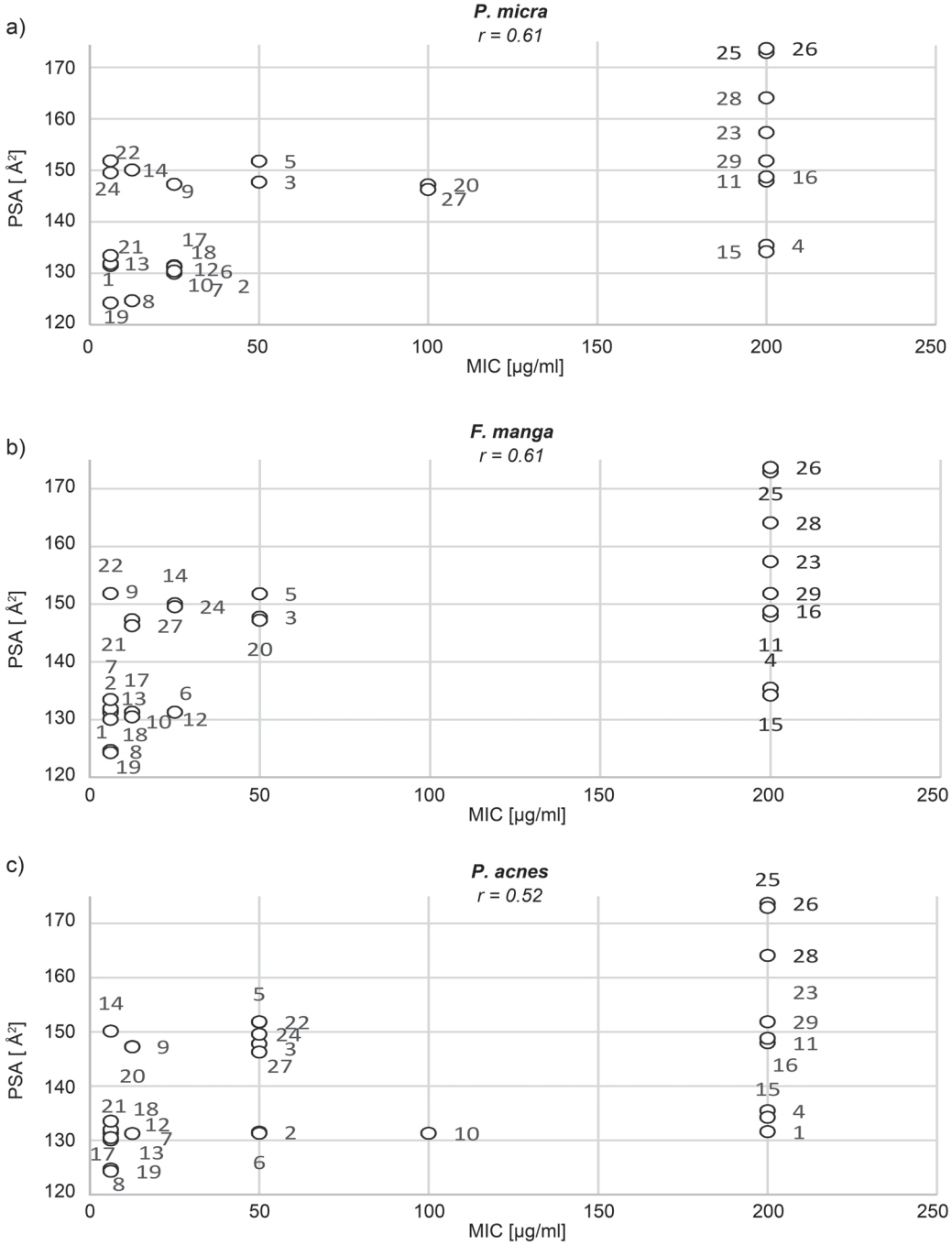

Fig. 1. Plots of antimicrobial activity of compounds **1–29** for *P. micra* (a), *F. magna* (b), *P. acnes* (c) vs calculated PSA. The correlation coefficients (*r*) ranged from 0.52 to 0.61.

area, dipole moment, lipophilicity for all compounds were calculated by using SPARTAN '08 software with B3LYP/6-31G* density functional model (SPARTAN '08). Atomic charges of sulphur and nitrogen at sulfonamide groups were also calculated. Statistical analyses of calculated descriptors were performed by STATISTIKA 10. The analysis of structural and electronic parameters has not adjudicated evident influence of these descriptors on biological activity of guanidines. The correlation coefficients (*r*, Fig. 1) showed that for the most susceptible bacteria strains (*P. micra*, *F. magna* and *P. acnes*) the PSA which is defined as the area due to nitrogen and oxygen and any hydrogens attached to nitrogen and oxygen was the best correlated descriptor to the experimental MIC values. The scatter plots (Fig. 1) shows that in the majority compounds with PSA values higher than 151.8 Å² are inactive against *P. micra*, *F. magna* and *P. acnes*. On the other hand, PSA values lower than 140 Å² describe the compounds with high antibacterial activity.

The role of PSA in governing passive diffusion has been widely discussed, as PSA seems to optimally

Table II
Cytotoxic activities of compounds **2**, **5**, **7**, **8** and **13**.

Compound	The human keratinocyte cell line (HaCaT)						
	Cell viability (%)					IC_{50} (μM)	IC_{50} μg/ml
	1 μM	10 μM	25 μM	50 μM	100 μM		
2	96 ± 5	100 ± 1	96 ± 2	5 ± 0.5	7 ± 0.8	35	18.4
5	95 ± 3	98 ± 1	92 ± 0.5	100 ± 0.4	71 ± 2	>100	> 53.0
7	99 ± 2	98 ± 3	100 ± 2	7 ± 0.6	8 ± 1	36	21.4
8	97 ± 3	97 ± 1	63 ± 3	6 ± 0.5	7 ± 2	30	17.8
13	95 ± 4	92 ± 0.2	48 ± 5	7 ± 2	6 ± 0.5	24	14.2

recapitulate the drug properties that play an important role in membrane penetration. Generally, compounds with PSA ≥ 140 Å^2 should exhibit poor cell penetration (≤ 10%), whereas compounds with PSA ≤ 60 Å^2 show high absorption (≥ 90%) (Ertl, 2007). Our studies revealed that low antibacterial activity of compounds with high PSA values is due to their limited cellular uptake.

To assess if the effect shown against bacterial cells could be related to a selected toxicity or to a more general toxic effect, we performed assay on the human keratinocytes (HaCaT cell line) to screen the most active compounds (**2**, **5**, **7**, **8** and **13**, Table II) for their general cytotoxic activity. The HaCaT cell line was cultured in Dulbecco's modified Eagle's medium (DMEM) supplemented with 4500 mg/l glucose, 10% fetal bovine serum, 2 mM glutamine, 10000 units penicillin, and 10 mg/ml streptomycin. Cultures were maintained in a humidified atmosphere containing 5% CO_2 at 37°C.

Cell viability was determined using the MTT(3-(4,5-dimethylthiazol-2-yl)-2,5-diphenyltetrazolium-bromide) assay (Ragab *et al*., 2013; Morales and Haza, 2013; Suresh *et al*., 2011). Cells were seeded in 96-well plates at a density of 5×10^3 cells/well and treated for 72 h with the guanidine derivatives in the concentration range 1–100 μM. Next, MTT (0.5 mg/ml) was added directly to the medium and cells were further incubated for 3 h at 37°C. The optical density of the formazan solution was measured at 550 nm with a plate reader (Victor, 1420 multilabel counter). Results are expressed as IC_{50} values. ± SD was calculated from at least three independent experiments.

Experiments indicated that the studied HaCaT cell line survived even at compound **5** concentration of 100 μM (53 μg/ml). The IC_{50} values of compounds **2**, **7**, **8** and **13** ranged from 24 μM (14.2 μg/ml) to 36 μM (21.4 μg/ml) and were higher than the lowest MIC values obtained for many bacterial strains (*P. anaerobius*, *P. micra*, *F. magna*, *P. acnes*, *S. aureus*, *E. faecalis*, *C. xerosis*).

Summarizing, the antibacterial agents found in this paper are useful leads for designing of new effective antibacterial compounds. Results of these preliminary studies need subsequent pharmacokinetic, mechanistic and toxicity evaluations, that will be the aim of new work in the near future.

Literature

Baquero F., J. Martínez-Beltrán and E. Loza. 1991. A review of antibiotic resistance patterns of *Streptococcus pneumoniae* in Europe. *J. Antimicrob. Chemother.* 28 Suppl. C: 31–38.

Brown G.M. 1962. The biosynthesis of folic acid. II. Inhibition by sulphonamides. *J. Biol. Chem.* 237: 536–540.

Chu D.T.W., J.J. Plattner J.J. and L. Katz. 1996. New directions in antibacterial research. *J. Med. Chem.* 39: 3853–3874.

Clinical and Laboratory Standards Institute. 2006. Methods of Dilution Antimicrobial Susceptibility Testing for Bacteria That Grow Aerobically; Approved Standard – Seventh Edition. CLSI document M7-A7. Wayne, PA. USA.

Clinical and Laboratory Standards Institute. 2007. Methods for Antimicrobial Susceptibility Testing of Anaerobic Bacteria; Approved Standard – Seventh Edition. CLSI document M11-A7. Clinical and Laboratory Standards Institute, Wayne, PA. USA.

Connor E.E. 1998. Sulfonamide antibiotics. *Prim. Care Update Ob Gyns* 5: 32–35.

Eells S.J., J.A. McKinnell, A.A. Wang, N.L. Green, P. O'Hara, M.L. Brown and L.G. Miller. 2013. A comparison of clinical outcomes between healthcare-associated infections due to community-associated methicillin-resistant *Staphylococcus aureus* strains and healthcare-associated methicillin-resistant *S. aureus* strains. *Epidemiol. Infect.* 141: 2140–2148.

Ertl P. 2007. Polar Surface Ares, pp. 111–125. In: Mannhold R., Kubinyi H., Folkers G., ed. Molecular drug properties: Measurement and Prediction. Wiley-VCH Verlag GmbH & Co. KGaA, Weinheim.

Forbes B.A., D.F. Sahn and A.S. Weissfeld. 2007. Bailey and Scott's Diagnostic Microbiology. 12th ed. Mosby Elsevier St. Louis, MO. USA.

Gadad A.K., C.S. Mahajanshetti, S. Nimbalkar and A. Raichurkar. 2000. Synthesis and antibacterial activity of some 5-guanylhydrazone/thiocyanato-6-arylimidazo[2,1-b]-1,3, 4-thiadiazole-2-sulfonamide derivatives. *Eur. J. Med. Chem.* 35: 853–857.

Holdeman L.V., E.P. Cato and W.E.C. Moore. 1977. Anaerobe Laboratory Manual. VPI 4th ed. Blacksburg, VA. USA.

Laxminarayan R., A. Duse, Ch. Wattal, A.K.M. Zaidi, H.F.L. Wertheim, N. Sumpradit, E. Vlieghe, G.L. Hara, I.M. Gould, H. Goossens and others. 2013. Antibiotic resistance-the need for global solutions. *Lancet Infect. Dis.* 13: 1057–1098.

Mishra R.P.N, E. Oviedo-Orta, P. Prachi, R. Rappuoli and F. Bagnoli. 2012. Vaccines and antibiotic resistance. *Curr. Opin. Microbiol.* 15: 596–602.

Morales P. and A.I. Haza. 2013. Antiproliferative and apoptotic effects of Spanish honeys. *Pharmacogn. Mag.* 9: 231–237.

Perry A.L. and P.A. Lambert. 2006. *Propionibacterium acnes*. *Lett. Appl. Microbiol.* 42: 185–188.

Perry A. and P. Lambert. 2011. *Propionibacterium acnes*: infection beyond the skin. *Expert Rev. AntiInfect. Ther.* 9: 1149–1156.

Ragab E.A., A.S. Mohammed, H.S. Abbass and S.I. Kotb. 2013. A new flavan-3-ol dimer from *Ficus sprague*ana leaves and its cytotoxic activity. *Pharmacogn. Mag.* 9: 144–148.

Rodríguez-Rojas A., J. Rodríguez-Beltrán, A. Couce and J. Blázquez. 2013. Antibiotics and antibiotic resistance: a bitter fight against evolution. *Int. J. Med. Microbiol.* 303: 293–297.

Sławiński J., B. Żołnowska, D. Pirska, A. Kędzia and E. Kwapisz. 2013. Synthesis and antibacterial activity of novel 4-chloro-2-mercaptobenzenesulfonamide derivatives. *J. Enzyme Inhib. Med. Chem.* 28: 41–51.

SPARTAN '08 Wavefunction Inc., Irvine, CA 92612, USA.

STATISTIKA 10 software, StatSoft. Inc., Tulsa, OK 74104, USA.

Steed M.E., C. Vidaillac, W.E. Rose, P. Winterfield, G.W. Kaatz and M.J. Rybak. 2011. Characterizing vancomycin-resistant Enterococcus strains with various mechanisms of daptomycin resistance developed in an *in vitro* pharmacokinetic/pharmacodynamic model. *Antimicrob. Agents Chemother*. 55: 4748–4754.

Suresh H.M., B. Shivakumar, K. Hemalatha, S.S. Heroor, D.S. Hugar and K.R. Rao. 2011. *In vitro* antiproliferative activity of *Annona reticulata* roots on human cancer cell lines. *Pharmacogn. Res.* 3: 9–12.

Veloo A.C., G.W. Welling and J.E. Degener. 2011. Antimicrobial susceptibility of clinically relevant Gram-positive anaerobic cocci collected over a three-year period in the Netherlands. *Antimicrob. Agents Chemother.* 55: 1199–1203.

Żołnowska B., J. Sławiński, A. Pogorzelska, J. Chojnacki, D. Vullo and C.T. Supuran. 2014. Carbonic anhydrase inhibitors. Synthesis, and molecular structure of novel series *N*-substituted *N*'-(2-arylmethylthio-4-chloro-5-methylbenzenesulfonyl)guanidines and their inhibition of human cytosolic isozymes I and II and the transmembrane tumor-associated isozymes IX and XII. *Eur. J. Med. Chem.* 71: 135–147.

Polish Journal of Microbiology
2015, Vol. 64, No 3, 307–310

SHORT COMMUNICATION

The Effect of Fe_3O_4 Nanoparticles on Survival of Probiotic Bacteria *Lactobacillus acidophilus* PCM2499 at Lower pH

ANDRZEJ JURKOWSKI[1]*, BARTŁOMIEJ ZAPOTOCZNY[2], JACEK J. KOZIOŁ[1] and MIROSŁAW R. DUDEK[2]

[1] Department of Biotechnology, University of Zielona Góra, Zielona Góra, Poland
[2] Institute of Physics, University of Zielona Góra, Zielona Góra, Poland

Submitted 11 November 2014, revised 6 March 2015, accepted 6 March 2015

Abstract

This paper presents a description of an experiment in which the survival rate of the probiotic bacteria *Lactobacillus acidophilus* PCM2499 was increased only due to the presence of Fe_3O_4 magnetic nanoparticles. The survival rate increased from 1.3 to 10 times compare to the control. It has been shown that the minimum concentration of NPs with a positive effect equals 8 mg/ml and the maximum concentration of the NPs equals 24 mg/ml.

K e y w o r d s: *Lactobacillus acidophilus* PCM2499, Fe_3O_4 nanoparticles, probiotic bacteria, survival at low pH

Generally, lactic acid fermentation is used to produce a wide variety of food products such as: cottage cheese, yogurt, kefir, *etc*. The major fermentation product of the investigated probiotic bacterium *Lactobacillus acidophilus* PCM2499 (Polish Collection of Microorganisms, Wrocław, Poland) is lactic acid. Lactic acid is an important factor in environmental stress, occurring during the fermentation of foods and beverages. The growth of LAB depends upon the pH value of the environment and therefore also on the concentration of lactic acid in the environment. The minimum value of pH for *Lactobacillus* sp. amounts to 3.8–4.4 (Piard and Desmazeaud, 1991).

The increase of bacterial survival rate at lowered pH is of great importance in the food industry. The lactic acid produced by LAB reduces the pH thus inhibiting the activity of these bacteria and reducing the efficiency of the process. Therefore, the development of a method to increase the survival of LAB would result in a more efficient process of lactic fermentation.

Previous studies have focused primarily on the impact of various stress factors on the survival of microorganisms, including the influence of pH on the survival rate of LAB (de Angelis and Gobetti, 2004). The main topic of the research was also concerned with the investigation of microorganisms' adaptation processes to low pH (Sánchez *et al*., 2007) as well as the tolerance of low pH (Bang *et al*., 2000; Bang *et al*., 2002; Matsui and Cvitkovitch, 2010; Senouci-Rezkallah *et al*., 2011). Studies on the clarification of the mechanism of intracellular pH (pH_i) homeostasis were also conducted (Baker-Austin and Dopson, 2007; Hutkins and Nannen, 1993; Kirsch, 2014; Quinn *et al*., 2012; Zhang *el al*., 2013). A number of programs that model stress factor-dependent survival have been created, such as *e.g.* Pathogen Modeling Program Version (http://www.usda.gov).

Adding $CaCO_3$ or other alkaline salts into the bacterial environment is a widely used method of increasing the pH. However, Zapotoczny *et al*. (2013) demonstrated the nanobuffering property of Fe_3O_4 magnetic nanoparticles (NPs). The buffering properties of NPs are explained by the change in superficial charge on the oxide NPs. It has been shown, both theoretically and experimentally, that pH value for acidic solution is less acidic in the NPs environment (measured in nanoparticles suspension gathered by external magnet), less alkaline in alkaline environment and remains at the same level when the pH value is close to the point of zero charge (PZC). NPs react neither with acids nor bases and the buffering effect is limited around the nanoparticles. Since the pH near the NPs surface is more neutral than in bulk, the effect was named nanobuffering. Within our area of interest there is a critical pH value for *L. acidophilus* PCM2499 which, as mentioned

* Corresponding author: A. Jurkowski, Department of Biotechnology, University of Zielona Góra, Zielona Góra, Poland; **e-mail: andrzej.jurkowski@wp.pl**

above, ranges 3.8–4.4. In that pH range the nanobuffering shown by Zapotoczny *et al.* (2013) is $\Delta pH \approx 0.5$. The change of pH value allows to be efficient to notice the difference in survival of LAB in the presence and absence of Fe_3O_4 NPs. Therefore, Fe_3O_4 magnetic nanoparticles were used to improve the survival of *L. acidophilus* PCM2499 at a lower pH.

All chemicals were of analytical reagents grade (iron sulphate $FeSO_4$ (ACS reagent, ≥ 99.0% (Sigma-Aldrich), iron chloride $FeCl_3 \cdot 6H_2O$ (POCH) and 25 % ammonia NH_4OH (POCH)) and used directly without further purification.

Fe_3O_4 NPs were synthesized by coprecipitation of iron salts in alkaline solution. Water solutions of 137 mM of $FeSO_4 \cdot 7\ H_2O$ and 274 mM of $FeCl_3 \cdot 6\ H_2O$ were placed in a beaker. Gaseous nitrogen was used for 30 minutes for degassing an aqueous solution and disposal of diluted oxygen. The solution was stirred mechanically at 1200 rpm and during that process 130 mM NH_4OH was added dropwise. The color of the solution changed from orange-brown to black indicating synthesis of Fe_3O_4 NPs. The final pH value exceeded 10. The stirring process was continued for 30 minutes. Then NPs were separated by external magnet and washed 5–7 times with distilled water until the pH value was lower than 7. Finally, the NPs were dried under vacuum for 500 minutes at 55°C.

The synthesized samples were investigated using different techniques. AFM (Bioscope Catalyst, Bruker) and TEM/EDX (Tecnai G2 F20 S Twin, Fei) were used to investigate the shape and size of synthesized nanoparticles. For AFM a small amount of dried NPs was dissolved in distilled water and sonicated for 1 hour. Then a single drop was put on a mica surface and air dried. The analysis of topography was conducted using a tapping mode. Crystallographic structure of NPs was investigated using X-ray diffraction (XRD) to determine the phase of synthesized iron oxides. The measurements were performed on a BRUKER D8 Advance diffractometer using Johansson monochromator ($\lambda Cu\ K_{\alpha 1} = 1{,}5406$Å). Additionally, Scherrer equation was used to calculate diameter of single crystals. The pH was measured with InLab Combination pH Micro Electrode (Mettler Toledo) on SevenExcellence™ pH/mV meter.

The influence of nanoparticles on survival was tested by culturing *L. acidophilus* PCM2499 at lower pH. The following experiment was performed. A 24 hour *L. acidophilus* PCM2499 starter culture in MRS broth (Merck) was employed. 96% acetic acid was used to lower the pH of the MRS broth to 3.901. The pH was measured with InLab Combination pH Micro Electrode (Mettler Toledo) on SevenExcellence™ pH/mV meter.

One hundred miligrams of Fe_3O_4 NPs and 1 ml of the 24 hour starter culture were added to the tubes containing 4 ml of this medium. The samples were incubated at 37°C in the following intervals of 0.5, 1.0, 1.5, 2.0, 2.5 hours. For each time variant a control culture without Fe_3O_4 NPs was set up. After incubation the samples were transferred to MRS agar in dilutions. Petri dishes were incubated at 37°C for 48 h. Colonies were counted to calculate the CFU/ml for each variant. The experiment was performed in triplicate. T-test analysis was performed. The starter culture was transferred to MRS agar in dilutions. Petri dishes were incubated at 37°C for 48 hours. Colonies were counted to calculate the CFU/ml.

A 24 hour *L. acidophilus* PCM2499 starter culture in MRS broth (Merck) was employed. 96% acetic acid was used to lower the pH of the MRS broth to 3.904. The pH was measured with InLab Combination pH Micro Electrode (Mettler Toledo) on SevenExcellence™ pH/mV meter. 0.16; 0.14; 0.12; 0.1; 0.08; 0.06; 0.04; 0.02 and 0 g of Fe_3O_4 NPs and 1 ml of starter culture were successively added to the tubes containing 4 ml of this medium. They were incubated at 37°C for 45 min. After the incubation they were transferred to MRS agar in dilutions. Petri dishes were incubated at 37°C for 48 h. Colonies were counted to calculate the CFU/ml for each variant. The experiment was performed in triplicate. T-test analysis was performed. The starter culture was transferred to MRS agar in dilutions. Petri dishes were incubated at 37°C for 48 hours. Colonies were counted to calculate the CFU/ml.

Due to magnetic attraction between NPs agglomerates were observed. Nevertheless single NPs were still easy to notice. The mean size equals 17–20 nm. Several NPs with different diameters were imaged and a few representatives were marked on a cross-section. The chosen NPs' diameter ranges from 10–35 nm, where the value of scan height was taken into consideration.

The XRD diffraction peaks correspond well to magnetite Fe_3O_4 (JCPDS file, No. 00-011-0614) indicating that the sample has a cubic crystal system. Also, we can see that no characteristic peaks of impurities were observed. To calculate the mean diameter of crystals of Fe_3O_4 NPs the Scherrer equation was used. The mean diameter is equal to:

$$D = \frac{\kappa \lambda}{\beta cos\ \theta}$$

where κ is shape factor and its value was assumed 0.94 for spheroidal shape of NPs, λ is X-ray wavelength (Cu 1,5406 Å), β is the line broadening at half the maximum intensity and θ is the Bragg angle. The value of β was calculated with the use of *Topas* software, where seven reflections were used to calculate the position and half-width values. Calculated mean diameter of obtained NPs is equal to 21 nm.

Bacterial growth was observed for samples with and without Fe_3O_4 NPs. Details of the number of bacteria

Table I
Number of survival bacteria *Lactobacillus acidophilus* PCM2499 in pH = 3.901 incubated with and without Fe_3O_4 NPs

Time of incubation [h]	Number of bacteria [CFU/ml]				t
	Culture with Fe_3O_4 NPs		Control without Fe_3O_4 NPs		
	Mean value	Standard deviation	Mean value	Standard deviation	
0	$6 \cdot 10^6$	0	$6 \cdot 10^6$	0	–
0.5	$2.19 \cdot 10^6$	$0.86 \cdot 10^6$	$1.69 \cdot 10^6$	$0.71 \cdot 10^6$	705717.3
1.0	$2.77 \cdot 10^5$	$1.76 \cdot 10^5$	$1.35 \cdot 10^5$	$0.86 \cdot 105$	85805.61
1.5	$3.92 \cdot 10^4$	$1.55 \cdot 10^4$	$0.6 \cdot 10^4$	$0.18 \cdot 10^4$	1769.82
2.0	$13 \cdot 10^3$	$9.56 \cdot 10^3$	$2.89 \cdot 10^3$	$0.22 \cdot 10^3$	220.56
2.5	$0.74 \cdot 10^3$	$0.72 \cdot 10^3$	$0.06 \cdot 10^3$	$0.05 \cdot 10^3$	48.29

and test t analysis are shown in Table I. Figure 1 shows the survival rate of *L. acidophilus* PCM2499 during 0–2.5 hours incubation with and without Fe_3O_4 NPs. Fig. 1 indicates the ratio of the survival of bacteria with Fe_3O_4 NPs to survival without NPs at each time variant.

In this experiment an investigation on the concentration of NPs below which there is no positive effect on survival rate was carried out. For all the variants (0.16; 0.14; 0.12; 0.1; 0.08; 0.06; 0.04; 0.02 and 0 g of Fe_3O_4 NPs in 5 ml of culture) colonies were obtained. The colonies were counted. T-test analysis was performed. Figure 2 shows the percentage of survival for different variants of the concentration of NPs.

Previous research using NPs was concerned with the antibacterial effect of gold and silver NPs (Jena *et al.*, 2014; Krishnaraj *et al.*, 2010; Nabikhan *et al.*, 2010; Mishra *et al.*, 2014; Puišo *et al.*, 2014). However no research was performed in order to overcome the harmful effects of stress factors.

The research conducted by our team has shown a positive effect of Fe_3O_4 NPs on the survival of *L. acidophilus* PCM2499 in conditions of low pH. During the cultivation of *L. acidophilus* under reduced pH we observed a higher survival rate of bacteria for all samples with Fe_3O_4 NPs than in the control group. T-test analysis shows that the results obtained for samples with Fe_3O_4 NPs are statistically significant. Graph 1 shows the ratio of the survival of the bacteria with NPs to survival without NPs. It can be noticed that the difference in bacterial survival increases along with increasing incubation time (trend line y = 1.25x). The survival rate increased from 1.3 to 10 times compared to the control group. T-test analysis shows that the minimum concentration of NPs having a positive effect

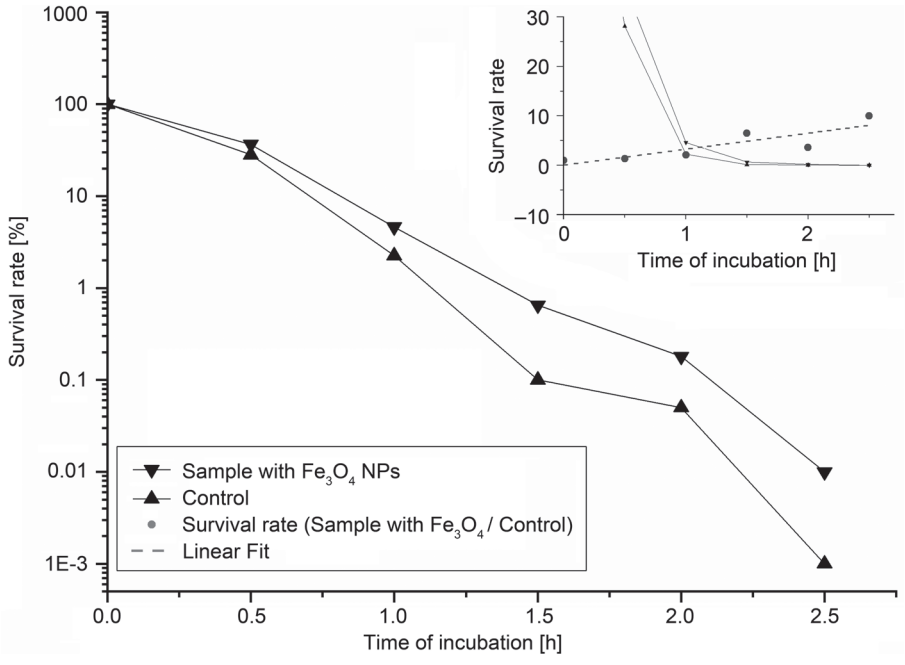

Fig. 1. Survival rate of *L. acidophilus* PCM2499 during incubation with and without Fe_3O_4 NPs. Insert shows survival rate (sample with Fe_3O_4 NPs to control ratio) and linear fit.

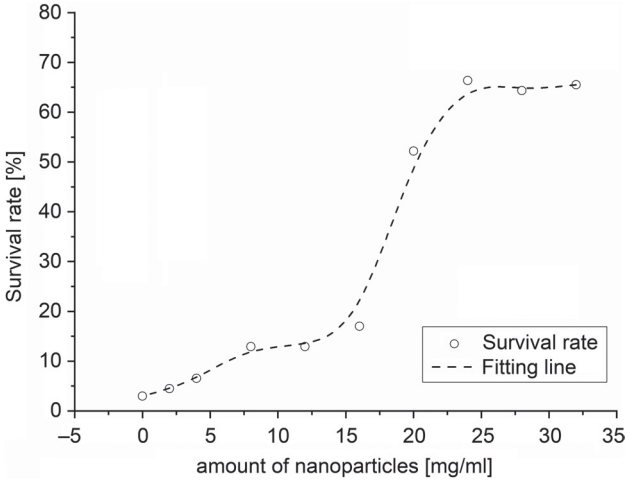

Fig. 2. Survival rate of *L. acidophilus* PCM2499 during incubation with Fe_3O_4 NPs. The fitting line is just a visual guide.

equals 8 mg/ml. In contrast, the maximum concentration of the NPs, above which no longer positive increase was observed equals 24 mg/ml. Along with the raise in the concentration of NPs an increase in the survival of the bacteria was also noted. From the obtained results it can be seen that in the range of 4–16 mg/ml the survival increases slightly (from 4.49% to 17%), while in the range of 20–24 mg/ml, a significant increase in survival was observed (52.17–66.37%). A further increase above 24 mg/ml no longer causes a further increase in the survival. The insignificant influence on the survival with small NPs concentration ranges (up to 16 mg/ml) may be due to the fact that such amount of NPs is able to change pH in a relatively small volume of culture resulting in an insignificant influence on survival increase. In contrast, the concentration of Fe_3O_4 NPs in the range of 20–24 mg/ml contains a sufficient amount of NPs to change the corresponding culture volume, and thus significantly affect the survival.

In conventional technologies the lactic acid created in fermentation is neutralized with calcium carbonate or calcium hydroxide. Then, to isolate the lactic acid from the post-fermentation solution calcium lactate is crystallized and then hydrolyzed with sulfuric acid. The use of Fe_3O_4 NPs during the lactic acid fermentation instead of calcium carbonate or calcium hydroxide could facilitate and increase the efficiency of the process. Lactic acid productivity growth by NPs needs to be confirmed in further studies.

Acknowledgments

One of the authors (B.Z.) is a scholar within Sub-measure 8.2.2 Regional Innovation Strategies, Measure 8.2 Transfer of knowledge, Priority VIII Regional human resources for the economy Human Capital Operational Program co-financed by European Social Fund and state budget.

Literature

Baker-Austin C. and M. Dopson. 2007. Life in acid: pH homeostasis in acidophiles. *Trends Microbiol.* 15: 165–171.

Bang I.S., B.H. Kim, J.W. Foster and Y.K. Park. 2000. *OmpR* regulates the stationary-phase acid tolerance response of *Salmonella enteric* serovar *typhimurium*. *J. Bacteriol.* 182: 2245–2252.

Bang I.S., J.P. Audia, Y.K. Park and J.W. Foster. 2002. Autoinduction of the ompR response regulator by acid shock and control of the Salmonella enterica acid tolerance response. *Mol. Microbiol.* 44: 1235–1250.

De Angelis M. and M. Gobetti. 2004. Environmental stress responses in *Lactobacillus*: A review. *Proteomics* 4: 106–122.

Hutkins R.W. and N.L. Nannen. 1993. pH Homeostasis in Lactic Acid Bacteria. *J. Dairy Sci.* 76: 2354–2365.

Jena J., N. Pradhan., B.P. Dash, P.K. Panda and B.K. Mishra. 2014. Pigment mediated biogenic synthesis of silver nanoparticles using diatom Amphora sp. and its bactericidal and antimicrobial activity. *J. Saudi Chemi. Soc.* "*in press*", doi:10.1016/j.jscs.2014.06.005.

Kirsch K.M. 2014. The impact of CO_2 on inorganic carbon supply and pH homeostasis in Corynebacterium glutamicum. PhD thesis. University of Cologne, Germany.

Krishnaraj C., E.G. Jagan, S. Rajasekar, P. Selvakumar, P.T. Kalaichelvan and N. Mohan. 2010. Synthesis of silver nanoparticles using *Acalypha indica* leaf extracts and its antibacterial activity against water borne pathogens. *Colloids Surf. B* 76: 50–56.

Matsui R. and D. Cvitkovitch. 2010. Acid tolerance mechanisms utilized by *Streptococcus* mutans. *Future Microbiol.* 5: 403–417.

Mishra A., M. Kumari, S. Pandey, V. Chaudhry, K.C. Gupta and C.S. Nautiyal. 2014. Biocatalytic and antimicrobial activities of gold nanoparticles synthesized by Trichoderma sp. *Bioresour. Technol.* 166: 235–242.

Nabikhan A., K. Kandasamy, A. Raj and N.M. Alikunhi. 2010. Synthesis of antimicrobial silver nanoparticles by callus and leaf extracts from saltmarsh plant, *Sesuvium portulacastrum* L. *Colloids Surf. B* 79: 488–493.

Piard J.C. and M. Desmazeaud. 1991. Inhibiting factors produced by lactic acid bacteria. 1. Oxygen metabolites and catabolism end-products. *Lait* 71: 525–541.

Puišo J., D. Jonkuvienė, I. Mačionienė, J. Šalomskienė, I. Jasutienė and R. Kondrotas. 2014. Biosynthesis of silver nanoparticles using lingonberry and cranberry juices and their antimicrobial activity. *Colloids Surf. B* 121: 214–221.

Quinn M.J., C.T. Resch, J. Sun, E.J. Lind, P. Dibrov and C.C. Hase. 2012. NhaP1 is a K+(Na+)/H+ antiporter required for growth and internal pH homeostasis of *Vibrio cholerae* at low extracellular pH. *Microbiology* 158: 1094–1105.

Sánchez B., M-Ch. Champomier-Vergès, M. del Carmen Collado, P. Anglade, F. Baraige, Y. Sanz, C.G. de los Reyes-Gavilán, A. Margolles and M. Zagorec. 2007. Low-pH adaptation and the acid tolerance response of *Bifidobacterium longum* biotype *longum*. *Appl. Environ. Microbiol.* 73: 6450–6459.

Senouci-Rezkallah K., P. Schmitt and M.P. Jobin. 2011. Amino acids improve acid tolerance and internal pH maintenance in *Bacillus cereus* ATCC14579 strain. *Food Microbiol.* 28: 364–372 .

Zapotoczny B., M.R. Dudek, J.J. Kozioł and J. Mleczko. 2013. Nanobuffering property of Fe_3O_4 magnetic nanoparticles in aqueous solution. *Phys. A.* 392: 1493–1499.

Zhang W., Y. Wang, Y. Song, T. Wang, S. Xu, Z. Peng, X. Lin, L. Zhang and X. Shen. 2013. A type VI secretion system regulated by *OmpR* in Yersinia pseudotuberculosis functions to maintain intracellular pH homeostasis. *Environ. Microbiol.* 15: 557–569.